

For my loving and supportive parents,

Nursen and Yilmaz Senturk

and for my dear grandfather Ramazan BIYIK who deeply wished but

could not join my graduations, sleep in peace...

EphrinB ligands are functional co-receptors for Reelin to regulate neuronal migration

Dissertation zur Erlangung des Doktorgrades
der Naturwissenschaften

vorgelegt beim Fachbereich Biowissenschaften
der Johann Wolfgang Goethe-Universität
in Frankfurt am Main

von

Msc. Aycan Senturk

aus Olpe

Frankfurt am Main (2010)

Vom Fachbereich Biochemie, Chemie und Pharmazie der Johann Wolfgang Goethe-
Universität als Dissertation angenommen.

Dekanin: Prof. Dr. Anna Starzinski-Powitz

Gutachter: Prof. Dr. Amparo Acker-Palmer

Prof. Dr. Thomas Deller

Datum der Disputation: 14.02.2011

The part of the work presented in this thesis was performed in the laboratory of Prof. Dr. Amparo Acker-Palmer, Junior Group – Signal transduction, at the Max-Planck-Institute of Neurobiology, Martinsried, Germany and completed in the laboratory of Prof. Dr. Amparo Acker-Palmer, Institute for Molecular Life Sciences (FMLS), Goethe University, Frankfurt.

1 Table of Contents

1	Table of Contents	5
2	Abbreviations.....	9
3	Zusammenfassung	13
4	Introduction	19
4.1	Development of the cerebral cortex (corticogenesis) in mice	19
4.1.1	Development of the neocortex.....	19
4.1.2	Development of the hippocampus	21
4.1.3	Development of the cerebellum.....	22
4.2	Neuronal migration and layering in the cerebral cortex during embryonic development and adulthood.....	24
4.2.1	Role of Reelin in cortical neuronal migration	25
4.2.2	Other functions of Reelin.....	28
4.3	Defects in cortical layer formation of mice.....	29
4.3.1	The <i>reeler</i> mice	30
4.3.1.1	Alterations in the cerebral cortex of the <i>reeler</i> mice	31
4.3.1.2	Alterations in the hippocampus of the <i>reeler</i> mice.....	33
4.3.1.3	Alterations in the cerebellum of the <i>reeler</i> mice	33
4.3.2	The <i>Yotari</i> and the <i>Scrambler</i> mice.....	34
4.3.3	The VLDLR and the ApoER2 knockout mice.....	35
4.4	Reelin pathway	38
4.4.1	Reelin	38
4.4.2	The lipoprotein receptors: VLDLR and ApoER2	39
4.4.3	Dab1 and signaling downstream of Dab1.....	41
4.4.3.1	Dab1 phosphorylation.....	42
4.5	Eph receptors and their ephrin ligands	45
4.5.1	Structure of Eph receptors and ephrins	46
4.5.1.1	Eph structure.....	46
4.5.1.2	Ephrin structure.....	47

4.5.2	Bidirectional signaling mechanisms between Eph receptors and ephrin ligands.....	48
4.5.2.1	Mechanisms of Eph receptor “Forward” signaling.....	49
4.5.2.2	Mechanism of ephrin ligand “Reverse” signaling.....	50
4.5.3	Roles of Eph and ephrins in nervous system development.....	53
4.5.3.1	Axon guidance.....	54
4.5.3.2	Synaptic Plasticity.....	55
4.5.3.3	Segmentation.....	55
4.5.3.4	Corticospinal tract formation.....	56
5	Results	59
5.1	Genetic interaction between Reelin and ephrinB pathways	60
5.1.1	Compound mice show <i>reeler</i> like phenotypes in the cerebral cortex.....	60
5.1.1.1	Cortical neurons invade the marginal zone in <i>rl/+; b3-/-</i> compound mutant mice.	61
5.1.1.2	Cortical layering is altered in the <i>rl/+; b3-/-</i> compound mutant mice.	62
5.1.1.3	Interneuron distribution is altered in the compound mutant mice.	68
5.1.1.4	BrdU birth dating study reveals neuronal migration defect in <i>rl/+; b3-/-</i> compound mutant mice.	70
5.1.1.5	Preplate splitting does not take place in the compound mutant embryos.....	75
5.1.1.6	Radial glia scaffold is altered in the <i>rl/+; b3-/-</i> compound mutant mice.	76
5.1.2	<i>rl/+; b3 -/-</i> compound mice show <i>reeler</i> like phenotypes in the hippocampus.	78
5.1.2.1	CA1 shows layering defects in the hippocampus of <i>rl/+; b3-/-</i> compound mutant mice. 79	
5.1.2.2	The granular cell layer in the dentate gyrus of <i>rl/+; b3-/-</i> compound mice is less compact.....	82
5.1.2.3	Mossy cells are dislocated in the <i>rl/+; b3-/-</i> compound mutant mice.	83
5.1.2.4	The radial glial scaffold of the dentate gyrus is altered in the <i>rl/+; b3-/-</i> compound mutant mice.	84
5.1.2.5	The dendritic branching of hippocampal pyramidal neurons is increased in the <i>rl/+; b3-/-</i> compound mutant mice.....	85
5.1.3	<i>rl/+; b3-/-</i> and <i>rl/+; b2-/-</i> compound mutant mice show <i>reeler</i> like phenotypes in the cerebellum.	88
5.1.3.1	Cerebellar Purkinje cell migration requires ephrinB ligands for proper migration	88
5.2	Reelin, Dab1 and ephrinB ligands are in the same signaling complex.....	94
5.2.1	Reelin and Dab1 binds to ephrinB ligands.....	94
5.2.2	Reelin and ephrinB ligands functionally interact.....	95
5.2.3	Dab1 phosphorylation levels are reduced in ephrinB3 knockouts.....	96

1 Table of Contents

5.2.4	EphrinB ligands are in complex with Reelin receptors, ApoER2 and VLDLR. 100	
5.2.5	Dab1 phosphorylation is induced following ephrinB3 activation.	101
5.3	EphrinB reverse signaling stimulation can rescue <i>reeler</i> phenotypes in the cerebral cortex.....	102
5.3.1	Activation of ephrinB ligands is sufficient to activate Reelin signaling in cortical neuron cultures.	102
5.3.2	Activation of ephrinBs rescues cortical migration defects in the <i>reeler</i> mouse.104	
6	Discussion	107
6.1	Concluding remarks.....	116
7	Material and methods	119
7.1	Material.....	119
7.1.1.1	Antibodies	119
7.1.2	Chemicals, Reagents, Commercial Kits & Enzymes	120
7.1.3	Consumable Material.....	122
7.1.4	Equipment.....	124
7.1.5	Oligonucleotides	126
7.1.6	Cell lines	127
7.1.7	Mice	127
7.1.8	Primary cells and tissues.....	127
7.2	Media and Standard Solutions.....	127
7.2.1	Media and Supplements for Cell Culture.....	130
7.2.2	Media and Supplements for Primary Cell Culture	131
7.2.3	Media for Organotypic Cultures	131
7.2.4	Solutions for Biochemistry	132
7.2.5	Solutions for BrdU staining	135
7.2.6	Solutions for Embedding of Vibratome & CryoSections.....	135
7.2.7	Solutions for histology	136
7.3	Methods	137
7.3.1	Molecular Biology	137
7.3.1.1	Genomic DNA extraction and genotyping polymerase chain reactions (PCR)	137
7.3.2	Cell culture	139

7.3.2.1	Mammalian cell lines.....	139
7.3.2.2	Cultivation of primary cortical neurons.....	141
7.3.3	Biochemistry	142
7.3.3.1	Cell Stimulation	142
7.3.3.2	Cell or Tissue Lysis and Protein Concentration Measurements	142
7.3.3.3	Immunoprecipitation and Pulldown Experiments.....	143
7.3.3.4	Immunoblotting.....	144
7.3.4	Mouse work	145
7.3.5	Histology	146
7.3.5.1	Fixation and perfusion.....	146
7.3.5.2	Cryosectioning.....	147
7.3.5.3	Vibratome sectioning	147
7.3.5.4	Immunocytochemistry	148
7.3.5.5	Immunohistochemistry	149
7.3.5.6	DAB staining	150
7.3.5.7	Negative controls	151
7.3.5.8	Nissl staining.....	151
7.3.5.9	DNA-labeling.....	151
7.3.6	Birthdating studies.....	152
7.3.6.1	Cumulative BrdU labeling.....	152
7.3.6.2	BrdU staining	152
7.3.7	Organotypic cultures.....	153
7.3.7.1	Preparation of embryonic cortical sections.....	153
7.3.7.2	Stimulation	153
7.3.7.3	Fixation and Immunohistochemistry of organotypic cultures	154
7.3.8	Tandem affinity purification (TAP) and mass spectrometry.....	154
7.3.9	Data analysis	155
8	Bibliography	157
9	Acknowledgements	173
10	Publication List	176
11	Curriculum Vitae	178

2 Abbreviations

ADHD, Attention deficit hyperactivity disorder

ApoER2, Apolipoprotein E receptor 2

ApoER2^{-/-}, Apolipoprotein E receptor 2 knockout mouse

BG, Bergmann glia

BrdU, 5'-bromodeoxyuridine

CA, Hippocampal areas

CNR Cadherin-related neuronal receptors

CP, Cortical plate

CR, Cajal-Retzius

CrkL, Crk like

Dab1, *disabled-1* gene

DG, Dentate gyrus

E, Embryonic day

ECM, Extracellular matrix

EGL, External granular layer

EGF, Epidermal growth factor

Ephrin, Eph-receptor-interacting proteins

Ephs, Eph receptor tyrosine kinases

FAK, Focal adhesion kinase

FGF, Fibroblast growth factor

GCL, Granule cell layer

GFAP, Glial fibrillary acidic protein

GPI, Glycosylphosphatidylinositol

HP, Hippocampal cortical plate

IGL, Internal granular layer

IHC, Immunohistochemistry

IML, Inner molecular layer

IMZ, Inner marginal zone

IZ, Intermediate zone
JIP, JNK interacting protein
JNK, c-Jun N-terminal kinase
LTP, Long-term potentiation
MAPKK, Map-kinase-kinase
MGL, Medial ganglionic eminence
ML, Molecular layer
MZ, Marginal zone
NPxY, Asn-Pro-x-Tyr, x means any amino acid
OML, Outer molecular layer
OMZ, Outer marginal zone
PB, Phosphate buffer
PBS, Phosphate-buffered saline
RC2,
PCL, Purkinje cell layer
PDGF, Platelet derived growth factor
PDZ, PSD-95 post-synaptic density protein, Discs large, Zona occludens tight junction protein
PFA, Paraformaldehyde;
PICK, Phosphatidylinositol 3-kinase
PKB, Protein kinase B
PP, Preplate
PTB, Phosphotyrosine binding
PTB-BL, Protein tyrosine phosphatase-basophil-like
PY, Pyramidal layer
Reln, Reelin gene
RTK, Receptor tyrosine kinases
SAM, Sterile α -motif
SDF-1, Stromal derived factor 1
SEM, Standard error of the mean
SFK, Src family kinase
SH2, SRC-Homolgy-2
SLM, Stratum lacunosum-moleculare

2 Abbreviations

SO, Stratum oriens

SP, Subplate

SP, Stratum pyramidale

SR, Stratum radiatum

SVZ, Subventricular zone

VLDLR, Very low density lipoprotein receptor

VLDLR^{-/-}, Very low density lipoprotein receptor knockout mouse

VZ, Ventricular zone

Y, Tyrosine

WM, White matter

3 Zusammenfassung

Der Neocortex der Säugetiere weist charakteristische Schichtungen auf, und jede dieser Schichten enthält verschiedene Typen von Neuronen, die in stereotypen Mustern angeordnet sind. Die Ausbildung dieser geschichteten Struktur ist nur dann möglich, wenn korrekte Migration von Neuronen von proliferativen Zonen zu deren Endpositionen stattfindet. Die exakte Migration und Schichtung wird von Mutationen beeinflusst, die entweder die migratorische Fähigkeit der Neuronen beeinträchtigen, oder deren Fähigkeit, die Position zu erkennen, an der sie die Wanderung beenden sollten (Gupta *et al.*, 2002, Rice *et al.*, 2001, Walsh *et al.*, 2000). In den letzten Jahren wurde das extrazelluläre Protein Reelin als wichtiger Faktor bekannt, der sich auf mehrere Schritte der neuronalen Migration und Schichtung in der Großhirnrinde auswirkt (zusammengefasst in (Tissir *et al.*, 2003). Das sekretierte Glykoprotein Reelin kontrolliert die Migration der Neuronen durch die Bindung an zwei Lipoproteinrezeptoren, den Very-low-density lipoprotein Rezeptor (VLDLR) und den Apolipoprotein E Rezeptor 2 (ApoER2) (D'Arcangelo *et al.*, 1999). Die Bindung von Reelin an ApoER2 und VLDLR ruft die Phosphorylierung von Disabled-1 (Dab1) (D'Arcangelo *et al.*, 1999, Howell *et al.*, 1997), einem Adapterprotein, das an die intrazelluläre Domäne der Rezeptoren bindet, hervor, indem sie Kinasen der Src-Familie (SFKs) aktiviert (Arnaud *et al.*, 2003, Bock *et al.*, 2003a). Außer der Bedeutung des Reelin-Signalwegs für die korrekte Entwicklung des Nervensystems und dem Wissen, dass die Unterbrechung dieses Signalwegs zu verschiedenen neurologischen Krankheiten wie Epilepsie, Schizophrenie und der Alzheimerkrankheit führt (Costa *et al.*, 2002, Botella-Lopez *et al.*, 2006, Herz *et al.*, 2006), ist die molekulare Grundlage der Aktivierung dieses Signalwegs an der Zellmembran noch kaum charakterisiert. Da VLDLR und ApoER2 keine intrinsische Kinaseaktivität besitzen, wurde die Existenz eines Korezeptors für mindestens eine Dekade vermutet, und die genaue Natur dieses Korezeptors ist unbekannt.

EphrinBs, Transmembranliganden für Eph-Rezeptoren, besitzen die Fähigkeit zur Signalgebung, die für synaptische Plastizität und Angiogenese durch Sprossung erforderlich ist, indem sie die Aktivität anderer Transmembranrezeptoren wie AMPAR beziehungsweise VEGFR2 beeinflussen (Sawamiphak *et al.*, 2010b, Segura *et al.*, 2007, Essmann *et al.*, 2008). Darüber hinaus führt die Stimulation von kortikalen Neuronen in Kultur mit löslichen EphB-Rezeptoren zur Rekrutierung und Aktivierung von SFKs in Membranpatches, in denen sich ephrinB-Liganden befinden (Palmer *et al.*, 2002). Deshalb nehmen wir an, dass ephrinB *in vivo* funktionell mit dem Reelin-Signalweg verbunden sein könnte.

Der Fokus dieser Arbeit liegt darin, zu zeigen, dass das neuronale Wegweiser-molekül ephrinB einen entscheidenden Korezeptor für die Reelin-Signalgebung während der Entwicklung geschichteter Strukturen im Gehirn darstellt.

Um zu erforschen, ob ephrinB und die Reelin-Signalgebung *in vivo* genetisch interagieren, wurden zuerst Mäuse mit Compound-Mutationen hergestellt, die eine Nullmutation im Gen für ephrinB3 tragen und heterozygot für Reelin sind ($rl/+; b3/-$). *Reeler* ist eine autosomal rezessive Mutation der Maus, die, wenn sie heterozygot auftritt, keinen offenkundigen Phänotyp aufweist (Caviness *et al.*, 1972, Caviness *et al.*, 1978). Wir zeigen, dass ephrinBs genetisch mit Reelin interagieren, da Mäuse mit Compound-Mutationen ($rl/+; b3 -/-$) und ephrinB1-, B2- und B3-Dreifach-Knockouts die verschiedenen Defekte in der Entwicklung phänokopieren, die im Neocortex, Hippocampus und Cerebellum der *reeler*-Mäuse beobachtet wurden. Eines der Kennzeichen des *reeler*-Phänotyps ist die gestörte Schichtung der Großhirnrinde mit einer Marginalzone (MZ), die eine äußerst große Zahl an Zellen enthält (Caviness, 1982). Sowohl die Compound-Mäuse als auch die Triple-ephrinB1B2B3-knockouts zeigten eine Zunahme der Zellzahl in der MZ. Um die kortikalen Defekte detailliert zu charakterisieren, wurde die Verteilung von postmitotischen migrierenden Neuronen im Cortex von $rl/+; b3/-$ Compound-Mäusen mit Hilfe von unterschiedlichen schichtenspezifischen Markern für früh (Tbr1) (Hevner *et al.*, 2001) und spät entstandene (SatB2 and Brn1) (Britanova *et al.*, 2008, McEvelly *et al.*, 2002) Neuronen, analysiert. Unsere Untersuchungen ließen die veränderte kortikale

3 Zusammenfassung

Schichtung in den *rl/+; b3-/-* Compound-Mäusen erkennen. So befanden sich früh entstandene Neuronen in den oberen cortikalen Schichten und spät entstandene in den unteren cortikalen Schichten, was für eine *outside-in*-Schichtung spricht, wie man sie von *reeler* kennt. Interessanterweise ist eine der frühesten strukturellen Abnormalitäten, die man im *reeler*-Cortex erkennen kann, die Unfähigkeit, die Preplate, die reich an extrazellulärer Matrix ist, in die Marginalzone und die Subplate aufzuspalten (Sheppard *et al.*, 1997). Zum Zeitpunkt E17.5 zeigten *rl/+; b3-/-* Compound-Mäuse eine beachtliche Anhäufung von Chondroitin-Sulfat-Proteoglykan (CSPG), einer Komponente der extrazellulären Matrix, im gesamten Neocortex mit einer ungeteilten Schicht an der Oberfläche, welche übermäßig viel CSPG enthielt und somit die abnorme Teilung der Preplate der *reeler*-Maus nachahmte.

Um zu bestätigen, dass die beobachteten Effekte auf die Schichtung des Cortex der *rl/+; b3-/-* Compound-Mäuse als Folge der Beeinträchtigung der neuronalen Migration auftritt, wurden zusätzlich BrdU-Puls-Experimente durchgeführt. BrdU wird in sich teilende Vorläuferzellen eingebaut und spiegelt deshalb das migratorische Verhalten von neu entstandenen Neuronen zum Zeitpunkt der Injektion wieder. Schwangeren Weibchen wurde BrdU zu den Zeitpunkten E12.5, E15.5 und E17.5 injiziert und die Gehirne wurden am postnatalen Tag 20 ausgewertet. Die Verteilung der mit BrdU gekennzeichneten Neuronen zu verschiedenen Zeitpunkten der Entwicklung in der Großhirnrinde bestätigte unsere Untersuchungen, die mit Hilfe der schichtspezifischen Marker durchgeführt worden waren. Deshalb deuten unsere Ergebnisse an, dass die beobachteten Defekte in der Schichtung des Cortex tatsächlich eine Folge von beeinträchtigter neuronaler Migration sind.

Es wurde beobachtet, dass auch geschichtete Strukturen im Hippocampus in den *rl/+; b3-/-* Compound-Mäusen verändert sind, was für einen Crosstalk zwischen ephrinB3 und Reelin auch während der Entwicklung des Hippocampus spricht. Die CA1-Region des Hippocampus zeigte eine lockere Verbindung der pyramidalen Zellschichten, welche zu einer signifikanten Erhöhung der Dicke dieser Region und zu einer Einwanderung von Pyramidalzellen in das Stratum oriens führte. Darüber

hinaus haben die Anomalien in den dendritischen Verzweigungen von Pyramidalneuronen der CA1-Region, die in Richtung der Reelin-produzierenden Cajal-Retzius-Zellen im stratum locunosum moleculare projizieren, in den *rl/+; b3-/-* Compound-Mäusen eine auffallende Ähnlichkeit mit denen, die in *reeler*-Mutanten beobachtet wurden. Reelin fungiert auch als Differenzierungsfaktor und Positionierungssignal für radiale Gliazellen, die positiv für glial fibrillary acidic protein (GFAP) sind und ein Gerüst für die korrekte Migration von neu entstandenen Granularzellen, die auf das Netzwerk der Granularzellen im Gyrus dentatus zuwandern (Forster *et al.*, 2002) bilden. In *rl/+; b3-/-* Compound-Mäusen ist dieses Gerüst aus radialen Gliazellen schwerwiegend beeinträchtigt, was ebenfalls zu einer lockeren Organisation der Granularzellen im Gyrus dentatus führt.

Die Ataxie in *reeler*-Mäusen ist das Ergebnis einer schwerwiegenden Fehlorganisation im Cerebellum dieser Mutanten (Tissir *et al.*, 2003). Interessanterweise wurden nur milde Defekte in den Granularzellen, die sich in der internen Granularschicht des Cerebellums von *rl/+; b3-/-* Compound-Mäusen angesammelt haben, und keine Defekte in der Migration und der Verzweigung der Purkinjzellschicht, festgestellt. Stattdessen ist ephrinB2 in den Purkinjzellen des Cerebellums stark exprimiert (Liebl *et al.*, 2003) und obwohl keine bedeutenden Defekte der Migration dieser Zellen festgestellt wurden, zeigte die Untersuchung der Verzweigung der Purkinjzellen in *b2-/-* Mäusen eindeutige Defekte, die bereits in einfachen ephrinB2-Mutanten auftraten. Bedeutend ist, dass die Defekte in der Verzweigung bei *rl/+; b2-/-* Compound-Mäusen signifikant verstärkt waren, was darauf hindeutet, dass der Reelin-Signalweg im Cerebellum spezifisch ephrinB2 benötigt.

Um Einblicke in den Mechanismus zu erhalten, wie ephrinB-Liganden den Crosstalk mit Reelin durchführen, um die korrekte Positionierung von Neuronen in den geschichteten Strukturen des Gehirns zu kontrollieren, wurde als nächstes die biochemische Interaktion dieser beiden Signalwege untersucht. In einer gerichteten proteomischen Untersuchung mit Hilfe der Tandem affinity purification-mass spectrometry-Methode (Angrand *et al.*, 2006) von Proteinen aus eine Neuroblastom-Zelllinie, die ephrinB binden, wurde Reelin als ein Protein, das mutmaßlich mit

3 Zusammenfassung

ephrinB interagiert, identifiziert. Zunächst bestätigten wir die Fähigkeit von Reelin, mit ephrinBs zu assoziieren mit Ko-Immünpräzipitation beider endogener Proteine aus Gehirnlisaten. Das extrazelluläre Protein Reelin zeigte eine starke Bindung an die extrazelluläre Domäne von ephrinB3 und auch von ephrinB2, was andeutet, dass beide ephrin-Liganden die Funktionen von Reelin *in vivo* beeinflussen könnten. Die Stimulierung von cortikalen Neuronen mit Reelin führt zu einer effektiven Tyrosin-Phosphorylierung des Adapters Dab1. Da die Stimulation von cortikalen Neuronen mit einer löslichen, vorgeclusterten Form von EphB-Rezeptoren zur Rekrutierung und Aktivierung von Src-Kinasen in ephrinB-Clustern führt (Palmer *et al.*, 2002), nehmen wir an, dass ephrinBs Src-Kinasen in VLDLR- und ApoER2-Rezeptor-Clustern rekrutieren und aktivieren könnten. Aktivierte Src-Kinasen phosphorylieren dann wiederum das Adapterprotein Dab1, das an VLDLR und ApoER2 gebunden ist und initiieren die weitere Signalgebung. In Übereinstimmung damit ko-immunpräzipitiert phosphoryliertes Dab1 zum Zeitpunkt E16.5 mit ephrinBs, während die neuronale Migration und die Schichtung des Cortex stattfindet. Darüber hinaus konnten wir beobachten, dass ephrinB3, das durch EphB3-Fc aktiviert wurde, sowohl Reelin, als auch ApoER2 und VLDLR in ephrinB3-Membranpatches in cortikalen Neuronen anhäuft. Die Aktivierung von ephrinB-Liganden durch Stimulation von cortikalen Neuronen mit EphB3-Fc führt zur Rekrutierung und Phosphorylierung von Dab1 in ephrinB-Clustern.

Als nächstes befassten wir uns mit der Notwendigkeit von der durch ephrinB vermittelten Rekrutierung und Aktivierung von Src-Kinasen für den Reelin-Signalweg, indem wir Loss-of-function-Studien sowohl in cortikalen Neuronen in Kultur als auch *in vivo* in Mäusen durchführten. Cortikale Neuronen, die aus ephrinB3- und ephrinB2-Knockouts isoliert wurden, zeigten eine signifikante Beeinträchtigung der durch Reelin vermittelten Phosphorylierung von Dab1 und die Phosphorylierungslevels von Dab1 in ephrinB3 Mausmutanten waren stark verringert, was andeutet, dass ephrinBs Korezeptoren, die notwendig für einwandfreie Signalgebung durch Reelin sind, darstellen. Um die Bedeutung von ephrinBs für die Kontrolle der Funktion von Reelin zu

untersuchen, arrangierten wir eine Reihe von Rescue-Experimenten sowohl in Neuronenkulturen als auch während der neuronalen Migration im Cortex *in vivo*. Aus *reeler*-Mäusen isolierte cortikale Neuronen zeigten die erwartete verringerte Phosphorylierung von Dab1, die rückgängig gemacht werden konnte, indem die Neuronen mit exogenem Reelin stimuliert wurden. Noch bedeutender ist die Tatsache, dass die Phosphorylierung von Dab1 durch die alleinige Aktivierung von ephrinBs mit EphB wiederhergestellt werden konnte, was die Bedeutung der ephrinBs als Korezeptoren für die Aktivierung des Signalwegs über die Rezeptoren für Reelin, VLDLR und ApoER2, widerspiegelt. Um die Rolle von ephrinBs als Korezeptoren für den Reelin-Signalweg während der neuronalen Migration in der Großhirnrinde zu unterstreichen, setzten wir ähnliche Rescue-Experimente in organotypischen Schnittkulturen an. In den Schnitten von *reeler*-Mäusen und Wildtyp-Wurfgeschwistern wurde die Migration von Neuronen, die durch Fc als Kontrolle und EphB3-Fc stimuliert wurde, nach drei Tagen in Kultur untersucht. Die *reeler*-Schnitte zeigten den typischen *reeler*-Phänotyp in der Großhirnrinde. In Übereinstimmung mit der Annahme einer wirksamen Regulation des Reelin-Signalwegs war die Aktivierung von ephrinB mit EphB-Rezeptoren in der Lage, die migratorischen Defekte in *reeler*-Schnitten aufzuheben.

Zusammengefasst identifizieren unsere Ergebnisse ephrinBs als Korezeptoren für den Reelin-Signalweg, die für die Funktion von Reelin in der neuronalen Migration während der Entwicklung der geschichteten Strukturen der Großhirnrinde, dem Hippocampus und dem Cerebellum notwendig sind. Unsere genetischen Analysen von ephrinB-Mutanten zeigen gemeinsam mit starken biochemischen Untersuchungen, dass ephrinBs *in vivo* für zahlreiche Aktivitäten von Reelin erforderlich sind.

4 Introduction

4.1 Development of the cerebral cortex (corticogenesis) in mice

The mammalian cerebral cortex is a highly ordered structure. Its development is very dynamic and involves complex processes. This structure is achieved by a delicately orchestrated program in which the assembly of cerebral cortex and other layered structures is precisely modulated, both temporally and spatially. This is achieved through the mastered use of signaling molecules, ultimately resulting in an intricate organism and tightly orchestrated movements of billions of cells during embryonic development.

4.1.1 Development of the neocortex

The neocortex is phylogenetically the most recent part of the cerebral cortex. It is defined as the outermost region of the cortex and comprises six layers of neurons, each of which consist of neurons that share similar morphological and functional characteristics (Angevine *et al.*, 1961, Kostovic *et al.*, 1980, Luskin *et al.*, 1985, Marin-Padilla, 1998, Rakic, 1974). This laminated structure is built in the mouse during embryonic days (E) 11 to 18 by the coordinated migration of principal neurons from germinal zones towards their destination in the upper layers. The first principal neurons originate from the proliferation of precursors that are generated in the germinal zones; ventricular zone (VZ), subventricular zone (SVZ) or the rhombic limb. These precursors first form a transient structure called the preplate (PP) between E10 and E12. Axonal projections from the preplate neurons subsequently separate the VZ from the pial surface and thus form the intermediate zone (IZ) (reviewed in (Rakic *et al.*, 1995) (Figure 4.1A). Simultaneously with this initial layer formation, the appearance of Cajal-Retzius (CR) cells takes place (Lavdas *et al.*, 1999, Meyer *et al.*, 1999). The subsequent generation of

neurons migrating from the VZ towards the pia, splits the PP into two zones; namely the superficial marginal zone (MZ) which contains the CR cells and the subplate (SP). These newly migrated neurons form then the cortical plate between the MZ and the SP (Marin-Padilla, 1998, Super *et al.*, 1998b) (Figure 4.1B). The next cohorts of neurons from the VZ form the remaining layers of the six-layered neocortex with this systematic radial glia migration, where younger cortical neurons occupy layers closer to the pial surface and older cortical neurons are positioned deeper inside and closer to the VZ. Therefore, this laminated structure of cortex is achieved in an “inside-out” pattern (Frantz *et al.*, 1996, McConnell *et al.*, 1991, Takahashi *et al.*, 1999) (Figure 4.1C).

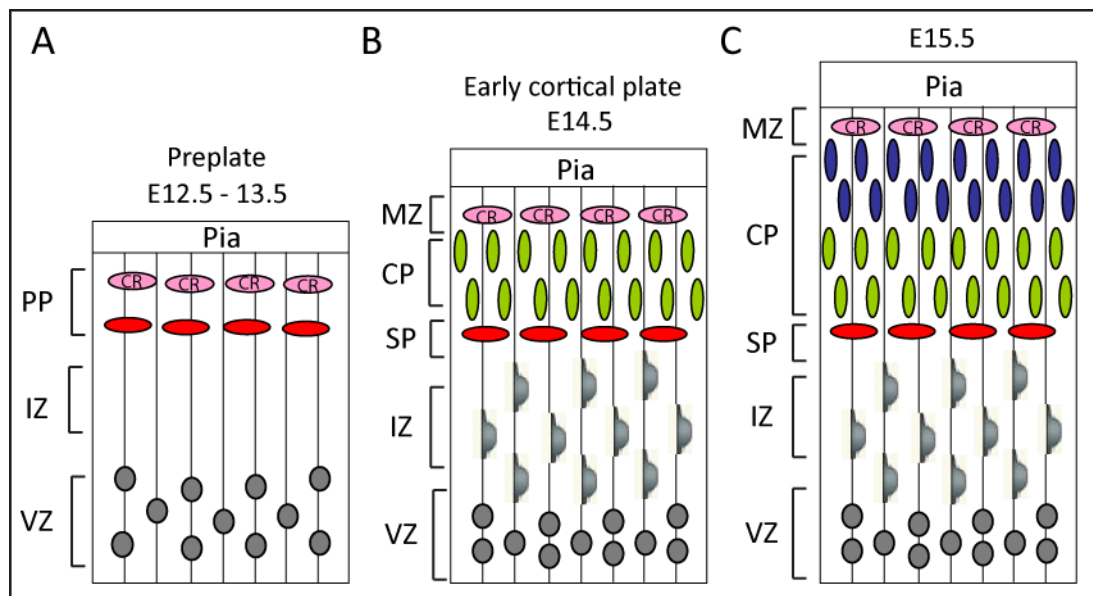


Figure 4.1 Schematic view of early cortical development in mice (Adapted from (Tissir *et al.*, 2003)). (A) At embryonic day (E) 12.5 pioneer neurons form the preplate (PP) with Cajal-Retzius cells (CR - pink) and subplate cells (SP - red). (B) At E14.5 new-born neurons from ventricular zone (VZ) invade the PP and condense in the cortical plate (CP - green), splitting the preplate into two MZ (pink) and SP. (C) At E15.5, the next cohort of neurons (blue) migrates through the cortical plate and settles superficially forming an inside to outside gradient. Cell free MZ and the five layers of cortical neurons constitute the mammalian neocortex. CP, Cortical Plate; CR, Cajal-Retzius cells; IZ, Intermediate zone; MZ, Marginal zone; PP, Preplate; SP, Subplate; VZ, Ventricular zone.

4.1.2 Development of the hippocampus

The hippocampal complex consists of the dentate gyrus (DG), the CA regions and the parahippocampal (subicular) cortex (Stanfield *et al.*, 1979b). Each of these structures is derived from distinct proliferative zones resided in the wall of the dorsal telencephalon, namely medial pallidum. The formation of the hippocampus in mouse becomes evident at E12 with the formation of a preplate containing pioneer neurons followed by the appearance of a cell dense cortical plate which splits the preplate zone into a subplate and a marginal zone. Unlike the neocortex, in the developing hippocampus the cortical plate does not become a multi-laminar structure but remains a cell dense layer (Figure 4.2, A, B). However, the marginal zone is subdivided into two segregated sub-layers: the inner marginal zone (IMZ) and the outer marginal zone (OMZ) (Figure 4.2C). First, the hippocampal pyramidal cells migrate from the site of their origin near the ventricle to their final destination along the radial scaffold formed by radial fibers in the inner marginal zone, which will form the stratum pyramidale (SP). The SP neurons form the CA layers with an inside-out pattern, in which the later generated neurons are aligned more superficially than the earlier generated neurons. In the adult hippocampus the outer marginal zone becomes the stratum lacunosum-moleculare (SLM) and the subplate becomes the stratum oriens (SO) (Figure 4.2). Unlike the CA layers, the DG develops in an outside-in manner over a protracted period into the adulthood (Forster *et al.*, 2006). In the DG the first generated neurons reside outside the dentate cortical plate, i.e., in the molecular layer and in the hilus, and guide commissural and entorhinal afferents, which are the two major afferent pathways, terminating in characteristic non-overlapping layers (Super *et al.*, 1994, Super *et al.*, 1998b). It has been shown that when entorhinal and commissural afferents enter the hippocampus they specifically invade different target layers, indicating the role of lamina specific cues in the hippocampus (Super *et al.*, 1994, Super *et al.*, 1998a, Super *et al.*, 1998b). The entorhinal afferents innervate the SLM of CA subfields and the outer molecular layer (OML) of the DG, the commissural/associational fibers innervate the SO and the stratum radiatum (SR) of CA subfields and

the inner molecular layer (IML) of the DG (Burwell *et al.*, 1995, Steward *et al.*, 1976, Swanson *et al.*, 1977).

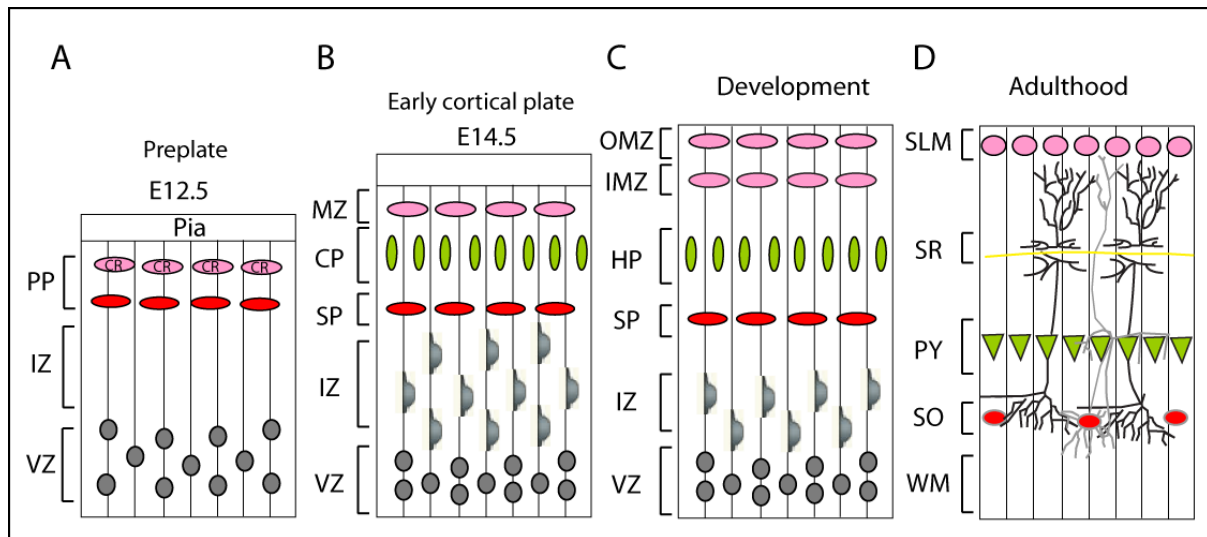


Figure 4.2 Laminated structure of the hippocampus (Super *et al.*, 1998b). The scheme shows the laminar organization of developing hippocampus. (A, B) Hippocampal development starts with the formation of preplate (PP) followed by appearance of a cell dense cortical plate (CP) by cell migrating from ventricular zone (VZ) which then splits the PP into subplate (SP) and marginal zone (MZ). (C) The MZ is divided into two segregated sublayers: the inner marginal zone (IMZ) and the outer marginal zone (OMZ). Developing hippocampal cortical plate (HP) remains a cell dense layer (PY). (D) The OMZ becomes stratum locunosum moleculare (SLM), the IMZ becomes the stratum radiatum (SR), and the subplate becomes the stratum oriens (SO). CP, Cortical plate; HP, Hippocampal cortical plate; IMZ, Inner marginal zone; IZ, Intermediate zone; MZ, Marginal zone, OMZ, Outer marginal zone; PP, Preplate; PY, pyramidal layer; SLM, Stratum locunosum moleculare; SO, Stratum oriens; SP; Stratum pyramidale; SR, Stratum radiatum; VZ, Ventricular zone; WM, White matter.

4.1.3 Development of the cerebellum

The cerebellum is the third well-defined laminated structure in the brain, composed of the molecular layer (ML), the Purkinje cell layer (PCL), the granule cell layer (GCL) and the white matter (including the cerebellar nuclei). Despite its structural simplicity, the development of the cerebellum is relatively complex. During embryonic development the cerebellum arises from an anlage on the floor of the fourth ventricle starting from E11 (Chizhikov *et al.*, 2003). As the development proceeds, two germinal zones; namely the rhombic lip and the VZ, gives rise to several classes of neurons. Rhombic lip, a structure found at the interface between the roof-plate of the fourth ventricle and

4 Introduction

the dorsal neuroepithelium, gives rise to granule cell precursors, which form the external granule layer (EGL). Other neuronal precursors are born near the VZ and migrate along radial fibers till the EGL, where a multilayered plate is formed. Purkinje cells, which are also born in the VZ and migrate outwardly along radial fibers, develop in the ML mostly in the first postnatal week. At this time, the granule cells migrate inwardly across the ML and the PCL to form the internal granule layer (IGL) (Figure 4.3).

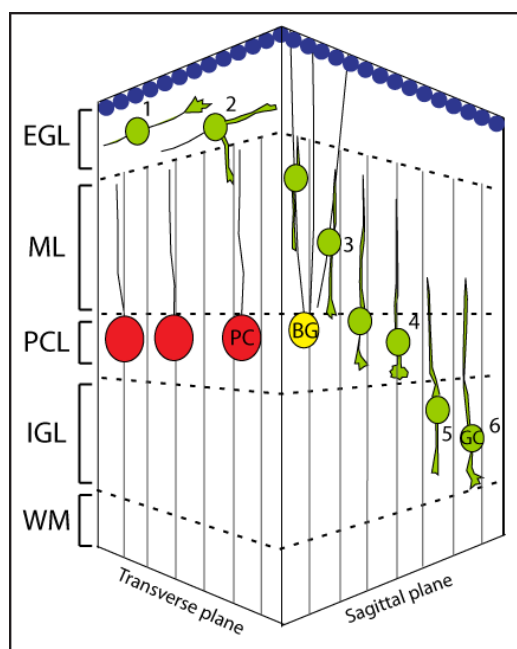


Figure 4.3 **Three-dimensional representation of cerebellar development** (Adapted from (Yacubova *et al.*, 2003). 1: Granule cells progenitors proliferate in the external granular layer (EGL); 2: then they differentiate and migrate tangentially in the middle of the EGL and develop vertical process near the EGL–ML (molecular layer) border; 3: followed by Bergmann glia-associated radial migration in the ML; 4: stationary state in the Purkinje cell layer (PCL); 5: and glia-independent radial migration in the inner granular layer (IGL); 6: completion of migration in the middle or the bottom of the IGL. The extensive postnatal proliferation of the EGL and subsequent migration of differentiating granule neuronal cells results in massive growth of the cerebellum. Foliation of the cerebellum is closely associated with both granule cell proliferation and ingrowth of cerebellar afferents, which also occurs during postnatal development. BG, Bergman glia; EGL, External granular layer; IGL, Inner granular layer; ML, Molecular layer; PC, Purkinje cell; PCL, Purkinje cell layer; WM, White matter.

4.2 Neuronal migration and layering in the cerebral cortex during embryonic development and adulthood

The assembly of the cerebral cortex and all layered structures during embryonic development is achieved by sequential migration of cells from their place of birth to their final position. New born neurons first reach the dorsal forebrain and then migrate to their final positions using two different modes of migration: radial migration or tangential migration. Radial migration is primarily used by excitatory cortical neurons that travel from the cortical VZ to their final destinations in the cortical plate, whereas, the vast majority of inhibitory interneurons are born in the germinal layers of the ganglionic eminence and invade to the cortex by tangential migration, in which cells migrate orthogonal to the direction of radial migration (Marin *et al.*, 2003, Nadarajah, 2003).

Accumulating data suggest the model of radial migration as the predominant route, by more than 80 % of all cortical neurons moving radially to reach their final destinations in the cortex (Edmondson *et al.*, 1987, Noctor *et al.*, 2002, Rakic, 1972, Rakic, 1974). Two distinct modes of cell movement are responsible for radial migration: nuclear translocation and glial-guided locomotion (Ghashghaei *et al.*, 2007, Nadarajah *et al.*, 2001). During nuclear translocation cells first extend a long process to the pial surface from the VZ and then loosen the ventricular attachment, thereby the nucleus moves through this elongated process to its final location at a speed of 60 μm / hour. This allows a radial glia independent migration, which is common for early born cortical neurons. During glial-guided locomotion, in contrast, migrating cells extend a motile process which maintains a constant length. The cells move forward with a speed of 35 μm / hour with short bursts of movements (Nadarajah *et al.*, 2001, Noctor *et al.*, 2004) and the entire cell moves along the radial fiber (Tabata *et al.*, 2003). Thus locomotion is mainly adapted by neurons that are born after the preplate splits (Gupta *et al.*, 2002).

4 Introduction

Radial glial cells provide the scaffold for specific migration in the brain. They arise throughout the neural tube during early development of the VZ and each radial glia cell has its cell body located in the VZ. Radial glial fibers reach the pial surface, where they display branches that are anchored to the basal membrane, and provide not only a physical scaffold for migrating neurons, but also remain as dynamic components of the developing cortex (Gadisseux *et al.*, 1989, Noctor *et al.*, 2001, Schmechel *et al.*, 1979).

Although radial migration is the primary mechanism by which neuronal precursors migrate to their destination, a subpopulation of cortical neurons migrates to their destinations by tangential migration (Austin *et al.*, 1990, O'Rourke *et al.*, 1995). These are mainly inhibitory GABAergic interneurons of the neocortex, olfactory bulb and hippocampus, which are derived from lateral and medial ganglionic eminences of the ventral telencephalon (Anderson *et al.*, 2001). Interneurons migrating towards the cortex follow a controlled route influenced by several factors such as motogenic factors and chemorepulsive or chemoattractive cues produced by the preoptic area and the cortex or the substratum (Marin *et al.*, 2003). Even though interneurons and projection neurons originate from different proliferative areas, the ones that are born at the same time share the same destination cortical layer (Kriegstein *et al.*, 2004).

4.2.1 Role of Reelin in cortical neuronal migration

Radial and tangential neuronal migration of projection and inhibitory cortical neurons during corticogenesis is a systematic process regulated by various factors across the cortex. It is not only accomplished by cell autonomous behavior; but also by cell-cell interactions and spatial and temporal factors. So far various genes have been identified that are important for neuronal migration (Bielas *et al.*, 2004). Some of these genes affect neuronal motility in a cell autonomous way, such as *filamin* (Sheen *et al.*, 2002), whereas others affect neuronal positioning in a non cell-autonomous way, such as Reelin (D'Arcangelo *et al.*, 1995), the molecule in focus of this thesis.

Reelin is an extracellular glycoprotein that is secreted from specific populations of neurons in the developing and mature brain (D'Arcangelo *et al.*, 1995, Alcantara *et al.*, 1998, Ogawa *et al.*, 1995). The three main structures where Reelin plays important roles during lamination are cerebral cortex, hippocampus and cerebellum. Immunohistochemical studies show the first detectable signal of Reelin at E9.5; later at E12.5 and E14.5 its expression becomes more prominent. The highest level of Reelin production during embryonic development is found in CR cells located in the MZ in the forebrain near the pial surface of the developing neocortex, and by the granular cells in the cerebellum (Rice *et al.*, 1998, Frotscher, 1998). Moreover, Reelin is also expressed in other laminated cortical structures, such as the olfactory bulb and at early stages of development in the tectum and in the spinal cord.

In the neocortex, Reelin is essential to accomplish the six-layered structure where the new born neurons bypass the older ones. In the embryonic and early post-natal hippocampus, Reelin is expressed by Cajal-Retzius cells in the fascia dentate, OML of the DG and in the SLM of the hippocampus proper (D'Arcangelo *et al.*, 1995, Alcantara *et al.*, 1998). Reelin plays an important role in the development of hippocampal connections (Borrell *et al.*, 1999, Del Rio *et al.*, 1997). Reelin is also believed to be required for the proper formation of the radial glial scaffold which is necessary for the proper outside-in migration of granular cells in DG, as well as for the inside-out migration of pyramidal cells in the stratum pyramidale. Presence of Reelin is also essential during development of the cerebellum. During embryonic development Reelin is expressed in the EGL, whereas postnatally from IGL of cerebellum (Miyata *et al.*, 1996, Schiffmann *et al.*, 1997).

Several hypotheses have been postulated to explain the function of Reelin. Some theories suggest Reelin as a chemo-attractant molecule for migrating neurons to bypass the predecessors, while others suggest Reelin as a repellent molecule for subplate neurons (Schiffmann *et al.*, 1997), thereby facilitating the invasion of the cortical plate or as an inhibitory molecule that is important for the detachment of cells from radial glial scaffold. When migrating neurons encounter Reelin their

4 Introduction

adhesion properties change and this results in the arrest of migration, which then serves as a detachment signal (Hack *et al.*, 2002). The detached neurons from radial glia translocate then to the pial surface (reviewed in (Marin *et al.*, 2003, Nadarajah *et al.*, 2001, Kriegstein *et al.*, 2004, Noctor *et al.*, 2004, Tabata *et al.*, 2003). The most commonly accepted theory suggests that Reelin is a stop signal (reviewed in (Lambert de Rouvroit *et al.*, 1998, Curran *et al.*, 1998). Nevertheless, so far none of these theories have been fully confirmed.

A study has shown that if Reelin is ectopically expressed in the precursor cells of the cortical VZ that normally do not express Reelin, in the background mice lacking Reelin most of the defects associated with Reelin loss can be rescued (Magdaleno *et al.*, 2002). This is in contradiction to the most proposed model where Reelin signaling affects mainly the neurons that are close to the MZ. Furthermore, when CR cells are missing the correct inside-out lamination is not impaired (Yoshida *et al.*, 2006) indicating other possible sources of Reelin can be sufficient for normal cortical development. Still it is important to emphasize that radial glial cells span the cerebral cortex, contacting the MZ as well as the ventral zone, and therefore able to mediate Reelin signaling throughout the cerebral cortex. Based on the association between radial glial cells and migrating neurons, a most recent study proposed the following model “Detach and Stop” for the function of Reelin (Cooper, 2008). Early-born neurons migrate a short distance till they encounter Reelin producing CR cells in the MZ and stop. These cells are arrested earlier than the later born neurons and due to increasing thickness of the cortical plate the late born neurons migrate longer distances to pass the elder ones and to reach MZ where they will stop (Frotscher, 1997) (Figure 4.4A).

The “Detach and Go” model has been proposed by other groups as an alternative to the ‘Detach and Stop’ model. The “Detach and Go” model is based on Reelin dependent but radial glial independent movement of early born neurons. These neurons first extend a leading edge to the MZ and upon their contact with Reelin they translocate themselves and settle on the corresponding layer in the subplate (Nadarajah *et al.*, 2001). The later born neurons migrate along radial glial scaffold and upon

passing the early born subplate neurons they detach from radial glial fibers (Frotscher, 1997). The ‘Detach and Go’ model explains the inverted layering phenotype of *reeler* mice as a result of prevention of final Reelin-dependent nuclear translocation to the top of the cortical plate (Figure 4.4B).

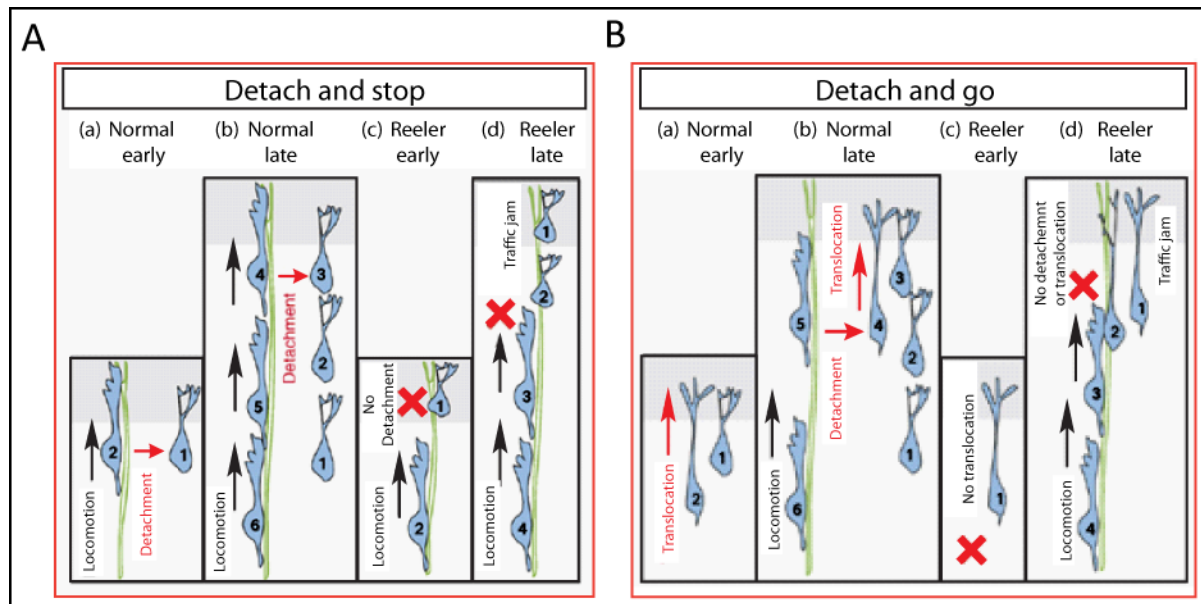


Figure 4.4 Migration models for Reelin mediated cortical layering (Frotscher, 1997). (A) “Detach and Stop” model for Reelin mediated cortical layering. (a) During early development neurons migrate along radial glia until they reach the Reelin secreting marginal zone (MZ) instructing them to detach, settle and differentiate. (b) Subsequent waves of neurons follow the same principle and rest above preexisting layers. (c) In the *reeler* mouse, neurons fail to detach from the radial glia scaffold and migrate into the MZ, hence (d) preventing later born neurons to pass preexisting layers, causing a “traffic jam”. (B) “Detach and Go” model for Reelin mediated cortical layering. (a) During early development neurons encounter Reelin in the MZ instructing them to initiate nuclear translocation just beneath the MZ. (b) Later born neurons migrate along radial glia until they reach the Reelin secreting MZ where they are instructed to detach and initiate nuclear translocation above preexisting neuronal layers. (c) In the *reeler* mouse, neurons fail to undergo nuclear translocation and (d) pile beneath the later born neurons which migrate along radial glia Reelin independently but fail to initiate the final Reelin dependent nuclear translocation past preexisting layers into the cortical plate, causing a “traffic jam”. (MZ in grey, neurons in blue are numbered in order of birth, radial glia in green, Reelin dependent events in red).

4.2.2 Other functions of Reelin

Reelin does not only play a key role in neuronal positioning during embryonic development, but also during adulthood (Hack *et al.*, 2002), especially during synaptic plasticity and in memory formation

by enhancing long-term potentiation (LTP) (Beffert *et al.*, 2005). Molecular studies suggesting the role of Reelin in synaptic complexity of hippocampal neurons revealed a cross-talk between Reelin signaling and NMDA receptors (Niu *et al.*, 2004) and also the role of Reelin in promoting dendritic spine development in hippocampal neurons during adulthood (Niu *et al.*, 2008). It has been also shown that Reelin signaling may act to fine tune Notch-1 activation in human neuronal progenitor cells (Keilani *et al.*, 2008). Another recent study shows the important role of Reelin in autism as reduced levels of Reelin was observed in the sera and in the brains of autistic patients (Kelemenova *et al.*, 2009). In addition to its signaling properties, Reelin can also act as a serine protease on adhesion molecules of the extracellular matrix, thus facilitating cellular migration (Quattrocchi *et al.*, 2002).

4.3 Defects in cortical layer formation of mice

Recent progress made in the study of cortical development identified various mechanisms have been identified that are important for the cortical layer formation. Attributed to the advances made in the development in mouse genetics, together with high genetic compatibility to human, the mouse has become the favored model system to study the basic of these molecular mechanisms. These animal models allow analysis of various malformations implicated in human brain development such as childhood epilepsy, schizophrenia, autism and attention deficit disorder (Francis *et al.*, 2006, Herz *et al.*, 2006). Thus, the studies will not only give insight into the molecular mechanisms of human psychiatric disorders but also will be essential to identify putative therapeutic targets for these neurological disorders. Among the several molecular mechanisms one of the most studied and characterized pathway is the Reelin pathway.

4.3.1 The *reeler* mice

In rodents the deficiency of Reelin gene causes the *reeler* phenotype. The “so called” *reeler* mouse was originally described over 60 years ago by Douglas Scott Falconer after its spontaneous appearance in a mouse stock at the Institute of Animals Genetics in Edinburgh in 1948 (Falconer, 1951). Following his observations Falconer concluded that *reeler* mice were ‘mentally deficient’. Consequently the *reeler* mouse was included in the Catalog of the Neurological Mutants of the Mouse, among the 90 by then to date known mutations affecting the nervous system (Sidman *et al.*, 1965). Since then it has been an excellent model to study behavior, as well as mechanisms and consequences of cell migration during nervous system development. With its long history of research it still serves as a powerful tool to study molecular mechanisms of brain morphogenesis.

The *Reeler* mouse is a mutant that displays behavioral abnormalities, such as ataxia, tremor, and reeling gaits (Falconer, 1951). The mutation does not affect the survival or vitality of neocortical cells (Rakic *et al.*, 1995) hence it provides a beneficial analysis model for classical histological studies of the central nervous system. These mice revealed architectonic abnormalities in several major layered cortical structures such as cerebrum, hippocampus and cerebellum (reviewed in (D’Arcangelo *et al.*, 1998, Lambert de Rouvroit *et al.*, 1998). Besides morphological anomalies, more subtle defects in cell clustering or laminar organization have been reported in several subcortical structures, including amygdala, olfactory tubercle, olfactory bulb, inferior olivary complex, dorsal cochlear nucleus, and facial nucleus (Caviness *et al.*, 1972, Goffinet, 1983, Goffinet, 1984, Martin, 1981, Wyss *et al.*, 1980). Moreover, other defects have been studied in other parts of the nervous system of the *reeler* mouse, such as thalamus, midbrain, retina, brainstem and spinal cord (Caviness, 1982, Goffinet, 1979, Hamburgh *et al.*, 1960, Hoffarth *et al.*, 1995, Ogawa *et al.*, 1995, Pinto-Lord *et al.*, 1982, Rice *et al.*, 2000, Yip *et al.*, 2000).

The role of Reelin in humans has also been a matter of interest in recent years. A mutation in the Reelin gene causes the Norman-Roberts type of lissencephaly in humans (Hong *et al.*, 2000) which

has a phenotype similar to the mouse model. Reelin deficiency has been observed also in human psychiatric disorders, such as autism, attention deficit hyperactivity disorder (ADHD), or in neurodevelopmental diseases, such as schizophrenia. Therefore, mice with similar Reelin deficiencies have been hypothesized as models for these neurological disorders (Costa *et al.*, 2002, Qiu *et al.*, 2006).

4.3.1.1 Alterations in the cerebral cortex of the *reeler* mice

During the brain development, via mechanisms described in section 4.2, the neuronal precursors migrate from their birthplace to their final destination where they form layers. In the *reeler* brain, the neuronal precursors are born normally and all major, morphologically distinguishable neural cell classes can be observed (Caviness *et al.*, 1973). The differentiation of neurons hardly affected and, with a few exceptions, the dendritic trees, the axons, and the connections with their targets are formed normally (Caviness, 1976, Simmons *et al.*, 1982, Steindler *et al.*, 1976, Terashima *et al.*, 1983) (Figure 4.5A). However, when the first cohort of cortical plate neurons migrate out of the VZ, they fail to invade the PP and to split it into MZ and subplate (Sheppard *et al.*, 1997). Failure of PP splitting results in the formation of a structure called the superplate (SPP). The superplate contains CR cells, superplate neurons and a few cortical plate neurons (Caviness, 1982, Derer, 1985). When compared to wild-type mice the MZ of the *reeler* mice is relatively cell-dense containing neuronal processes and some scattered cortical plate neurons (Figure 4.5B). The following cohort of neurons migrating out from VZ cannot penetrate their predecessors, which leads to accumulation of these neurons beneath the superplate. This causes an inversion of the cortical layers called “outside-in” layering, instead of the normal “inside-out” layering (Caviness, 1982) (Figure 4.5C; Figure 4.6A, B).

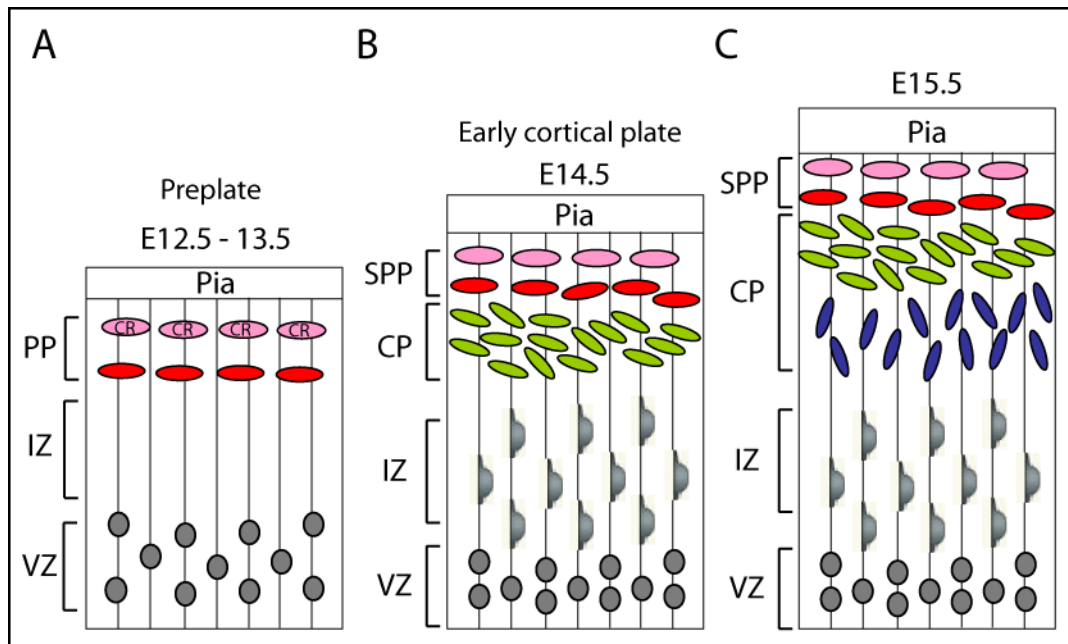


Figure 4.5 Schematic view of early cortical development in *reeler* mice (Adopted from (Tissir *et al.*, 2003). (A) At embryonic day (E) 12.5 pioneer neurons form the preplate with Cajal-Retzius cells (pink) and subplate neurons (red). At this stage, the *reeler* phenotype is not evident. (B) At E14.5 new cells that are migrating from the ventricular zone (green) towards the pia cannot split the preplate into two components and form superplate (SPP). (C) At E15.5, the second cohort of neurons (blue) settles in the deep tiers of the cortical plate, forming an outside-in pattern. CP, Cortical plate; IZ, Intermediate zone; SPP, Superplate; VZ, Ventricular zone.

This phenomenon has been studied in detail by autoradiography and it was shown that cortical patterning is missing in *reeler* mice. Cortical layers further characterized by layer specific markers showed the inverted layering of the *reeler* cortex. This has become possible due to recently gained insights into the temporal sequence of gene expression during corticogenesis. For example *Cux1* is specifically expressed in upper layers (layer II/III) in wild-type mice however, it is observed in the deep part of the *reeler* cortex (Ferrere *et al.*, 2006). *Tbr1* is expressed in layer V/VI of the normal cortex, however *Tbr1* expressing neurons are located in more superficial layers in the *reeler* cortex (Hevner *et al.*, 2001).

Moreover, the role of radial glial scaffold in the inverted cortical layering in *reeler* mice has been studied extensively using radial glia markers; such as glial fibrillary acidic protein (GFAP), astrocyte-

specific glutamate transporter (GLAST) and RC2 (Levitt *et al.*, 1980, Misson *et al.*, 1988, Shibata *et al.*, 1997). Several observations in the *reeler* mice suggested that the Reelin signaling directly affects radial glia morphology and that Reelin controls the neuronal migration by acting on the radial glial scaffold (Forster *et al.*, 2002, Frotscher *et al.*, 2003, Weiss *et al.*, 2003).

4.3.1.2 Alterations in the hippocampus of the *reeler* mice

In the hippocampus Reelin is expressed superficially to the migrating cells and as expectedly when Reelin is absent, in *reeler* mice, the neuronal organization of hippocampus is severely disrupted (reviewed in (Forster *et al.*, 2006). Granule cells are malpositioned and distributed across the entire DG (Stanfield *et al.*, 1979b) and pyramidal cells form a split layer in the hippocampus (reviewed in (Forster *et al.*, 2006) (Figure 4.6C, D). In *reeler* mutants the commissural fibers and the perforant pathway is also altered. The commissural fibers follow their misrouted target cells (Deller, 1998) and the perforant pathway fails to cross the hippocampal fissure to its target and instead takes an aberrant curving parallel to the fissure (Muraoka *et al.*, 2007) due to increased gliosis (Woodhams *et al.*, 1999, Woodhams *et al.*, 2000). The affected radial glial scaffold of the *reeler* hippocampus (Weiss *et al.*, 2003) suggests that Reelin is involved in the differentiation of radial glial cells, and thereby affects neuronal migration. In the adult *reeler* brain the dramatic decrease on the number of newly generated neurons in the DG suggests that the balance of neurogenesis and gliogenesis is regulated by Reelin (Zhao *et al.*, 2007).

4.3.1.3 Alterations in the cerebellum of the *reeler* mice

A major phenotype of the *reeler* mice is the uncoordinated walking behavior that is largely explained by cerebellar defects. In the *reeler* cerebellum the typical appearance of the folia is missing. The size of the granular layer is severely reduced and the arrangement of Purkinje cells is disrupted. Purkinje cells normally form a single-cell-layer around the granular layer, whereas in *reeler* mice only 5% of

the Purkinje cells are observed in Purkinje cell layer and the rest is ectopically localized throughout the cerebellum forming loose segregations (Hamburgh *et al.*, 1960, Mariani *et al.*, 1977) (Figure 4.6E, F). The ataxic walking behavior of the *reeler* mice has been mainly explained by defects in the cerebellum and in humans disruption of the Reelin gene leads to cerebellar hypoplasia which results in severe ataxia (Hong *et al.*, 2000).

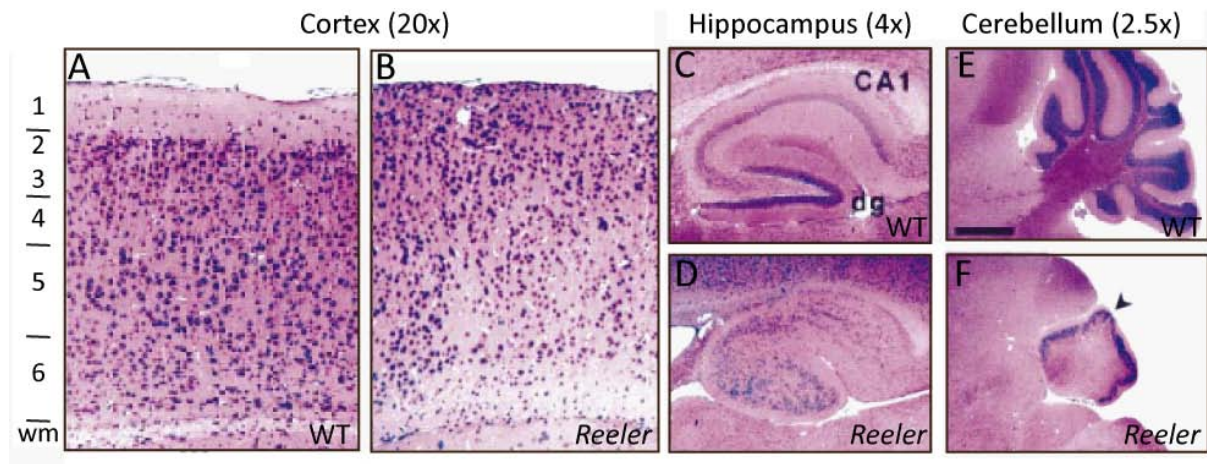


Figure 4.6 Histological analysis of WT and *Reeler* mice (adapted from (Trommsdorff *et al.*, 1999). Cortical layering and histoanatomy of the hippocampus and cerebellum from wild-type and *reeler* mice. Sagittal sections of wild-type (A) and *reeler* (B) brains of P13 mice were stained with hematoxylin/eosin (H&E). Normal cortical layers are indicated by numbers 1-6 next to (A). Histoanatomy of the hippocampus at 4x (C, D) and the cerebellum at 2.5x (E, F) magnification is visualized with H&E staining. The splitting of CA1 region is seen in the *reeler* mouse hippocampus (D). The small rim of dysplastic granule cells in the *reeler* mice is indicated with the arrow in (F). Scale bars = 1 mm (2.5x) (E), 625 μ m (4x), 125 μ m (20x). CA1, Hippocampal area; DG, Dentate gyrus; WT, Wild-type.

4.3.2 The *Yotari* and the *Scrambler* mice

Similar phenotypes that are indistinguishable to that of the *reeler* mice have been observed in two other mouse strains, namely *scrambler* and *yotari*, which were caused by mutations in the *disabled-1* (*Dab1*) gene. *Yotari* is an autosomal recessive mutant mouse which appeared during the generation of the receptor for inositol-1,4,5-triphosphate null mice (Howell *et al.*, 1997, Sheldon *et al.*, 1997). *Scrambler* is a spontaneous mutation that appeared in the inbred mouse strain DC/Le (dancer) in 1991 (Sweet *et al.*, 1996). These two mouse lines exhibited several *reeler*-like phenotypes such as

abnormality in the laminar organization of brain structures like the 'outside-in' layering in the cerebral cortex, disruption of the DG organization, lack of Purkinje cell plate and lack of the cerebellar foliation (Rice *et al.*, 1999). Despite these defects Reelin expression in *yotari* and *scrambler* mutants is not altered (Goldowitz *et al.*, 1997).

The indistinguishable phenotypes of *yotari* and *scrambler* suggests that Reelin and Dab1 are part of the same signaling pathway where Reelin is present in the extracellular space and Dab1 acts as an intracellular adaptor protein. Yet, the signaling depends on cell surface receptors that bind to the Reelin and transmit the incoming signals to Dab1.

4.3.3 The VLDLR and the ApoER2 knockout mice

Very low density lipoprotein receptor (VLDLR) and apolipoprotein E receptor 2 (ApoER2) are two lipoprotein (LDL) receptors that were identified as the cell surface receptors for Reelin. VLDLR binds to apolipoproteins in the blood circulation and VLDLR knockout mice (VLDLR^{-/-}) was generated in 1990s with the intention to analyze the profile of lipoproteins. However, besides being smaller and leaner than their littermates, the mice showed no changes in the lipoprotein profiles, and until specific brain regions were analyzed, no significant phenotype was observed. VLDLR^{-/-} mice showed only a modest phenotype in cortical lamination (Figure 4.7B,a, b) and a loosely packed neuronal layering in the hippocampus (Figure 4.7A,a, c); whereas, the cerebellum of VLDLR^{-/-} mice was smaller and less foliated than their littermates, with a less compact granule cell layer and large numbers of ectopic Purkinje cells (Figure 4.7A,b, d) (Trommsdorff *et al.*, 1999).

ApoER2 knockout (ApoER2^{-/-}) lines were generated by Trommsdorff *et al.* (1999) and revealed grossly normal phenotypes except for subtle defects in cortical structures. The cortical lamination was more strikingly altered in ApoER2^{-/-} mice when compared to VLDLR^{-/-} mice showing horizontally oriented but indistinguishable layers (Figure 4.7B,a, c). The DG of ApoER2^{-/-} mice

showed a less compact organization compared to control littermates, a clear split into two in pyramidal layers (Figure 4.7A,a, e) and a reduction in size of the cerebellum (Figure 4.7A,b, f) (Trommsdorff *et al.*, 1999).

Although the single knockout mouse strains of ApoER2 and VLDLR do not show ataxia, which is a strong characteristic of *reeler*, they show mild complementary phenotypes. Loss of ApoER2 or VLDLR alone causes subtle but distinguishable phenotypes, indicating that VLDLR is more important for the development of the cerebellum whereas ApoER2 for lamination of the cortex. Moreover, it has been shown recently that ApoER2 is indispensable for the correct migration of late-generated neurons, whereas the VLDLR mediated Reelin signal prevents neurons from entering the MZ (Hack *et al.*, 2007). These studies further suggest divergent roles for VLDLR and ApoER2, which explains why single knockout mice do not show strong *reeler*-like defects. Interestingly, simultaneously deletion of both receptors results in *reeler*-like phenotype, including inverted cortical layering, hypoplasia of the cerebellum, ataxia, gait and tremor (Trommsdorff *et al.*, 1999). Double knockout mice gave the first evidence that the two LDL receptors are linked to neuronal migration and that ApoER2 is critical for normal neuronal positioning in the neocortex (Figure 4.7B, a-d) and the hippocampus (Figure 4.7A,a, g), and together with the VLDLR for the development of the cerebellum (Figure 4.7 A,b, h) (Trommsdorff *et al.*, 1999).

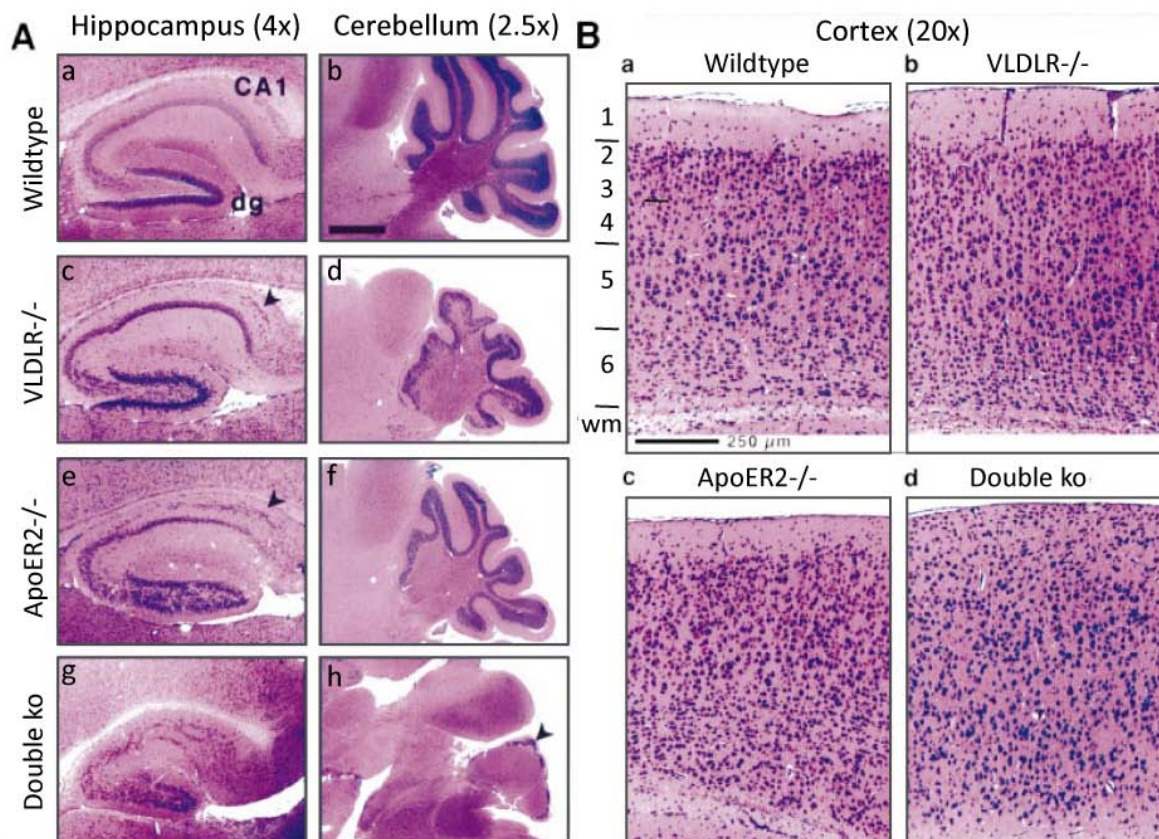


Figure 4.7 Anatomy of the hippocampus, the cerebellum and the cortex in wild-type, *VLDLR*^{-/-}, *ApoER2*^{-/-}, and *VLDLR*^{-/-}/*ApoER2*^{-/-} double knockout mice (Trommsdorff *et al.*, 1999). (A) Hematoxylin/eosin staining of sagittal sections of the hippocampus (a, c, e, and g), the cerebellum (b, d, f, and h), and (B) the cortex of P20 wild-type, *VLDLR*^{-/-}, *ApoER2*^{-/-}, and *VLDLR*^{-/-}/*ApoER2*^{-/-} mice. The arrow in (c) points to the split in the CA1 region, which is a characteristic feature of *reeler* mice. The arrow in (h) points to the small rim of dysplastic granule cells in the double knockout mice. Scale bars = 250 μ m.

Since the discovery of *reeler* and various mouse mutants showing similar phenotypes as the *reeler* mouse numerous reports dealing with these mice have been published. Histopathological studies greatly advanced the knowledge about brain development, neuronal migration and the molecular mechanisms underlying the defects appearing in *reeler* and *reeler* related mice mutants. The finding that all mice mutants for the components of Reelin signaling pathway share the same anatomical alterations during cortical lamination strongly suggests a linear signal transduction cascade for the formation of the cortical architecture.

4.4 Reelin pathway

Reelin pathway, which is partially or totally defected in *reeler*, *scrambler*, *yotari*, *VLDLR*^{-/-} and *ApoER2*^{-/-} mice, involves the extracellular matrix protein Reelin, two members of LDL receptor family, *ApoER2* and *VLDLR*, and the intracellular adaptor protein *Dab1* as the main mediators of an intricate signaling cascade involved in correct brain development (Howell *et al.*, 1997, D'Arcangelo *et al.*, 1999, Sheldon *et al.*, 1997, Trommsdorff *et al.*, 1999).

4.4.1 Reelin

The Reelin gene (*Reln*), responsible for the *reeler* phenotype, is mapped to chromosome 5 in mice or chromosome 7q22 in human, spread over a genomic region of 450 kb (Bar *et al.*, 1995, DeSilva *et al.*, 1997, Royaux *et al.*, 1997, Tissir *et al.*, 2003). Reelin is composed of 65 exons encoding for a large glycoprotein which has 3461 amino acids. The sequence starts with an N-terminal signal peptide that is followed by a region similar to F-spondin and a consensus cleavage site which leads to eight adjacent repeats of 350 to 390 amino acids. Each of these repeats is composed of two sub-domains, A and B, which are similar to each other, and each A – B subunit is separated by an epidermal growth factor (EGF) motif (D'Arcangelo *et al.*, 1995). The protein ends with an arginine rich C-terminal region which is required for secretion (Rice *et al.*, 2001).

Reelin has a predicted size of 385 kDa; however, on the SDS-gel it appears at 427 kDa which indicates that the protein is glycosylated (D'Arcangelo *et al.*, 1997). Moreover, Reelin is cleaved into smaller fragments putatively by a metalloproteinase, resulting in six different fragments of size between 100 to 320 kDa (Lambert de Rouvroit *et al.*, 1999). The cleavage was shown to occur between the repeats 2 - 3 and 6 – 7. The two major fragments are; a 180 kDa N-terminal fragment including a 120 kDa central fragment and a 100 kDa C-terminal fragment. Although the functions of most of the fragments are unknown, the fragmentation of Reelin has been proven to be required for

4 Introduction

in vivo mechanisms of Reelin (Jossin *et al.*, 2007). For example, in a slice culture assay the reintroduction of the central fragment, containing the repeats 3-6, has been shown to rescue the preplate splitting (Jossin *et al.*, 2004). The N terminus is responsible for the oligomerization of Reelin (Utsunomiya-Tate *et al.*, 2000) since monoclonal antibody CR-50, which recognizes this region, disrupts oligomerisation (D'Arcangelo *et al.*, 1997). The fragment, composed of repeats 5 and 6, has been identified as the receptor binding region (Yasui *et al.*, 2007) and the Carboxyl terminal part of Reelin is suggested to play a role in Reelin secretion as well as in Reelin signaling (D'Arcangelo *et al.*, 1997, Nakano *et al.*, 2007) (Figure 4.8).

Although the structure of Reelin is well studied, the precise mechanism of how the Reelin signaling events are actually linked to the *in vivo* behavior of individual neural cells during migration remains unknown. A coherent model of Reelin function is still missing.

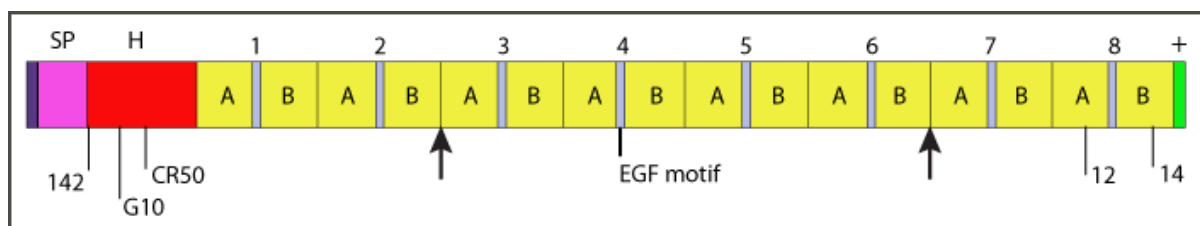


Figure 4.8 Scheme of the Reelin protein (Tissir *et al.*, 2003). The sequence begins with a signal peptide of 27 residues, followed by a region with similarity to F-spondin (segment 'SP', amino acids 28–190). A unique region (segment 'H') between amino acids 191 and 500 is followed by eight repeats of about 350 amino acids (repeat 1, residues 501–860; repeat 2, 861–1220; repeat 3, 1221–1596; repeat 4, 1597–1947; repeat 5, 1948–2314; repeat 6, 2315–2661; repeat 7, 2662–3051; repeat 8, 3052–3428). Each repeat contains an epidermal growth factor (EGF) motif in the center, flanked by two subrepeats, A and B, which show a weak similarity to each other. The protein terminates with a stretch of 33 amino acids that is rich in basic residues (3429–3461, +). The epitopes recognized by the antibodies 142, G10, CR50, 12 and 14 are indicated. The two arrows point to the estimated sites of processing *in vivo*.

4.4.2 The lipoprotein receptors: VLDLR and ApoER2

The two LDLRs, VLDLR and ApoER2, play important roles in extracellular protein endocytosis, cross-membrane signal transduction and in the modulation of synaptic function (reviewed in (Rogers *et al.*, 2008). Besides their role in hepatic cholesterol transport and metabolism, VLDLR and ApoER2 are

important for the transmission of extracellular signals across the membrane, which includes changes in the organization of cytoskeleton and therefore, regulation of neuronal migration in the embryonic and postnatal brain (Herz *et al.*, 2000, Trommsdorff *et al.*, 1998). In order to accomplish neuronal migration Reelin interacts with these two lipoprotein receptors, with a higher affinity to ApoER2 (D'Arcangelo *et al.*, 1999, Andersen *et al.*, 2003, Hack *et al.*, 2007). This affinity difference has been reasoned by the fact that ApoER2 is associated to lipid rafts determined by its extracellular domain, whereas VLDLR is strictly excluded from these microdomains (Cuitino *et al.*, 2005, Duit *et al.*, 2010). Reelin binds to the LDLRs via their extracellular domains, containing 7 or 8 cysteine-rich repeats of about 40 amino acids, in a calcium dependent manner and leads to the clustering of the receptors (Borrell *et al.*, 1999, Benhayon *et al.*, 2003, Hiesberger *et al.*, 1999, Strasser *et al.*, 2004). The extracellular domains of LDLRs are followed by two EGF repeats, a β -propeller segment with YWTD motif, and another EGF repeat, a paramembrane region of O-linked glycosylation, the transmembrane segment and a cytoplasmic region. The intracellular domains of these receptors are required for the recruitment of intracellular proteins to regulate cellular events such as kinase signaling, cytoskeletal re-organization and receptor endocytosis (Gotthardt *et al.*, 2000). The c-Jun N-terminal kinase (JNK) interacting protein (JIP1) has been identified as a linker between kinesin-1 and ApoER2 (Verhey *et al.*, 2001). JIP's can bind to the intracellular tails of ApoER2 and VLDLR and thereby further activate kinase pathways like map-kinase-kinase (MAPKK) and JNK, which assemble on JIP (Gotthardt *et al.*, 2000, Horiuchi *et al.*, 2007). Moreover, ApoER2 has been recently studied for its role in several neurological diseases including Alzheimer's disease most strongly with its role in amyloid deposits (reviewed in (Rogers *et al.*, 2008). The two lipoprotein receptors also contain NPxY (Asn-Pro-x-Tyr, x means any amino acid) sequence in their intracellular region (Schneider *et al.*, 2003) and plays a key role in clathrin-mediated endocytosis of these receptors. More importantly this is the docking site for the Dab1 protein (Howell *et al.*, 1999a).

4.4.3 Dab1 and signaling downstream of Dab1

Dab1 is an intracellular adapter protein, encoded by the *disabled-1* gene located on mouse chromosome 4 or human chromosome 1p32-p31 (Lambert de Rouvroit *et al.*, 1998). It is expressed in migrating neurons destined to the cortical plate, in pyramidal cells in the hippocampus and in the external germinal layer of the cerebellum, all of which are Reelin target cells (Howell *et al.*, 1997). The N-terminus of Dab1 contains a phosphotyrosine binding domain (PTB domain) which is a motif known as protein interaction/phosphotyrosine binding domain and mediates the association between Dab1 and ApoER2/VLDLR. The interaction between the PTB domain and the NpxY motif of receptors depends on phosphorylation of the NPxY motif (Margolis, 1996). However, this interaction is not dependent on tyrosine phosphorylation, instead, clustered LDL receptors, upon binding to Reelin, induces phosphorylation of Dab1 on specific tyrosine residues (Howell *et al.*, 1999a). Phosphorylated Dab1 interacts transiently with a variety of intracellular proteins that presumably carry out the molecular program necessary for the final stages of neuronal migration and the assembly of cellular layers (D'Arcangelo, 2005). At present it is not clearly known which pathways downstream of Dab1 are involved in the Reelin signaling. Various biochemical studies focus on proteins that are able to bind to Dab1 through its phosphorylation sites and several SH2 domain-containing proteins have been described. Among them Crk (CrkI and CrkII), Crk-like (CrkL) and Crk-binding protein, Dok1, have been identified in complexes bound to tyrosine-phosphorylated Dab1 through mass spectrometry (Chen *et al.*, 2004, Ballif *et al.*, 2004). Crk and Dock1 and others (as Nck) have been reported to be involved in the cytoskeletal network assembly by regulating cell migration downstream of integrins in mammals (Cheresh *et al.*, 1999, Petit *et al.*, 2000). Cells lacking focal adhesion kinase (FAK) or Src kinases, which are activated by integrin signaling or by their substrates paxillin or p130Cas, show reduced adhesion turnover rates and therefore, reduced migration. This is in accordance to the study of Webb *et al.*, (2004) implicating the importance of integrin induced tyrosine kinase activation for migrating cells. Nck and Crk proteins are adaptor proteins without any

catalytic activity and can induce tyrosine phosphorylation of Dab1 in a Src family kinase (SFK) dependent manner (Huang *et al.*, 2005).

Another SH2 domain containing and Dab1 interacting protein is the phosphatidylinositol 3-kinase (PI3K) regulatory subunit P85 α . Interaction of P85 α by Dab1 results in the activation of AKT/protein kinase B (PKB) and inhibition of the glycogen synthase kinase 3 beta (GSK3 β), which is a kinase for tau protein (Bock *et al.*, 2003b, Beffert *et al.*, 2002, Jossin *et al.*, 2007). Dab1 has also been shown to interact with proteins containing no SH2 domain, such as the non-catalytic region of the tyrosine kinase adapter protein β (Nck β) (Bock *et al.*, 2003a, Pramatarova *et al.*, 2003) and Lis1, in a Dab1 phosphorylation dependent manner (Assadi *et al.*, 2003). Lis1 and doublecortin (DCX) are two microtubule-stabilizing proteins (Sapir *et al.*, 1997, Horesh *et al.*, 1999) and are also causative gene products of human lissencephaly (Gleeson *et al.*, 1998), suggesting that microtubule regulation has crucial roles in cortical development.

4.4.3.1 Dab1 phosphorylation

In order to mediate downstream mechanisms of Dab1 signaling it is essential that Dab1 is phosphorylated. At the C-terminus of the PTB domain Dab1 contains five tyrosine residues, each of which has relative importance for the transmission of the Reelin signal (Morimura *et al.*, 2009). Among them Y198, Y220 and Y232 are the main Reelin dependent phosphorylation sites (Keshvara *et al.*, 2001, Pramatarova *et al.*, 2003) and their phosphorylation is carried out by non receptor kinases of the SFK through a feed-forward mechanism (Strasser *et al.*, 2004).

By various studies it has been shown that in response to Reelin Dab1 becomes polyubiquitinated and therefore, tyrosine phosphorylation targets Dab1 to degradation in proteosomes via the E3 ubiquitin ligase component Cullin 5 (Arnaud *et al.*, 2003, Feng *et al.*, 2007). In *reeler* mice Dab1 is not phosphorylated and therefore cannot be degraded by the proteosome. This leads to an accumulation of Dab1 protein in the cytosol (Rice *et al.*, 1998). As tyrosine phosphorylation of Dab1

4 Introduction

is required for its degradation, as well as signaling events to take place, phosphorylation event is a hallmark feature of Reelin signaling and it has been generally used as a marker to evaluate effects of other factors on Reelin signaling.

In order to study the role of tyrosine phosphorylation of Dab1 a 5F knock-in mice, by replacing the 5 potential phosphorylated tyrosine to phenylalanine (F), has been generated (Howell *et al.*, 2000). In this mutant Dab1 protein was not phosphorylated on tyrosine residues and was not upregulated to the extent observed in the *reeler* or the ApoER2/VLDLR receptor mutants. The 5F mutant shows similar phenotype to the *reeler* mice and therefore suggests that Dab1 tyrosine phosphorylation is required for Reelin signaling (Howell *et al.*, 2000). Another supportive study indicating the necessity of Dab1 phosphorylation was done by Herrick and Cooper (2002) where they partially rescued the phenotypes of Dab1^{-/-} mice by replacing the gene with a partial cDNA coding for the PTB domain and the region corresponding to the tyrosine residues of Dab1.

The search for the kinases responsible for Dab1 tyrosine phosphorylation focused on members of SFKs (Howell *et al.*, 2000); hence Dab1 was originally identified as a Src binding protein in a yeast two-hybrid screen (Howell *et al.*, 1997). The mechanism by which Reelin stimulates Dab1 phosphorylation is unclear. Src and Fyn were shown to catalyze Dab1 tyrosine phosphorylation and phosphorylation of Dab1 is required for full activity of Src/Fyn. One possible role of Reelin is to recruit Dab1 and SFKs to a common location on a Dab1 dependent way; on the other hand Dab1 phosphorylation by SFKs stimulates the SFKs, suggesting that phosphorylation of Dab1 and activation of Src/Fyn form a positive feedback loop downstream to Reelin (Ballif *et al.*, 2003, Bock *et al.*, 2003a). A possible explanation for the positive feedback loop is that when Reelin oligomers bind to LDL receptor clusters the receptors and this clustering induces the accumulation of Dab1 and activation of the Src/Fyn. Another study supporting the amplification of Reelin signaling upon receptor aggregation has been done by Yasui *et al* (2007) and showed that in order to induce

maximum Dab1 tyrosine phosphorylation not only two Reelin repeats but the full length Reelin was required.

Yet, possibly due to functional redundancy neither *Fyn*^{-/-}, *Src*^{-/-} nor *Fyn*^{-/-}/*Src*^{+/-} show a *reeler*-like phenotype (Arnaud *et al.*, 2003). However, treatment of brain slices with PP2a, a specific inhibitor for SFK, induces the characteristic *reeler* like phenotype (Jossin *et al.*, 2007), as well as double *Src*/*Fyn* knockouts show some of the defects associated with Reelin loss (Kuo *et al.*, 2005).

In accordance to many studies it has been accepted that tyrosine phosphorylation of Dab1 is central to Reelin signaling, yet neither VLDLR nor ApoER2 contain a kinase domain in their cytoplasmic tails, it has been postulated that Reelin binds to other cell surface receptors to form a macromolecular complex required for SFK recruitment/activation and Dab1 phosphorylation. The present thesis elucidates the role of ephrinB ligands as an essential co-receptor for Reelin signaling during the development of laminated structures in the brain.

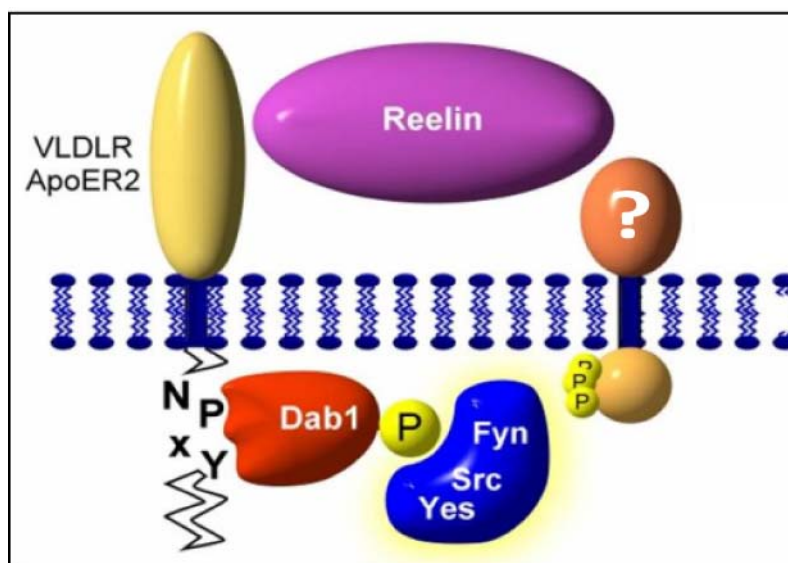


Figure 4.9 Hypothetical pathway of the Reelin-signaling (Adapted from Alexander Weiss, 2004). Reelin binds to the receptors VLDLR and ApoER2 on the cell surface and to a co-receptor that recruits and activates SFKs. mDab1 is then recruited to the cell-surface and binds to the cytoplasmic NPXY-motif of VLDLR and ApoER2 and is phosphorylated by SFKs. Signaling is initiated by recruitment of adaptor proteins which bind to phosphorylated Dab1.

4.5 Eph receptors and their ephrin ligands

Eph receptor tyrosine kinases (Ephs) and their membrane-bound ligands, the ephrins, have captured the interest of developmental biologists with their various functions during embryogenesis and adulthood. They mediate cell-cell instructive cues in a variety of developmental programs including the guidance of migrating cells and axonal processes, segmentation, neural crest cell migration, synaptic plasticity, angiogenesis, as well as serving other distinct functions in tissue morphogenesis (reviewed in (Palmer *et al.*, 2003).

The first Eph receptor was discovered in a screen for novel tyrosine kinases involved in cancer cells and its cDNA was cloned from the erythropoietin-producing hepatocellular carcinoma cell line (Eph) (Hirai *et al.*, 1987). Subsequently, other Eph receptor family members were discovered and today Eph receptors form the largest known subfamily of receptor tyrosine kinases (RTKs) (Orioli *et al.*, 1997). In vertebrates 14 members of Eph receptors exist and in invertebrates (*Drosophila melanogaster* and in the nematode *C. elegans*) one Eph receptor has been reported (reviewed in (Wilkinson, 2001). Based on sequence similarities and ligand binding characteristics mammalian Eph receptors can be divided into two subgroups, A and B. A subclass is comprised of nine receptors (EphA1-A8 and EphA10) and B subclass contains five receptors (EphB1-B4 and EphB6). Their overall structure is similar but their binding affinity to ephrin ligands differs. EphA receptors bind promiscuously to the A-type ephrins, whereas EphB receptors bind to the B-type ephrins. Binding across subclasses does not occur with the exception of EphA4 receptor that has also been found to bind ephrinB2 (Flanagan *et al.*, 1998) and ephrinB3 (Gale *et al.*, 1996). Additionally, a recent study showed that EphB2 receptors interact with ephrinA5 (Himanen *et al.*, 2004).

The first ligands for Eph receptors were identified some years later by different research groups (Bartley *et al.*, 1994, Cheng *et al.*, 1994). In 1997 an international nomenclature committee coined the family of receptors 'Eph' and the ligands 'ephrin' (Eph-receptor-interacting proteins) (Eph

Nomenclature Committee, 1997). Ephrin ligands have 9 members in vertebrates, in invertebrates the nematode *C. elegans* has four ephrin genes and *Drosophila melanogaster* has one gene encoding for ephrin (reviewed in (Wilkinson, 2001). The mammalian ephrin ligands are also subdivided into two classes, A and B, depending on their membrane attachment mode. A-sub class of ephrins (ephrinA1-A5) are anchored to the membrane via glycosylphosphatidylinositol (GPI)-anchor, whereas the B-sub class of ephrins (ephrinB1-B3) have a single pass transmembrane domain and a short cytoplasmic tail.

4.5.1 Structure of Eph receptors and ephrins

4.5.1.1 Eph structure

All Eph receptors conform to the structure of RTKs. They have an extracellular N-terminal glycosylated ligand binding domain, a single membrane-spanning domain, and a cytoplasmic region with a tyrosine kinase domain. The extracellular region harbors the N-terminal ligand binding domain, a cysteine-rich region containing an EGF like motif which is thought to function in receptor-receptor oligomerization, and two fibronectin type III repeats (reviewed in (Kullander *et al.*, 2002). The intracellular part of Eph receptors contains four functional units: the juxtamembrane domain that contains two conserved tyrosine residues, a classical protein kinase domain, a sterile α -motif (SAM), and a postsynaptic PDZ-domain binding motif (PSD-95 post-synaptic density protein, Discs large, Zona occludens tight junction protein).

The juxtamembrane domain is involved in signal activation by mediating the kinase activity via autophosphorylation of two tyrosine residues. In the unphosphorylated state the conformation of the juxtamembrane domain represses the activation of the kinase domain through an intracellular mechanism involving the N-terminal KD lobe. In the active state, upon phosphorylation of tyrosine residues, the kinase domain is relieved from the juxtamembrane region and can get its active

conformation (Wybenga-Groot *et al.*, 2001). The solved structure of SAM domain indicates that it could participate in protein-protein interactions forming dimers and oligomers. Another protein-protein interaction motif is PDZ motif which mediates interactions with PDZ-domain containing proteins in a sequence-specific fashion.

4.5.1.2 Ephrin structure

Ephrin ectodomains commonly have a conserved ~20kDa N-terminal ephrin domain involved in Eph receptor interactions, followed by a ~40 amino acid unstructured spacer that links the domain to the membrane. The ephrin domain, an eight stranded β -barrel, with three α helices connecting the strands, and two conserved buried disulfide bonds stabilizing the structure, has a primary sequence that shares no similarity with any other known protein (Toth *et al.*, 2001). While all ephrins share this unique domain, ephrinA ligands are attached to the exoplasmic leaflet of the cell membrane by a GPI-anchor, and the ephrinB ligands have a short, single transmembrane domain, followed by a highly conserved cytoplasmic tail (Figure 4.10).

The cytoplasmic tails of ephrinB ligands contain 5 conserved tyrosine residues and a C-terminal PDZ-binding motif. Three of these tyrosines (residues 312, 317 and 332) have been identified as the major *in vivo* tyrosine phosphorylation sites (Kalo *et al.*, 2001), which become rapidly phosphorylated upon activation of ephrinB ligands. This phosphorylation is accomplished by clustered soluble ectodomain of Eph receptor stimulation (Palmer *et al.*, 2002) with the fibroblast growth factor (FGF), presumably by the co-expressed FGF receptor, and by stimulation of the endogenous PDGF (platelet derived growth factor) receptor (Bruckner *et al.*, 1997). This rapid phosphorylation is mediated by SFKs, which upon stimulation by EphB receptors, are activated and recruited to ephrinB-containing membrane clusters (Palmer *et al.*, 2002). The cytoplasmic tails of ephrinB ligands are also phosphorylated in one serine residue (Ser-9) which regulates the binding of PDZ-containing proteins and has been shown to be important for the ephrinB2-mediated regulation

of AMPA receptor trafficking at the synaptic membrane during synaptic plasticity (Essmann *et al.*, 2008).

As the known range of biological functions performed by this family of multitasking receptors and ligands continues to expand, focus is shifting to determining how these molecules transduce such important and diverse signals into the cells.

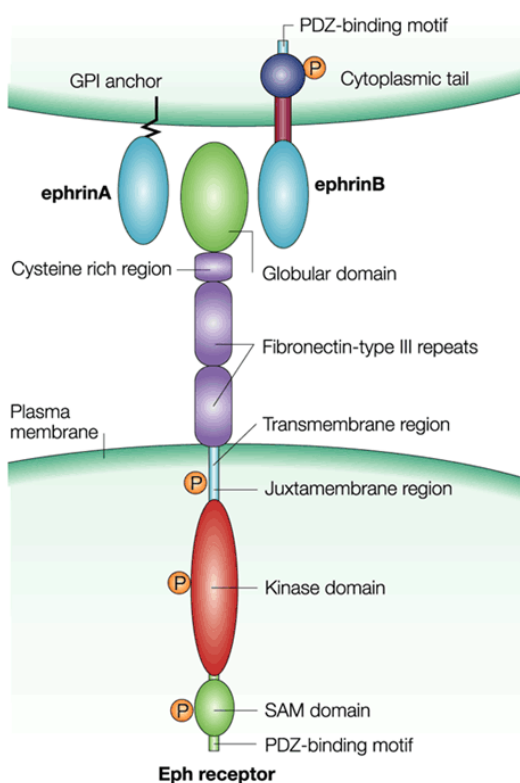


Figure 4.10 General features of Eph receptors and ephrins (Kullander *et al.*, 2002). The Eph receptor family of receptor tyrosine kinases (bottom) and the ephrin ligands (top) are membrane bound molecules interacting upon cell-to-cell contact. Eph and ephrins are classified into two groups, A and B, depending on sequence similarities and binding affinities. EphrinA ligands are membrane anchored by GPI and engage with EphA receptors, ephrinB ligands possess a short cytoplasmic domain and bind to EphB receptors. Ligand-receptor interactions (green), which take place at the extracellular receptor/ligand binding domain, have been mapped in detail and uncovered dimeric and oligomeric Eph-ephrin complexes (not shown). GPI, Glycosylphosphatidylinositol; SAM, Sterile α -motif.

4.5.2 Bidirectional signaling mechanisms between Eph receptors and ephrin ligands

Eph receptor family members, unlike most RTKs are not activated by soluble ligands. They autophosphorylate upon binding to their cognate ephrin ligands and subsequently activate signaling cascades. For functional signaling, multimerization of both receptors and ligands to distinct clusters at plasma membrane is required (Himanen *et al.*, 2001). These clusters allow initiation of so called

bi-directional signaling cascade where ephrin ligands induce signaling downstream of Eph receptors and also signal themselves into the cell that expresses them, acting as both 'receptor' and 'ligand' simultaneously, and named as 'forward' and 'reverse' signaling.

4.5.2.1 Mechanisms of Eph receptor "Forward" signaling

Eph receptors regulate crucial cellular events; therefore, their catalytic activity is tightly regulated. When Eph receptors are not activated they are either in monomeric or dimeric form on the cell surface. Upon binding of ephrin ligands Eph receptors are stabilized and initially form a high affinity heterodimer between their N domains. Binding sites between tetramers then favour formation of high order clusters (Himanen *et al.*, 2001), allowing trans-phosphorylation of tyrosine residues in the cytoplasmic domain via receptor kinase domain (Schlessinger, 2000) and removal of inhibitory interaction between the juxtamembrane region and the kinase domain. This conformational change in the kinase domain is achieved by steric and electrostatic forces pushing the phosphorylated juxtamembrane region away from the kinase domain. The new conformational state increases the affinity of Eph receptors to substrate binding (Kalo *et al.*, 1999). The phosphorylated kinase domain allows recruitment and phosphorylation of different phosphotyrosine-binding adaptor proteins, including kinase domains of neighbouring Eph receptor, to the membrane, and thereby initiate downstream signaling cascade.

The downstream adaptor molecules are capable of binding to the juxtamembrane domain of Eph receptors through their SRC-Homology-2 (SH2), SH3 and PDZ domains (reviewed in (Kullander *et al.*, 2002, Palmer *et al.*, 2003). There are some SH2-domain containing proteins downstream of Eph receptor, such as the SFKs Src and Fyn, Ras-GTPase activation protein (RasGAP), non-receptor tyrosine kinase Abl-related gene (Arg), Abelson (Abl), PI3K, and growth-factor receptor bound 2 (Grb2) (Zisch *et al.*, 1997). There are also several PDZ domain containing proteins that bind to PDZ domains of Eph receptors such as protein interacting with C kinase Pick1, Syntenin, a syndecan-

interacting protein, and two glutamate receptor interacting proteins; GRIP1 and GRIP2 (reviewed in (Kullander *et al.*, 2002). These proteins, which often do not possess intrinsic kinase activity, however, are able to bind to phosphorylated tyrosine motifs of the receptor via their SH2 domain, and are important for the formation of protein complexes to connect signaling molecules to upstream and downstream signaling events.

Eph receptor propagated signaling pathways generally tend to converge on cytoskeletal remodeling via Rho family GTPases, which include Rho, Rac and Cdc42 (Hall *et al.*, 2000). They can induce differential effects, such as activation of Rho as well as inhibition of Rac and Cdc42, shifting actin dynamics towards contraction and reduced extension (Shamah *et al.*, 2001). In another example, the Rac specific GTPase-activating protein (Rac-GAP) alpha2-chimaerin mediates EphA4 triggered growth cone collapse in response to ephrinB3 (Iwasato *et al.*, 2007, Wegmeyer *et al.*, 2007). Additionally Eph receptors also interact with non receptor tyrosine kinases Abl and Arg, which are known regulators of actin cytoskeleton (Yu *et al.*, 2001). Moreover, Eph receptors have also been shown to be involved in the regulation of integrin-mediated adhesion pathways (Zhou *et al.*, 1999). Forward signaling pathways have been studied intensively in several other cellular mechanisms, however, ephrin ligand reverse signaling mechanisms are largely unknown and are the focus of this thesis.

4.5.2.2 Mechanism of ephrin ligand “Reverse” signaling

Crystallographic studies indicate that upon binding to Eph receptors, the ephrin-ephrin heterodimers are disrupted and a circular tetrameric structure comprising of two receptors and two ligand molecules is formed (Himanen *et al.*, 2001). Oligomerization and clustering of Eph receptors and ephrins at the surface is essential for activation of membrane attached ephrin ligands and to enable their signaling function, named as “reverse signaling” (Kullander *et al.*, 2002). As both ephrinA and ephrinB ligands do not possess catalytic activity, help of cytoplasmic proteins is essential for signal transduction. So far two types of molecular partners; PDZ-domain containing proteins binding to

4 Introduction

carboxyl termini of ephrinB and SH2 domain containing proteins have been identified that are associated physically with cytoplasmic tails of ephrinB ligands. Yet, little is known about the signaling pathway that acts downstream of ephrin ligands.

Binding of EphB receptors to ephrinB ligands induces rapid phosphorylation of the cytoplasmic tyrosine residues of ephrinB ligands (Bruckner *et al.*, 1997). This phosphorylation is mediated by SFKs that are recruited to large ephrinB patches in the membrane and thereby become activated (Palmer *et al.*, 2002). The phosphorylation of ephrinB ligands on tyrosine residues creates docking sites for the SH2 and SH3-domain containing adaptor proteins such as growth-factor-receptor-bound protein4 (Grb4) (Cowan *et al.*, 2001). Grb4 is a SH2-SH3 adaptor protein and via its SH3 domain interacts with other proteins involved in the reorganization of the actin cytoskeleton, leading to the disassembly of F-actin-containing stress fibers and increased FAK activation, thereby triggering further events regulating the cytoskeleton dynamics (Cowan *et al.*, 2001). However, short after the tyrosine phosphorylation, the PDZ-domain-containing protein, PTP-BL (protein tyrosine phosphatase-basophil-like) is recruited to phosphorylated ephrinB and dephosphorylates ephrinB and SFK (Palmer *et al.*, 2002), creating a switch from phosphotyrosine-dependent signaling to PDZ-dependent signaling. Subsequently, proteins containing PDZ domains -as the adaptor protein GRIP1- bind to the cytoplasmic tail of ephrinB ligands (Bruckner *et al.*, 1999). An example is PDZ-regulator of heterotrimeric G-protein signaling (PDZ-RGS3), which, following ephrinB activation, acts to neutralize CXCR4 attraction to Stromal derived factor 1 (SDF-1), and activates a signaling pathway that leads to decreased cell migration of cerebella granule cells, contributing to correct layering of these cells in the cerebellum (Lu *et al.*, 2001). Similarly, ephrinB ligands may perform other functions downstream of CXCR4 in other cell types, where expression of ephrinB ligands and CXCR4 expression overlap. Many other PDZ domain interacting proteins are associated to ephrinB ligands, including GRIP2, Pick1, mPAR-3 and synthenin. As PDZ-RGS3, mPAR-3 and synthenin are also important to control the cytoskeletal stress by ephrinB reverse signaling (Cowan *et al.*, 2002).

Not only ephrinBs but also ephrinA ligands transmit signals across the membrane. The GPI-linked ephrins (ephrinAs) also activate a Fyn member of the SFK, which mediates integrin mediated cell adhesion and morphology (reviewed in (Davy *et al.*, 2005). Although a signaling mechanism is still unclear, it has been shown that ephrinA ligands like ephrinB ligands are localized to lipid rafts, indicating ephrin ligands may activate a number of signaling pathways (Huai *et al.*, 2001).

Lipid rafts are liquid-ordered membrane microdomains that represent an assembly of glycosphingolipids and cholesterol. These specialized membrane microdomains have a role in a wide variety of processes, including signal transduction (Simons *et al.*, 2000). It has been hypothesized that lipid rafts can serve as sites of signal integration since many molecules known to be involved in intracellular signaling are enriched within them (Zajchowski *et al.*, 2002). Examples of these signaling molecules include GPI-anchored proteins (such as ephrinA), transmembrane proteins (such as ephrinB and ApoER2) and dually palmitoylated and myristoylated proteins (such as SFKs) (Duit *et al.*, 2010, Varma *et al.*, 1998). Therefore, rafts act as platforms for the signal transduction and lateral clustering can lead to fusion of dispersed rafts to larger patches, thereby forming higher order signaling units (Simons *et al.*, 2000).

Regulated signal transduction in these lipid rafts is an attractive strategy for achieving spatial and temporal specificity in Eph/ephrin signaling. As it is the case for many GPI-anchored proteins, ephrinA5 is highly enriched in lipid rafts and its downstream signaling has been found to be initiated from these local domains (Davy *et al.*, 1999, Gauthier *et al.*, 2003). It has been also reported that ephrinB1 association with lipid rafts is important in tailoring its signaling responses. The cytoplasmic tail of ephrinB1 is able to specifically recruit GRIP into lipid rafts when they are expressed together (Bruckner *et al.*, 1999). The regulation of tyrosine phosphorylation of ephrinB1 by SFKs was also taking place in lipid rafts (Palmer *et al.*, 2002). Signaling pathways downstream and upstream of Eph and Ephrin are summarized in Figure 4.11

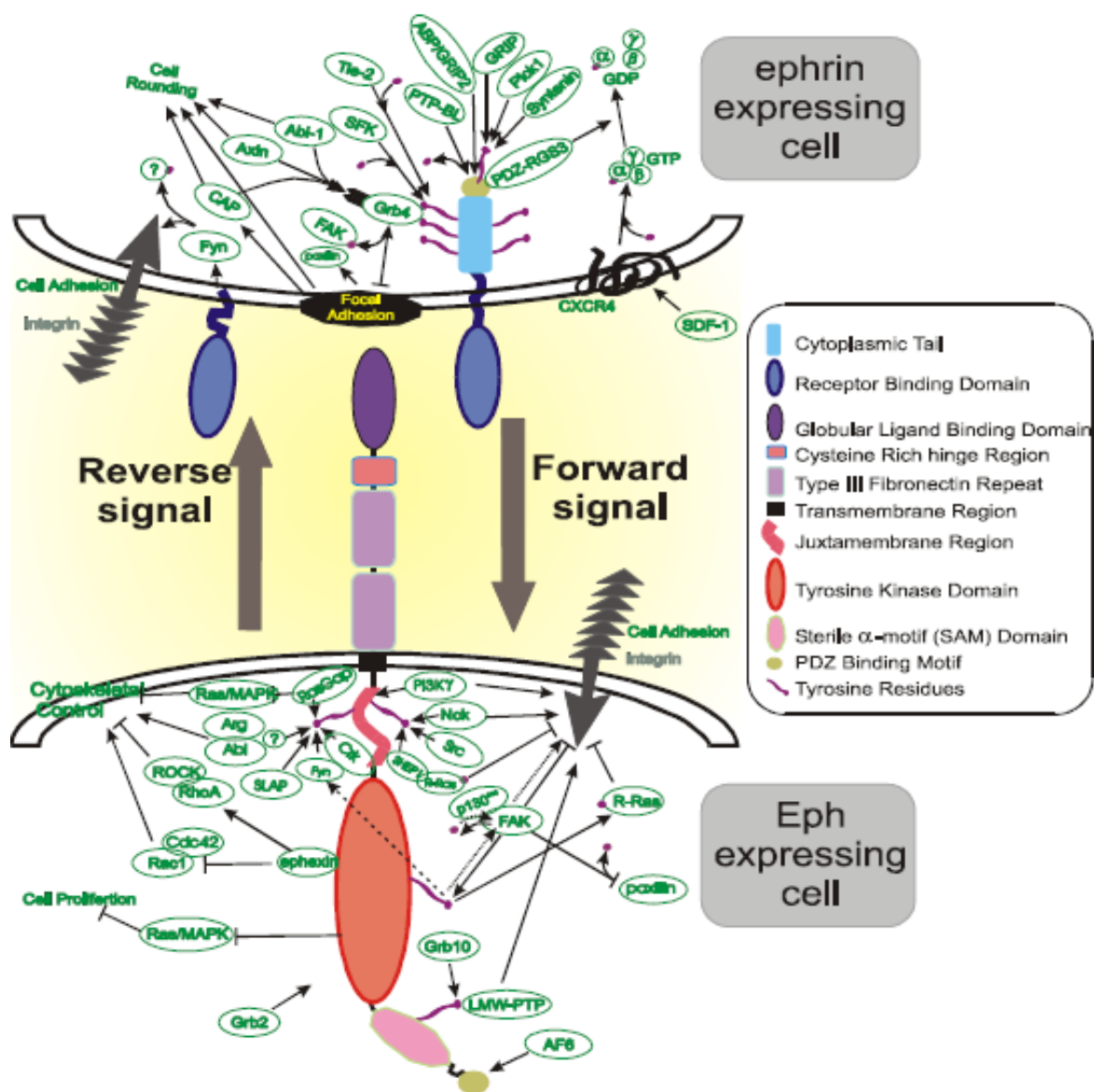


Figure 4.11 A schematic representation of Eph and ephrin cell signaling (Adapted from Vearing *et al.*, 2005). Structurally and functionally significant domains within Eph and ephrin proteins along with signaling molecules/cascades involved in Eph/ephrin activation. Arrows indicate positive response and flat end lines indicate negative response.

4.5.3 Roles of Eph and ephrins in nervous system development

The Eph receptor tyrosine kinases and their ligands, ephrins, are well known for mediating cell migration, and various studies using different mouse lines with different mutations in Eph and ephrin ligands revealed their role in axonal outgrowth and pathfinding, cell adhesion, topographic

mapping and axon fasciculation during development (Egea *et al.*, 2007, Pasquale, 2005). They mediate cell-contact-dependent signaling and are primarily involved in the generation and maintenance of patterns of cellular organization. At cellular level, downstream signaling mechanisms of Eph receptors and ephrins are required for correct migration of cells during embryogenesis or their processes, and to regulate cell adhesion by regulating the cytoskeleton. Depending on the cell type and the players of Eph/ephrins, along with several potential downstream partners, the control of cytoskeletal dynamics can be attractive, adhesive or repulsive.

4.5.3.1 Axon guidance

The Eph receptors and ephrin ligands were first studied for their role acting as cellular contact cues for axon guidance, via repulsive or attractive cues (reviewed in (Davy *et al.*, 2005). In this respect the first studied model for axon guidance is retinotectal topographic mapping, wherein Eph and ephrins work by forming complementary gradients in mutually exclusive way (Flanagan *et al.*, 1998). It has been shown that cells expressing Eph receptors avoid territories where ephrin is expressed thereby guiding the axons to appropriate targets (reviewed in (Palmer *et al.*, 2003).

Role of Eph/ephrins in thalamocortical projections has been the focus of several groups. Mammalian neocortex and limbic cortex is composed of well defined layers. The laminar organization of neocortex and the role of Reelin signaling has been explained in section 4.1.1. Eph / ephrins play an important role during the formation of the highly specific branching pattern of the neurons that are positioned at specific layers. Previous work by Bonhoeffer, Castellani and Bolz (1997) described a repulsive guidance signal of ephrin ligands during cortical layering by using membrane stripes of ephrinA5 transfected and control tissue in the Bonhoeffer assay (Bonhoeffer *et al.*, 1985). EphrinA5 has been shown as a branch promoting factor and also a repellent guidance cue of limbic thalamic fibers (Mann *et al.*, 2002). These *in vivo* and *in vitro* studies supported the dual biological activity pattern of Eph signaling, which suggest that repulsive effects of ephrins can become attractive.

4.5.3.2 Synaptic Plasticity

Eph and ephrins have important functions in spine morphology and synapse formation and thus control synaptic plasticity. Eph receptors and ephrinB ligands are expressed in distinct regions of mouse hippocampus and via regulating molecular pathways such as Rho GTPases they play important roles in spine formation. Regarding the role of forward signaling Henkemeyer *et al.*, (2003) showed that EphB1/B2/B3 receptor deficiency led to impaired spine formation. Among a number of studies investigating the role of ephrinB ligands, reverse signaling, in spine formation another recent study described the importance of ephrinB ligand reverse signaling for proper spine formation via Grb4 and GIT1 recruitment (Segura *et al.*, 2007). EphrinB2 ligands also have different roles during synaptic plasticity involving regulation of AMPA receptor trafficking and their surface distribution at synapses (Essmann *et al.*, 2008). EphrinB3 ligands have been also implicated in synaptic plasticity and remodeling in the hippocampus, where their interaction and activation by EphA4 causes activation of Ephexin and Cdk5 complex, resulting in dendritic spine retraction (Fu *et al.*, 2007, Grunwald *et al.*, 2004, Tremblay *et al.*, 2007).

4.5.3.3 Segmentation

EphB-ephrinB signaling is important for establishing hind- and forebrain segmentation during the development. Eph/ephrins mediate this cell sorting at the rhombomeres by providing positional information to the different cell populations (Kiecker *et al.*, 2005), and therefore, generating boundaries between cells that form different parts of the embryo. In vertebrate hindbrain there are seven rhombomeres (1-7) and these specify the identity and the origin of certain nerves, as well as different neural crest cells. The complementary and alternating expression of Eph/ephrins in rhombomeres results in a repulsive action of ephrins, where cells that express the ligand will sort away the receptor expressing cells, and vice versa (reviewed in (Palmer *et al.*, 2003). For example EphA4 receptors expressed in the odd-numbered rhombomeres 3 and 5 repulse and ephrinB2

expressed in cells in the even-numbered rhombomeres 2, 4, and 6. The sorting of rhombomeres is found to be directed by bi-directional signaling between Eph and ephrins. Similar ectopic-expression studies in zebra fish embryos showed requirement of the cytoplasmic domain of ephrin ligands to mediate cell sorting at boundaries (reviewed in (Palmer *et al.*, 2003).

4.5.3.4 Corticospinal tract formation

The corticospinal tract guidance mechanism is another example of signaling that is induced by Eph/ephrins. EphrinB3 is expressed in the midline of the spinal cord, whereas EphA4, a binding partner of ephrinB3, is expressed at the ventral gray matter in the growth cones of developing axons (Kullander *et al.*, 2001a, Kadison *et al.*, 2006). Upon binding of EphA4 to ephrinB3 the axon growth cone collapses due to activation of signaling pathways associated with cytoskeletal motility (Kullander *et al.*, 2001a). Therefore, ephrinB3 forms a barrier for neurons that express EphA4 and confine them to stay on the ipsilateral side of the spinal cord (Kullander *et al.*, 2001a, Yokoyama *et al.*, 2001)

In ephrinB3 and EphA4 knockout mice many anatomical defects have been described. These involve the aberrant re-crossing of corticospinal axons in the ventral midline of the spinal cord (Coonan *et al.*, 2001, Yokoyama *et al.*, 2001). This leads to an abnormal walking behavior in the ephrinB3 and EphA4 knockout mice in which instead of normal alterations between left and right legs a synchronous movement of hind limbs produces the hopping gait (Kullander *et al.*, 2001b, Kullander *et al.*, 2003).

EphrinB3 ligands, besides their role in corticospinal tract formation, have also been reported to be expressed in postnatal myelinating oligodendrocytes, and by using primary CNS neurons possess an inhibitory activity (Benson *et al.*, 2005). Another role of ephrinB ligands is related to their expression at the SVZ and in the rostral migratory stream. EphrinBs have been suggested to influence the

4 Introduction

neurogenesis by affecting proliferation and apoptosis. Eph/ephrin signaling disturbance leads to defects in the migration and proliferation in the SVZ (Chumley *et al.*, 2007, Conover *et al.*, 2000). Ricard *et al.*, (2006) have shown an increase in cell proliferation in the subventricular zone of ephrinB3 knockout mice.

5 Results

Despite the importance of the Reelin signaling pathway for proper nervous system development and that disruption of this pathway results in several neurological disorders such as epilepsy, schizophrenia and Alzheimer's disease (Herz *et al.*, 2006), molecular characterization of the activation of this pathway at the cellular membrane remains poorly understood. Since VLDLR and ApoER2 do not possess intrinsic kinase activity the existence of a co-receptor that locally activates Src kinases has been proposed for at least a decade but compelling evidence of its existence and the exact nature of this co-receptor are so far unknown. EphrinBs, transmembrane ligands for Eph receptors, have signaling capabilities that are required for axon guidance and sprouting angiogenesis (reviewed in (Davy *et al.*, 2005, Palmer *et al.*, 2003). Interestingly, we have shown that ephrinB ligands physically associate and regulate the activity of other transmembrane receptors both during synaptic plasticity (Essmann *et al.*, 2008) as well as developmental and tumor angiogenesis (Sawamiphak *et al.*, 2010). Since stimulation of cultured cortical neurons with soluble EphB receptors leads to the recruitment and activation of SFKs in ephrinB ligand-membrane patches (Palmer *et al.*, 2002) we investigated whether ephrinB ligands would be the missing co-receptors for Reelin signaling.

All members of the ephrinB gene family are abundantly expressed in the nervous system, including cells in the subventricular zone and ventricular zone during embryogenesis and show spatiotemporal changes in many regions. The expression profiles of ephrinB ligands and their role in development have been studied extensively by various groups (Palmer *et al.*, 2003). Mice lacking individual ephrinB ligands show several defects during development and plasticity of the nervous system (Conover *et al.*, 2000, Fu *et al.*, 2007, Grunwald *et al.*, 2004, Kadison *et al.*, 2006, Ricard *et al.*, 2006) but, they don't have ataxia which is a hallmark of *reeler* and mDab1-deficient *scrambler* mice.

Therefore, to explore whether ephrinB2 and ephrinB3 ligands share overlapping functions with Reelin signaling pathway, we generated compound mutant mice. This is a commonly used method to study the genetic interaction between two or more proteins. The mice were generated by crossing ephrinB2 (b2^{-/-}) or ephrinB3 knockout (b3^{-/-}) mice with heterozygous *reeler* (rl^{+/+}) mice. The progeny of this mating was interbred to generate wild-type (+/+), rl^{+/+}, b2^{-/-} or b3^{-/-}, and compound mutant mice (rl^{+/+}; b2^{-/-} or rl^{+/+}; b3^{-/-}) (Figure 7.2). With this strategy we intend to increase the penetration of ephrinB phenotypes upon reduction of Reelin protein. *Reeler* heterozygous mice do not have any *reeler*-like phenotypes and are therefore suitable for this analysis (Caviness *et al.*, 1972, Caviness *et al.*, 1978).

5.1 Genetic interaction between Reelin and ephrinB pathways

In the first part of the project we studied the interaction of ephrinB ligands with Reelin signaling pathway by investigating the cerebral cortex, the hippocampus, and the cerebellum of ephrinB knockout mice as well as compound mutant mice for major *reeler*-like phenotypes.

5.1.1 Compound mice show *reeler* like phenotypes in the cerebral cortex.

The most significant phenotype of the *reeler* cerebral cortex is the undistinguishable marginal zone (MZ) and the inversion of inside-out layering (reviewed in (Rice *et al.*, 2001). This is due to the failure of preplate splitting and formation of a structure called superplate. In the *reeler* mice the superplate contains Cajal-Retzius cells, scattered cortical plate neurons with neuronal processes and therefore, when compared to normal MZ, it is relatively cell-dense (Figure 5.1, Figure 4.4). The next cohort of neurons migrating out from ventricular zone cannot penetrate their predecessors, which leads to accumulation of these neurons beneath the superplate. This causes inversion of cortical layers to an “outside-in” layering, instead of the normal “inside-out” layering (Caviness, 1982) (Figure 4.4).

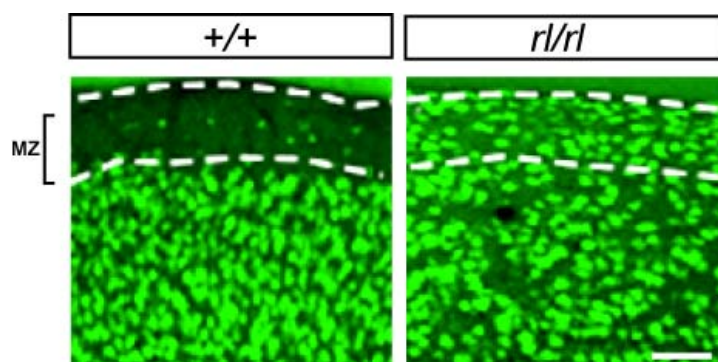


Figure 5.1 Cortical layering is altered in *reeler* mice. NeuN immunostaining of coronal brain sections through the neocortex of adult mice showed only few neurons in the Marginal zone (dashed line) of wild-type mice (+/+), whereas *reeler* (*rl/rl*) MZ was filled with cells and cortical layering was disturbed due to outside-in layering. Immunostaining signals were detected using Alexa-Fluor 488-conjugated secondary antibody. Scale bar = 100 μm . MZ, Marginal zone.

5.1.1.1 Cortical neurons invade the marginal zone in *rl/+*; *b3*^{-/-} compound mutant mice.

In order to visualize the neurons in the MZ of ephrinB2, ephrinB3 knockout mice (*b2*^{-/-} and *b3*^{-/-}) and ephrinB2 and ephrinB3 compound mutant mice (*rl/+*; *b2*^{-/-} and *rl/+*; *b3*^{-/-}) we first performed NeuN immunostaining on coronal brain sections from postnatal (P21) mice. NeuN (Neuronal Nuclei) reacts with most neuronal cell types throughout the nervous system. Developmentally, immunoreactivity is first observed shortly after neurons have become postmitotic, and the staining is primarily localized in the nucleus of the neurons with lighter staining in the cytoplasm. Thus, NeuN immunohistochemistry allowed us to study cell invasion into the MZ of the different mice (Figure 5.1, Figure 5.2). When compared to confocal images taken from +/+, *rl/+*, and single ephrinB knockouts both compound mice lines showed *reeler*-like cell invasion into the MZ (Figure 5.1, Figure 5.2A). Cell density in the MZ (dashed line) was assayed by counting cell number and averaging to 100 μm^2 area. Quantification of neurons in the MZ and subsequent statistical analysis revealed a significant increase in NeuN+ neurons in ephrinB3 compound mutant (*rl/+*; *b3*^{-/-}) mice from 11.73 ± 0.47 cells/100 μm^2 (wild-type control, +/+) to 17.49 ± 0.75 cells/100 μm^2 . A significant increase in cell density was also observed in ephrinB2 compound mice (*rl/+*; *b2*^{-/-}), from 12.08 ± 0.31 (wild-type control, +/+) to 16.51 ± 0.84 . Cell densities of *rl/+* (13.09 ± 1.00 , 13.62 ± 0.54), *b3*^{-/-} (11.65 ± 0.72) as

well as $b2^{-/-}$ (13.25 ± 0.43) MZ didn't show any significant difference with wild-type control mice (Figure 5.2B, C).

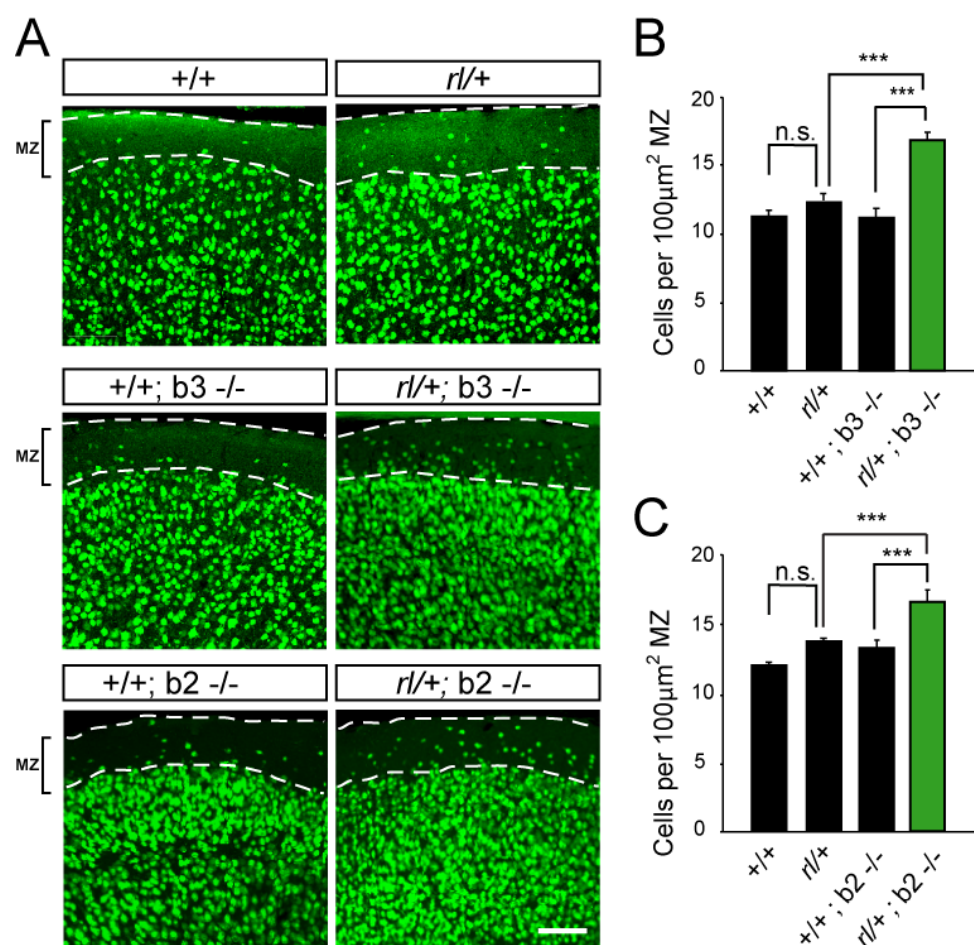


Figure 5.2 Cortical neurons of compound mutant mice invade into MZ. (A) Neuron distribution of marginal zone (MZ) (dashed line) of $+/+$, $rl/+$, $b3^{-/-}$, $b2^{-/-}$, $rl/+; b3^{-/-}$ and of $rl/+; b2^{-/-}$ were detected with NeuN immunostaining on coronal brain sections through the neocortex of adult (P21) mice. In the MZ of $+/+$, $rl/+$, $b3^{-/-}$ and $b2^{-/-}$ only few neurons were detected, whereas in the compound mutant mice ($rl/+; b3^{-/-}$ and $rl/+; b2^{-/-}$) neurons invaded into MZ. Immunostaining signals were detected using Alexa-Fluor 488-conjugated secondary antibody. Scale bar = 100 μm . (B, C) Stereological quantification of cell numbers in the MZ of $+/+$, $rl/+$, $b3^{-/-}$ and $rl/+; b3^{-/-}$ and of $+/+$, $rl/+$, $b2^{-/-}$ and $rl/+; b2^{-/-}$ are shown representatively. Quantification were performed from 4 different animal groups and pictured as number of cells in 100 μm^2 MZ (SEM, *** $P < 0.0001$; n.s., not significant). MZ, Marginal zone.

5.1.1.2 Cortical layering is altered in the $rl/+; b3^{-/-}$ compound mutant mice.

We next analyzed the cell layering in the ephrinB3 knockout and $rl/+; b3^{-/-}$ compound mutant mice.

First we performed 4',6-Diamidin-2-phenylindol (DAPI) staining on coronal cortical sections of $+/+$,

5 Results

rl/+, *b3-/-* and *rl/+*; *b3-/-* mice (Figure 5.3). DAPI is a fluorescent stain that binds strongly to DNA and allows detection of gross morphology. In *rl/+*; *b3-/-* compound mutant mice DAPI staining showed alterations in cell layering compared to *+/+*, *rl/+* and *b3-/-* mice.

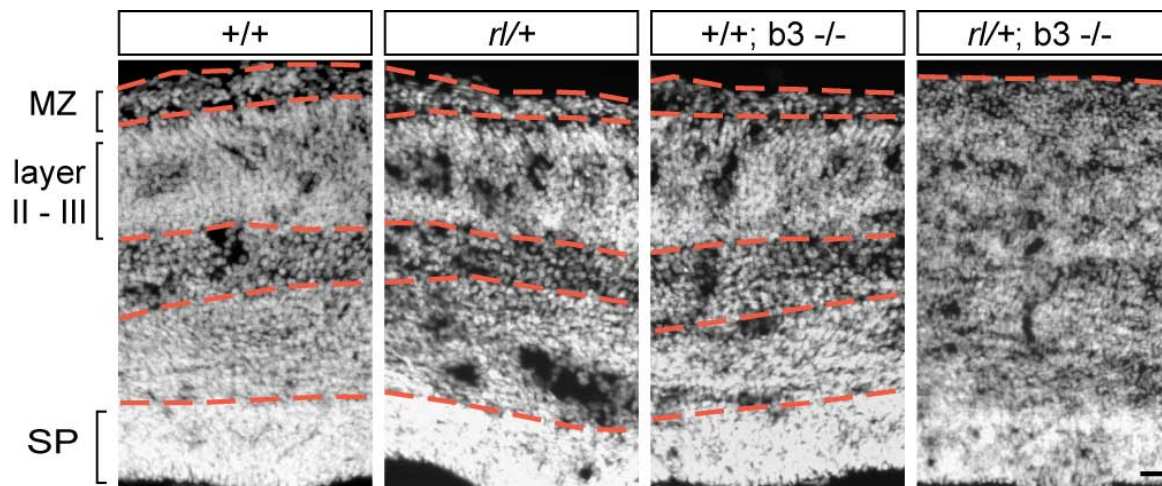


Figure 5.3 Cell layering in the *rl/+*; *b3-/-* compound mutant mice at E17.5 was altered. Coronal sections of embryonic mice (E17.5) were immunostained with DAPI to observe cellular layering in *+/+*, *rl/+*, *b3-/-* and *rl/+*; *b3-/-* mice. Cell free MZ and normal cortical layers are observed in *+/+*, *rl/+* and *b3-/-* mice, whereas in the cerebral cortex of *rl/+*; *b3-/-* compound mice cortical layers were no longer clearly separated and cellular invasion into the MZ is observed. Scale bar = 100 μ m. MZ, Marginal zone; SP, Subplate.

We then proceeded to characterize cortical layers by specific markers. Recent insight into the temporal sequence of gene expression of different transcription factors during corticogenesis has provided a wide range of markers to study cortical layering (reviewed in (Molyneaux *et al.*, 2007)). Some examples of layer specific genes are *Cux1*, *Cux2*, *Lhx2*, *SatB2* as markers for layer II/III to IV (Nieto *et al.*, 2004, Britanova *et al.*, 2008, Bulchand *et al.*, 2003, Nakagawa *et al.*, 1999, Zimmer *et al.*, 2004); *Brn1* and *Brn2* as markers for layer II-III and V (McEvelly *et al.*, 2002, Sugitani *et al.*, 2002); *Rorb* as a marker for layer IV (Schaeren-Wiemers *et al.*, 1997); *Foxp2* as a marker for layer VI (Ferland *et al.*, 2003); *c-Neu* (also known as ErbB2) as a marker for layer V neurons (Miller *et al.*, 2000). Some of these genes are expressed in individual cell types within a layer or across layers, such as *Tbr1*, which is expressed at high levels in neurons of layer V-VI and at low levels in layer II (Hevner *et al.*, 2001); *Scip*, which is expressed mainly in subcerebral neurons of layer V and at much lower

levels in neurons of layer II-III (Frantz *et al.*, 1994); and *er81* which is expressed in cortico-cortical and subcerebral projection neurons of layer V (Hevner *et al.*, 2003).

Analysis of early born cortical neurons

In order to study cortical layering in more detail we first investigated the organization of early born cortical neurons in the *rl/+; b3-/-* compound mutant mice using specific lower layer markers, such as *Tbr1* and *FoxP2*. *Tbr1* is a transcription factor of the T box family that is expressed soon after cortical progenitors begin to differentiate. It is highly expressed in early-born neurons of the preplate and layer V-VI (Bulfone *et al.*, 1995) and is a common genetic determinant for the differentiation of early-born glutamatergic neocortical neurons, as well as for functions of these neurons as regulators of cortical development (Hevner *et al.*, 2001). In *reeler* cortex the expression of *Tbr1*, due to outside-in layering, has been observed in more superficial layers (Hevner *et al.*, 2001) and in our immunohistochemistry studies, *Tbr1* revealed the strongest signal in deep cortical layers of *+/+*, *rl/+*, and *b3-/-* mice, whereas in *rl/+; b3-/-* compound mutant mice an invasion towards more superficial cortical layers was observed (dashed line) (Figure 5.4A). The quantification of the *Tbr1*⁺ cells in the upper cortical layers showed increased cell density in the *rl/+; b3-/-* compound mutant mice (6.38 ± 0.27), compared to wild-type control (2.42 ± 0.06). The cell density of *rl/+* (1.50 ± 0.03) and *b3-/-* (0.83 ± 0.04) mice showed no significant change compared to wild-type mice. (Figure 5.4B). Moreover, the analysis of the distribution of *Tbr1*⁺ neurons among cortical layers showed the alterations in the migration of early born neurons (Figure 5.4C).

Deeper layers can also be studied with *FoxP2*, expressed in the developing and adult mouse brain, including the striatum, thalamus, and cerebral cortex. *Foxp2* is another marker for layer VI (Ferland *et al.*, 2003) as its expression is restricted to dopamine and cyclic adenosine 3',5'-monophosphate-regulated phosphoprotein, 32 kDa (DARPP-32)⁺ neurons of layer VI (Hisaoaka *et al.*, 2009). The

5 Results

immunostaining of coronal cortical sections of $+/+$, $rl/+$ and $b3^{-/-}$ mice revealed a corresponding staining pattern at layer VI (dashed line) with virtually no $FoxP2^{+}$ neurons stained in the upper layers. However, in the $rl/+$; $b3^{-/-}$ -compound mutant mice $FoxP2^{+}$ neurons were observed in upper cortical layers (arrowheads) (Figure 5.4 C).

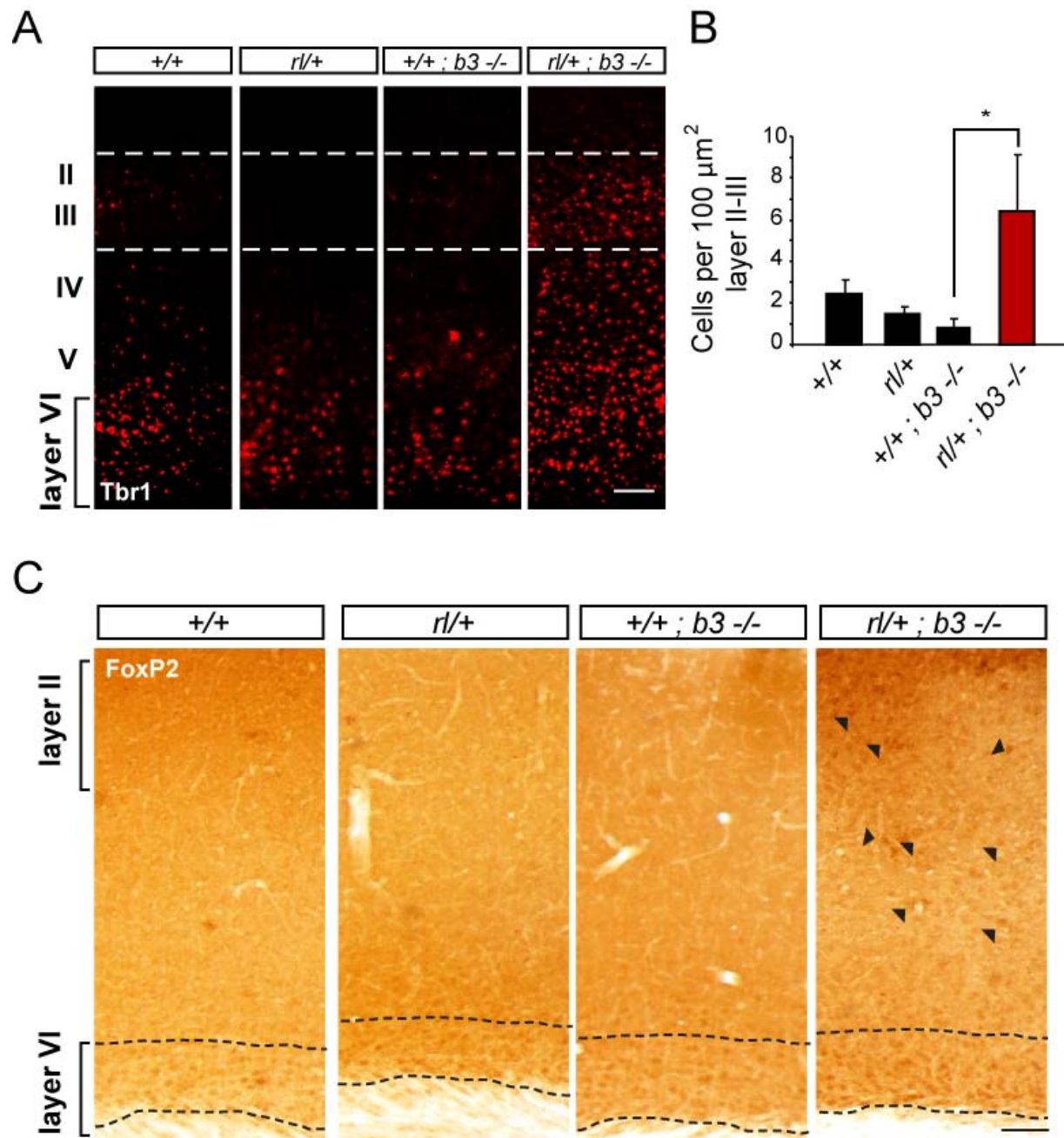


Figure 5.4 Early born neurons shows altered cortical layering in the compound mice. (A) Coronal sections of adult mice (P21) were immunostained for Tbr1, a deep layer marker. Confocal images of *+/+*, *rl/+*, *b3-/-* and *rl/+; b3-/-* displayed Tbr1+ cells in lower layers. However, Tbr1+ cells were also accumulated in the upper cortical layers (II-IV – dashed line) of the *rl/+; b3-/-* compound mutant mice. Immunostaining signals were detected using cy3-conjugated secondary antibody. Scale bar = 75 μm (B) Quantification of the Tbr1+ cell number in 100 μm^2 cortical area represented. (SEM, * $P < 0.05$). (C) The cerebral cortex from both *rl/+; b3-/-* compound mutant mice and control brain sections divided into ten equal bins, and the number of Tbr1+ neurons in each bin was plotted to represent the relative distribution of neuronal migration from the ventricular surface to the pial surface. (D) Immunostaining for FoxP2, another deep layer marker, of *+/+*, *rl/+*, *b3-/-* and *rl/+; b3-/-*. In *+/+*, *rl/+*, and *b3-/-* cortex FoxP2+ cells were located only in layer VI, whereas in *rl/+; b3-/-* compound mice several FoxP2+ neurons were observed in the upper cortical layers. Immunostaining signals were detected using DAB staining protocol (See Methods). Scale bar = 75 μm .

Moreover, by crossing the *rl/+; b3-/-* compound mutant mice with Thy1-GFP M-line, in which YFP is expressed in a subset of layer V pyramidal neurons in the neocortex, we analyzed the large pyramidal neurons that constitute the layer V of cerebral cortex (Figure 5.5, dashed line). In accordance to our marker analysis with *Tbr1* and *FoxP2*, we detected an absence of pyramidal neurons in layer V in the *rl/+; b3-/-* compound mutant mice and instead observed these pyramidal cells in more superficial layers (arrowheads) (Figure 5.5).

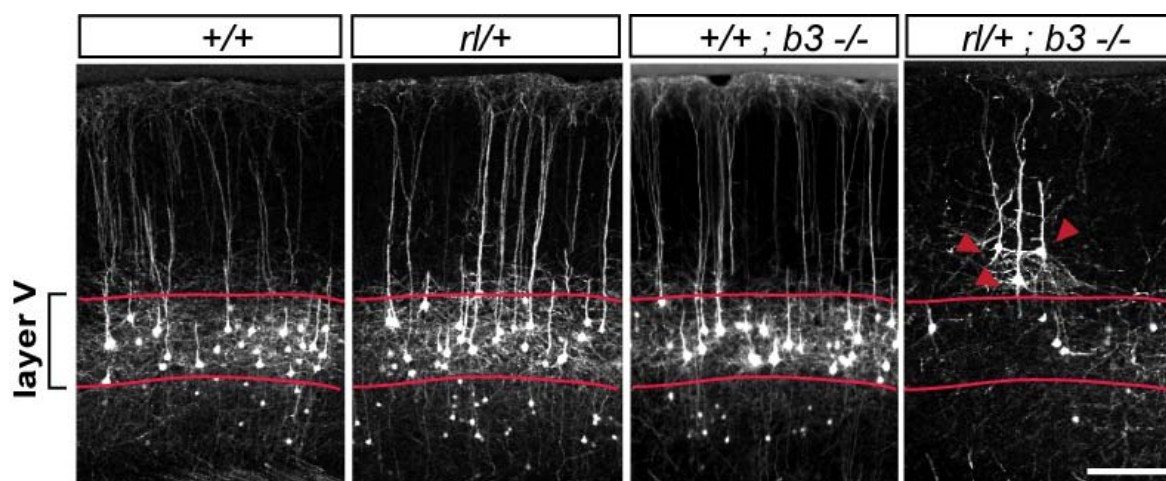


Figure 5.5 Pyramidal neurons of cortical layer V shows distribution alterations in the *rl/+; b3-/-* compound mutant mice. Thy1-GFP+ transgenic mice lines generated to detect YFP+ subset of pyramidal neurons in layer V of *+/+*, *rl/+*, *b3-/-* and *rl/+; b3-/-*. Confocal images showed loss of pyramidal neurons in layer V in the *rl/+; b3-/-* compound mutant mice and several GFP+ neurons in more superficial layers. Scale bar = 50 μm .

Analysis of later born cortical neurons

Specific alterations in the cortical layering in the *rl/+; b3-/-* compound mutant mice were also observed in superficial cortical layers by *Brn1* and *SatB2* immunostaining. *Brn1* and *Brn2* are expressed during the development of the forebrain throughout the cortical plate but at highest levels in a subset of neurons in cortical layers II to IV (McEvelly *et al.*, 2002). In the *+/+*, *rl/+* and *b3-/-* mice the *Brn1*⁺ neuronal population was detected mainly between layer II and IV. However, in the *rl/+; b3-/-* compound mice the *Brn1*⁺ neurons were mainly observed in the lower cortical layers as in the *reeler* cortex (Figure 5.6) as well as in the *Dab1-/-* *scrambler* mice (Herrick *et al.*, 2004).

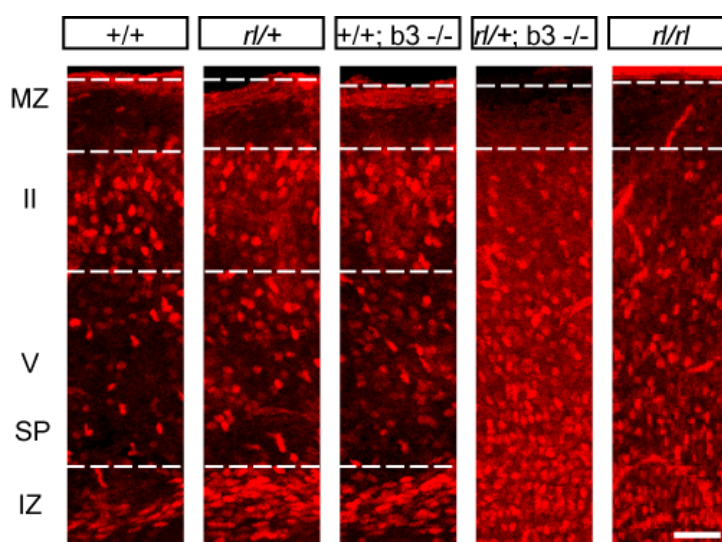


Figure 5.6 Later born neurons shows altered cortical layering in the *rl/+; b3-/-* compound mutant mice. Immunostaining for *Brn1*, an upper layer marker, of the cortex of *+/+*, *rl/+*, *b3-/-*; *rl/rl* and *rl/+ b3-/-* mice. In *+/+*, *rl/+* and *b3-/-* cortex upper layer specific staining observed. In the *rl/+; b3-/-* compound mice a *reeler*-like cell distribution observed, where *Brn1*⁺ cells located in lower cortical layers. Immunostaining signals were detected using cy3-conjugated secondary antibody. Scale bar = 50 μ m. MZ, Marginal zone; SP, Subplate; IZ, Intermediate zone.

SatB2 is a postmitotic determinant for upper-layer neurons in the neocortex (Britanova *et al.*, 2008) and as expected *SatB2* immunostaining of the wild-type, *rl/+* and *b3-/-* mice allowed detection of upper-layer neurons. The *rl/+; b3-/-* compound mutant neocortex showed reduced cell density in the upper layers and increased number of cells in the lower layers (Figure 5.7).

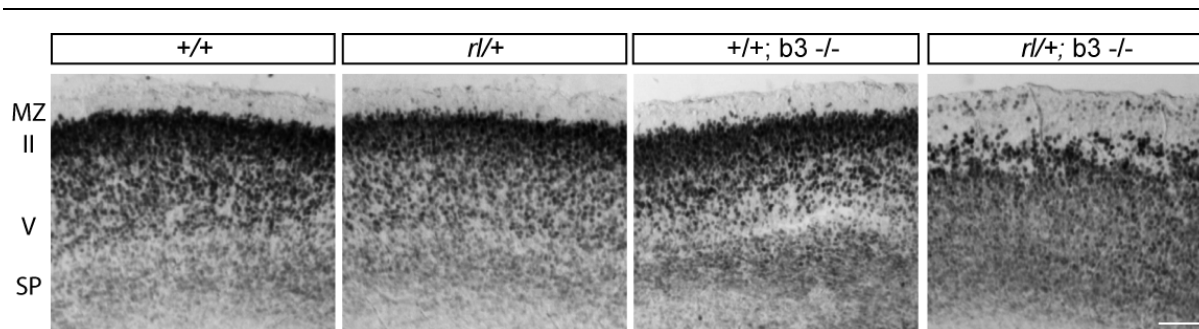


Figure 5.7 Later born neurons shows altered cortical layering in the *rl/+ b3-/-* compound mutant mice. Immunostaining for SATB2, an upper layer marker, of the cortex of *+/+*, *rl/+*, *b3-/-* and *rl/+ b3-/-* mice. In *+/+*, *rl/+* and *b3-/-* cortex upper layer specific staining observed. In the *rl/+; b3-/-* compound mice a *reeler*-like cell distribution observed, where SATB2+ cells located in lower cortical layers. Immunostaining signals were detected using DAB staining protocol. Scale bar = 50 μ m. MZ, Marginal zone; SP, Subplate.

5.1.1.3 Interneuron distribution is altered in the compound mutant mice.

The correct positioning of both projection neurons and local circuit interneurons is crucial for proper functioning of the mature cortex. Like projection neurons, GABAergic interneurons form layers though not as clearly distinguishable as projection neurons. Birth-dating and transplantation studies have demonstrated relationships between the timing of interneuron generation and their layer destinations (Miller, 1986, Hevner *et al.*, 2004, Peduzzi, 1988, Valcanis *et al.*, 2003, Yozu *et al.*, 2004). Interneuron layering is formed following two phases of migration. First, tangential migration of cells from the subpallidum to the pallidum takes place. Afterwards, they migrate radially from the MZ or from the SVZ into the CP and finally adopt the defined laminar position. Although cortical neurons and interneurons of the cerebral cortex follow different developmental programs (Anderson *et al.*, 1997), and interneurons migrate through much greater distances than projection neurons, GABAergic interneurons tend to adopt the same cortical layer as synchronically generated projection neurons (Miller, 1985, Fairen *et al.*, 1986, Valcanis *et al.*, 2003).

Interneurons express Dab1 as laminar formation proceeds (Herz *et al.*, 2006) and Reelin as they settle in the cortex (Alcantara *et al.*, 1998). Therefore, when the members of Reelin signaling pathway is absent in the cortex, as in the *reeler* mice, the laminar arrangement of GABAergic

5 Results

interneurons are severely impaired (Hevner *et al.*, 2004). Within this context we studied the distribution of GABAergic neurons in the cortex of *rl/+; b3-/-* compound mice at postnatal day 20. We examined neocortical interneurons that originated from the subcortical telencephalon by immunostaining with antibody for Calbindin at P20. Calbindin is expressed by layer II-III neurons (Benhayon *et al.*, 2003) and we observed a tight band of immunoreactivity near the pial surface at the somatosensory cortex of the control mice (*+/+*, *rl/+* and *b3-/-*) (Figure 5.8A). However, in *rl/+; b3-/-* compound mutant cortex the distribution of Calbindin+ neurons in layer II-III was altered, the cells were dispersed in deeper positions (Figure 5.8A, B). Summary histograms depict Calbindin+ interneuron distribution throughout the cortex of *b3-/-* and *rl/+; b3-/-* compound mice. In *b3-/-* animals interneurons were located mainly in layer II-III (73 % layer II-III and 25 % layer IV-V) whereas in *rl/+; b3-/-* compound mice they were scattered towards lower cortical parts of the cortex (55.7 % in layer II-III and 36 % in layer IV-V) (Figure 5.8B, C). Previous studies have established that the layering of projection neurons is inverted in *reeler*, *scrambler* and *yotari* mice (Howell *et al.*, 1997, Sheldon *et al.*, 1997); hence, the interneuron inversion observed here is consistent with the notion that, when Reelin signaling is impaired, both interneurons and deep layer projection neurons are inverted.

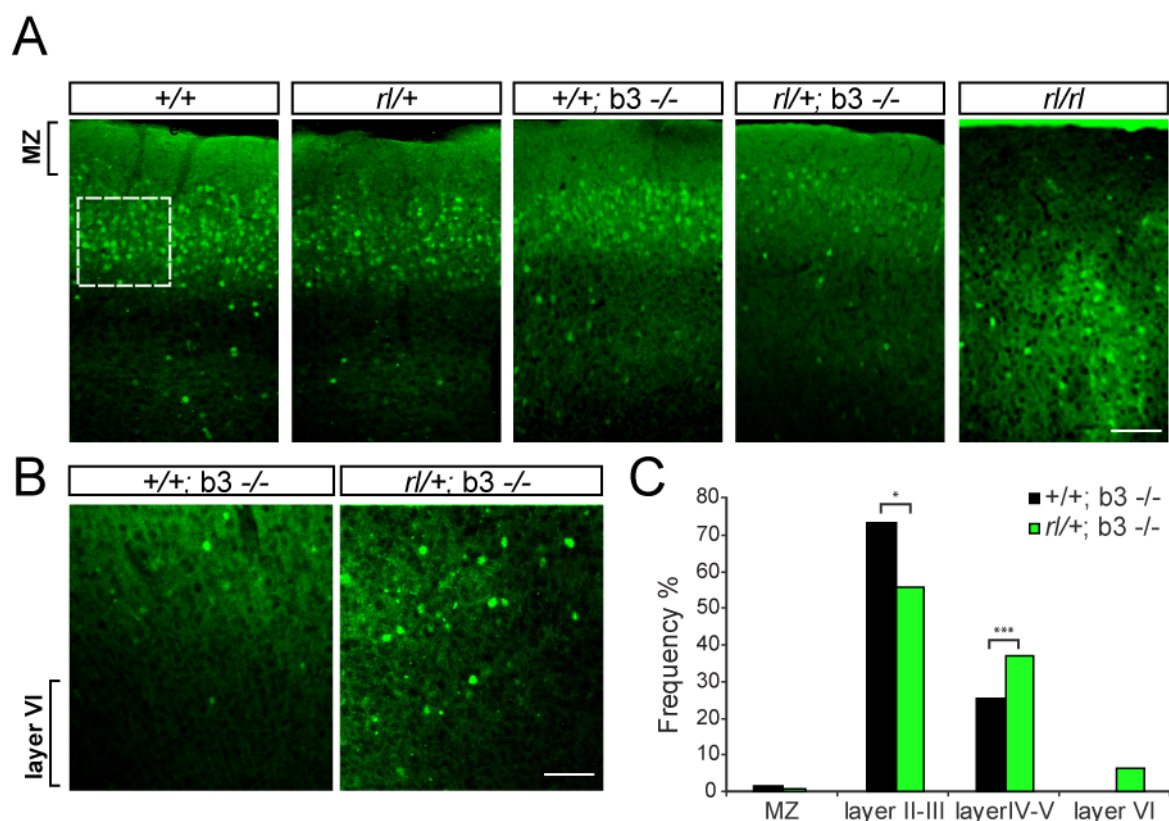


Figure 5.8 Interneuron distribution is altered in *rl/+; b3^{-/-}* compound mutant mice. (A) Calbindin immunostaining of coronal sections of adult *+/+*, *rl/+*, *b3^{-/-}* and *rl/+; b3^{-/-}* mice. Calbindin immunoreactivity at the somatosensory cortex of *+/+*, *rl/+* and *b3^{-/-}* mice showed proper interneuron distribution, whereas in the *rl/+; b3^{-/-}* compound mice the cell density reduced significantly in the upper cortical layers, revealing defects in the latter stages of neuronal migration. Immunostaining signals were detected using Alexa-Fluor-488-conjugated secondary antibody. Scale bar = 100 μ m (B) Confocal images of layer V showed more interneurons in the *rl/+; b3^{-/-}* compound mutant cortex. Scale bar = 50 μ m. (C) Stereological quantification of cell number in layer II-III was performed in the dashed areas (200x200 μ m) of 4 animals from each group and % of cells at each layer, and cell number in lower layers was quantified from confocal images as shown in (B) and was plotted relative to total cell number in the whole cortex. (SEM, * $P < 0.05$; *** $P < 0.0001$). MZ, Marginal zone.

Taken together, these results indicate that ephrinB3 reverse signaling plays an important role during cortical lamination of principal neurons and interneurons.

5.1.1.4 BrdU birth dating study reveals neuronal migration defect in *rl/+; b3^{-/-}* compound mutant mice.

One of the hallmarks of *reeler* phenotype is the roughly inverted cell layering among the cortical plate which has been confirmed by birth dating analysis (Caviness, 1982). As the laminar

5 Results

organization of the cerebral cortex of *rl/+; b3-/-* compound mutant mice showed several *reeler*-like alterations we examined whether the abnormalities in cortical layering reflected impaired neuronal migration. Therefore, we used the thymidine analog 5-bromo-2'-deoxuridine (BrdU) birth dating. BrdU is incorporated into the DNA of dividing progenitor cells and serves as a permanent marker if progenitors are labeled during the S phase of cell cycle. Mice were labeled at E12.5, E15.5 and E17.5 by BrdU injection and analyzed at postnatal day 20. Analysis of distribution of BrdU+ cells in the CP at different stages allowed us to examine the migration pattern of these cells. Neurons labeled at E12.5 with BrdU were confined to the inferior aspect of the cortex, corresponding to layer V in the wild type mice, *rl/+* and ephrinB3 knockouts (*b3-/-*) (Figure 5.9A). In contrast, BrdU-labeled cells in the *rl/+; b3-/-* compound mutant littermate were highly accumulated at upper layers (layer II-III) (Figure 5.9A). A significant number of neurons labeled with BrdU were located superficially in *rl/+; b3-/-* compound mutant cortex (67 %), with a smaller number in the region corresponding to layer IV-V (10 %), as it is the case in the *reeler (rl/rl)* cortex (71 % in layer V and 17 % in lower layers) (Figure 5.9B). The cortex was divided into ten equal bins starting from MZ to ventricular zone and the distance of each cell to the MZ was measured in order to observe the distribution of neurons among cortical layers. As expected wild-type (+/+) and *rl/+* didn't show a difference in cell distribution, as well as *b3-/-* mice. (Figure 5.9C). The *rl/+; b3-/-* compound mutant mice showed predominant distribution alterations distinguishable from that in +/+, *rl/+* and *b3-/-* mice where early born neurons were located in most superficial parts of the cortex.

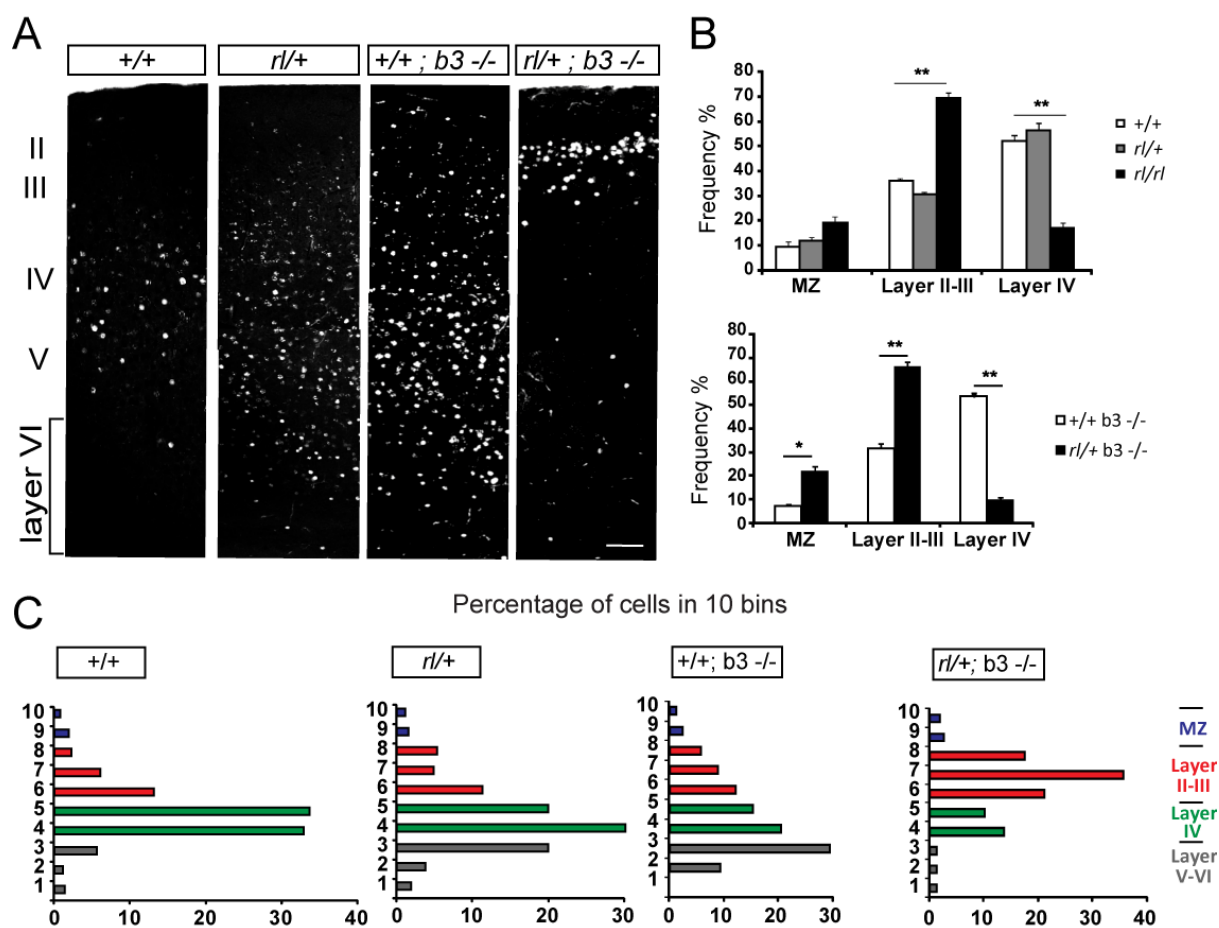


Figure 5.9 Neurons born at E12.5 do not migrate to lower layers in the *rl/+; b3-/-* compound mutant mice. (A) Pregnant mice were injected intraperitoneally with BrdU (50 $\mu\text{g/g}$ of body weight) at E12.5. The animals were analyzed 4 weeks postnatally. BrdU+ neurons in the cerebral cortex were detected by immunostaining with a mouse monoclonal antibody to BrdU (1:1000, Chemicon). Compound mutant mice (*rl/+; b3-/-*) showed *reeler*-like inversion of cortical layers, with early born neurons located in most superficial part of the cortex. Immunostaining signals were detected using cy3-conjugated secondary antibody. Scale bar = 50 μm . (B) The frequency of BrdU+ neurons of +/+, *rl/+* and *rl/rl* (left panel) and of *rl/+; b3-/-* compound mutant mice versus *b3-/-* (right panel) were plotted. (SEM, * $P < 0.05$; ** $P < 0.001$) (C) The cerebral cortex from both *rl/+; b3-/-* compound mutant mice and control brain sections divided into ten equal bins, and the number of BrdU+ neurons in each bin was plotted to represent the relative distribution of neuronal migration from the ventricular surface to the pial surface. Two brains were analyzed for each genotype.

Neurons born at later stages were labeled with BrdU at E15.5, occupying an area corresponding to layer II-III in +/+, *rl/+* and *b3-/-* mice (Figure 5.10A). In *rl/+; b3-/-* compound mutant cortex the BrdU+ cells were scattered throughout the cortex, with a tendency towards the deeper half of the cortex (Figure 5.10A). The cell number in each layer was quantified and their distribution in the cortex was measured. In the *rl/+; b3-/-* compound mutant cortex frequency of cells in superficial layers was

5 Results

significantly less than control animals (48 %, 71 % respectively) and the increase in lower layers was also significant (from 47 % to 22 %) as in the *reeler* cortex. *Reeler* cortex showed 44 % decrease in cell number in upper layers and 40 % increase in cell number in lower layers when compared to the wild-type (+/+) and *rl/+* mice. The distribution plots confirmed the observed alteration where later born neurons were located in deeper layers of the cortex (Figure 5.10C).

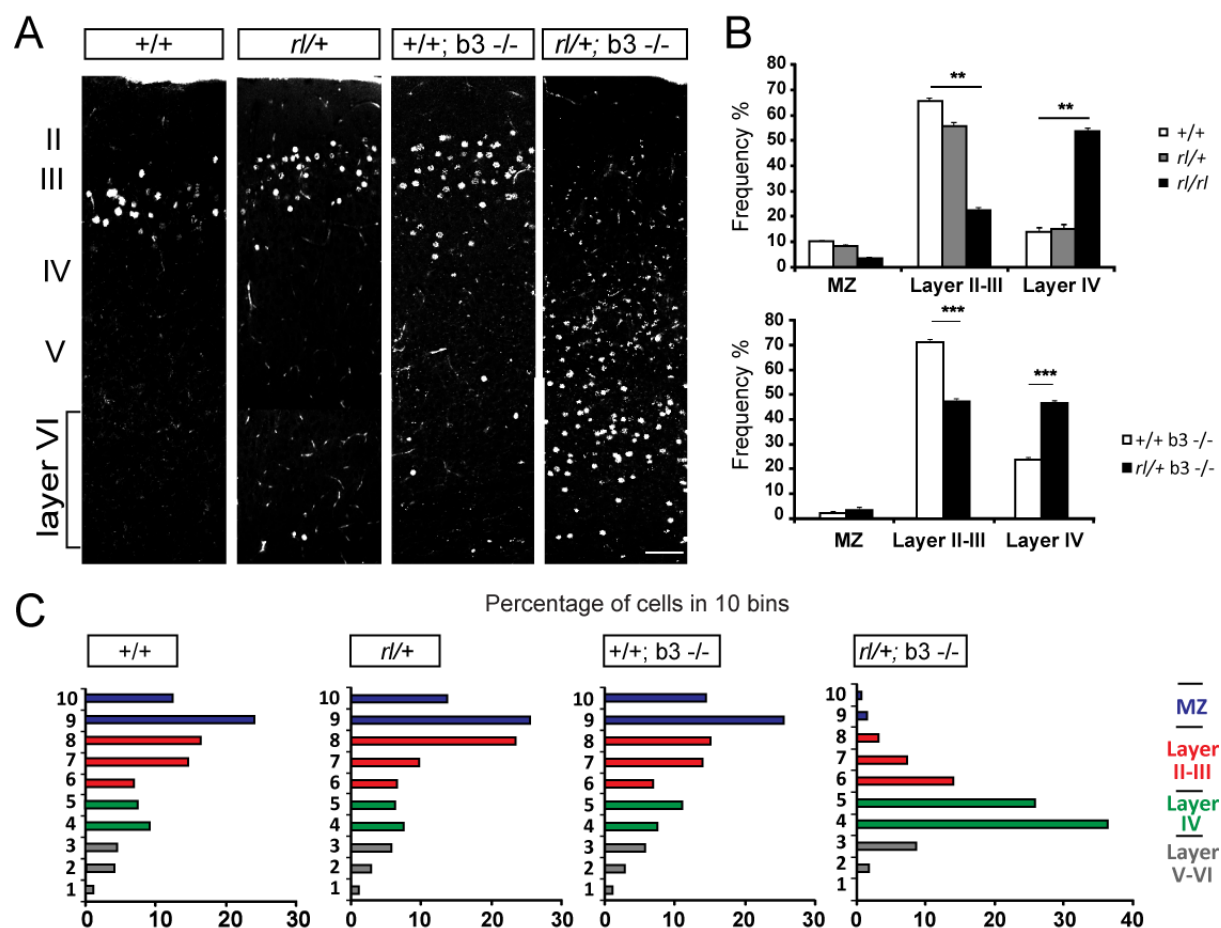
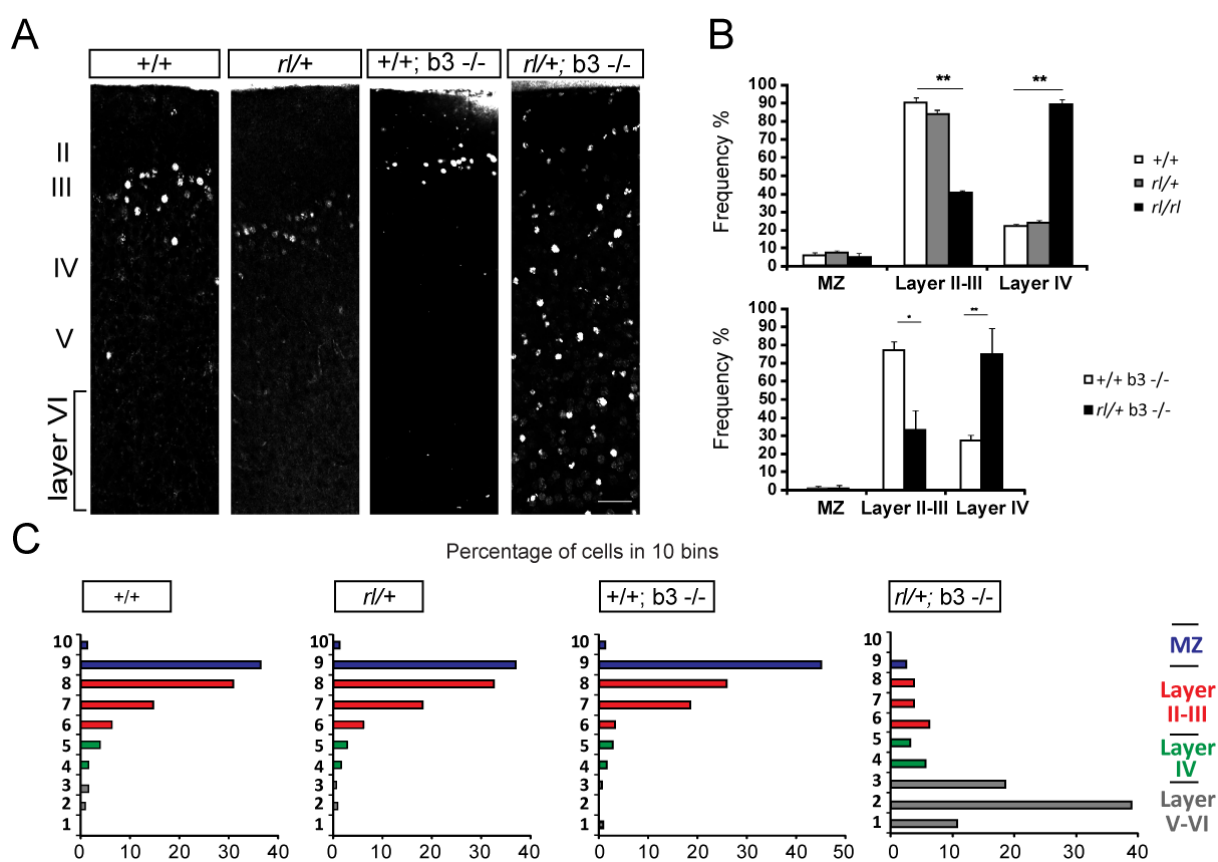


Figure 5.10 Neurons born at E15.5 do not migrate to upper cortical layers in the *rl/+; b3^{-/-}* compound mutant mice. (A) Pregnant mice were injected intraperitoneally with BrdU (50 mg/g of body weight) at E15.5. The animals were analyzed 4 weeks postnatally. BrdU+ neurons in the cerebral cortex were detected by immunostaining with α -BrdU antibody (1:1000, Chemicon). Compound mutant mice (*rl/+; b3^{-/-}*) showed *reeler*-like inversion of cortical layers, with late born neurons located in deeper part of the cortex. Immunostaining signals were detected using cy3-conjugated secondary antibody. Scale bar = 50 μ m. (B) The frequency of BrdU+ neurons of *+/+*, *rl/+* and *rl/rl* (left panel) and of *rl/+; b3^{-/-}* compound mutant mice versus *b3^{-/-}* (right panel) were plotted. (SEM, ** $P < 0.001$; *** $P < 0.0001$) (C) The cerebral cortex from both *rl/+; b3^{-/-}* compound mutant mice and control brain sections divided into ten equal bins, and the number of BrdU+ neurons in each bin was plotted to represent the relative distribution of neuronal migration from the ventricular surface to the pial surface. Two brains were analyzed for each genotype.

At E17.5 neurogenesis is low, so very few labeled neurons can be observed in mice (Figure 5.11). The BrdU labeling of these late born neurons showed only few cells in layer II-III of *+/+*, *rl/+* and *b3-/-* cortices, whereas, BrdU-labeled cells in a *rl/+; b3-/-* compound mutant littermate were spread throughout the width of the cortex (Figure 5.11A). Quantification of cell number in each layer shows the decrease in cell number in upper cortical layers in *reeler* mice (91 % to 39 %) and in the *rl/+; b3-/-* compound mutant mice cortex (78 % to 32 %) when compared to respective control animals. In lower cortical layers of the *rl/+; b3-/-* compound mutant mice the BrdU+ cells were increased from 29 % to 75 %, similar to *reeler* cortex (Figure 5.11B). Cell distribution plots show the shift of BrdU+ cells towards lower layers in the *rl/+; b3-/-* compound mice, whereas in the others are restricted to layer II-III (Figure 5.11C).



5 Results

Figure 5.11 Neurons born at E17.5 do not migrate to upper cortical layers in the *rl/+; b3-/-* compound mutant mice. (A) Pregnant mice were injected intraperitoneally with BrdU (50 mg/g of body weight) at E17.5. The animals were analyzed 4 weeks postnatally. BrdU+ neurons in the cerebral cortex were detected by immunostaining with a mouse monoclonal antibody to BrdU (1:1000, Chemicon). Compound mutant mice (*rl/+; b3-/-*) showed *reeler*-like inversion of cortical layers, with latest born neurons located in deeper parts of the cortex. Immunostaining signals were detected using cy3-conjugated secondary antibody. Scale bar = 50 μ m. (B) The frequency of BrdU+ neurons of *+/+*, *rl/+* and *rl/rl* (left panel) and of *rl/+; b3-/-* compound mutant mice versus *b3-/-* (right panel) were plotted. (SEM, * $P < 0.05$; ** $P < 0.001$). (C) The cerebral cortex from both *rl/+; b3-/-* compound mutant mice and control brain sections divided into ten equal bins, and the number of BrdU+ neurons in each bin was plotted to represent the relative distribution of neuronal migration from the ventricular surface to the pial surface. Two brains were analyzed for each genotype.

Taken together, birth dating analysis of *rl/+; b3-/-* compound mutant mice showed that cortical layers are inverted, which results from a migratory impairment of the newly generated neurons to colonize the upper layers in the cortex.

5.1.1.5 Preplate splitting does not take place in the compound mutant embryos.

Abnormal splitting of preplate cells is one of the earliest structural defects detected in the *reeler* neocortex (Caviness, 1982, Sheppard *et al.*, 1997). The preplate is composed of Cajal-Retzius neurons and subplate neurons. In the *reeler* cortex the subplate neurons remain close to the Cajal-Retzius neurons and are displaced above the developing cortical plate to form a 'superplate'. These changes in the preplate splitting can be analyzed using extracellular matrix components, such as fibronectin and chondroitin sulfate proteoglycan (CSPG). Fibronectin and CSPG are first distributed throughout the proliferative zone, however, their distribution changes with newly generated cells forming the preplate. CSPG becomes more prominent in the preplate and fibronectin in the processes of preplate neurons. As the cortical plate neurons divide the preplate association persists and by CSPG immunolabeling MZ and subplate can be visualized.

CSPGs are secreted from subplate neurons (Sheppard *et al.*, 1991). They are closely associated with the preplate, even when the preplate neurons are abnormally positioned, as in the *reeler* neocortex,

their distribution is defected (Sheppard *et al.*, 1997). As a step in defining the molecular environment for development of the mammalian cerebral cortex we examined the preplate splitting in wild-type (+/+) and *rl/+*; *b3*^{-/-} compound mice by CSPG immunohistochemistry. As shown in Figure 5.12, the subplate was easily detected in E17.5 embryos of +/+, *rl/+* and *b3*^{-/-} and was absent in *reeler* mice (*rl/rl*). Surprisingly, CSPG staining was more dispersed in neocortex of compound mutant mice suggesting an improper splitting closer to *reeler* phenotype (Figure 5.12). Defects observed in the preplate splitting plausibly contribute to the increased cell number in the marginal zone of the compound mutant mice (Figure 5.2).

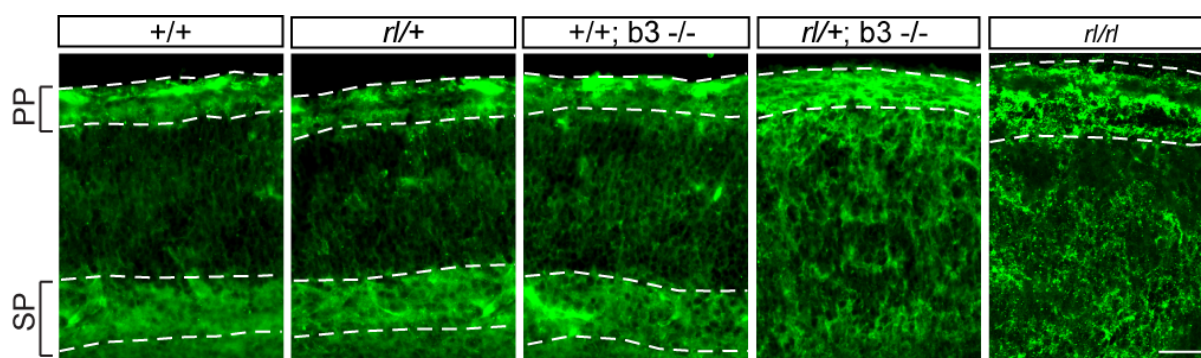


Figure 5.12 Preplate splitting does not take place in the compound mutant embryos. Coronal sections from E17.5 mice labeled with α -CSPG (mouse, 1:1000, Chemicon). The immunostaining revealed the preplate (PP) splitting (white dashed line) in the +/+, *rl/+*, and *b3*^{-/-} mice. In the *rl/+*; *b3*^{-/-} compound mice an intense staining in the PP (white dashed line) and a weak staining in SP was observed, suggesting the PP splitting doesn't completely take place. In *reeler* (*rl/rl*) cortex a thick staining is observed at PP and SP was not detected as described previously (Sheppard *et al.*, 1997). Immunostaining signals were detected using Alexa-Fluor-488-conjugated secondary antibody. Scale bar= 50 μ m. PP, Preplate; SP, Subplate.

5.1.1.6 Radial glia scaffold is altered in the *rl/+*; *b3*^{-/-} compound mutant mice.

In the developing brain we can distinguish two modes of migration, tangential and radial. Radial migration is the most common form of migration in the developing cortex with a specialized scaffold of cells on the cerebral wall formed by radial glia cells (Hatten, 1999, Rakic, 1972). Radial glia cells are characterized by a soma situated near the ventricular surface and an elongated fiber shaft that

5 Results

transiently spans the entire width of the cerebral wall. The radial glia scaffold is present only during neuronal development and subsequently transforms into astrocytes in the cerebral cortex and Bergman fibers in the cerebellum (Hatten, 1999, Rakic, 1972). In *reeler* mutant mouse the later-born neurons seem to have difficulty to pass the earlier born neurons, which migrate in close contact to radial glial fibers (Pinto-Lord *et al.*, 1982). Several observations in *reeler* mice, such as branching of subpial endfeet (Pinto-Lord *et al.*, 1982, Hunter-Schaedle, 1997), suggested that Reelin signaling directly affects radial glia morphology (Frotscher *et al.*, 2003), and therefore Reelin controls the neuronal migration by acting on the radial glial scaffold (Weiss *et al.*, 2003, Forster *et al.*, 2002, Frotscher *et al.*, 2003). The cortex is also inverted in *Dab1* mutants, and *Dab1* mutant neurons remain closely associated with radial glial fibers (Gonzalez *et al.*, 1997, Howell *et al.*, 1997, Sanada *et al.*, 2004). Since *rl/+; b3-/-* compound mouse displays defects in cell migration and layering and preplate splitting, we analyzed the radial glia morphology in these mice.

The radial glial scaffold can be investigated using various markers, such as glial fibrillary acidic protein (GFAP), astrocyte-specific glutamate transporter (GLAST), Nestin and RC2 (Levitt *et al.*, 1980, Misson *et al.*, 1991, Misson *et al.*, 1988, Shibata *et al.*, 1997, Storck *et al.*, 1992). We used RC2 as radial glia markers and stained coronal sections of E17.5 mice. Radial processes appeared to be normal in the wild-type, *rl/+* and *b3-/-* cortex, whereas in the *rl/+; b3-/-* compound mutant cortex the radial organization was defected with non-radial and disorganized fibers (Figure 5.13A - arrowheads). We next observed the alignment of neuronal processes in the cortex of the *rl/+; b3-/-* compound mice by MAP2 immunohistochemistry at E18.5. MAP2 staining revealed the radial alignment of neuronal processes in the *+/+*, *rl/+*, *b3-/-* mice whereas a failure of neuronal dendritic arborization in the cortex of the *rl/+; b3-/-* compound mice (Figure 5.13B).

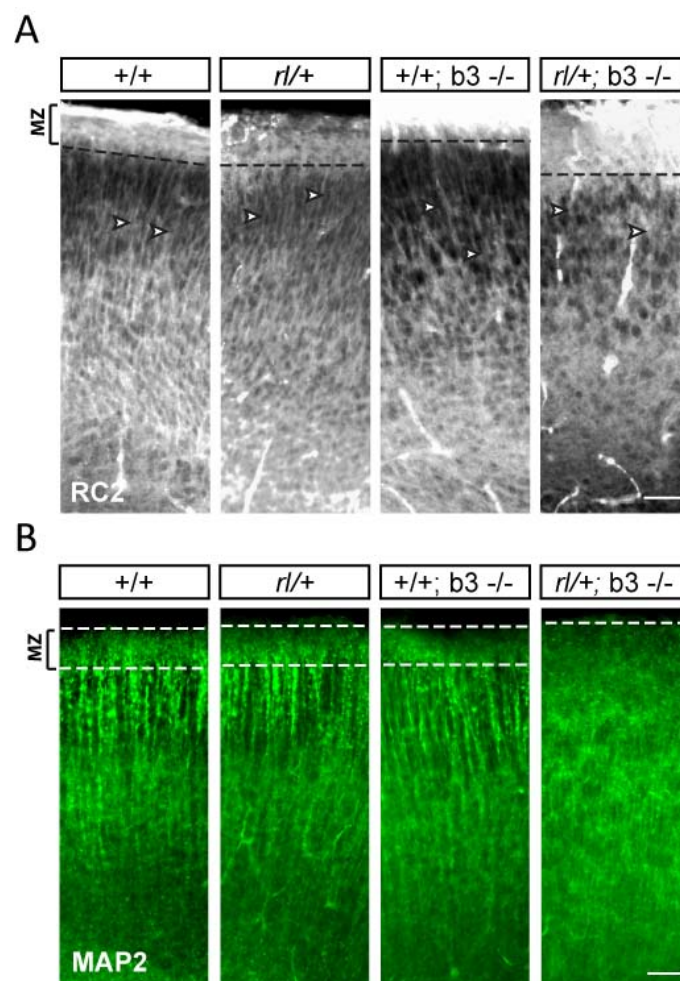


Figure 5.13 RC2 staining shows radial glial scaffold in the cortex. (A) Radial glial scaffold analyzed at E17.5 of *rl/+; b3 -/-* compound mutant mice using RC2 as a marker. Radial elongation of glial cells was observed in the *+/+*, *rl/+* and *b3 -/-* mice, whereas in the *rl/+; b3 -/-* compound mice this radial elongation was disturbed. (B) Analysis of dendritic arborization at E18.5 and P20. MAP2 staining shows radially oriented neuronal processes as well as cell free MZ in *+/+*, *rl/+* and *b3 -/-* mice. However, the neuronal processes in the cortical plate of *rl/+; b3 -/-* compound mice were misoriented (arrows) and many of the processes invaded the MZ (arrowheads). Immunostaining signals were detected using Alexa-Fluor-488-conjugated secondary antibody. Scale bars = 75 μm . MZ, Marginal zone.

5.1.2 *rl/+; b3 -/-* compound mice show *reeler* like phenotypes in the hippocampus.

In the embryonic and early postnatal hippocampus, Reelin is expressed by the Cajal-Retzius cells in the fascia dentate, outer marginal layer (OML) of the dentate gyrus (DG) and in the stratum locunosum moleculare (SLM) of the hippocampus proper (D'Arcangelo *et al.*, 1995, Alcantara *et al.*,

1998). When Reelin is absent granular and pyramidal cell migration is altered (reviewed in (Forster *et al.*, 2006). Besides Reelin and among all ephrinBs, ephrinB3 is highly expressed in the DG and in the CA1 region of hippocampus (Grunwald *et al.*, 2004). Therefore, after observing migration defects in the cerebral cortex of *rl/+; b3 -/-* compound mutant mice we also investigated possible defects in the hippocampus. We focused our analysis on the primary *reeler*-like phenotypes in the *rl/+; b3 -/-* compound mutant mice.

5.1.2.1 CA1 shows layering defects in the hippocampus of *rl/+; b3 -/-* compound mutant mice.

Hippocampal pyramidal cells migrate along radial fibers and position themselves according to an inside-out gradient in the stratum pyramidale (SP). In the normal hippocampus CA forms a sharply laminated pyramidal layer. In contrast, *reeler* mice show a poor segregation of the cell-rich and cell-poor laminae and results in the splitting of two rows of pyramidal cells (Stanfield *et al.*, 1979a, Stanfield *et al.*, 1979b). In order to investigate the cell distribution in the pyramidal cell layer of *rl/+; b3 -/-* compound mutant mice we performed NeuN immunohistochemistry on coronal vibratome sections of adult mice. First *+/+* and *rl/rl* hippocampi were analyzed to reproduce the expected layering defects (Figure 5.14).

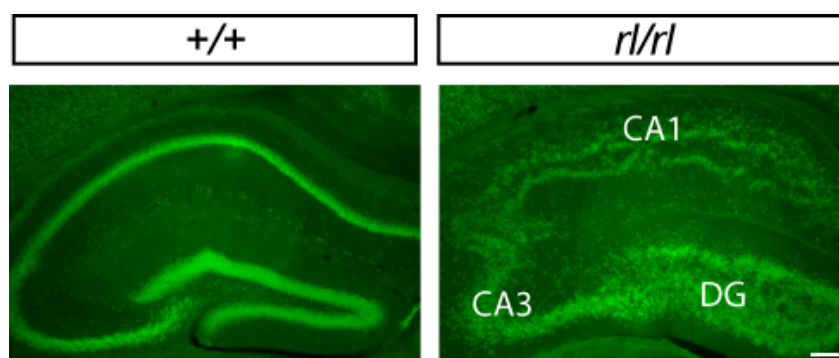


Figure 5.14 Granular layer distortion of *reeler* hippocampus. Granular layer of wild-type (*+/+*) and *reeler* (*rl/rl*) coronal sections stained with NeuN antibody and confocal images were taken. A compact, well-defined granular and CA layering was observed in *+/+* mice, whereas, *rl/rl* hippocampus showed the splitting of CA1 layer and disorganized granular cells in the dentate gyrus. Immunostaining signals were detected using Alexa-fluor-488-conjugated secondary antibody. Scale bar = 100 μ m. DG, Dentate gyrus; CA1 and CA3 are hippocampal areas.

Next, the $+/+$, $rl/+$, $b3-/-$ and $rl/+; b3-/-$ hippocampi were stained with NeuN-antibody. The pyramidal cell layers of $+/+$, $rl/+$ and $b3-/-$ mice were tightly packed, whereas, they were more loosely associated in the $rl/+; b3-/-$ compound mutant mice and this resulted in the increased thickness of the pyramidal cell layer from 75 μm to 150 μm in the $rl/+; b3-/-$ compound mutant mice (Figure 5.15 A, C). Moreover, the cell distribution in the apical part of the pyramidal cell layer showed an increase in the $rl/+; b3-/-$ compound mice (Figure 5.15A, B).

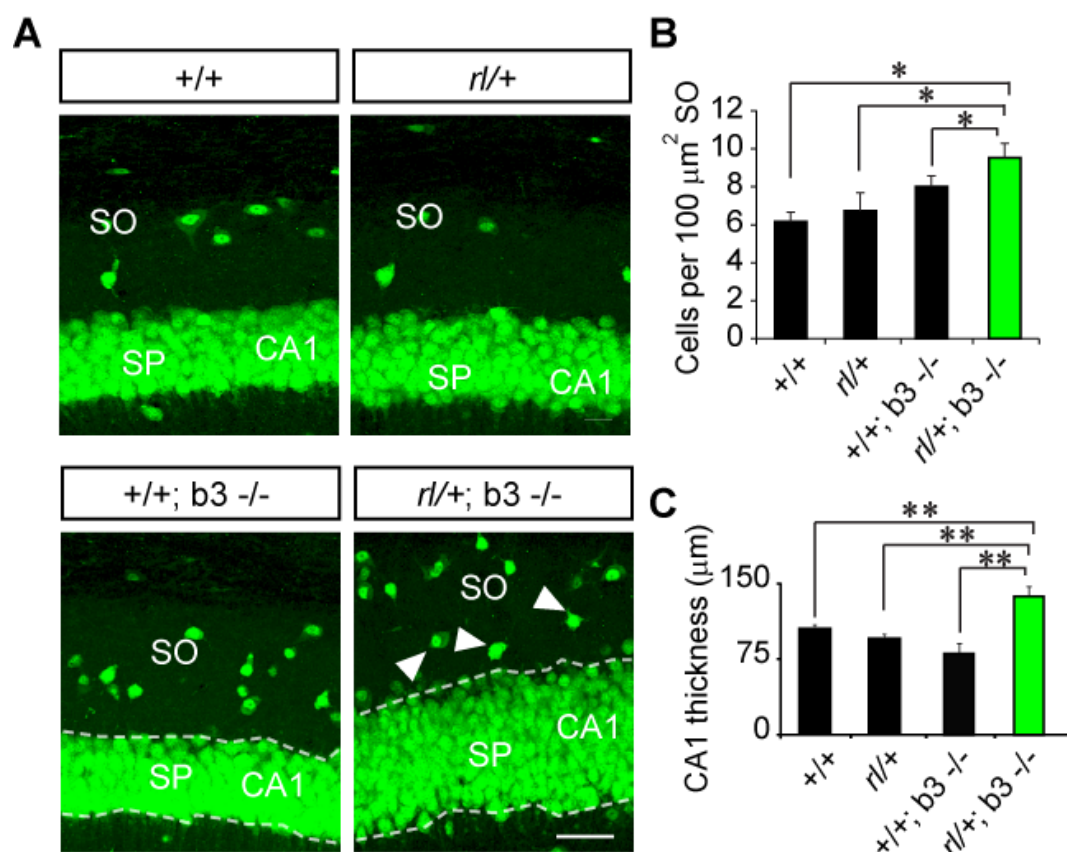


Figure 5.15 CA1 region of compound mutant mice shows alterations in its layering. (A) Invasion of the pyramidal cells of CA1 into stratum oriens (SO) observed by NeuN immunostaining of coronal sections through the neocortex of adult wild-type ($+/+$), $rl/+$, $b3-/-$ and compound mutant mice ($rl/+; b3-/-$). In the SO of $+/+$, $rl/+$ and $b3-/-$ mice there were only few neurons, whereas many NeuN+ cells were found (arrowheads) in the SO of $rl/+; b3-/-$ compound mutant mice. Also the thickness of SO was increased, showing a less dissociated CA1 layer. Immunostaining signals were detected using Alexa-fluor-488-conjugated secondary antibody. (B) Quantitative analysis of cell numbers in 100 μm^2 of SO revealed the impairment of dense packing of granular cell layer in the $rl/+; b3-/-$ compound mice. The CA1 thickness was measured in 3 animals and 6 CA1 regions. (SEM, $*P<0.5$; $**P<0.001$). Scale bar = 50 μm . CA1, Hippocampal areas; SP, Stratum pyramidale; SR, Stratum radiens; SO, Stratum oriens.

5 Results

The increased cell number in the apical part of the CA1 area was further investigated, in order to detect whether these cells were also born at the stage of hippocampal formation, as well as to exclude the fact that they were not interneurons but are principal neurons. Therefore, we first performed BrdU labeling of hippocampal neurons by injecting pregnant mice at E16.5 and observed BrdU+ cells at postnatal stage (P20), after the hippocampal development is completed. Quantification of BrdU+ cell density in the stratum oriens (SO) confirmed the increase in the cell density observed with the NeuN immunohistochemistry (Figure 5.16).

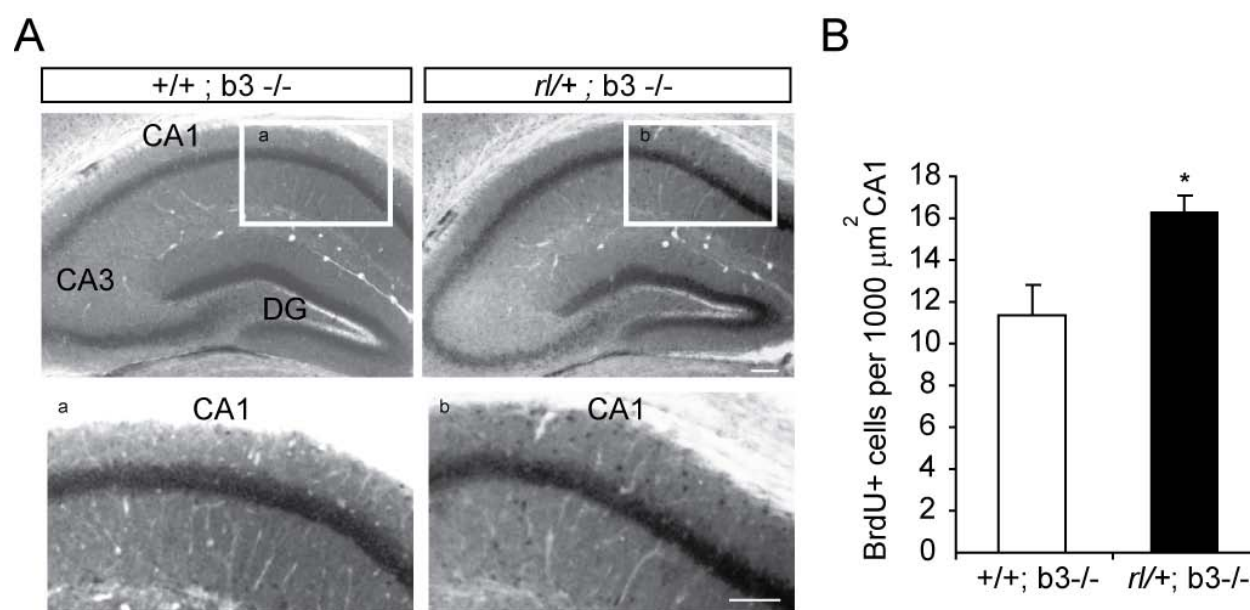


Figure 5.16 BrdU staining of CA1 region is shows altered cell layering. (A) Pregnant mice were injected intraperitoneally with BrdU (50 μg/g of body weight) at E16.5. The animals were analyzed 4 weeks postnatally. BrdU+ neurons were detected by immunostaining with a mouse monoclonal antibody to BrdU (1:1000, Chemicon). In b3-/- mice a compact CA layering was observed, whereas in rl/+; b3-/- compound mutant mice more BrdU+ cells were detected in the apical part of the CA1 region (blow ups, a and b respectively). Immunostaining signals were detected using DAB staining protocol. Scale bar = 50 μm. (B) The density of BrdU+ neurons of +/+; b3-/- versus rl/+; b3-/- in 1000 μm² were plotted. (SEM, *P<0.05). CA1 and CA3 are hippocampal areas; DG, Dentate gyrus.

Taken together, our observations reveal the defects of neuronal migration in SO of hippocampus in rl/+; b3-/- compound mutant mice.

5.1.2.2 The granular cell layer in the dentate gyrus of *rl/+*; *b3*^{-/-} compound mice is less compact.

Hippocampal pyramidal cells position themselves according to an inside-out gradient in the SP, whereas, in the DG the granular cells migrate in an outside-in gradient and form a compact granular cell layer. In *reeler* mice the granular cell layer of DG is also affected. The granular cells are scattered around and do not form a compact layer (Weiss *et al.*, 2003). Therefore, we studied the granular layer of DG in the *rl/+*; *b3*^{-/-} compound mutant mice with NeuN immunohistochemistry. In the *+/+*, *rl/+*, and *b3*^{-/-} hippocampus a compact granular layer was observed, however, in the *rl/+*; *b3*^{-/-} compound mice the granular layer was loosely dissociated (Figure 5.17).

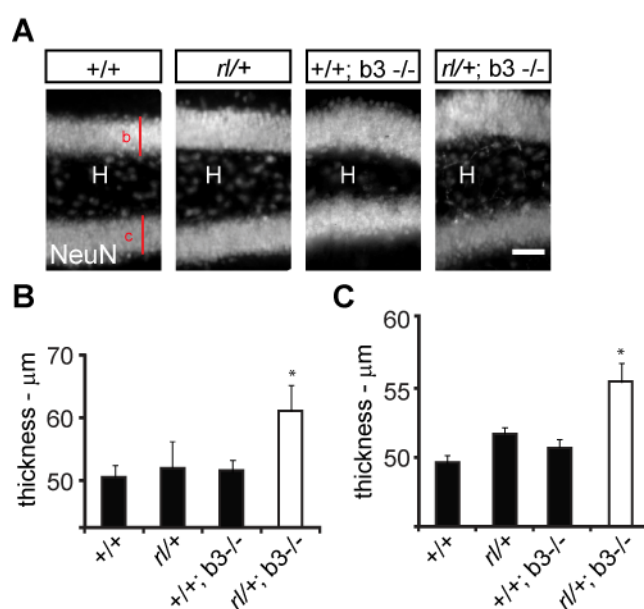


Figure 5.17 Granular layer thickness increased in the *rl/+*; *b3*^{-/-} compound mutant mice. (A) The granular cell layer of DG was labeled with NeuN immunohistochemistry. A compact granular layer was detected in *+/+*, *rl/+* and *b3*^{-/-} mice, whereas, in the *rl/+*; *b3*^{-/-} compound mutant mice the granular layer was loosely associated. Immunostaining signals were detected using Alexa-fluor-488-conjugated secondary antibody. Scale bar = 50 μm . (B, C) Thickness of granular layer was measured from 3 animals and 6 DG. In order to get a value for each DG, the thickness was measured from 5 different points and was averaged and plotted. The graphs show expansion of the layer thickness (thickness of b is represented in B and of c in C). (SEM, * $P < 0.05$). H, Hilus.

5.1.2.3 Mossy cells are dislocated in the *rl/+; b3-/-* compound mutant mice.

Granule cells express Calbindin and hilar mossy cells express Calretenin. These two cells have a clear segregation in wild-type mice (Liu *et al.*, 1996), however, in *reeler* mice these two layers intermingle (Drakew *et al.*, 2002). In order to further study the granular layer of *rl/+; b3-/-* compound mutant mice we performed Calretenin immunostaining and analyzed the distribution of hilar mossy cells. Calretenin immunostaining of *+/+*, *rl/+*, *b3-/-* and *rl/+; b3-/-* mice showed the mossy cells and their dendritic projections in the inner molecular layer (IML) (Figure 5.18A). In the *rl/+; b3-/-* compound mutant mice we observed several mossy cells in the granular layer (arrowheads) and quantification of mossy cell number in $100 \mu\text{m}^2$ of the stratum granulare (SG) revealed an increase in the number of mislocated mossy cells, suggesting a migration failure of mossy cells from DG, from their birth place to the granular layer (Figure 5.18B).

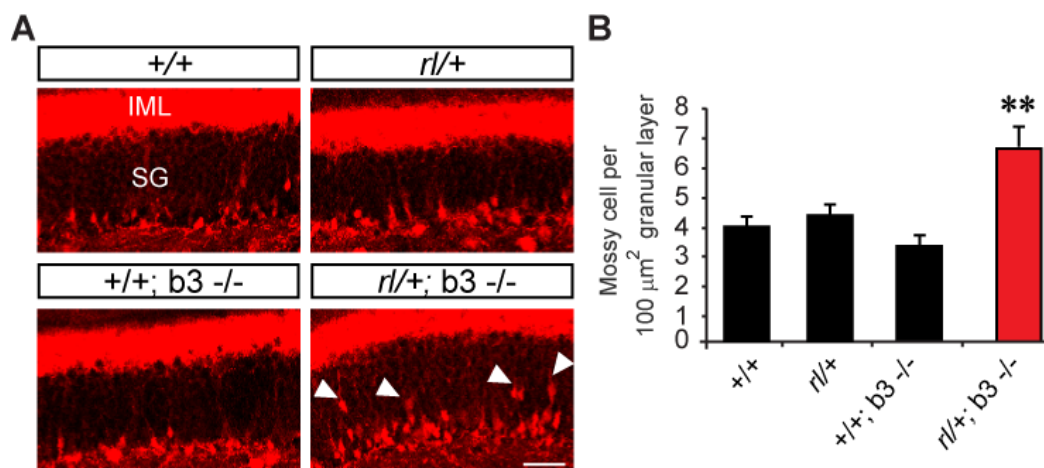


Figure 5.18 Mossy cells were observed in the granular layer of *rl/+; b3-/-* compound mutant mice. (A) Calretenin immunohistochemistry was performed to label the hilar mossy cell in the DG of *+/+*, *rl/+*, *b3-/-* and *rl/+; b3-/-* mice. The analysis revealed mislocated mossy cells in the granular layer (SG) of the *rl/+; b3-/-* compound mutant mice. Immunostaining signals were detected using cy3-conjugated secondary antibody. Scale bar = $50 \mu\text{m}$. (B) The cell number in the SG was measured and plotted as cell number per $100 \mu\text{m}^2$ area. In the *rl/+; b3-/-* compound mice the misled cell number increased. (B). (SEM, ** $P < 0.001$). IML, Inner molecular layer; SG, Stratum granulare.

5.1.2.4 The radial glial scaffold of the dentate gyrus is altered in the *rl/+; b3-/-* compound mutant mice.

As in cerebral cortex, hippocampal layering is achieved by proper migration of pyramidal and granular cells from their birth of origin to final locations. In hippocampus neurons are born in proliferative zone in the DG which also persists in postnatal life since the DG is fully developed only in the postnatal life. Late generated granule cells have to migrate from proliferative zone of hilus through and integrate into a fully differentiated dentate granule network. This migration in the DG, in contrast to most other brain regions, takes place via a persisting radial glia scaffold postnatally (Forster *et al.*, 2002, Weiss *et al.*, 2003). These glial cells provide a pool of granule cell precursors (Seri *et al.*, 2001) and also form a template for migrating granule cells. Reelin is required to achieve a proper radial glial scaffold and proper granule cell migration (Zhao *et al.*, 2004). Reelin has specific effects on these GFAP+ radial glia cells, which are required for the migration of hippocampal neurons (Forster *et al.*, 2002). It is a differentiation factor and a positional cue for the GFAP+ glial cells. In *reeler* mice the radial glial scaffold is severely altered (Forster *et al.*, 2002); therefore, it is likely that the migration defects of *reeler* mice are, at least in part, a consequence of malformations of the radial glial cells (Stanfield *et al.*, 1979b, Drakew *et al.*, 2002). In order to analyze the radial glial scaffold in *rl/+; b3-/-* compound mutant mice we performed GFAP immunostaining on *+/+*, *rl/+*, *b3-/-* and *rl/+; b3-/-* mice (Figure 5.19). A characteristic radially oriented glial scaffold was visualized both in the suprapyramidal and the infrapyramidal blade of the DG of postnatal (P10) *+/+*, *rl/+*, and *b3-/-* mice. In the *rl/+; b3-/-* compound mutant mice the GFAP+ cells had very short, ramified processes, and we observed a premature transformation of glial cells into astrocytes (Figure 5.19). Loss of proper radial glial scaffold in *rl/+; b3-/-* compound mutant mice could be, at least partially as in *reeler* mice, responsible for the granular and pyramidal cell layering defects.

5 Results

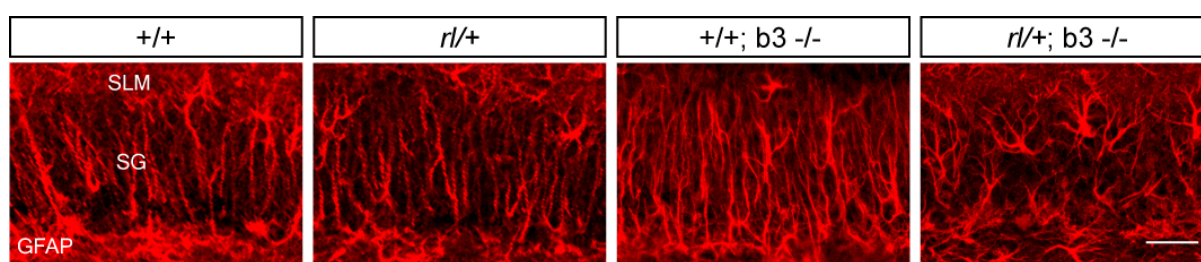


Figure 5.19 Radial glial scaffold is altered in the *rl/+; b3-/-* compound mutant mice. Staining for GFAP in the dentate gyrus was performed on coronal sections of *+/+*, *rl/+*, *b3-/-* and *rl/+; b3-/-* mice (P10). GFAP+ radial glial fibers of *+/+*, *rl/+* and *b3-/-* mice run perpendicular to the granular layer, whereas, in the *rl/+; b3-/-* compound mutant mice GFAP+ cells have short processes, thus resembling typical astrocytes. Immunostaining signals were detected using cy3-conjugated secondary antibody Scale bar = 50 μ m. H, Hilus; SG, Stratum granulare; SLM, Stratum locunosum moleculare.

5.1.2.5 The dendritic branching of hippocampal pyramidal neurons is increased in the *rl/+; b3-/-* compound mutant mice.

In the embryonic and early postnatal hippocampus Reelin is secreted at high levels from Cajal-Retzius cells into the SLM of the hippocampus proper (D'Arcangelo *et al.*, 1995). Pyramidal neurons of the CA1 region project towards the Reelin-rich SLM and thus are more likely to be affected in the *rl/+; b3-/-* compound mice. To investigate the dendritic branching of the pyramidal neurons, projecting from the SP to the SLM, we performed immunostaining using α -Calretenin antibody. The labeled neurons appeared to be normally laced in the pyramidal layer of *+/+*, *rl/+*, and *b3-/-* mice, however, there were ectopic neurons in the *rl/+; b3-/-* compound mutant mice (Figure 5.20A - arrowhead). The overall length and the orientation of the apical tree of the CA1 pyramidal neurons and their projections appeared normal in *+/+*, *rl/+*, and *b3-/-* mice, whereas these projections were misoriented in the *rl/+; b3-/-* compound mutant mice as well as in *rl/rl* mice (Figure 5.20A). The long projections from SP towards SLM were missing and *rl/+; b3-/-* compound mice showed high order branches, especially close to the cell body, compared to wild-type mice. To study this dendritic branching in detail we performed Sholl analysis on the pyramidal neurons. This is a commonly used quantitative analysis method to characterize the morphological characteristics of a neuron and is based on counting the number of dendrite intersections after concentric circles of gradually

increasing radius have been drawn starting from the center of the cell body (Sholl, 1953). Our Sholl analysis data revealed more than 50 % increased branching close to the cell body of pyramidal neurons in the *rl/+; b3-/-* compound mice compared to *+/+*, *rl/+* and *b3-/-* mice (Figure 5.20B, C).

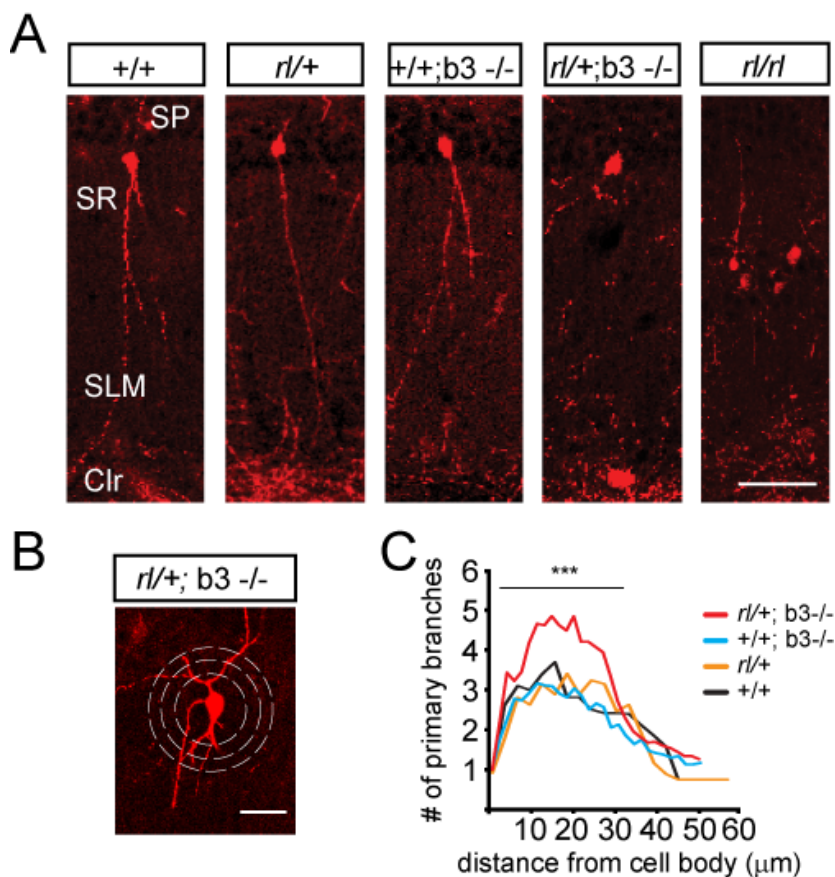


Figure 5.20 *Reeler*-like branching defects of pyramidal neurons was observed in the *rl/+; b3-/-* compound mutant mice. (A) Cell morphology of pyramidal neurons projecting from stratum pyramidale (SP) towards stratum locunosum moleculare (SLM) was analyzed. Single, long projections were observed in the wt (*+/+*), *rl/+* and *b3-/-* mice, whereas these projections were misoriented and misbranched in the *rl/+; b3-/-* compound mutant mice. Immunostaining signals were detected using cy3-conjugated secondary antibody. Scale bars = 25 μm . (B) Sholl analysis obtained from 20 neurons from each pyramidal layer of 3 animals showed increased branching 40 μm distance to the cell body of the *rl/+; b3-/-* compound mutant mice. (SEM, *** $P < 0.0001$). SG, Stratum granulare; SLM, Stratum locunosum moleculare; SP, Stratum pyramidale.

We also observed the dendritic branching by using a transgenic mouse line expressing YFP postnatally. YFP expression, under the control of *Thy1* promoter, is maintained through the adulthood in only a selection of neuronal populations (line M). These mice were bred with *rl/+; b3+/-* compound mice in order to get *b3-/-; YFP+* and *rl/+; b3-/-; YFP+* mice. The pyramidal neurons

5 Results

projecting towards SLM in hippocampal sections from P20 mice were examined by fluorescent confocal microscopy. Similar higher order branching pattern was observed in the *rl/+; b3-/-* compound mutant mice confirming the results from the Calretenin immunostaining (Figure 5.21A). Sholl analysis performed on YFP+ branches of both mice lines and the branching of the pyramidal cells of *rl/+; b3-/-* compound mutant mice showed again 48 % increase in branching observed in the *rl/+; b3-/-* compound mutant mice (Figure 5.21B).

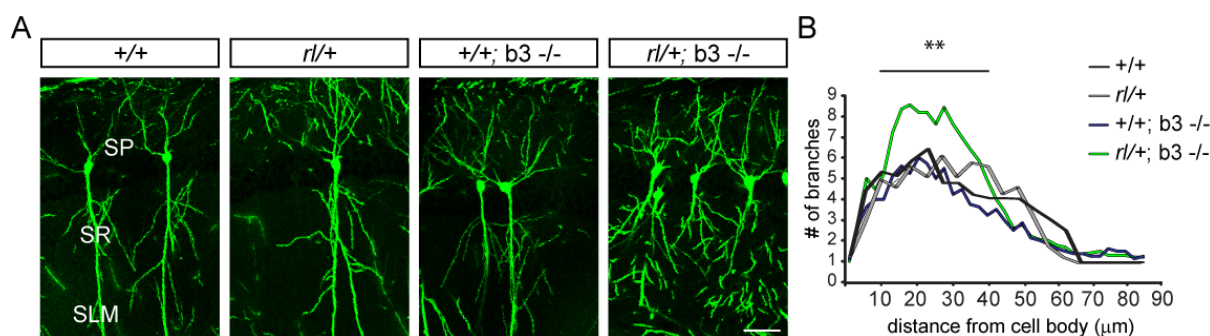


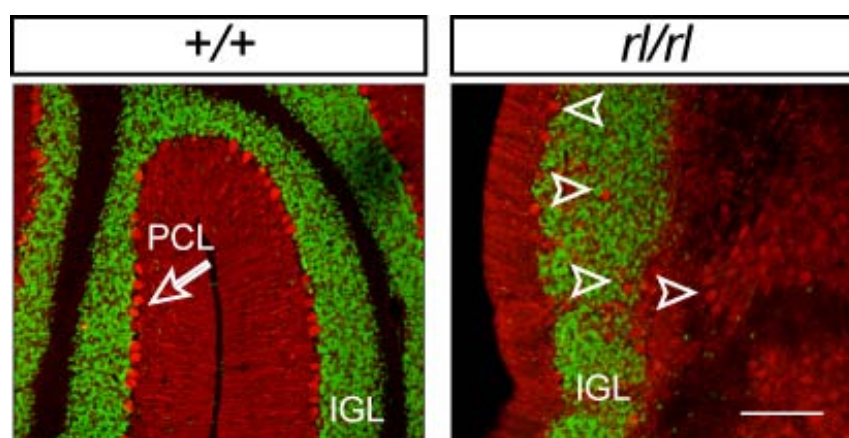
Figure 5.21 *Reeler*-like branching defects of pyramidal neurons were observed in YFP+; *rl/+; b3-/-* compound mutant mice. (A) Cell morphology of pyramidal neurons projecting from stratum pyramidale (SP) toward stratum locunosum moleculare (SLM) was analyzed. Single, long projections were observed by fluorescent confocal microscopy in the *b3-/-* mice, whereas these projections were misoriented and misbranched in the *rl/+; b3-/-* compound mutant mice. Scale bar = 25 μm. (B) Sholl analysis showed increased branching 40 μm close to the cell body of the *rl/+; b3-/-* compound mutant mice. Quantifications performed from 2 animals and 20 neurons from each pyramidal layer. (SEM, ** $P < 0.001$). SG, Stratum granulare; SLM, Stratum locunosum moleculare; SP, Stratum pyramidale.

These findings indicate further genetic interaction between Reelin and ephrinB3 signaling pathway, as *rl/+; b3-/-* compound mutant mice showed not only in cerebral cortex but also in hippocampus several *reeler*-like phenotypes.

5.1.3 *rl/+; b3-/-* and *rl/+; b2-/-* compound mutant mice show *reeler* like phenotypes in the cerebellum.

5.1.3.1 Cerebellar Purkinje cell migration requires ephrinB ligands for proper migration

Formation of cerebellum starts with the birth of Purkinje cells between E11 and E13. They migrate outwards along the radial glial cells and form the Purkinje cell layer (PCL), below the external granular layer (EGL). During the development of cerebellum Reelin is expressed by the granular cells and when Reelin is absent, although the Purkinje cells are born normal they do not form the PCL (Rice *et al.*, 2001) most probably due to the disorganized radial glial scaffold (Yuasa *et al.*, 1993). In *reeler*, *dab1* mutant *scrambler*, or *src/fyn* mutant mice Purkinje cells are misplaced and observed in clusters between the EGL and the ventricular zone (Kuo *et al.*, 2005). Purkinje cells can be stained by using a Calbindin antibody (Jande *et al.*, 1981) as well as antibodies against Dab1 (Rice *et al.*, 1998). As ephrinB2 ligands are expressed by Purkinje cells and ephrinB3 by granular cells (Migani *et al.*, 2007) we analyzed the PCL and EGL using Calbindin antibody to detect Purkinje cells and NeuN antibody to detect granular cells both in single knockout and *rl/+; b3-/-* and *rl/+; b2-/-* compound mutant mice. First the PCL and granular cell layer of *+/+* with *rl/rl* and then *b3-/-* with *rl/+; b3-/-* were investigated. The *rl/rl* cerebellum showed PCL and granular cell layering defects (arrowheads) (Figure 5.22).



5 Results

Figure 5.22 Granular and Purkinje cell layering shows defects in the cerebellum of *reeler* mice. Cerebellum of wild type (+/+) and *reeler* (*rl/rl*) coronal sections stained with NeuN (green) and Calbindin (red) antibody and analyzed by confocal microscopy. A compact NeuN+ granular layer with Calbindin+ Purkinje cell layer (arrow) was detected in the wild-type mice, whereas in the *rl/rl* mice the Purkinje cells were misplaced (arrowheads) and the granular cell layer was disturbed. Immunostaining signals were detected using Alexa-fluor-488 and cy3-conjugated secondary antibodies. Scale bar = 150 μm . PCL, Purkinje cell layer.

In order to investigate the role of ephrinB3 we next analyzed the wild-type, *rl/+*, *b3-/-* and *rl/+; b3-/-* compound mice (Figure 5.23). In *rl/+*, *b3-/-* as well as in *rl/+; b3-/-* compound mice Purkinje cells were aligned as in wild-type (Figure 5.23A) and neither Purkinje cell branching (Figure 5.23B) nor in cell layering (Figure 5.23C) major changes were observed.

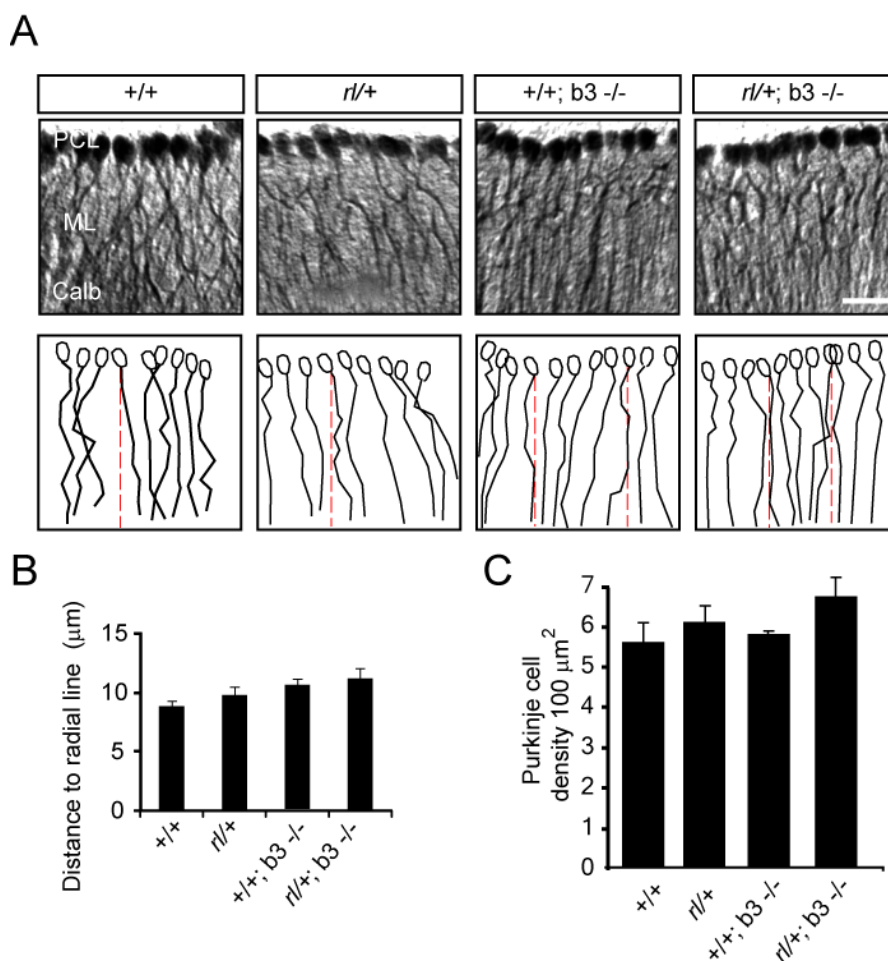


Figure 5.23 Purkinje cell branching and layering in *rl/+; b3-/-* compound mice was normal. (A) Purkinje cell layer and dendritic branching of Purkinje cells of sagittal sections of the adult cerebellum from *+/+*, *rl/+*, *b3-/-* and *rl/+; b3-/-* mice were analyzed using Calbindin immunolabelling. Immunostaining signals were detected using the DAB staining protocol. (A, B) Distance of the primary branches to the perpendicular radial line (dashed line) was measured and no differences were observed in the *rl/+; b3-/-* compound mice compared to controls. (C) Purkinje cell distribution showed no changes in the *rl/+; b3-/-* compound mice. Scale bars = 50 μ m. ML, Molecular layer; PCL, Purkinje cell layer.

The granular cells are produced in the EGL and then migrate along radial glial fibers to the inner granular cell layer (IGL). As ephrinB3 is expressed in the granular cell layer, we investigated the granular cells further with NeuN immunostaining and analyzed their layering (Figure 5.24). In *+/+*, *rl/+* and *b3-/-* mice the granular cell layer was normal, whereas in the *rl/+; b3-/-* compound mice an accumulation of granular cells in the IGL was observed (Figure 5.24A). The quantification of cells in 100 μ m² of IGL showed the significant increase in granular cell density (Figure 5.24B).

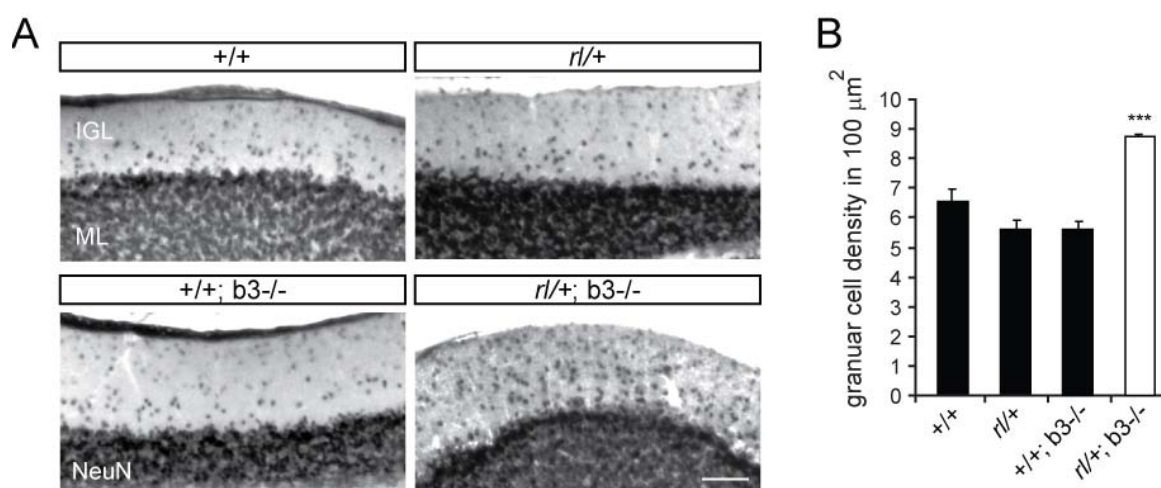


Figure 5.24 Granular cell layering is disorganized in *rl/+; b3-/-* compound mutant mice. (A) NeuN immunohistochemistry performed on *+/+*, *rl/+*, *b3-/-* and *rl/+; b3-/-* postnatal cerebellum (P20). Granular cells were mainly observed as densely packed in the inner granular layer (IGL). In the IGL of *+/+*, *rl/+* and *b3-/-* few cells were detected, whereas in the IGL of *rl/+; b3-/-* cerebellum the granular cell density was higher. Immunostaining signals were detected using the DAB staining protocol. Scale bar = 50 μ m. (B) Quantifications were performed on 4 images obtained from 6 cerebellum of each genotype and number of cells in 100 μ m² were plotted. (SEM, *** P <0.0001). IGL, Inner granular layer; ML, Molecular layer.

5 Results

Next, we analyzed the cerebellum of the ephrinB2 knockout and *rl/+*; *b2*^{-/-} compound mutant mice using Calbindin immunolabelling (Figure 5.25). Purkinje cells are born in the VZ and migrate outwardly to form the PCL. As ephrinB2 ligands are expressed by Purkinje cells we investigated the wild-type, *rl/+*, *b2*^{-/-} and *rl/+*; *b2*^{-/-} mice and didn't detect any gross morphology alteration (Figure 5.25A, C). Next we studied the Purkinje cells and observed PCL in *b2*^{-/-} as in the *+/+* mice, however, the neuronal processes of *b2*^{-/-} mice were shortened and not radially elongated as it is in the wild-type mice (left panel) (Figure 5.25A, B). Defects were aggravated in the *rl/+*; *b2*^{-/-} compound mice indicating that ephrinB2 is necessary for Reelin function during cerebral PC branching.

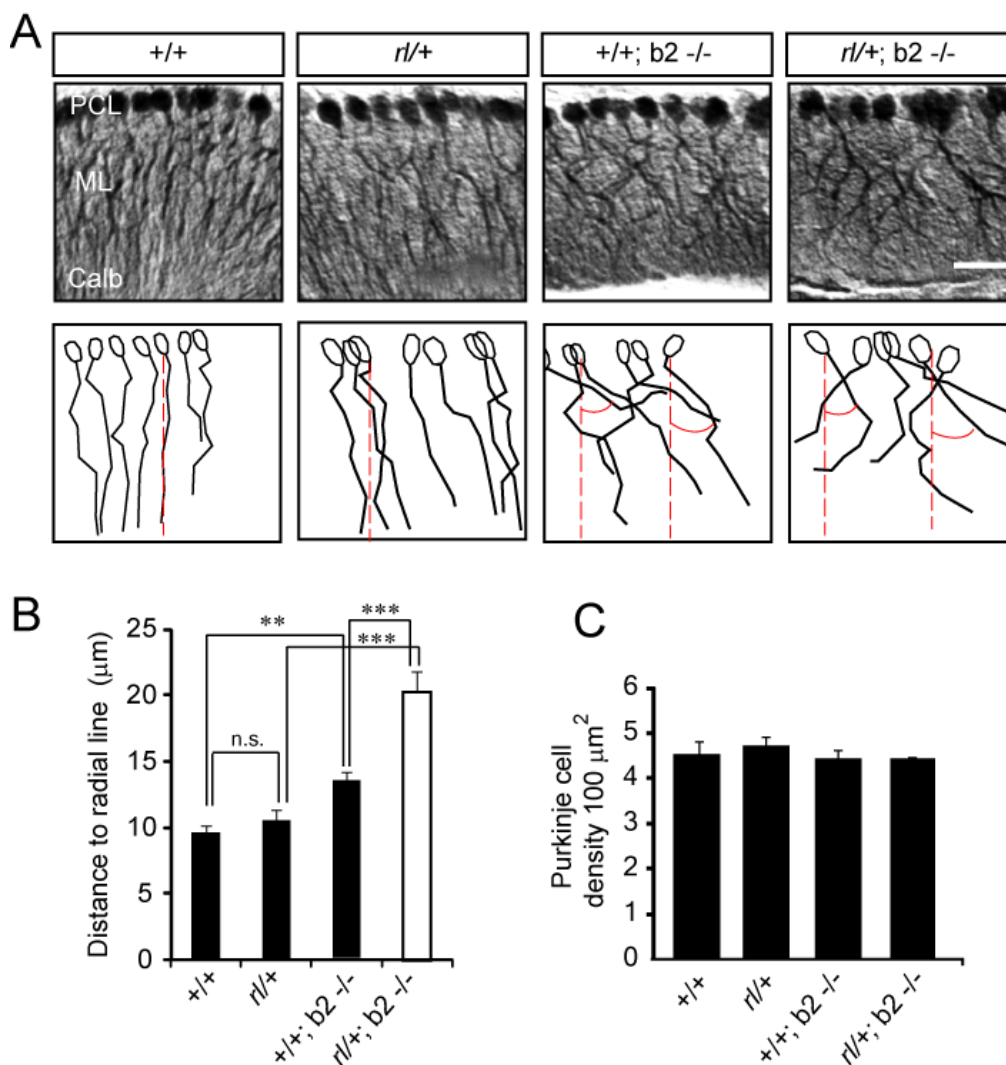


Figure 5.25 Dendritic branching but not layering of Purkinje cells were altered in the *rl/+; b2/-* compound mice. Dendrite structure of Purkinje cells in the Purkinje cell layer was visualized by Calbindin immunolabelling of adult cerebellum of *+/+*, *rl/+*, *b2/-* and *rl/+; b2/-*. Immunostaining signals were developed using the DAB protocol. (B) Distance of primary branches to the radial perpendicular line (dashed line) showed altered dendritic branching of Purkinje cells in the single ephrinB2 knockout (*b2/-*) and stronger alterations in the *rl/+; b2/-* compound mice. (C) The PCL cell density of *b2/-* and *rl/+; b2/-* mice showed no defects. (SEM, ** $P < 0.001$, *** $P < 0.0001$, n.s. not significant). Scale bars = 50 μm . IGL, Inner granular layer; PCL, Purkinje cell layer.

Taken together, our results identify ephrinBs as co-receptors for Reelin signaling required for the function of Reelin in neuronal migration during the development of the layered structures in the cerebral cortex, hippocampus and cerebellum. Some defects, for example in the arborization of Purkinje cells in the cerebellum, were already detectable in single ephrinB2 knockouts although lowering the dosage of Reelin allowed a better penetrance of the defects caused by the loss of function of individual ephrinB ligands. This suggests a certain redundancy between the three ephrinBs with regard to activation of Reelin signaling. In agreement, triple ephrinB1/B2/B3 mutant mice showed phenotypes resembling the *reeler* mouse (Figure 5.26). In order to visualize the neurons in the MZ of the triple ephrinB1B2B3 knockout mice (*b1b2b3/-*) we performed NeuN immunostaining on coronal brain sections from postnatal (P21) mice. NeuN immunohistochemistry allowed us to study cell invasion into the MZ of the triple knockout mice. When compared to confocal images taken from *b3/-* mice the triple knockout mice showed *reeler*-like cell invasion into the MZ (Figure 5.26A). Cell density in the MZ (dashed line) was assayed by counting cell number and averaging to 100 μm^2 area. Quantification of neurons in the MZ and subsequent statistical analysis revealed a significant increase in NeuN+ neurons in the triple knockout mice from 11.31 ± 0.41 cells/100 μm^2 (wild-type control, *+/+*) to 12.57 ± 0.82 cells/100 μm^2 (Figure 5.26B). Next, the *b3/-* and *b1b2b3/-* hippocampi were stained with NeuN-antibody. The layering of CA3 was strongly affected in triple knockout (arrows) and an expansion of CA1 region was observed (Figure 5.26C).

5 Results

Despite this redundancy, the differences in the phenotypes associated with ephrinB2 and ephrinB3 loss-of-function suggest that the two ephrins might have differential roles in activating Reelin signals at different brain structures.

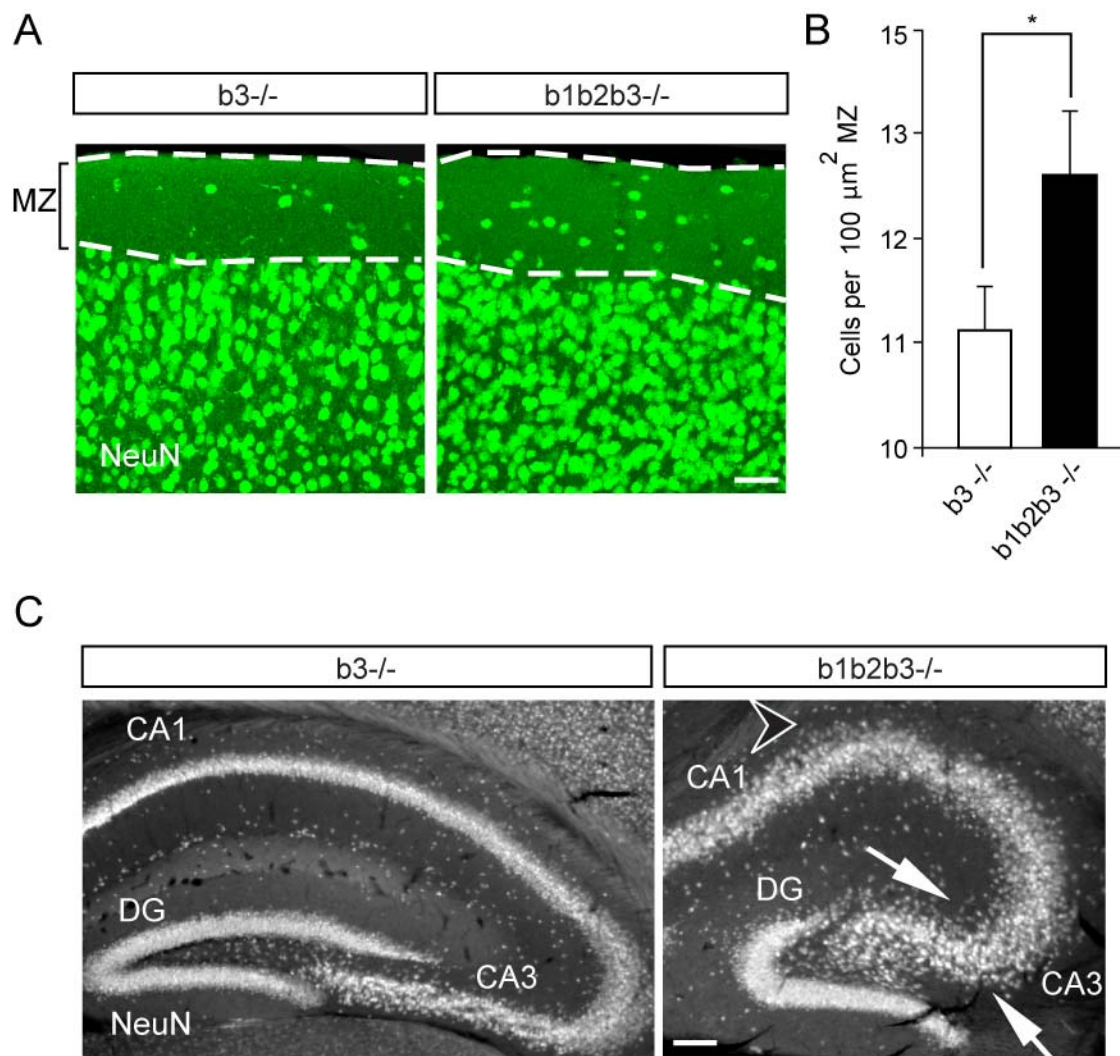


Figure 5.26 EphrinB1B2B3 triple knockout phenocopies the reeler mutation. (A) NeuN immunostaining of coronal cortical sections through the neocortex of adult ephrinB3 knockout (b3^{-/-}) showed only few neurons in the Marginal zone (dashed line), whereas the MZ of triple ephrinB knockout mice (b1b2b3^{-/-}) shows invasion of neurons in the MZ (defined with dashed lines). (B) Stereological quantification of cell numbers in the MZ of b3^{-/-} and b1b2b3^{-/-} are shown representatively. Quantification were performed from 2 different animal groups and pictured as number of cells in 100 μm^2 MZ. (C) Histological analysis of adult hippocampus of b3^{-/-} and b1b2b3^{-/-} mice with NeuN immunostaining. The layering of CA3 was strongly affected in triple knockout (arrows) and an expansion of CA1 region was observed (arrowhead). (SEM, ** P>0.001). Scale bars: 50 μm (A), 100 μm (C). MZ, Marginal zone, DG, Dendate gyrus, CA1 and CA3, hippocampal areas.

5.2 Reelin, Dab1 and ephrinB ligands are in the same signaling complex.

In order to get mechanistic insights on how ephrinB ligands can crosstalk to Reelin signaling to control the correct position of neurons in the layered structures in the brain we next assessed the biochemical interaction of these two pathways. We performed a directed proteomic analysis of ephrinB-binding proteins from a neuroblastoma cell line using the tandem affinity purification–mass spectrometry methodology (Angrand *et al.*, 2006) and identified Reelin as a putative ephrinB-interacting protein (data not shown).

5.2.1 Reelin and Dab1 binds to ephrinB ligands.

In order to confirm the proteomics data we first studied the biochemical interaction of ephrinB ligands with Reelin. First, Reelin was collected from 293T cells, stably expressing Reelin or GFP, as control, concentrated and analyzed by Western blot (Figure 5.27A). This concentrated Reelin was bound to Sepharose beads and used for pull-down experiments from mouse brain lysates. Reelin efficiently pulled down ephrinBs (Figure 5.27B). Moreover, Reelin was also strongly bound to the extracellular domain of ephrinB3 and also to ephrinB2, suggesting that both ephrinBs could influence the *in vivo* functions of Reelin signaling (Figure 5.27C). We further confirmed the ability of Reelin to associate with ephrinBs by co-immunoprecipitation of both endogenous proteins from brain lysates (Figure 5.27D). In the control pre-immune serum Reelin protein was not detectable. These suggested that Reelin and ephrinB ligands are in the same signaling complex *in vivo*.

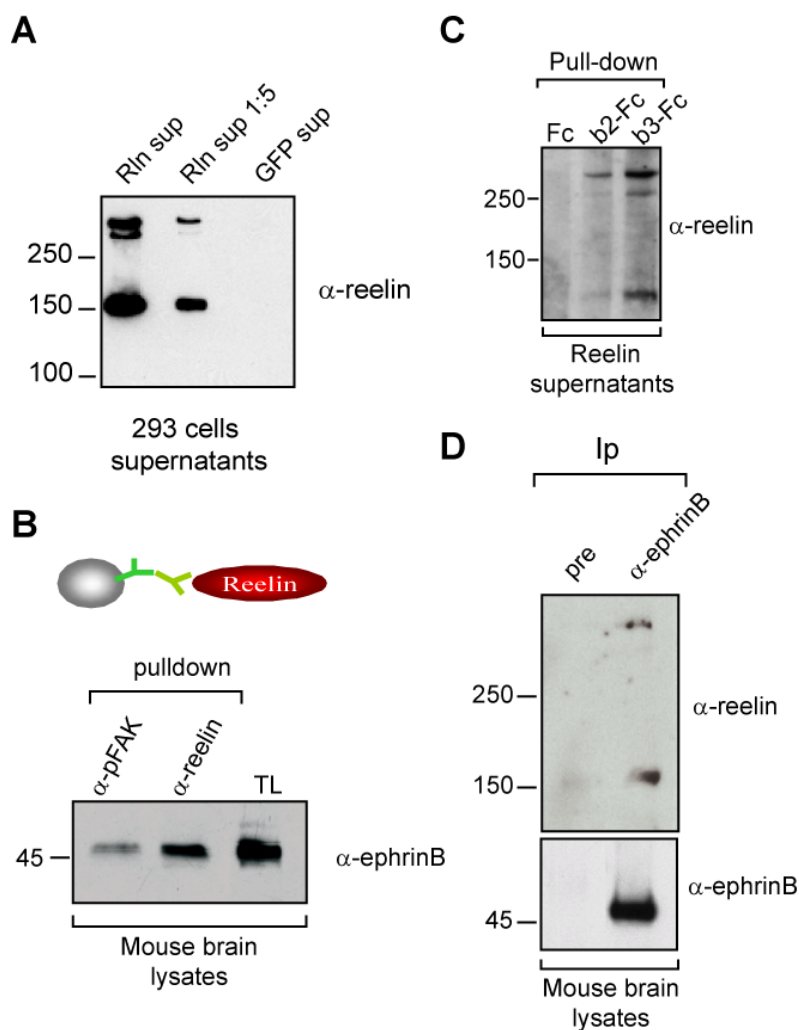


Figure 5.27 Reelin binds to ephrinB ligands. (A) Reelin-containing supernatants were collected from 293T cells grown in DMEM without serum and 5x concentrated. Reelin protein was detected using Western blot analysis with α -Reelin antibody (1:500, Chemicon). (B) Binding of Reelin and ephrinB was investigated by pulldown assay. Mouse embryonic brain lysates were incubated with Reelin bound to Sepharose beads and ephrinB was detected using α -ephrinB antibody (1: 200, Santa Cruz). (C) The extracellular domain of ephrinB2 and ephrinB3 binds to Reelin. Supernatants of 293 cells expressing Reelin were incubated with ephrinB2-Fc, ephrinB3-Fc or Fc as a control. (D) Reelin was precipitated from embryonic mouse brain (E16.5) lysates using α -ephrinB antibodies. Reelin was detected in ephrinB precipitates but not in the control pre-immune serum.

5.2.2 Reelin and ephrinB ligands functionally interact.

We next analyzed the functional interaction between Reelin signaling pathway with ephrinB ligands.

Dab1 is an intracellular adapter protein, which is expressed in migrating neurons and gets phosphorylated by Src kinases upon binding of Reelin to the two lipoprotein receptors. In

accordance to many studies it has been accepted that tyrosine phosphorylation of Dab1 is central to Reelin signaling (Howell *et al.*, 2000, Herrick *et al.*, 2002). In order to study the interaction between ephrinB ligands and Dab1 embryonic brain cortices of E16.5 and mice were homogenized and immunoprecipitated with an antibody against ephrinB ligands. At E16.5, when corticogenesis is actively taking place, Dab1 protein and phosphorylated Dab1 was detected in the ephrinB immunoprecipitates (Figure 5.28). Dab1 protein has a molecular weight of 80 kDa and the phosphorylated Dab1 was detected by using an antibody against phospho-Tyrosine (P-Tyr) with the corresponding band at 80 KDa. These binding analyses suggest that ephrinBs are recruiting the different players required for Reelin signaling.

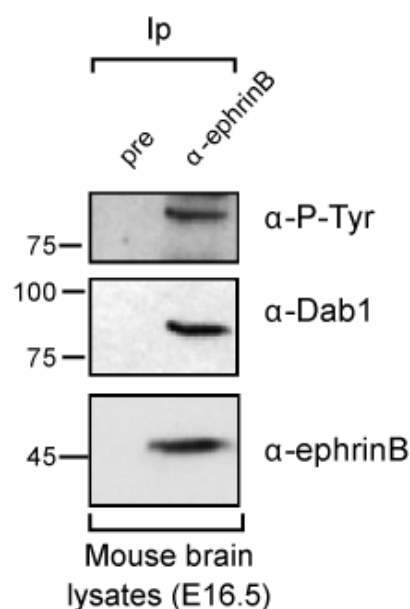


Figure 5.28 Dab1 is in complex with ephrinB ligands. Brain lysates from E16.5 brain cortices and E12.5 heads were homogenized. The lysates were immunoprecipitated with α -ephrinB antibody and analyzed with Western-blot using α -Dab1, α -pTyr and α -ephrinB antibodies. The middle blot shows the Dab1 protein and at the corresponding molecular weight. P-Tyr antibody detected phosphorylated Dab1 protein (upper blot).

5.2.3 Dab1 phosphorylation levels are reduced in ephrinB3 knockouts.

To reveal the requirement of ephrinB-mediated recruitment and activation of Src kinases for Reelin signaling embryonic brain lysates of wild-type, *rl/rl* and *b3^{-/-}* were monitored for Dab1 and pDab1

5 Results

levels (Figure 5.29). Expectedly, in mice lacking the Reelin protein Dab1 phosphorylation was not detected and Dab1 levels were increased. Upon its phosphorylation Dab1 is degraded via proteosomes leading to accumulation of Dab1 protein (Arnaud *et al.*, 2003). Interestingly, in mice lacking ephrinB3 ligands Dab1 phosphorylation levels were greatly reduced that correlated with an increase in Dab1 total levels suggesting that ephrinB ligands are required for efficient Reelin signaling.

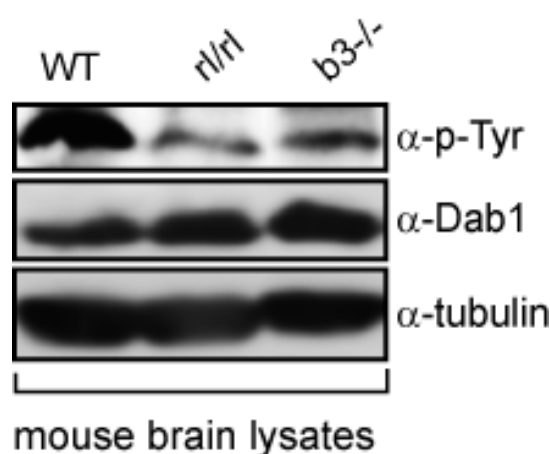


Figure 5.29 pDab1 levels were reduced in the absence of ephrinB3 ligands. Total brain lysates (P20) of wild-type, *rl/rl* and *b3-/-* mice were analyzed for levels of Dab1 and phosphorylated Dab1 using Dab1 (1:1000, Chemicon) and pTyr antibodies (1:1000, Upstate). Western blots showed a lack of phosphorylation in *reeler* mice and reduction of Dab1 phosphorylation levels in the absence of ephrinB3 ligands. A corresponding increase in Dab1 levels was observed when phosphorylation levels were reduced both in *rl/rl* and *b3-/-* mice.

The requirement of ephrinB ligands for efficient Reelin signaling was also analyzed using cortical neurons in culture. Primary cortical neuron cultures from E16.5 mice were grown for 5 days (5 DIC) and then stimulated with Reelin and GFP supernatants as a control, to observe Dab1 phosphorylation as a read out for Reelin-induced signaling. Stimulated wild-type primary cortical neurons with Reelin showed phosphorylated Dab1 as bright puncta in the dendritic shaft of neurons (Figure 5.30A,a) as well as around the cell periphery (Morimura *et al.*, 2005). This increase was also confirmed by quantifying the pDab1 signal intensity on dendritic branches (Figure 5.30A,b) as well as by Western blot using α-Dab1 and α-pTyr antibodies (Figure 5.30A,c). After setting up our culture

system we addressed the requirement of ephrinB-mediated recruitment and activation of Src kinases for Reelin signaling and investigated in primary cortical neurons lacking ephrinB ligands the phosphorylated Dab1 levels upon Reelin and GFP supernatant stimulation for 1 h. Reelin activates Src family kinases (SFKs) which then phosphorylates Dab1 on Tyr-220 residue, one of the major Reelin-induced phosphorylation sites of Dab1 (in cultured neurons in (Howell *et al.*, 1999b, Arnaud *et al.*, 2003, Keshvara *et al.*, 2001). Therefore, we used Tyr-220 as well as Tyr-232 specific pDab1 antibodies to compare phosphorylated Dab1 levels in cells upon Reelin stimulation. Levels of Dab1 phosphorylation were reduced in ephrinB2 and ephrinB3 knockout cultures compared to their wild-type controls (Figure 5.30B). An accumulation of Dab1 protein was observed, again correlating with the fact that in absence of Reelin, mDab1 protein is not degraded (Figure 5.30B,a, b, lower blots). We also confirmed our biochemical assays by immunocytochemistry. Wild-type and ephrinB3 knockout cortical neurons were stimulated with Reelin and GFP supernatants, and pDab1 was visualized as bright puncta on dendritic shafts (Figure 5.30C,a). The pDab1 levels in b3^{-/-} mice were already altered in un-stimulated case and upon stimulation the pDab1 signal intensity was reduced in b3^{-/-} neurons compared to wild type (Figure 5.29C,b)

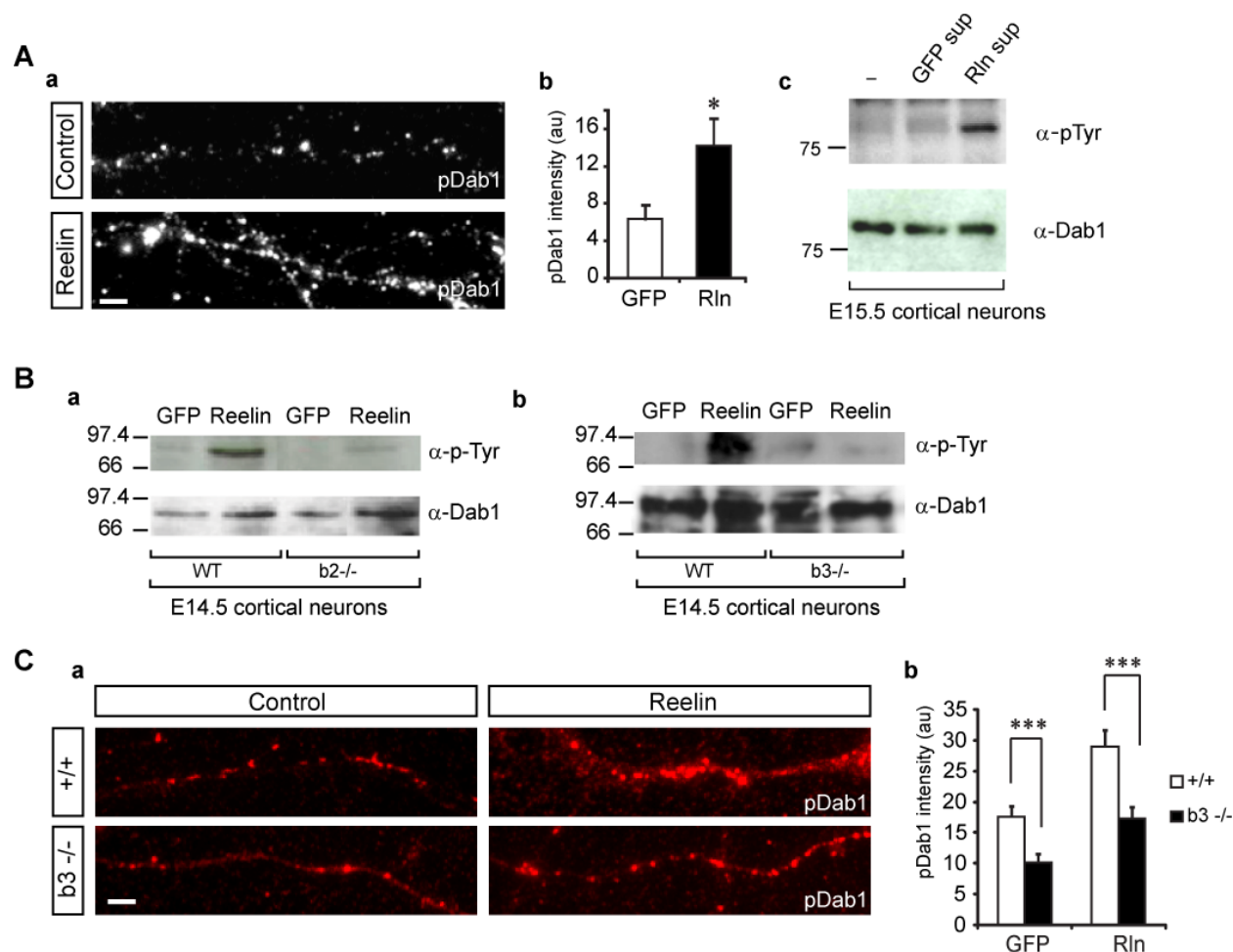


Figure 5.30 Phosphorylation of Dab1 is impaired in the absence of ephrinB ligands. (A) Wild-type primary cortical neurons stimulated with Reelin and GFP to observe phosphorylated Dab1 (pDab1) levels. Reelin stimulation activated Dab1 phosphorylation. Scale bars: 2 μ m. The increase was confirmed by measuring pDab1 intensity on dendrites as well as on cell lysates by Western blot. (B) Cortical neuron cultures from b3^{-/-} and b2^{-/-} mice and their wild-type litter mates were prepared from E16.5 embryonic brains. The neurons were cultured 5 days in vitro and Dab1 phosphorylation was induced by Reelin and GFP stimulation. Lysates from these cells were analyzed by Western Blot using α -phospho Dab1 (p-Dab1) antibody. The blots showed a reduction in Dab1 phosphorylation upon Reelin stimulation in both ephrinB ligand lacking cultures and a corresponding increase in Dab1 levels. (C) Stimulation of wild-type cortical neurons with Reelin enhanced Dab1 phosphorylation whereas; ephrinB3 knockout cultures didn't show same levels of phosphorylation (C, a). (C, b) Quantification of pDab1 intensity showed a significant impairment in Dab1 phosphorylation of ephrinB3 knockout cultured neurons. Immunostaining signals were detected using Alexa-Fluor-488-conjugated secondary antibody. (SEM, *P<0.05; ***P<0.0001).

5.2.4 EphrinB ligands are in complex with Reelin receptors, ApoER2 and VLDLR.

We next investigated the interaction of LDL receptors, ApoER2 and VLDLR with ephrinB ligands. It has been shown that stimulation of cortical neurons with a soluble pre-clustered form of EphB receptors ectodomains fused to the Fc portion of human IgG (EphB3-Fc) leads to the activation of Src kinases in ephrinB clusters (Palmer *et al.*, 2002). As ephrinB3 binds with high affinity to EphB3 (Liu *et al.*, 2006b) we stimulated cortical neuron cultures (from E16.5 mice) with EphB3-Fc to detect ephrinB clusters on the cell membrane. EphB3-Fc, but not Fc control, stimulation of primary cortical neurons induced the formation of large ephrinB clusters at the membrane (Figure 5.31) that co-localized extensively with both Reelin receptors, ApoER2 and VLDLR. (Figure 5.31 A, B). These results indicate that the two membrane bound receptors for Reelin are clustered in the same complex with ephrinB ligands.

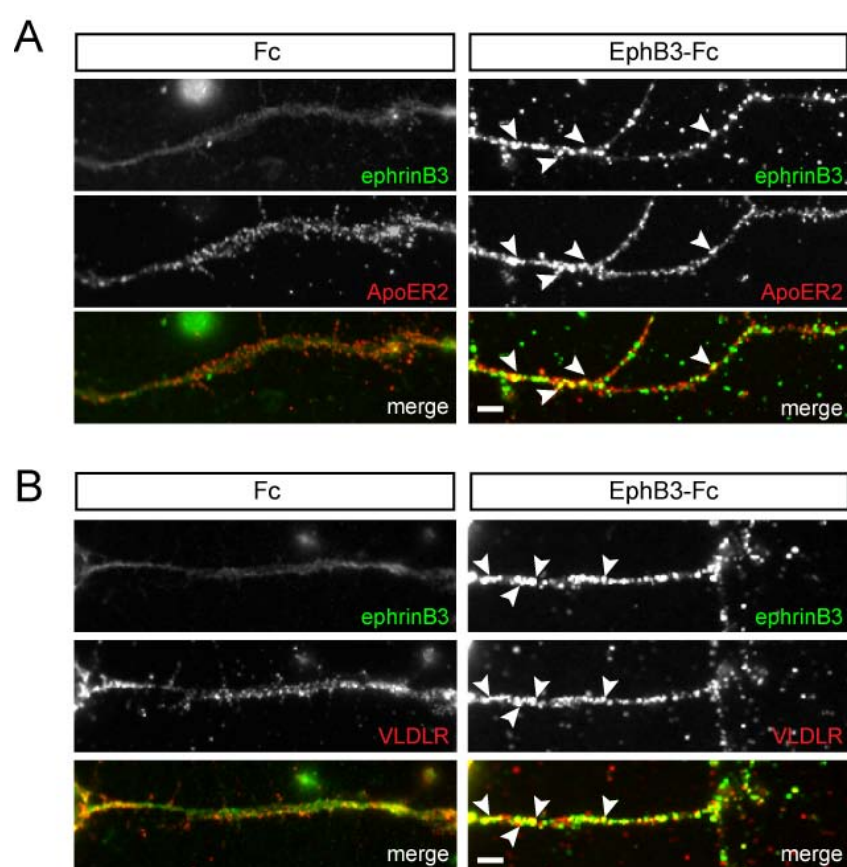


Figure 5.31 ApoER2 and VLDLR are in the same complex with ephrinB3 ligands. (A, B) Primary cortical neurons from E16.5 mice were stimulated with soluble EphB3-Fc and Fc to visualize ephrinB3 cluster on the membrane (green puncta). ApoER2 and VLDLR were visualized using specific antibodies for those receptors (red puncta). Analysis of double immunolabelling revealed co-localization of ephrinB3 ligands with ApoER2 and VLDLR, (arrowheads in A and B respectively). Immunostaining signals were detected using cy2- and cy3-conjugated secondary antibodies. Scale bars: 2 μ m.

5.2.5 Dab1 phosphorylation is induced following ephrinB3 activation.

In order to investigate whether ephrinB3 reverse signaling regulates Dab1 phosphorylation, we stimulated cultured primary mouse cortical neurons (from E16 mice) with soluble EphB receptor. EphB3-Fc, but not control Fc, stimulation of primary cortical neurons induced the formation of large ephrinB clusters at the membrane seen as bright puncta in dendritic shafts (Figure 5.32). On the same dendritic branches phosphorylation of Dab1 was visualized using antibodies specific for tyrosine residues, Tyr-220 and Tyr-232, of Dab1. Double immunofluorescence showed co-localization of big ephrinB patches with pDab1 clusters upon stimulation with EphB3 (Figure 5.32A, arrowheads) showing that activation of ephrinB3 ligands by stimulation of cortical neurons with EphB3-Fc leads to the recruitment and phosphorylation of Dab1 in ephrinB clusters.

Interestingly, co-stimulation of cortical neurons with Reelin and EphB3-Fc enhanced the Dab1 phosphorylation compared to only Reelin or only EphB3-Fc stimulation levels (Figure 5.32B,a). Quantification of pDab1 signal intensity on dendritic branches and western-blot analyses (Figure 5.32B, b&c) showed a significant enhancement in pDab1 levels, supporting the interaction between two signaling pathways and the co-receptor function of ephrinBs .

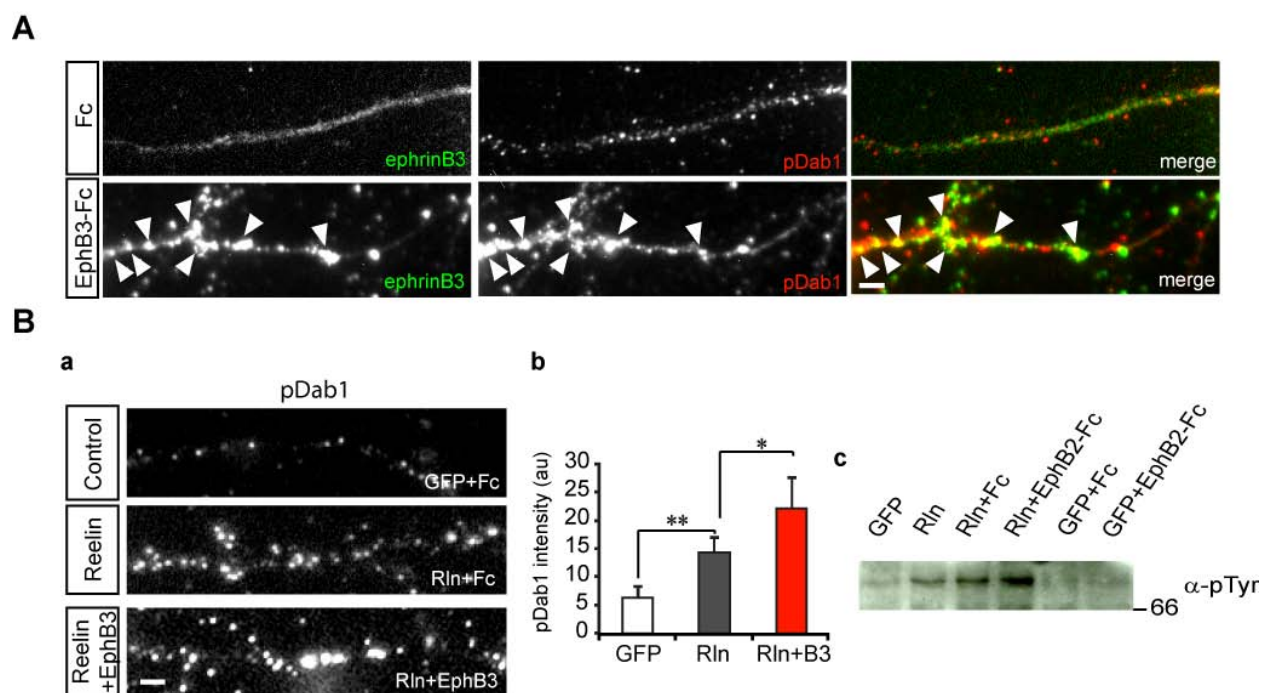


Figure 5.32 Dab1 phosphorylation is induced by Reelin and EphB3 stimulation. (A) Analysis of Reelin signaling in WT cortical neurons cultures from E16.5 + 5DIC. EphrinB3 ligands were activated by stimulation of pre-clustered form of EphB3-Fc and Fc as control. Activation of ephrinB reverse signaling lead to formation of ephrinB patches (green puncta) as well as pDab1 phosphorylation (red puncta). Moreover, ephrinB ligands and pDab1 co-localized (arrowheads). Immunostaining signals were detected using Alexa-Fluor-488- and cy3-conjugated secondary antibodies. Scale bar: 2 μ m. (B) Cortical neurons were stimulated with GFP/Fc as control, Rln, and Rln+EphB3-Fc. Co-stimulation of Reelin pathway and ephrinB reverse signaling enhanced Dab1 phosphorylation. Immunostaining signals were detected using cy3-conjugated secondary antibody (B, a). (B, b) Signal enhancement was observed by measuring pDab1 signal intensity on dendrites. (B, c) Stimulated cells were lysed and pDab1 levels were analyzed by Western blot. Scale bar = 2 μ m. (SEM, * P <0.05; ** P <0.001).

5.3 EphrinB reverse signaling stimulation can rescue *reeler*

phenotypes in the cerebral cortex.

5.3.1 Activation of ephrinB ligands is sufficient to activate Reelin signaling in

cortical neuron cultures.

Collectively, our data suggested that ephrinB ligands and Reelin are in the same signaling complex and lack of ephrinB ligands cause various alteration both in the signaling pathway and also in cortical

5 Results

morphology. Next, we addressed the question if activation of ephrinB ligands could also activate the Reelin signaling pathway and rescue the *reeler* phenotype. We first prepared cortical neuron cultures from *reeler* mice (E16.5) and stimulated both wild-type and *reeler* cultures with Reelin. Cortical neurons isolated from *reeler* mice showed the expected decreased Dab1 phosphorylation compared to the cortical neurons isolated from the wild-type littermates and, as has been shown in several studies, stimulating *reeler* neuron cultures with exogenous Reelin rescued Dab1 phosphorylation (Howell *et al.*, 1999b) (Figure 5.33). More importantly, Dab1 phosphorylation in *reeler* neurons was rescued solely by activation of ephrinBs with EphB receptors reflecting the importance of ephrinBs as co-receptors to activate signaling through the Reelin receptors VLDLR and ApoER2 (Figure 5.33A, B).

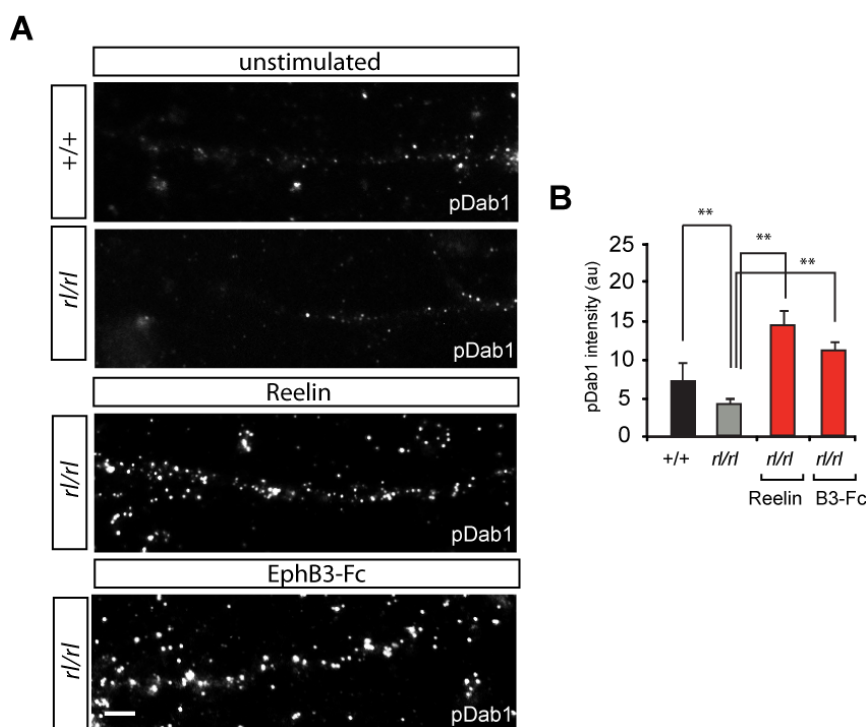


Figure 5.33 Activation of ephrinB ligands is sufficient to activate Reelin signaling in cortical neuron cultures. (A) Cortical neuron cultures from wt (+/+) and *reeler* (*rl/rl*) mice were analyzed for Dab1 phosphorylation after different stimulations. Stimulation of cultures with Reelin induced Dab1 phosphorylation not only in +/+ but also in *rl/rl* mice. Pre-clustered EphB3-Fc stimulation of cortical neurons also induced Dab1 phosphorylation in *rl/rl* neurons. Immunostaining signals were detected using cy3-conjugated secondary antibody. Scale bar = 2 μ m. (B) The intensity of phosphorylated Dab1 was measured on 100 dendritic branches of 30 different neurons of each genotype from 3 different experiments. A representative graph is shown. (SEM, **P<0.001).

5.3.2 Activation of ephrinBs rescues cortical migration defects in the *reeler* mouse.

We next analyze whether it was possible to rescue the migration defects observed in *reeler* mice by solely activating ephrinB reverse signaling. Over the past few years, the analysis of cell migration has greatly improved by the development of organotypic slice cultures that recapitulate, both in time and space, the movement of cortical neurons from the ventricular zone to the cortex (*Anderson et al.*, 1997).

We prepared organotypic slice cultures of embryonic brains from *reeler* and wild type mice. The pregnant females (E16.5) were injected with BrdU 1 hour prior embryonic brain isolation and slice preparation. The BrdU labels the later born neurons which constitute layer II-III after migration. The embryos were removed and organotypic slices of 300 μm thickness were prepared. After 4 hours recovery, slices were stimulated with pre-clustered EphB3-Fc to activate ephrinB3 reverse signaling as well as with pre-clustered Fc fragment as a negative control. Following 3 days of repeated stimulation the BrdU labeled neurons were labeled with BrdU immunohistochemistry (Figure 5.34A). As expected, in wild-type cultures the BrdU+ neurons were mainly located at layer II-III, whereas in *reeler* cultures, the BrdU labeled neurons were at deeper layers, representing the outside-in layering of *reeler* phenotype. Remarkably, in EphB3-Fc stimulated *reeler* cultures the BrdU labeled cells were observed in more superficial layers, as in the wild-type cultures (Figure 5.34B, C), suggesting that activation of ephrinB ligands is sufficient to induce the proper migration in the cortex in absence of Reelin.

5 Results

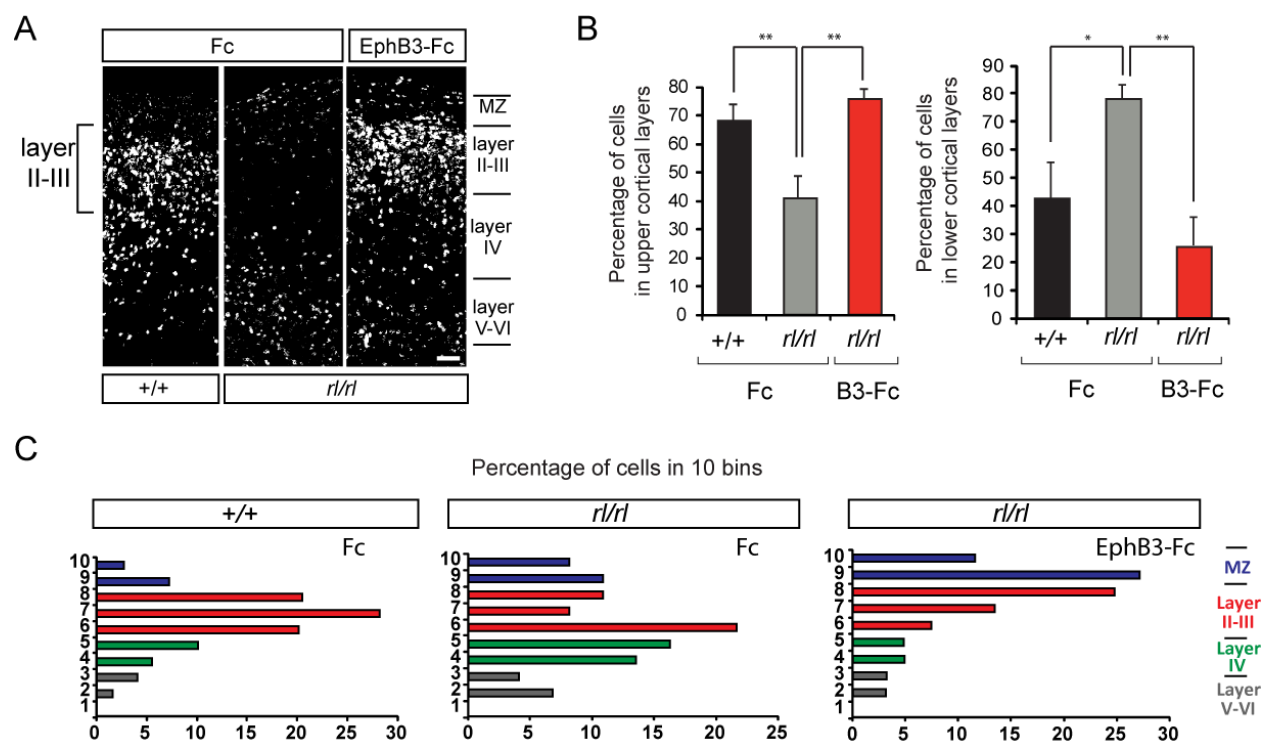


Figure 5.34 Activation of ephrinB ligands rescues the cortical migration defects of *reeler* mouse. (A) Heterozygous *reeler* (*rl/+*) females, crossed with *rl/+* males, were injected with BrdU at E16.5 and organotypic cultures were prepared from wild-type (*+/+*) and *reeler* (*rl/rl*) embryos upon 1 hour of injection. Cultures were stimulated with pre-clustered EphB3 and Fc in order to study the role of the ephrinB3 reverse signaling during cell migration. Stimulation of wt cultures with Fc showed normal cortical migration. Fc stimulated *reeler* cultures showed outside-in cell migration and BrdU+ cells observed in deeper layers. Immunostaining signals were detected using Alexa-Fluor-488-conjugated secondary antibody. (B) Activation of ephrinB3 signaling by EphB3 stimulation of *reeler* cultures rescued *reeler* phenotype, as BrdU+ cells were located in superficial cortical layers as *+/+* mice. Scale bar = 50 μ m. (C) The cortex was divided into 10 equal bins, starting from ventricular zone and distance of each BrdU+ cell to the MZ was measured. Then the percentage of cells in each bin was plotted as frequency versus distance to MZ. 4 pictures were taken for each genotype and a representative of 3 different experiments is shown. (SEM, * $P < 0.05$, ** $P < 0.001$).

Taken together, our results identify ephrinBs as co-receptors for Reelin signaling required for the function of Reelin in neuronal migration during the development of the layered structures in the cerebral cortex, hippocampus and cerebellum. Our genetic analysis of ephrinB mutants together with a strong biochemical analysis show that ephrinBs are required *in vivo* for various Reelin actions.

6 Discussion

In the present study we focused on the role of ephrinB ligands as co-receptors for Reelin signaling. Reelin, an extracellular matrix protein, binds to the extracellular binding domain of the two lipoprotein receptors (LDLR), apolipoprotein E receptor 2 (ApoER2) and very low density lipoprotein receptor (VLDLR) (Trommsdorff *et al.*, 1999). Reelin binding to the receptor complex relays a signal across the membrane that leads to the binding of the cytoplasmic protein Dab1 to the NPxY domain of the receptors (Stolt *et al.*, 2005). Reelin binding to the receptor complex also leads to the activation of cytoplasmic tyrosine kinases, Fyn and Src, both of which then phosphorylates Dab1 (Howell *et al.*, 1997, Sheldon *et al.*, 1997). This linear signaling pathway have been identified following several genetic studies performed on *reeler* (reviewed in (D'Arcangelo *et al.*, 1998, Lambert de Rouvroit *et al.*, 1998) and *scrambler* (Howell *et al.*, 1997, Rice *et al.*, 1998, Sheldon *et al.*, 1997), naturally occurring mouse mutants in which the Reelin and Dab1 genes, respectively, are defective. Following studies showed that double knockout (KO) of ApoER2/VLDLR, as well as Fyn/Src KO mice also shows *reeler* and *scrambler* like phenotypes (D'Arcangelo *et al.*, 1999, Hiesberger *et al.*, 1999, Kuo *et al.*, 2005, Trommsdorff *et al.*, 1999). Taken together, to study the role of a protein in Reelin signaling pathway the common approach is to analyze *reeler*-like phenotypes in a mouse model that is lacking the gene of interest. The signaling pathway has been always supported *in vivo* by cortical defects that are similar to *reeler* mice: i.e. invasion of neurons into the cell-sparse marginal zone (MZ), failure to split the preplate into MZ and subplate and the inverted neuronal layering in the neocortex. In this study, to show that ephrinB ligands are genetically interacting with the Reelin signaling pathway, we used the same approach and analyzed ephrinB2 and ephrinB3 KO and ephrinB3 compound mice (*rl/+; b3-/-*) (Figure.7.2). As heterozygous *reeler* mice do not show any *reeler*-like defects, by generating compound mice we could increase the penetrance of ephrinB2 and ephrinB3 phenotype upon reduced Reelin levels and interestingly observed several *reeler* like

defects in cerebral cortex, hippocampus and cerebellum of ephrinB2 and ephrinB3 compound mice. Some of these defects, such as branching of Purkinje cells in the cerebellum, were already apparent in single knockout ephrinB2 animals suggesting that ephrinB2 is a potent and non-replaceable regulator of Reelin signaling in the cerebellum. In the other structures in the brain such as neocortex and hippocampus redundancy of the different ephrinB family members might occur. In agreement with this migration defects related to the *reeler* phenotype were systematically seen in the triple ephrinB1B2B3 knockouts.

First, we analyzed the cerebral cortex and migration of cortical neurons. The MZ of the compound mice is hypercellular and the cortical plate is inverted, which is shown by BrdU birthdating studies. In order to detect if also the cytoarchitecturally defined lamination of cerebral cortex was inverted we used the advantage that during development, different types of cortical projection neurons are distinguished by various transcription factors expressed in a layer-specific manner (Hevner *et al.*, 2003, Leone *et al.*, 2008). Among these transcription factors, SatB2, Brn1, Tbr1 and FoxP2 are used as markers for corticocortical, corticospinal, and corticothalamic projection neurons, respectively (Britanova *et al.*, 2008, Hevner *et al.*, 2001, Arlotta *et al.*, 2005, Hisaoka *et al.*, 2009). Our analysis showed that in the compound mice the projection neurons have migration defects in cerebral cortex consistent with the BrdU birthdating results. Moreover, another hallmark of *reeler* cortex is the failure of the preplate splitting (Sheppard *et al.*, 1997). To investigate the contribution of the molecular environment to the developmental defects of the cortex of the compound mice we performed CSPG staining, which is one of the major extracellular matrix proteins and is distributed throughout the proliferative zone. CSPG has a role in defining the destination of migrating neurons that form the cortical plate and in delineating the pathway for early axonal extension. Upon splitting of the preplate the ECM component becomes most prominent in the MZ and in the subplate in the wild-type developing cortex, whereas in *reeler*, as well as in our compound mutant mice, although the cortical plate formed, the CSPG staining was more prominent in the MZ but absent from the

subplate, suggesting that the preplate splitting cannot take place in those mutants. This suggests that the inverted cortical layering of compound mice could be due to the failure of the preplate splitting.

Accumulating evidence indicates that the laminar identities of cortical neurons are genetically determined (McConnell *et al.*, 1991) and therefore it is believed that specific sets of genes expressed in progenitors and/or their neuronal progeny determine laminar fate (Hevner *et al.*, 2003, Zhong *et al.*, 2004). We compared the expression profiles of ephrinB ligands and the Reelin in the developing mouse brain. In the neocortex Reelin is expressed mainly by Cajal-Retzius (CR) cells in the MZ (D'Arcangelo *et al.*, 1995) and ephrinB2/3 expression is observed throughout the cortex as well as in the ventricular zone (VZ) where the glutamergic neurons of cortical plate are generated (Marin *et al.*, 2003, Parnavelas, 2000). Importantly, VZ cells express high levels of ApoER2, VLDLR and Dab1 proteins (Forster *et al.*, 2002, Magdaleno *et al.*, 2002, Sheldon *et al.*, 1997, Trommsdorff *et al.*, 1999, Luque *et al.*, 2003) and hence contain all the protein machinery required to perceive Reelin-signals. Moreover, as observed for the components of the Reelin signaling pathway, strong ephrinB3 expression is also observed in the medial ganglionic eminence (MGE) (Liebl *et al.*, 2003) where the interneurons are generated (Kriegstein *et al.*, 2004). As early born interneurons are located at upper cortical layers, it is suggested that they receive their information from lower layer projection neurons, underlying the requirement of a functional Reelin signaling pathway for proper upper layer positioning (Hammond *et al.*, 2006). Consistent with the layering defects of upper layer neurons in compound mice, an expected migration defect of interneurons was also detected with Calbindin immunohistochemistry.

Next we analyzed the hippocampus and observed that pyramidal neurons invade to the stratum oriens, granular cells invade to the hilus and mossy cells were observed in the granular cell layer, all suggesting migration defects in the hippocampus. Moreover, hippocampal pyramidal cells migrate along radial fibers and position themselves according to an inside-out gradient in the stratum

pyramidale. Consistent with the recent studies showing importance of Reelin signaling for dendritic branching (Niu *et al.*, 2008), we observed *reeler*-like branching defects of pyramidal neurons in the compound mice. Importantly, Reelin is expressed by the CR cells in the fascia dentata, outer marginal layer of the DG and in the stratum locunosum moleculare of the hippocampus proper (Alcantara *et al.*, 1998, D'Arcangelo *et al.*, 1995) and ephrinB3 is the highest expressed family member among all ephrinBs in the DG and in the CA1 region (Grunwald *et al.*, 2004). Therefore, migration defects of granular and pyramidal cells are most probably due to alterations in the Reelin signaling in the compound mice due to lack of ephrinB ligands. One of the primary functions of ephrinB ligands is the patterning of cell and axonal populations from the earliest stages of development. EphrinB ligands are also important for formation of organized axonal projections through their expression gradients across interconnected brain regions (reviewed in (Palmer *et al.*, 2003), suggesting that the defects of pyramidal neuron branching most probably occur due to the lack of ephrinB3 ligand in the hippocampus.

Although the cortical layering of compound mutant mice is *reeler* and *scrambler*-like, the hippocampal phenotype of the compound mice is still distinguishable from *reeler* and *scrambler*. The hilar mossy cells and the granular cells are not strongly affected in the compound mice. Given that these cells are generated between E15-21, (Bayer, 1980) and differentiate in the hilar region, they are no longer able to migrate later. So, only late-generated granule cells can take advantage of the late-forming radial glial scaffold (Weiss *et al.*, 2003) and migrate to the granule cell layer (Zhao *et al.*, 2004). The dentate gyrus (DG) develops according to an outside-in gradient and neurogenesis continues well into the second postnatal week. This could be also explained by functional compensation of ephrinB3 protein by other ephrinB ligands, ephrinB1 and ephrinB2, at least to its function in establishing laminated brain structures. It is also important to note that during embryonic development and adulthood ephrinB1 ligands are also expressed at low levels in the DG

6 Discussion

(Migani *et al.*, 2009), whereas, ephrinB2 ligands are strongly expressed in the CA1 region and low in the DG (Grunwald *et al.*, 2004, Migani *et al.*, 2007).

In the cerebellum ephrinB3 is expressed in the granular layer, whereas ephrinB2 is mainly expressed by the Purkinje cells. The defects observed in the ephrinB3 and ephrinB2 compound mice are consistent with these expression profiles. EphrinB2 KO mice and ephrinB2 compound mice showed strong branching phenotypes in the Purkinje cells while migration of granular cells was unaffected. EphrinB3 is expressed in the granular layer but defects in the cerebellum of ephrinB3 compound mice were mild suggesting redundancy with ephrinB1. Interestingly, also the Reelin receptors show differential phenotypes in the cortex and the cerebellum with VLDLR showing a stronger phenotype in the cerebral structures (Trommsdorff *et al.*, 1999). As double ApoER2/VLDLR KO mice shows *reeler* like phenotypes it will be interesting to analyze the double ephrinB2/3 KO mice more in detail. Our preliminary results show that the double and the triple knockout ephrinB mice have stronger phenotypes compared to the single knockout mice.

Following our results showing a genetic interaction between Reelin signaling pathway and ephrinB ligands we also investigated their molecular interaction. Consistent with the idea that Reelin links the ephrinB ligands to the LDL receptors, and ephrinB ligands show overlapping expression profiles to the Reelin signaling pathway molecules, we were able to show the interaction of Reelin, ephrinB ligands, Dab1 and phosphorylated Dab1 (pDab1) in both immunoprecipitation and immunofluorescence studies. Moreover, in immunofluorescence co-localization studies we detected interaction of ephrinB ligands with both LDL receptors, ApoER2 and VLDLR, providing further evidence that these two pathways interact at the molecular level and are located in the same signaling complex.

One factor crucial for Reelin signaling is the phosphorylation of Dab1 via SFKs. The ablation of Dab1 phosphorylation leads to pronounced defects in cortical layering. We used two different approaches (total brain lysates and primary cortical neuron cultures) to verify the impact of ephrinB molecules

on Dab1 phosphorylation. Ablation of the ephrinB3 resulted in a small, but significant, decrease in Dab1 phosphorylation upon Reelin stimulation compared to the wild-type neurons. Thus the decreased Dab1 phosphorylation levels in the ephrinB3 KO neurons strongly support the role of ephrinB3 ligands in phosphorylation of Dab1 protein. Both in total brain lysates and in dissociated cortical neuron cultures, we not only observed a decrease in Dab1 phosphorylation levels, but also accumulation of Dab1 protein in the ephrinB2 and the ephrinB3 KO mice. Upon phosphorylation Dab1 also becomes polyubiquitinated and degraded via the proteasome pathway (Bock *et al.*, 2004, Feng *et al.*, 2007), therefore, reduction of Dab1 phosphorylation leads to an accumulation of Dab1 protein in *reeler*, as well as in double ApoER2/VLDLR KO mice (Rice *et al.*, 1998, Howell *et al.*, 1999a,b). In agreement with these, reduction of functional ephrinB ligands reduced Dab1 phosphorylation levels and led to accumulation of Dab1 protein, as in *reeler*, *scrambler* or ApoER2/VLDLR KO mice suggesting that ephrinB3 ligands are required for proper Reelin signaling.

Early steps in ephrinB reverse signaling involve its phosphorylation on tyrosine residues (Bruckner *et al.*, 1997), interaction with PDZ proteins via its C-terminus (Bruckner *et al.*, 1999, Torres *et al.*, 1998) and activation of SFKs (Palmer *et al.*, 2002). Induction of ephrinB/EphB-Fc complexes leads to recruitment and activation of Src to the ephrinB clusters. In the present study we used primary cortical neuron cultures and stimulated ephrinB3 reverse signaling by EphB3-Fc and observed large ephrinB clusters. Moreover, we also observed increased pDab1 levels, showing that Reelin signaling pathway can be activated upon stimulation of ephrinB reverse signaling. As our immunoprecipitation experiments, by double immunocytochemistry we confirmed that phosphorylated Dab1 proteins and ephrinB3 ligands are colocalized on dendritic membrane patches. Moreover, by immunocytochemistry we also observed that ApoER2 and VLDLR colocalize with ephrinB3 ligands. Interestingly, as ephrins, ApoER2 associates with lipid rafts, which can be a mechanism to ensure colocalization in the plasma membrane (Duit *et al.*, 2010, Palmer *et al.*, 2002). In addition, co-stimulation of cortical neurons with both Reelin containing supernatant and EphB3 led to enhanced

6 Discussion

Dab1 phosphorylation, promoting further evidence for the interaction between the ephrinB3 ligands and the Reelin signaling pathway.

Taken together, these findings suggest that Reelin and ephrinB ligands are obligate components of a signaling pathway that mediates transmission of the Reelin signal across the plasma membrane to intracellular kinases that regulate neuronal migration during development. We propose that binding of Reelin to both ephrinB ligands and LDL receptors, ApoER2 and VLDLR, leads to phosphorylation of Dab1 via the recruitment and activation of SFKs by ephrinB3 ligands.

Some other candidates have also been suggested to act as coreceptors for Reelin signaling. CNR1 is a Fyn binding protein and has been implicated in recruiting kinases to the Reelin-receptor-Dab1 complex (Senzaki *et al.*, 1999). The same study showed binding of Reelin with CNR1, where Reelin-AP fusion protein was obtained from cell lysates but not secreted, therefore might not be properly folded. However, a following study showed no binding between Reelin and ectodomain or the CV1 region of CNR1, whereas under same conditions Reelin binding to lipoprotein receptors was observed consistently (Jossin *et al.*, 2004). They also indicate that events acting parallel to Dab1 phosphorylation might be required for full activity. Another candidate molecule was the $\alpha 3\beta 1$ integrin receptor complex, which is a transmembrane receptor and is important for cell migration by linking the extracellular matrix to the cytoskeleton (reviewed in (Magdaleno *et al.*, 2001). Integrins became important for Reelin signaling first with the work of Anton *et al.*, 1999, where the $\alpha 3$ integrin deficient mice showed disrupted neuronal migration and laminar organization. Then Dulabon *et al.*, 2000, showed co-expression of $\alpha 3\beta 1$ integrin with Dab1 suggesting the association of Reelin and $\alpha 3$ integrin during corticogenesis, and Schmidt *et al.*, 2005 showed that this interaction takes place between the N-terminal region of Reelin (a site distinct from the region of Reelin shown to associate with lipoprotein receptors) and Dab1 can associate with $\alpha 3\beta 1$ integrin receptor complex. Thus, suggesting that $\alpha 3\beta 1$ integrin–Reelin interactions may contribute to appropriate neuronal placement during cortical development (Schmidt *et al.*, 2005). However, the phenotype

observed in $\alpha 3$ integrin deficient mice does not correlate to the *reeler* phenotype and the conditional $\beta 1$ KO mice confirmed that $\beta 1$ integrin is not required for the formation of cell layers in cerebral cortex (Graus-Porta *et al.*, 2001, Belvindrah *et al.*, 2007). Moreover, the integrin mouse has proper inside-out layering and integrin does not control Dab1 phosphorylation (Dulabon *et al.*, 2000). Recent genetic evidence suggests a promigratory function of Reelin molecule from deeper cortical layers (IV-VI) (Yoshida *et al.*, 2006) which is incompatible with a mechanism by which binding of Reelin to integrin inhibits migration. Although integrins are important with their role in radial glia fiber outgrowth and their attachment to basement membrane, as well as being a signal for detachment of neurons from radial glial scaffold and defects in radial glia cells affect the morphological differentiation of pyramidal neurons (Belvindrah *et al.*, 2007), proper inside-out cortical layering and Dab1 phosphorylation suggests that Reelin signaling is mediated by the receptors independently of any $\beta 1$ integrin (Luque, 2004, Magdaleno *et al.*, 2001).

We have convincingly showed that activation of ephrinB reverse signaling can rescue the *reeler*-phenotypes indicating that ephrinBs are potent regulators of Reelin signaling. We used 2 different approaches, dissociated cortical neuron cultures (E15) and organotypic slice cultures (E15 cortex), to verify the impact of the ephrinB molecules on Dab1 phosphorylation and activation of the Reelin signaling. In both assays phosphorylation of Dab1 and migration properties of neurons under non-stimulated conditions (GFP or Fc fragment) and upon Reelin stimulation were consistent with previous findings (Bock *et al.*, 2003a). In primary cortical neurons, activation of ephrinB3 ligands led to activation of Dab1 phosphorylation and a rescue of the *reeler* phenotype as efficient as exogenous stimulation with Reelin. Neuronal migration takes place from proliferative zones towards their destinations through Reelin signaling. In the *reeler* cortex neuronal precursors are born normally and the preplate is formed, however, the preplate splitting doesn't take place, therefore, the outside-in patterning is observed. In our organotypic culture assays, as expected, the *reeler* cultures showed outside-in migration patterning, whereas stimulation of cultures with soluble EphB3-Fc and,

consequently stimulation of Dab1 phosphorylation, rescued cell layering in the cerebral cortex. This strongly suggests the role of ephrinB3 ligands for Dab1 phosphorylation in Reelin signaling pathway.

Three models have been proposed to explain the phenotype of *reeler* mice and the mechanism of Reelin signaling pathway. One model suggests that Reelin acts as a repellent for subplate neurons thereby facilitates the split of preplate into the MZ and the subplate (Schiffmann *et al.*, 1997). In another model, a Reelin gradient selectively induces cortical plate neurons to migrate past the subplate neurons by acting as a chemo-attractant. In a third model, Reelin is thought to act as an inhibitory or as a stop signal that instructs migrating neurons to detach from their glial guidance fiber (Dulabon *et al.*, 2000). One of the most recent hypothesis has been recently compiled in the 'Detach and Go' model by Cooper *et al.*, 2008, where Reelin was proposed to promote detachment of migrating neurons from glial fibers and their translocation to the outermost area of cortex (Cooper, 2008, Frotscher, 1997). Another model, called as 'Detach and Stop' (Cooper, 2008, Frotscher, 1997) is based on the finding that the initial, radial glia independent, movement of cortical neurons past the subplate is Reelin dependent, while later, glia dependent migration relies on the other factors (Nadarajah *et al.*, 2001). Therefore, in this model, future layer VI neurons extend a leading edge towards the MZ where they encounter the Reelin source that instructs their translocation through the subplate and settle in their corresponding layer. Later in development, when younger neurons that migrate along the radial glia scaffolds, encounter Reelin, they are instructed by Reelin to detach from the glial fiber and initiate nuclear translocation to past the preexisting layers and settle above them. We observed that upon activation of Reelin signaling pathway with EphB3 stimulation, in the absence of Reelin, later born neurons can migrate towards the upper cortical layers, providing further evidence that Reelin acts as a stimulant for migration but is not a chemo-attractant as we did not stimulate *reeler* organotypic cultures locally. In *reeler*, except Reelin protein, the signaling pathway molecules are expressed and functional, therefore, stimulation of ephrinB reverse signaling recruit SFKs and lead to the phosphorylation of Dab1 protein which then

initiates migration and allows later born neurons to pass the elder ones. In a similar study it has been shown that ectopically expressed Reelin, in the *reeler* background, induced tyrosine phosphorylation of Dab1 in the VZ and rescued some, but not all, of the neuroanatomic and behavioral abnormalities characteristic of *reeler* (Magdaleno *et al.*, 2002). Results of both the work of Magdaleno *et al.*, 2000 and the work of this thesis indicate that Reelin does not function simply as a positional signal. Rather, it appears to participate in multiple events critical for neuronal migration and cell positioning.

6.1 Concluding remarks

In conclusion, the work presented in this thesis elucidated the role of the ephrinB ligands in the Reelin signaling. We describe, for the first time, the requirement of ephrinB ligands for Reelin signaling pathway, thus shedding a light onto the molecular mechanism involved in the phosphorylation of Dab1.

The regulation of Reelin signaling by ephrinB ligands represents a new example of how ephrinB ligands regulate the action of other membrane receptors. EphrinB ligands regulate for example cerebella granule cell migration by controlling SDF-1-mediated activation of the G protein-coupled chemokine receptor CXCR4 (Lu *et al.*, 2001). We have shown in the past that ephrinB2 reverse signaling regulates the trafficking of AMPA receptors at the synapse thereby controlling synaptic transmission (Essmann *et al.*, 2008). In the vasculature recent studies have unraveled that ephrinB2 controls the internalization and activation of VEGFR2 to induce tip cell filopodia extension and vascular sprouting both during development and during tumor angiogenesis (Sawamiphak *et al.*, 2010) Now we show that ephrinB ligands are the missing co-receptors for Reelin signaling and induce the formation of a macromolecular complex required for the Src activation and Reelin signaling. Thus, ephrinB ligands emerge now as major regulators of cellular signaling implicated in a

6 Discussion

broad array of functions and as potential therapeutic targets not only for cancer therapies but also for neurological disorders such as Alzheimer disease associated with loss of Reelin protein.

7 Material and methods

7.1 Material

7.1.1.1 Antibodies

Table 7-1: Primary Antibodies

Primary Antibodies	Ordering information	Supplier
Anti-ApoER2, rabbit	#A3481	Sigma
Anti-ephrinB (#23), rabbit		R&D
Anti-ephrinB1 (C-18) , rabbit	#SC-910	Santa Cruz
Anti-Brn-1 (C-17), goat	#sc-6028	Santa Cruz
Anti-BrdU, mouse	#MAB3424	Chemicon
Anti Calbindin (CL-300), mouse	#ab9481	Abcam
Anti-Calbindin (D-28K), rabbit	#ab1778	Chemicon
Anti-Calreteinin, rabbit	#ab5054	Chemicon
Anti-Calreteinin (6B3), mouse	#6B3	Swant
Anti-Chondroitin sulfate (CSPG), mouse	#C8035	Sigma
Anti Dab1, rabbit	#AB5840	Chemicon
Anti-Dab1, goat	#sc-7827	Santa Cruz
Anti-FoxP2, rabbit	#ab16046	Abcam
Anti GFAP, rabbit	#2015-02	Dako
Anti-GFAP, mouse	#MAB3402	Chemicon
Anti-MAP2, mouse	#MAB3418	Chemicon
Anti-NeuN, mouse	#MAB377	Chemicon
Anti-phospho-Dab1 (Tyr232), rabbit	#3327	Cell Signaling
Anti-phospho-FAK	#3284	Cell Signaling
Anti-Reelin, mouse	#MAB5364	Chemicon
Anti-RC2, mouse	#MAB5740	Millipore

Anti-SatB2, rabbit	#ab34735	Abcam
Anti-Tbr1, rabbit	#ab9619	Chemicon
Anti-tubulin, rabbit	#MRB-435P	Covance
Anti-VLDLR, goat	#AF2258	R&D systems
Anti-Phospho-Tyrosine clone 4G10,	#05-321	Upstate

Table 7-2 : Primary Antibodies

Secondary Antibodies	Ordering information	Supplier
Donkey anti-mouse minx cy2	#715-225-151	Dianova (Jackson)
Donkey anti-mouse minx cy3	#715-165-151	Dianova (Jackson)
Donkey anti-rabbit minx cy2	#711-225-152	Dianova (Jackson)
Donkey anti-rabbit minx cy3	#711-165-152	Dianova (Jackson)
Goat anti-human IgG Fc-fragment	#109-005-098	Dianova (Jackson)
Goat anti-mouse Alexa488	#A11029	Invitrogen
Goat anti-mouse HRP	#115-035-146	Dianova (Jackson)
Goat anti-rabbit HRP	#111-035-003	Dianova (Jackson)

7.1.2 Chemicals, Reagents, Commercial Kits & Enzymes

Table 7-3: Chemicals, reagents, commercial kits& enzymes

Chemicals	Ordering information	Supplier
30 % (w/v) Acryamide/Bis solution 29:1 (3.3 % C)	#161-0157	BioRad
Agarose beads		BioRad
Agarose, high	#01280	Biomol
Agarose, low melting	#A9419	Sigma
Ammonium persulfate (APS)	# 161-0700	BioRad
BES	#B-6420	Sigma
BioRad DC Protein Assay	#500-116	BioRad
Blotting grade milk powder	#T145.2	Roth
Borax	#B-3545-500G	Sigma
Boric acid	#203667	Merck

7 Material and methods

Bovine albumin powder	#7906	Sigma
Cresyl echt violet	#C3886	Sigma
5-bromo-2'-deoxyuridine (BrdU)	#B5002	Sigma
Complete EDTA-free, proteinase inhibitor	#1873580	Roche
DAB Substrate Kit	#D-0426	Sigma
DAPI	#6335.1	Roth
Diethylether	#3942.1	Carl Roth
DL-2-Amino-5-phosphonopentanoic acid (APV)	# A5282-10MG	Sigma
DMSO	#41641	Fluka
DNA ladder GeneRuler Ladder mix	#M0331	Fermentas
ECL Western blot detection reagent	#S RPN2134	GE Healthcare
Ethidium bromide	#7870.1	Carl Roth
Eukitt	#03989	Fluka Analytical
Fetal Bovine Serum (FBS)	#11020-106	Invitrogen
Fluorescent Mounting Medium	#S3023	Dako
Gelatin	#G9382	Sigma
Gluteraldehyd 25 %	#354400	Merck
Histomount	#00-8030	Zymed
HNO ₃ (Nitric acid) 65 %	#84381-1L	Sigma
Human IgG Fc-fragment	#009-000-008	Dianova
Immobilized NeutrAvidin™	#29200	Pierce
Isofluoran	#B506	Frone
Mouse EphB3 - Fc chimera	#432-B3	R&D
Natural mouse laminin	#23017015	Invitrogen
Nitric acid	#84382	Fluko
Normal donkey serum	#017-00-121	Dianova
Normal goat serum	#005-000-121	Dianova
OrangeG	#O-1625	Sigma
OCT	#4583	Sakura Finetek
PFA (Paraformaldehyd)	#1.04005.1000	VWR
Poly-D-Lysine hydrobromide	#P7886-1G	Sigma

Ponceau S solution	#33427	Serva
Precision plus protein standard	#161-0373	Bio-Rad
ProLong Antifade Kit	#P7481	Invitrogen
Protein A sepharose CL-4B	#17-0780-01	GE Healthcare
Protein G sepharose 4 fast flow	#17-0618-01	GE Healthcare
Roti coll	#0258.1	Carl Roth
Sekunden Kleber	#623554	Uhu
Sodium Fluoride (NaF)	#S-1501-100G	Sigma
Sodium ortho vanadate (NO ₃ VO ₄)	#S-6508	Sigma
Sodium Pyrophosphate (NaPP)	#221368-100G	Sigma
Sucrose	#5737	Merck
Taq DNA polymerase	#M0267L	New England
TEMED	#161-0801	Bio-Rad
Tissue-Tek O.C.T. compound	#4583	Sakura Finetek
TritonX (TX)-100 solution	#37238	Serva
Trypsin-EDTA	#25300-054	Invitrogen
Tween 20 (Polyoxyethylene sorbitan	#P5927-500ML	Sigma
β-Mercaptoethanol	#M-7522	Sigma
Vectastain ABC reagent, mouse	4002	Vector
Vectastain ABC reagent, rabbit	4001	Vector
Vectastain ABC reagent, rat	4004	Vector
Xylene	#CN-80.1	Roth

7.1.3 Consumable Material

Table 7-4: Consumable Material

Material	Type	Supplier
96 well PCR plate	#AB-0900	ABgene
Brush		Toppoint
Cell scrapers	# 831830	Sarstedt

7 Material and methods

Centrifugal filter devices	#YM-100	Millipore
Combitips plus	2 ml, 5 ml, 10 ml	Eppendorf
Cover slips 12/13mm Ø	#01-115-30	Marienfeld
CryoTubes, Nunc	#343958 1.5 ml	Nunc
Ear tags		National band & Tag
Embedding molds	#18646A	PolySciences
Filtered pipette tips	10µl, 20µl, 200µl, 1000µl	G. Kisker
Gel-saver tips 0.5-10 µl	#GS1025	G. Kisker
Hyperfilm ECL 8x10 in	#28-9068-39	GE Healthcare
ImmEdge™ Pen	#H-4000	Vector Laboratories
Latex gloves, powder-free	Size S6-7	Semperguard
Microscope slides	#J3800AZMNZ	Thermo Scientific
Multiwell cell culture plates	6, 24 well	TPP
Multiwell-inserts	#PICM03050	Millipore
Needles	26G, #NN-2623R	Terumo
Nitril gloves, powder-free	Size S6-7	Semperguard
Omnifix® - F1	#CE0123	Braun
Parafilm®	“M”laboratory film	Pechiney plastic
Pastuer pipettes, glass	#150.01	Poulsen & Graf
Pipette tips	10µl, 20µl, 200µl, 1000µl	Sarstedt
Plastic pipettes, Cellstar	5 ml, 10 ml, 50 ml	Greiner
Plastic pipettes, Falcon	1 ml, 2 ml, 5 ml, 10 ml, 25	Becton Dickinson
Polypropylene round bottom tube,	14 ml, 5 ml	Becton Dickinson
Polystyrene, Polypropylene conical	15 ml, 50 ml	Becton Dickinson
Protean extra thick blot paper	#1703969	BioRad
Reaction tube, safelock	1.5 ml, 2 ml	Eppendorf
Steritop, bottle top filter	250 ml, 500 ml (0.22 µm)	Millipore
Storage box 50 slides	#N953.1	Roth
Strips of 8 domed caps	#AB-0602	ABgene
Syringe	5 ml, 10 ml, 50 ml	Becton Dickinson
Syringe driven filter unit	0.22 µm, 0.45 µm	TPP

Tissue culture plastic dishes, Falcon	10 cm Ø, 6 cm Ø	Becton Dickinson
Tissue culture plastic dishes, Nunclon™	10 cm Ø, 6 cm Ø	Nunc
Whatman Protran nitrocellulose	#10401196	Schleicher& Schuell

7.1.4 Equipment

Table 7-5: Equipment

Equipment	Model	Supplier
+ 4°C fridge	Premium	Liebherr
-20 °C freezer	Liebherr comfort GS-5203	Liebherr
-80°C freezer	Ultra low freezer	Thermo Scientific
Balance	#SI-203	Denver Instruments
Burner	Fireboy eco	Integra Biosciences
Cell culture Hood	HERAsafe	Kendro
Centrifuge	Varifuge 3.0R	Kendro
Centrifuge	Megafuge 11/11R	Thermo Fischer
Centrifuge table	Centrifuge 5415D	Eppendorf
Centrifuge table, re Fridg.	Centrifuge 5415R	Eppendorf
CO ₂ incubator	HERAcell 240	Heraeus
Confocal Microscope	TCS SP5	Leica Instruments
Cryostat	#CM3050 S	Leica Instruments
Digital camera	16.4 4 MP Slider	Visitron systems
Electrophoresis apparatus	MicroPulser™	Bio-Rad
Epifluorescence microscope	Zeiss Axioplan	Zeiss
Fine balance	#SI234	Denver Instrument
Gel documentation system	UV-Transilluminator, Felix CCD	Biostep
Glas homogenizer	#S1149	B. Braun, Melsungen AG
Heating block	DRI-Block DB2D & 2A	Techne
Hemocytometer	Neubauer improved	Brand
Incubator shaker	Unitron-Pro	Infors
Laminar flow hood	HERAGuard	Kendro

7 Material and methods

Liquid Nitrogen Tank	#1007754	Air Liquide
Magnetic stirrer (heating)	MSH-20A	IDL GmbH
Magnetic stirring bar	50x8 mm, 30x8 mm	Brand
Microplate Absorbance	iMark™	Bio-Rad
Microwave	Severin 700	Severin
Multi channel pipette	0.5-10 µl, research	Eppendorf
Multi channel pipette	20-200 µl, Transferpette-8	Brand
Multi pipette	Multipipette®plus	Eppendorf
Oven	Heraeus 0-250 °C	Thermo Fisher
PCR machine	Flex Cycler	Analytic Jena
Peristaltic pump	Minipuls 3	Gilson
pH meter	Lab 850	Schott Instruments
Pipette boy	Pipetteboy acu	Integra Biosciences
Pipettes	P2, P20, P200, P1000	Gilson
Power supply	EPS 601	Amersham
Rotator	NeoLab rotator 2-1175	NeoLab
Rotor	GSA rotor & type 3	Sorvall
Shaker	#3966	GFL
Small microscope	Leica DM IL HC Fluo	Leica
Spectrometer	Ultrospec 3000	Amersham
Stereomicroscope	DFC 420	Leica
Thermo mixer	Thermomixer compact	Eppendorf
Vacuum system	#AC02	HLC BioTech
Vortex	Top-Mix 11118	Fisher Scientific
Vibratome	VT1200S	Leica Instruments
Water bath	Polystat 24	Fischer Scientific
Water purification system	Milli-Q Biocel A10	Millipore
Western Blot analysis:		
Semidry blotting apparatus	Trans-blot SD cell	BioRad
BioRad gel system	Mini PROTEAN® 3 cell	BioRad
X-ray Film Processor	#MI-5	Medical Index

Dissection tools:

Biology tip Dumostar 5	#11295-10	Fine Science Tools
Forceps narrow pattern	#11002-13	Fine Science Tools
FST Sterilizer	#19000-45	Fine Science Tools
Spencer Ligature Scissors	#14078-10	Fine Science Tools
Spring scissors strait	#15003-08	Fine Science Tools
Spring scissors strait	#15025-10	Fine Science Tools
Tissue scissors strait	#14028-10	Fine Science Tools
Tweezers	#11254-20	Fine Science Tools

7.1.5 Oligonucleotides

Table 7-6: Oligonucleotides

Primer	Sequence
B1wts2	5'-TTA GGA CAA AGG GCT CCC CTA GC-3'
Hb1as1	5'-GCC ATC TTG ACA GTG TTG TCT GC-3'
B1wtas1	5'-TGA CAG CAG GGT GTG GAC TCA CAT-3'
B2Cs1	5'-CTT CAG CAA TAT ACA CAG GAT G-3'
B2Cas1	5'-TGC TTG ATT GAA ACG AAG CCC GA-3'
B3-161F	5'-GGG ATA TGG AAG CTT TGA GAC-3'
B3-308R	5'-GGT TC ACC ACC CAC AAC CAG C-3'
B3-Neo3'ds85	5'-GAG ATC AGC AGC CTC TGT TCC-3'
Cre1	5'-GCC TGC ATT ACC GGT CGA TGC AAC GA-3'
Cre2	5'-GTG GCA GAT GGC GCG GCA ACA CCA TT-3'
<i>reeler</i> _wt_for	5'-CTG CTA CAC AGT TGA CAT ACC TTA ATC TAC-3'
<i>reeler</i> _wt_rev	5'-AGA GCC TAG AGG TTA GGG ACA CAA CTC TTC-3'
<i>reeler</i> _ko_for	5'-TAA GGG AGT CCT GGT CTC TTT CTG TCT TTA-3'
Thy1-F	5'TCT GAG TGG CAA AGG ACC TTA GG-3'
Thy1-R	5'CGC TGA ACT TGT GGC CGT TTA CG-3'

7.1.6 Cell lines

Cell lines

Line	Origin	Culture medium
293 Rln HEK	Human embryonic kidney cells	DMEM, FBS
293 GFP HEK	HEK stably expressing GluR2	DMEM, FBS, Geneticin

Stably expressing Reelin and GFP cell lines were kindly provided by Magdalena Goetz (GSF, Munich).

7.1.7 Mice

EphrinB1 and ephrinB2 were kindly provided by Ruediger Klein, MPI for Neurobiology, Martinsried.

EphrinB3 was kindly provided by George D. Yancopoulos, Regeneron Pharmaceuticals Inc., New York.

Reeler and Thy1-GFP mice were obtained from Jackson Laboratories,

7.1.8 Primary cells and tissues

Primary cells and animal tissues were obtained from C57BL6/J mice. EphrinB3 and *reeler* knockout mice and their wild-type litter mates were used to isolate neurons. EphrinB2 knockout neurons and control cells were isolated from conditional ephrinB2^{lox/lox} knockout mice (Grunwald et al., 2004) crossed with Nestin Cre⁺ or Nestin Cre⁻. These mice express cre recombinase under the Nestin promotor that specifically deletes ephrinB2 from the central nervous system.

7.2 Media and Standard Solutions

6x Agarose gel-loading buffer

50 % Glycerol (v/v)

1x TAE buffer

0.2 % Orange G (w/v)

Add distilled water to 100 ml total volume and store at room temperature (RT).

10x DPBS

137 mM NaCl

2.7 mM KCl

8 mM Na₂HPO₄

1.5 mM KH₂PO₄

Dissolve ingredients in 800 ml of sterile water. Adjust solution to pH 7.4 with HCl, fill up to 1 l total volume and sterilize by autoclaving. Store at RT.

Dulbeccos Phosphate-buffered saline (DPBS)

137 mM NaCl

2.7 mM KCl

8 mM Na₂HPO₄

1.5 mM KH₂PO₄

Dissolve ingredients in 800 ml of sterile water. Adjust solution to pH 7.4 with HCl, fill up to 1l total volume and sterilize by autoclaving. Store at RT.

0.5 M EDTA, pH 8.0

Disodium EDTA·2H₂O

Dissolve disodium EDTA in 800 ml of sterile water. Adjust solution to pH 7.4 with HCl, fill up to 1 l total volume and sterilize by autoclaving. Store at RT.

4 % Paraformaldehyde (PFA)

PFA (w/v)

10x D-PDS

10 N NaOH

Heat 800 ml of sterile water in the water bath to approximately 70°C, add PFA powder and stir thoroughly. Add NaOH to completely dissolve the PFA and let it cool down to RT. Add 100 ml 10x

7 Material and methods

DPBS and fill up to 1 l total volume with water. Adjust the pH to 7-7.3, filtered the solution using Whatman paper and store at -20°C in aliquots of adequate volume. Use a freshly thawed aliquot each time.

PDS-Tween (PBS-T)

1x D-PBS

0.1 % Tween®20

Store at RT.

Sodium phosphate buffer, pH 7.2

1 M Na₂HPO₄

1 M NaH₂PO₄

2 % SDS

Store at RT.

50x Tris-acetate-EDTA (TAE) electrophoresis buffer

Tris base

Glacial acetic acid

0.5 M EDTA (pH 8.0)

Add distilled water to 1 l total volume, the pH should be ~8.3. Store at RT. Dilute stock solution with distilled water to prepare both agarose gels and the electrophoresis buffer.

Tris-EDTA (TE) buffer, pH 8.0

10 mM Tris-HCl

1 mM EDTA

Adjust to pH 8.0 by adding concentrated HCl and fill up to 1 l volume. Sterilize by autoclaving and store at RT.

1M Tris-HCl, pH 7.4, 8.0 or 8.3

Tris base

Dissolve Tris base in 800 ml of sterile water. Adjust solution to the desired pH with concentrated HCl, fill up to 1 l total volume. Sterilize by autoclaving and store at RT.

10x TBS, pH 7.4

500 mM Tris.HCl, pH 7.4

1500 mM NaCl

Dissolve ingredients in 800 ml distilled water. Adjust solution to pH 7.4 with HCl, fill up to 1 l total volume and sterilize by autoclaving. Store at RT.

TBS, pH 7.4

50 mM Tris.HCl, pH 7.4

50 mM NaCl

Adjust to pH 7.4 by adding concentrated HCl and fill up to 1 l volume. Sterilize by autoclaving and store at RT.

7.2.1 Media and Supplements for Cell Culture**293 Rln and GFP growth medium**

DMEM (Invitrogen, #61965-059)	500 ml
Geneticin (Invitrogen, #10131-027)	360 μ l
2 mM L-Glutamine (100x) (Invitrogen, #25030-024)	5 ml
FBS, heat inactivated (Invitrogen, #110270-106)	50 ml
Penicilin/Streptomycin (100 μ g/ml) (PAA, #P11-010)	5 ml

Store at 4°C.

293 Rln and GFP starving medium

The same composition as the 293 growth medium, but without FBS.

7.2.2 Media and Supplements for Primary Cell Culture

Borate buffer

Boric acid	1.55 g
Borax	2.375 g

Dissolve in 500 ml distilled water, adjust to pH 8.5 and store at 4°C. For coating, dissolve poly-D-lysine (10 mg/ml) in borate buffer and sterilize by filtration.

Neurobasal medium (NB)

Neurobasal medium (Invitrogen, #21103-049)	500 ml
B-27 supplement (Invitrogen, #17504-044)	10 ml
L-Glutamine, stable 200mM (PAA, #M11-004)	1.25 ml

Store at 4°C.

Serum medium (SM)

DMEM (Invitrogen, #61965-026)	100 ml
FBS, heat inactivated (Invitrogen, #F-7524)	10 ml

Sterilize by filtration through a 0.22 µm pore size membrane and store at 4°C. FBS is kept in aliquots of 10 ml at -20°C.

Dissection medium (DM)

HBSS (Invitrogen, #24020-091)	500 ml
Penicillin/Streptomycin (Invitrogen, #15070-063)	5 ml
1 M HEPES (Invitrogen, #15630-056)	3.5 ml
L-Glutamine 200mM (PAA, #M11-004)	5 ml

Store at 4°C and keep on ice during dissection.

7.2.3 Media for Organotypic Cultures

Preparation medium

MEM (Invitrogen, #21575-022)	500 ml
------------------------------	--------

Penicillin/Streptomycin (Invitrogen, #15070-063)	5 ml
1 M Hepes (Invitrogen, #15630-056)	12.5 ml
L-Glutamine 200mM (PAA, #M11-004)	5 ml
Glucose, 45 %	5 ml
1 N NaOH	2 ml

Sterile filter the solution, adjust the pH to 7.4. Store at 4°C and keep on ice during preparation.

Incubation medium

MEM (Invitrogen, #21575-022)	42 ml
Penicillin/Streptomycin (Invitrogen, #15070-063)	1 ml
1M Hepes (Invitrogen, #15630-056)	2.5 ml
L-Glutamine 200mM (PAA, #M11-004)	1 ml
Glucose, 45 %	1.5 ml
Horse Serum (Sigma, #H1138)	25 ml
BME (Invitrogen, #41010-026)	25 ml
Sodium bicarbonate, 7.5 % (Sigma, #S5761)	2 ml
N-2 (Invitrogen, #17502-048)	1 ml
B-27 supplement (Invitrogen, #17504-044)	1 ml

Sterile filter the solution, adjust the pH to 7.4. Store at 4°C and keep on ice during preparation.

7.2.4 Solutions for Biochemistry

Blocking solution for Western blot analysis

Depending on the requirements of the primary antibody use PBST, PBS or TBS with 3-5 % milk powder (Roth) or 3-5 % BSA (Sigma). Prepare fresh, storage at 4°C overnight possible.

HNTG buffer

20 mM HEPES (pH 7.5)

150 mM NaCl

10 % Glycerol

0.1 % Triton-X100

7 Material and methods

Dissolve all ingredients in distilled water, adjust the pH to 7.5 and keep buffer at 4°C. Add 1 mM Na_3VO_4 and 1 % complete inhibitor cocktail (Roche) freshly right before use.

5x Laemmli electrophoresis buffer

Tris base	154.5 g
Glycerin	721 g
SDS	50 g

Add distilled water to 10 l total volume, store at RT.

Laemmli stacking gel, 10 ml

30 % (w/v) Acrylamid/bisacrylamid	1.3 ml
0.5 M Tris-HCl pH 6.8, 0.4 % SDS	2.6 ml
H ₂ O	6.1 ml
10 % APS	100 µl
TEMED	10 µl

Always prepare fresh, add APS and TEMED just before pouring the gel.

Laemmli separating gel

Concentration	6 %	7.5 %
30 % (w/v) Acrylamid/bisacrylamid	2 ml	2.5 ml
1.5 M Tris-HCl pH 8.8, 0.4 % SDS	2.6 ml	2.6 ml
H ₂ O	5.35 ml	4.85 ml
10 % APS	50 µl	50 µl
TEMED	5 µl	5 µl

Always prepare fresh, add APS and TEMED just before pouring the gel. Load distilled water on top to smoothen the edge of the polymerizing gel.

LBA Lysis buffer

50 mM Tris-HCl, pH 7.5

150 mM NaCl

0.5-1 % Triton X (TX)-100

Add distilled water to 500 ml and store at 4°C.

Add fresh to 50 ml:

1 mM Sodium ortho vanadate (Na_3VO_4)

10 mM NaPPi

20 mM NaF

Proteinase inhibitor cocktail tablet

6x sample buffer for reducing and non-reducing conditions

12 % SDS

300 mM Tris-HCl, pH 6.8

600 mM DTT

0.6 % Bromphenol blue

60 % Glycerol

Add distilled water to 30 ml, store aliquots at -20°C. For reducing conditions add 50 μl β -mercaptoethanol to 1 ml of 4x sample buffer or 25 μl to 1 ml of 2x sample buffer.

Stripping buffer

5 mM Sodium phosphate buffer, pH 7-7.4

2 mM β -Mercaptoethanol

2 % SDS

Store at RT. Add β -Mercaptoethanol right before use.

10x Transfer buffer

Tris base 60.5 g

Glycerin 281.5 g

SDS 25 g

Add distilled water to 2.5 l total volume, store at RT. Add 20 % methanol to the 1x transfer buffer right before use.

7.2.5 Solutions for BrdU staining

2x SSC buffer

0.3 M NaCl

0.03 M Sodium citrate

Store at RT.

Endogenous peroxidase blocking buffer

0.6 % H₂O₂

Dissolve in TBS. Store at RT.

Blocking buffer

0.25 % TritonX-100

3 % Donkey serum

Always prepare fresh and with TBS.

BrdU solution for injection

5 mg/ ml (m/w) BrdU dissolved in saline (0.9 % NaCl).

7.2.6 Solutions for Embedding of Vibratome & CryoSections

Acetate buffer, pH 6.5

1 M Sodium acetate

1 M Acetic acid

Sterile filter the solution, adjust the pH to 6.5 and adjust volume to 1 l. Store at RT.

Embedding solution for vibratome sectioning

Ovalbumin (Sigma, #A-S253) 90 g

0.1 M Acetate buffer, pH 6.5 200 ml

Dissolve albumin in acetated buffer by string for several hours at RT. Filter the solution with gauze to remove air bubbles and big clumps of undissolved albumin.

Gelatin (Sigma, #2500) 1.5 g

7.3 Methods

7.3.1 Molecular Biology

7.3.1.1 Genomic DNA extraction and genotyping polymerase chain reactions (PCR)

DNA preparation

DNA was obtained by boiling 0.1 – 0.5 cm long mouse tails at 95°C in 100 µl 50 mM NaOH for 45 min in the PCR machine. The lysates were neutralized by adding 10 µl of 1.5 M Tris pH 8.3.

Genotyping PCR

PCR-master mix for 50 µl reaction volumes were prepared as indicated in the Table 9.7 and 2 µl of DNA samples were placed to 96 well PCR reaction tubes.

Table 7-7: PCR master mix

Genotype	Reeler	B3
dNTPs (25 mM each)	0.4 µl	0.4 µl
10x Taq pol buffer (NEB)	5 µl	5 µl
Primer 1 (100 mM)	0.5 µl <i>reeler</i> -wt-for	0.5 µl B3-161F
Primer 2 (100 mM)	0.5 µl <i>reeler</i> -wt-rev	0.5 µl B3-308R
Primer 3 (100 mM)	0.5 µl <i>reeler</i> -ko-for	0.5 µl B3-Neo3'ds85
Taq Polymerase (NEB)	0.5 µl	0.25 µl
Distilled H ₂ O	41.15 µl	40.85 µl

Genotype	Cre	B2lox	Thy1-GFP
dNTPs (25 mM each)	0.4 µl	0.4 µl	0.4 µl
10x Taq pol buffer (NEB)	5 µl	5 µl	5 µl
Primer 1 (100 mM)	0.5 µl Cre1	0.5 µl B2cs1	0.5 µl Thy1-gfp-forward
Primer 2 (100 mM)	0.5 µl Cre2	0.5 µl B2cas1	0.5 µl Thy1-gfp-reverse

Taq Polymerase (NEB)	0.25 µl	0.5 µl	0.5 µl
Distilled H₂O	41.35 µl	41.1 µl	41.1 µl

The mice were checked for the presence of the indicated gene using appropriate PCR program.

PCR programs

Table 7-8: Genotyping PCR program

<p><u>Reaction Program for <i>Reeler</i>:</u></p> <p>95°C 2 min</p> <p>95°C 30 sec } 30 x</p> <p>63°C 30 sec } 30 x</p> <p>72 °C 1 min } 30 x</p> <p>72 °C 10 min } 30 x</p> <p>10 °C forever</p>	<p><u>Reaction Program for B3:</u></p> <p>94°C 2 min</p> <p>94°C 15 sec } 39 x</p> <p>58°C 30 sec } 39 x</p> <p>72 °C 40 sec } 39 x</p> <p>72 °C 5 min } 39 x</p> <p>10 °C forever</p>	<p><u>Reaction Program for B2:</u></p> <p>94°C 1 min</p> <p>94°C 45 sec } 34 x</p> <p>62°C 45 sec } 34 x</p> <p>72 °C 45 sec } 34 x</p> <p>72 °C 5 min } 34 x</p> <p>10 °C forever</p>
<p><u>Reaction Program for Cre:</u></p> <p>95°C 3 min</p> <p>95°C 40 sec } 34 x</p> <p>67°C 30 sec } 34 x</p> <p>72 °C 40 sec } 34 x</p> <p>72 °C 5 min } 34 x</p> <p>10 °C forever</p>	<p><u>Reaction Program for Thy1-</u></p> <p><u>GFP:</u></p> <p>95 °C 2 min</p> <p>95 °C 30 sec } 35 x</p> <p>60 °C 30 sec } 35 x</p> <p>72 °C 40 sec } 35 x</p> <p>72 °C 5 min } 35 x</p> <p>10 °C forever</p>	<p><u>Reaction Program for B1:</u></p> <p>94°C 2 min</p> <p>94°C 30 sec } 39 x</p> <p>60°C 45 sec } 39 x</p> <p>72 °C 1 min } 39 x</p> <p>72 °C 9 min } 39 x</p> <p>10 °C forever</p>

Separation of DNA on agarose gels

The agarose gel was prepared by boiling 2 % agarose in TAE buffer until complete dissolution of the agarose and then allowed to cool down until circa 40°C. Ethidium bromide was added and the solution poured into a gel chamber, where it solidified. Subsequently the comb used to create the pockets was removed and the chamber was filled with TAE buffer. The DNA mix and 6× loading

buffer were loaded onto gel and run for 30 minutes at 200 V. After electrophoresis a photograph of the gel was taken in the transilluminator on a UV light box and printed.

7.3.2 Cell culture

7.3.2.1 Mammalian cell lines

Maintaining 293 cells

The 10 cm tissue culture dish with 293 cells were prepared with 8 ml of medium and kept at 37°C, 7.5 % CO₂ and 95 % relative humidity in a CO₂ incubator. Before cells reach 100 % confluency, they were washed with 4 ml DPBS (at RT) and incubated with 2 ml Trypsin/EDTA at 37°C until all detach completely. Then the cells were diluted with 8 ml of pre-warmed growth medium and after brief dissociation one tenth of total volume were transferred to a new 10 cm tissue culture dish with 7 ml of pre-warmed growth medium.

Freezing of 293 cells

As the cells reach ~80 % confluency they were harvested as described above, collected in a 15 ml Falcon tube and spun for 5 min at 800 rpm. The cells were then re-suspended in 925 µl growth medium and 925 µl FBS for each vial with 5 % DMSO and 2 ml was transferred to cryo-vials. For gentle freezing vials were placed in an isopropanol isolated box and stored -80°C overnight and for long term storage they were transferred to the liquid nitrogen tank.

Thawing of 293 cells

The frozen cells were thawed by quickly placing them into a 37°C water bath and 10 ml of pre-warmed growth medium was added. After spinning for 5 minutes at 1000 rpm cells were collected, re-suspended and seeded onto the culture plates containing 7 ml of pre-warmed growth medium.

Collecting Reelin

Confluent cells expressing either GFP or Reelin were split in a ratio of 1/10 and kept in the incubator overnight. Next day the cells were washed twice with DPBS (at RT) and starved in the pre-warmed 293 starving medium for two days. The supernatant was transferred to a falcon tube and spun at 4000 rpm at 4 °C for 5 minutes to remove the cell debris. To concentrate the protein, 13 ml of the supernatant were transferred to 100 kDa centrifugal filter units and spun at 4000 rpm at 4°C for 20 minutes and this process was repeated until the supernatant was concentrated 20x or 40x, depending on the experimental requirements. Subsequently, the supernatant was transferred to Eppendorf tubes and either snap-frozen in liquid nitrogen and stored at -80°C or used immediately. The high content of Reelin protein in the medium collected from Reelin-expressing but not from GFP expressing cells was confirmed by Western blotting using a directed antibody against Reelin (Figure 7.1).

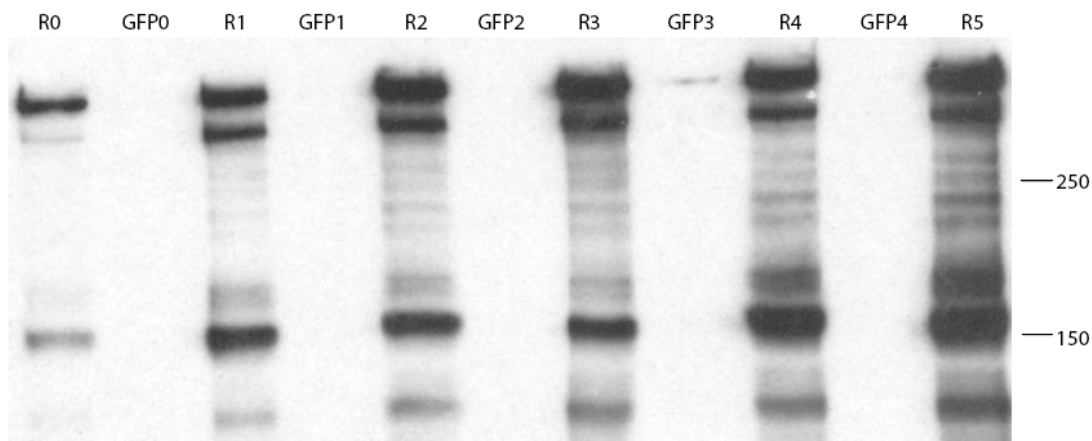


Figure 7.1 A western blot is depicted showing the presence of Reelin protein in Reelin conditioned medium but not in the control medium. Reelin supernatant from 293-Rln cells was concentrated in 5 steps (R0-R5), and samples from each step loaded on a 6% SDS-PAGE gel and analyzed by western blotting with α -Reelin (40-189) antibody. Samples from 293-GFP cells were also concentrated in parallel in 5 steps and used as a control (GFP0-GFP4).

7.3.2.2 Cultivation of primary cortical neurons

Coverslip (CVS) treatment and coating

CVS were first treated with nitric acid in a glass beaker at RT over night. The next day, in order to remove the acid, the CVS were washed 3 - 4 times quickly with H₂O then 4 times each for 30 minutes. The CVS were then spread separately on Whatmann paper to dry, and to sterilize the dried CVS were baked in the oven at 165°C. The CVS were then placed into 24 well plates and incubated with 1 mg/ml poly-D-lysine in Borate-Buffer (400 µl/well) at 37°C for minimum 5 hours. Then the CVS were washed 3 times with distilled sterile H₂O and air dried in sterile hood for 20 minutes and then coated with 5 µg/ml laminin in DPBS (400 µl/well) for minimum 2 hours at 37°C. Then the CVS were washed 3 times with DPBS and filled with 400 µl neurobasal (NB) medium and left in the incubator to equilibrate pH and the temperature.

Isolation of Cortical Neurons (adapted from (Zhang *et al.*, 2005))

On day E15.5 or E16.5 the pregnant mouse was anaesthetized and after cervical dislocation the uterus was removed and the embryos were taken out into ice-cold dissection medium (DM). The heads were then cut with sharp scissors. Fine-tip tweezers were used to hold the isolated brain. First the skull was removed by cutting the skull along both of the basal-lateral sides by another pair of tweezers and a fine scissor. The brains were then first cut into two halves and brain cortices were removed from the midbrain and brainstem and then transferred into a new dish containing fresh DM. Under a dissection microscope the meninges were removed and pooled together in a 15 ml tube containing ice-cold DM. After cortices from all brains were collected, the DM was carefully replaced with 1-2 ml pre-warmed trypsin and the tube put into the water bath for 15 minute incubation at 37°C. After removing the trypsin the reaction was stopped by washing the cortices 3 times with the pre-warmed serum medium (SM) and twice with the pre-warmed NB medium. The cortices were then triturated in 1.5 ml NB by passing through the fire polished Pasteur pipette 30 times (carefully avoided to make bubbles as neurons do not like oxygen) and centrifuged for 5 minutes at 650 rpm. The supernatant was removed and the cells were resuspended in pre-warmed

NB medium with the fire-polished Pasteur pipette. The cell number was counted using a Neubauer counting chamber, and 60.000 - 70.000 cells/well (24 well plates) and 5.000.000 cells/6 cm dish plates cultured for 3 - 5 days in vitro (DIV) at 37°C in a humidified incubator.

7.3.3 Biochemistry

7.3.3.1 Cell Stimulation

EphB and ephrinB stimulation

Eph receptors and ephrin ligands were activated with multimeric ligands or receptors, respectively. The EphB-Fc, ephrin-Fc or as control Fc were preclustered for 30 minutes at RT with anti-human-Fc using 1/10 (w/w). In biochemistry experiments 1 µg/ml (cells) or 4 µg/ml (neurons) and in immunocytochemistry experiments 4 µg/ml of pre-clustered recombinant Eph-Fc, ephrin-Fc or Fc was used. Before stimulation the neurons were washed with warmed DPBS (+CaMg) and then stimulated for 30 - 60 min, depending on the assay conditions.

Reelin and GFP stimulation

Before stimulation cortical neuron cultures were washed 3 times with DPBS and then stimulated for 60 minutes with 250 µl of 20x Reelin or GFP as control for biochemistry and immunocytochemistry experiments. Organotypic slice cultures were stimulated 3 subsequent days with 250 µl of 20x Reelin and GFP supernatants.

7.3.3.2 Cell or Tissue Lysis and Protein Concentration Measurements

Cell and Tissue Lysis

Stimulated cells were washed once with ice-cold DPBS and lysed in chilled lysis buffer on ice (e. g. 250 µl/6 cm Ø dish). The cells were collected using cell scrapers and the tissue was homogenized using glass homogenizers on ice. The lysates were collected into Eppendorf tubes and incubated in the lysis buffer on spinning wheel at 4°C for 1 hour. Then, in order to remove insoluble material

7 Material and methods

(nuclei, cytoskeletal components and insoluble membrane), cell lysates were centrifuged at 10,000 g for 10 minutes and homogenized tissue for 45 minutes at 4°C. The supernatant was placed in a fresh Eppendorf tube and directly used to measure the protein concentration.

Protein Concentration Measurement

The protein concentration of cell and tissue lysates was determined using the BioRad DC Protein Assay kit. Different BSA concentrations were used as standard and assayed together with the samples. Based on the standard, the protein amount in each sample was determined and equal amounts were used for further assays.

7.3.3.3 Immunoprecipitation and Pulldown Experiments

Immunoprecipitation

10 µl of appropriate agarose beads (Table 7.9) per sample were washed 3 times with PBS by centrifugation at 2.8 rpm for 2.5 minutes. After the last wash the beads were incubated with appropriate amount of antibody on a rotating wheel at RT for 40 - 60 minutes. The bead-antibody complexes were then loaded with 2 mg of tissue or cell lysates and incubated at 4°C on a spinning wheel for 2 hours. Following incubation the tubes were spun at 3.0 rpm for 3 minutes and the supernatant was discarded. The beads were washed three times with lysis buffer to remove the traces of unbound proteins by centrifugation at 3.0 rpm for 3 minutes with ice-cold lysis buffer and the immunoprecipitates were eluted by boiling in 25 µl of 2x sample buffer at 95°C for 5 minutes. Proteins in immunoprecipitates were detected by running on SDS gels, to separate the precipitated proteins, and analyzed by immunoblotting.

Table 7-9: Agarose beads and antibody specificity

Product	Specificity
Protein A-Agarose	mouse IgG _{2a} , IgG _{2b} & IgA, rabbit polyclonal, human IgG ₁ , IgG ₂ & IgG ₄ antibodies

Protein G PLUS-Agarose	mouse IgG ₁ , IgG _{2a} , IgG _{2b} & IgG ₃ , rat IgG ₁ , IgG _{2a} , IgG _{2b} & IgG _{2c} , rabbit and goat polyclonal, human IgG ₁ , IgG ₂ , IgG ₃ &IgG ₄ antibodies
Protein A/G PLUS	All of the above antibodies

Pulldown Experiments

In order to study highly specific ligand-receptor-interaction, pulldowns were used to isolate and to study the ephrinB molecules and their interaction partners. To pulldown ephrinB molecules from cell or tissue lysates, the extracellular part of Eph receptors fused to Fc portions of human antibodies (EphB2-Fc) were used (Cowan *et al.*, 2001). To pulldown Reelin α -Reelin (mouse) and for Dab1 α -Dab1 (rabbit) antibodies were used.

10 μ l of agarose beads per sample were taken and washed 3 times with PBS by centrifugation at 2.8 rpm 2.5 minutes. The beads were loaded with 5 μ g EphB-Fc, ephrinB-Fc or Fc (control for unspecific binding) together with the lysates and incubated over night at 4°C on a rotating wheel. The beads were pre-cleaned by incubation of only beads for 30 minutes at 4°C and the supernatants added only after. The beads were washed 3 times with ice cold lysis buffer by centrifugation at 3.0 rpm for 3 minutes, and the pulldowns were mixed with 25 μ l sample buffer and boiled at 95°C for 5 minutes. The proteins were then separated on SDS page gels.

7.3.3.4 Immunoblotting

The samples eluted in loading buffer and boiled at 95°C were separated on 6 % or 7.5 % SDS page gels and transferred to nitrocellulose membrane using a semi-dry blotting chambers (1 mA per cm² for 1 to 1.5 hours) in transfer buffer (20 % methanol). The membranes were first blocked in blocking solution depending on antibody-specific-requirements for 1 hour at RT and then incubated with the primary antibody for 1 hour at RT or overnight at 4°C. Subsequently membranes were washed 3 times for 10 minutes at RT in PBST. Secondary antibodies, linked to horseradish peroxidase (HPR),

7 Material and methods

were used to specifically detect primary antibodies. After incubating with secondary antibodies for 1 hour at RT the membranes were washed again 3 times 10 minutes in PBST and the signal was visualized using chemiluminescent reagent ECL for 1 minute at RT. The membranes were then wrapped in plastic wrap, placed in a film cassette and after different exposure times the films were developed in the developing machine.

7.3.4 Mouse work

All the mouse strains C57BL6/J were bred in the animal house of Goethe University, Frankfurt am Main, GERMANY. Animals were separated from their parents around postnatal day (P) 20 and males and females were housed separately. The animals were ear-tagged and tail biopsies were taken for genotyping. Transgenic mice were crossed with C57BL6/J genetic background, namely a heterozygous male was crossed with a wild-type female. *Reeler* mice (*rl/+*, stock number 000235, The Jackson Laboratory) were also backcrossed to C57BL6/J. For ephrinB3 knockout line wild type (WT) and homozygous littermates were obtained by heterozygous crossings. For ephrinB2 knockout line Cre^+ ephrinB2^{lox/lox} mouse was interbred with a Cre^- ephrinB2^{lox/lox} mouse. To generate compound mutant mice heterozygous *reeler* (*rl/+*) mice were crossed with homozygous or heterozygous ephrinB2 (b2) and ephrinB3 (b3) knockout animals. The progeny of this mating was interbred to generate *rl+*, *rl/+*, *b2-/-* or *b3-/-*, and *rl/+*; *b2-/-* or *rl/+*; *b3-/-* compound mutant mice (Figure 7.2). Depending on experimental design ephrinB3 mouse were bred with Thy1-GFP line as a heterozygous cross. For experiments with embryos formation of vaginal plugs on female mice was tracked daily from the first day of breeding. The day a plug was recorded as embryonic day 0.5 (E0.5). Embryos were taken according to experimental procedures between E14.5 – E18.5. The day of birth was recorded as P0. All animal experiments were carried out in accordance with the appropriate governmental authorities.

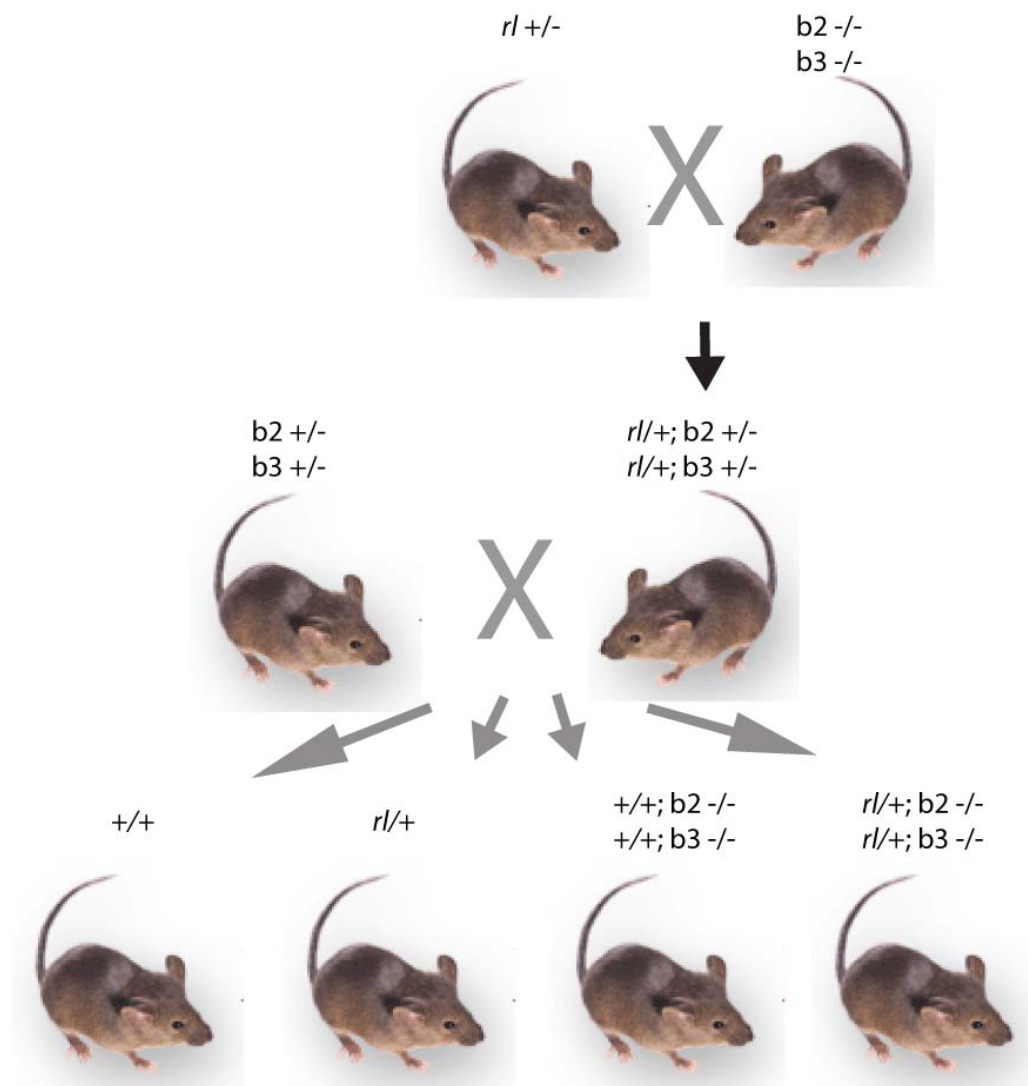


Figure 7.2 Generation of compound mutant mice. First heterozygous *reeler* ($rl/+$) mice were crossed with homozygous ephrinB2 ($b2$) or ephrinB3 ($b3$) knockout animals. The progeny of this mating was interbred to generate wild-type ($+/+$), heterozygous *reeler* ($rl/+$), ephrinB2 knockout ($b2 -/-$), or ephrinB3 ($b3 -/-$), and heterozygous *reeler* ephrinB2 or ephrinB3 knockout ($rl/+; b2 -/-$ or $rl/+; b3 -/-$) compound mutant mice. Cre recombinase containing ephrinB2^{lox/lox} mice were called as $b2 -/-$, and $b2+/+$ abbreviation was used to refer to a Cre^+ and a Cre^- ephrinB2^{lox/lox} crossing.

7.3.5 Histology

7.3.5.1 Fixation and perfusion

Pregnant animals were first anesthetized with diethylether and then sacrificed by cervical dislocation. Embryos were removed, the whole brains dissected out quickly and washed with 15 ml

7 Material and methods

ice cold DPBS to remove blood. The brains were then fixed in 4 % paraformaldehyde (PFA) overnight. For cryosectioning the brains were first fixed in 4 % PFA/4 % sucrose overnight and then cryoprotected in 30 % sucrose in DPBS overnight at 4°C. Brains of young post-natal mice were immersion fixed in 4 % PFA at 4°C overnight. Mice older than 5 days were perfused. Postnatal mice were first anesthetized with isoflurane and then perfused transcardially under anesthesia first with DPBS and then with 4 % PFA in DPBS. After perfusion the brains were dissected out from the skull and post-fixed overnight in 4 % PFA at 4°C and after washing in DPBS either embedded directly for sectioning or stored in DPBS + 0.01 % sodium azide at 4°C.

7.3.5.2 Cryosectioning

Cryosections were used for immunohistochemistry of various mice lines. Therefore, perfused brains were placed into embedding medium (Tissue-Tek) by putting the olfactory bulbs to the front of the embedding molds on a cooling platform. Sagittal or coronal sections were cut at a thickness of 20 µm using a microtome. Single sections were picked up with a fine brush and placed on the microscope slides. The sections were dried on a 37°C heating platform overnight and stored at 4°C for short term storage and at -20°C for long term storage.

7.3.5.3 Vibratome sectioning

Vibratome sections were used for immunohistochemistry of various cortical areas in different mice lines. For vibratome sectioning perfused brains were embedded in embedding medium. Therefore, an 11-ml aliquot of embedding medium (27 % albumin, 4.5 % gelatin in DPBS + 0.04 % sodium azide) was thawed at 37°C and cooled down at RT to prevent rapid polymerization after glutaraldehyde addition. First a base was prepared by adding 100 µl of 25 % glutaraldehyde to 2 ml embedding medium, mixed quickly and poured into the molds. After the polymerization took place brains were placed onto the base. Then the 4 ml of the embedding medium was mixed with 200 µl of 25 %

glutaraldehyde and quickly poured onto the sample. For complete solidification the polymerized sample was stored 1 hr at 4°C in DPBS. With histoacryl-tissue glue the gelatin block was glued on the flat metal block of the vibratome. Then vibratome sections were cut sagittally or coronally at 50 µm thickness using a Leica vibratome. Sections were picked up with a fine brush and placed in DPBS containing 24 well plates until they were processed for immunohistochemistry.

7.3.5.4 Immunocytochemistry

Primary cortical neurons, to be analyzed by fluorescence imaging, were seeded onto glass coverslips in a 24-well plate. After stimulation or required growth was achieved the neurons were fixed with 4 % PFA/4 % sucrose in DPBS for 12 minutes on an ice tray (4°C). After PFA was removed the cells were rinsed twice with DPBS and incubated with 50 mM NH₄Cl in DPBS for 10 minutes at 4°C to remove the excessive PFA. The NH₄Cl was rinsed off twice with cold DPBS and then the cells were permeabilized for 5 minutes with ice cold 0.1 % Triton X-100 (in DPBS). After washing the cells 3 times for 5 minutes with DPBS, the cells were incubated in blocking solution (2 % bovine serum albumin, 4 % donkey and/or 4 % goat serum) for 30 minutes at RT and then incubated with primary antibodies for 60 - 90 minutes at RT, or over night at 4°C. pDab1 (1:1000, Cell Signaling, Danvers, U.S.A.), ApoER2 (1:500, Sigma, GERMANY) and VLDLR (1:20, R&D, Minneapolis, U.S.A.) were used to visualize the phosphorylated Dab1 and the two LDL receptors, and human-Fc was used to visualize the clustered ephrinB patches on the neuronal branches. Following 3 subsequent washes each of 5 minutes the cells were incubated with secondary antibodies for 60 minutes at RT in a dark chamber. Finally, the cover slips were washed 3 times for 5 minutes with DPBS, once with H₂O and mounted on slides using the Gel/Mount anti-fading medium (Biomedica corp). Fluorescent images were acquired with a digital camera (SpotRT; Diagnostic Instruments) attached to an epifluorescence microscope (Zeiss) to visualize neurons.

7.3.5.5 Immunohistochemistry

Cryosections, collected on gelatin coated glass microscope slides, were first washed with DPBS for 5 minutes. The sections were then boiled in 0.1 % sodium citrate buffer (ph 8.0) 3 times in microwave for antigen retrieval and cooled down between boiling steps on ice. After the last boiling sections were washed with DPBS shortly and placed on a humidified chamber for the rest of the staining procedure. Sections were incubated 1 hr at RT in 0.2 % TX-100 (in DPBS)/10 % serum (blocking solution). The primary antibody was diluted in the blocking solution and incubated overnight at 4°C. After washing three times with DPBS for about 30 minutes, slices were either incubated with fluorescent labeled secondary antibody diluted in DPBS for 2 hours at RT or processed for DAB staining. After 3 washes with DPBS slices were mounted in Gel/Mount media and dried at RT.

Free floating vibratome sections were first permeabilized in 0.4 % TritonX 100 (in DPBS) for 30 minutes at RT on a rocker. Then blocked in 0.2 % TritonX 100 (in DPBS) + 2 % serum (typically from the same animal species used for the production of the secondary antibody) as standard blocking solution, otherwise antibody specific blocking solution was used to block unspecific binding at RT for 1 hour. Following blocking the sections were incubated with primary antibody in 0.05 % TritonX-100 (in DPBS)/1 % serum over 2 nights at 4°C then washed 3 times with DPBS each for 5 minutes and incubated with either fluorescent labeled secondary antibody in DPBS/0.5 % serum or processed for DAB staining. After 3 washes in DPBS slices were mounted in Aqua Poly/Mount mounting medium on glass slides and dried at RT.

To visualize the cell layers in the dentate gyrus and hippocampus proper, as well in MZ of cortex, mouse anti-NeuN (1:1000, Chemicon, Hofheim, Germany), a neuronal marker, was used. Rabbit polyclonal Tbr1 (1:1000, Chemicon), goat Brn1 (1:100, Santa Cruz, California, U.S.A.), rabbit FoxP2 (1:100, Abcam, Cambridge, UK) and rabbit polyclonal SatB2 (1:100, Abcam) were used to analyze the cortical layering of various compound mice. Rabbit polyclonal anti-GFAP (1:500, DAKO, Denmark)

and mouse monoclonal RC2 (1:1000, Chemicon) were used to stain the glial fibrillary acidic protein of radial glial cells. Mouse monoclonal MAP2 (1:1000, Chemicon) was used to analyze the dendritic processes of cortical neurons. For dentate granule cells, mouse monoclonal anti-calbindin (1:500, Chemicon) which recognizes the calcium-binding protein contained in dentate granule cells, in the cerebral cortex, and Purkinje cells in cerebellum was used. Rabbit Polyclonal anti-calretinin (1:3000, Swant, Bellinzona, Switzerland) and goat polyclonal anti-calretinin (1:2000, Chemicon) were used to label the calcium-binding protein contained in GABAergic interneurons and mossy cells of the dentate gyrus from wild-type and compound mice. Rabbit polyclonal anti- ApoER2 (1: 1000, Santa Cruz Biotechnology) was used to stain against the intracellular domain of the ApoER2 receptor. Mouse monoclonal anti-chondroitin sulfate (CS-56) (1:500, Sigma) recognizes the chondroitin sulfate chains of the CSPGs (Miller *et al.*, 1995).

7.3.5.6 DAB staining

Following primary antibody incubation the sections were washed with the indicated washing buffer and for non-fluorescent detection ABC kit was used. The sections were first incubated with secondary antibody in 1:300 dilution in DPBS containing 1.5 % serum for 1 hour at RT. The sections were then washed with DPBS and incubated in the Avidin-Biotinylated immuno-peroxidase enzyme complex (Vector Laboratories) for 1 hour at RT (The enzyme complex was prepared 1 hour prior to use, as the manufacturer's instruction). The sections were then washed several times with DPBS and staining was visualized with the 3, 3'-Di-amino-benzidine substrate (Sigma, UK) with 0.003 % H₂O₂ in distilled water. The reaction was controlled under stereomicroscope and stopped by washing the slices several times with DPBS and once with distilled water. The sections were then mounted using Eukitt on the microscope slides.

7.3.5.7 Negative controls

To rule out any unspecific binding of the secondary antisera, control experiments were performed by either leaving out the primary antibody or by using a primary antibody against an antigen that is not present in the respective tissue or at the respective developmental stage.

7.3.5.8 Nissl staining

This staining is based on the attraction of the basic dye cresyl violet to acidic ribonucleic acids which are enriched at the smooth endoplasmic reticulum in the perinuclear cytoplasm of neurons. It leads to a violet labeling of the somata of neurons and glial cells. With this staining, the cytoarchitecture of cortex was visualized.

Cryosections were first incubated in 50 % methanol/50 % isopropanol overnight at -20°C to de-fat the sections. The sections were then rehydrated through decreasing ethanol concentrations, 100 %, 95 %, 70 %, 50 % and distilled water, each for 5 minutes. Dehydrated sections were then stained in cresyl violet solution for 3 minutes and washed immediately with distilled water twice for 5 minutes. The sections were re-hydrated through increasing ethanol steps; 50 %, 70 %, 95 %, twice 100 % each for 5 minutes and then incubated twice for 5 minutes in xylene. Sections were then mounted with Eukitt on microscope slides and left to dry in a hood overnight.

7.3.5.9 DNA-labeling

For detection of the cell nuclei sections were stained with DAPI (4,6-diamino-2-phenylindole; (Naimski *et al.*, 1980) or propidium-iodide (PI) (Crissman *et al.*, 1976). DAPI-staining results in blue, PI in red and both substances are dyes that intercalate into nucleic acid molecules of DNA and RNA. DNA staining (DAPI 1µg/ml in PBS; PI 5µg/ml in PBS containing 50U/ml RNaseA) was performed after immunohistochemistry in sections for 5-10 minutes at RT followed by three consecutive washing steps in PBS at RT.

7.3.6 Birthdating studies

7.3.6.1 Cumulative BrdU labeling

For birthdating studies and to determine the number of dividing cells, the timed-pregnant female mice were injected intraperitoneally at different stages of pregnancy (E12.5, 15.5 and E17.5) with a single pulse (50 mg/kg body weight) of BrdU (5 mg/ml dissolved in saline). In order to study cortical layering in compound mice BrdU injected mice were analyzed at embryonic stages (E17.5 and E18.5) as well as at postnatal stages (P20). Therefore, if the embryonic brains were required, the female mice were anesthetized and the brains of embryos were fixed and embedded either for micratome or for vibratome sectioning, as described in the previous section. If postnatal animals were required, the mice were perfused and the brains were embedded for vibratome sectioning as described. In order to label new born neurons in organotypic cultures of *reeler* cortex, the pregnant mice were injected at E15.5 and after 2 hours the embryos were removed and the cortical organotypic cultures were prepared as described in following section.

7.3.6.2 BrdU staining

BrdU staining was performed as described previously (Nowakowski *et al.*, 1989). First the endogenous peroxidase activity was quenched by incubation with 0.6 % H₂O₂ (in TBS) for 30 minutes at RT. The sections were then incubated in 2xSSC/50 % formamide for 2 hours at 65°C and following the incubation rinsed twice each for 5 minutes with 2xSSC. To denature the DNA sections were incubated in 2 M HCl at 37°C for 1 hour and rinsed for 10 minutes in 0.1M Boric acid (pH8.5) at RT. After blocking for 30 minutes in 0.25 % TritonX (in TBS)/3 % normal goat serum sections were incubated with α -BrdU (1:1000, Chemicon) primary antibody in blocking solution overnight at 4°C. After washing twice with TBS for 5 minutes sections were incubated either with fluorescent labeled secondary antibody in TBS/ 0.2 % goat serum at RT for 2 hours or processed for DAB staining and mounted on the microscope slides.

7.3.7 Organotypic cultures

7.3.7.1 Preparation of embryonic cortical sections

Pregnant *rl/+* female mice were injected with 0.2 ml of 10 mg/ml BrdU at E15.5. After 2 hours, the females were decapitated under hypothermic anesthesia and then the wounds and the skin were disinfected with 100 % isopropanol. All next steps were performed under almost sterile conditions. The embryos were removed and placed in a dish on ice. After cutting the head skin with fine scissors along the longitudinal fissure and under the ears, the skin was pulled ventrally. The skull was opened by cutting along its caudal to rostral axis with fresh scissors. The second cut pointing towards the left or right ear was made perpendicular to the first cut to make a cross-cut. To expose the brain completely, the skull was carefully opened with a fine forceps. By means of a spatula, the brain was removed from the base of the skull into a plastic dish containing ice-cold preparation medium. The dishes had been placed on a pre-cooled metal block before the preparation. After removing the cerebellum, the brain hemispheres were glued on the metal vibratome cutting block and free floating coronal section of 300 μm were obtained in dissection medium using vibratome (speed: 10-20 mm/s, Amplitude: 0.9 mm) and placed on 0.4 μm culture plate inserts moistened with 1 ml of dissection medium. The filters were put in a sterile 6-well plate containing 1 ml incubation medium per well and the cultures were maintained in a humidified incubator with 5 % CO_2 at 35°C for 4 days. The incubation medium was changed first after 4 hours of recovery and then every two days.

Tails were collected for subsequent genotyping.

7.3.7.2 Stimulation

The embryos and new born mice were genotyped and after 4 hours of recovery time, *reeler* and wild-type explants were stimulated with recombinant mouse EphB3-Fc chimera or with human IgG, Fc fragment as a control. For effective initiation of the signaling, for each stimulated well 15 μl of the

stimulants (0.2 µg/µl) were used. If cultures were kept longer than one day, then the stimulation was repeated after 24 hours and the incubation medium was changed every second day. For better orientation in the brain slices during subsequent confocal imaging, agarose beads (Biorad) were placed in the ventricles of the slices. Before applying the beads on the tissue, they were washed 3 times with distilled water and 4 times with DPBS.

7.3.7.3 Fixation and Immunohistochemistry of organotypic cultures

After 1 - 4 days in culture the brain slices were fixed by replacing the medium with 4 % PFA/2 % sucrose in DPBS for 1 - 3 hours at RT. Subsequently, the slices were transferred to 48 well plates and washed 5 times for 10 minutes with TBS pH 8. The slices were kept in TBS at 4°C at least 24 hours before they were stained.

Fixed and washed brain slices were incubated in 0.6 % H₂O₂ in TBS for 30 minutes to kill endogenous peroxidase. To detect the BrdU labeled nuclei the slices were stained as described previously. Images were obtained using a confocal microscope (Leica, 15 µm stacks, 20X objective) and the maximum intensity was used for subsequent quantification of the number of BrdU-positive cells in the cortical layers using Metamorph software.

7.3.8 Tandem affinity purification (TAP) and mass spectrometry

Grb4-CTAP (C-terminal fusion) was generated as described in Stefan Weinges thesis (Bouwmeester *et al.*, 2004, Weinges, 2006). TAP purification, protein digestion, mass spectrometry and protein identification were done as described in Stefan Weinges thesis (Angrand *et al.*, 2006, Weinges, 2006).

7.3.9 Data analysis

Immunofluorescence

Neuron cultures and cryostat section images were acquired using a digital camera (SpotRT; Diagnostic Instruments) attached to an epifluorescence microscope (Zeiss) equipped with a 40X and a 63X objective (Plan-Apochromat; Zeiss). All quantitative measurements were performed using MetaMorph software (Molecular Devices).

Vibratome sections were analyzed at a two-channel confocal laser-scanning microscope (CLSM) using 20x to 40x objectives. Single optical section images (thickness 1-10 μm) and maximum intensity images (thickness 10-150 μm) were derived.

Quantification

Quantification of NeuN+ cells in MZ layer and in CA1 region of hippocampus, Tbr1+ cortical layer V neurons, calbindin+ interneurons, BrdU birthdating analysis of cortical neurons and for BrdU labeled cell distribution in cortical organotypic cultures images were made from sections using the 20x objective of a CLSM. The cells were counted throughout the rostral-caudal extent of the cortex (minimum of 6 sections per level, per animal, per condition). The quantification of BrdU labeled cell distribution was performed by further subdividing the cortex into 10 bins and the percentage of cells in each bin was plotted. In all counts, the experimenter did not know the condition of each animal. The distribution of cell in cortical layers were done by dividing each coronal strip into 5 or 6 bins arranged parallel to the pial surface that these corresponded to the different layers of the developing or developed cortex (VZ/SVZ, IZ, SP, CP, MZ). The extent of each layer was determined by Nissl counter staining, which is a cytoplasmic neuronal marker.

Quantification of pDab1 phosphorylation was based on fluorescence intensities. The intensity of signal was calculated for dendrite stretches of 100-200 μm from at least 10 different neurons (n= 50-100).

Sholl analysis

Sholl analysis was performed to study the dendritic branching of hippocampal pyramidal neurons. Sholl analysis is a quantitative method to characterize the morphological characteristics of a neuron and is based on counting the number of dendrite intersections after concentric circles of gradually increasing radius have been drawn starting from the center of the cell body (Sholl, 1953).

Statistics

For all data sets, the arithmetic average $\bar{x} = \frac{1}{n} \sum_{i=1}^n x_i$ was calculated and the standard deviation

and the standard error of the mean $SEM = \frac{s}{\sqrt{n}}$ were computed. Error bars depict the SEM. The Student's t-test was used to examine whether data sets differed significantly.

Data were considered as significant with $p < 0.05$ and as highly significant with $p < 0.01$. Calculations of the arithmetic average, the standard deviation, the standard error of the mean were performed with Microsoft Excel.

8 Bibliography

- Alcantara, S., Ruiz, M., D'Arcangelo, G., Ezan, F., de Lecea, L., Curran, T., *et al.* (1998). Regional and cellular patterns of reelin mRNA expression in the forebrain of the developing and adult mouse. *J Neurosci* **18**, 7779-7799.
- Andersen, O.M., Benhayon, D., Curran, T. and Willnow, T.E. (2003). Differential binding of ligands to the apolipoprotein E receptor 2. *Biochemistry* **42**, 9355-9364.
- Anderson, A., Belelli, D., Bennett, D.J., Buchanan, K.I., Casula, A., Cooke, A., *et al.* (2001). Alpha-amino acid phenolic ester derivatives: novel water-soluble general anesthetic agents which allosterically modulate GABA(A) receptors. *J Med Chem* **44**, 3582-3591.
- Anderson, S.A., Eisenstat, D.D., Shi, L. and Rubenstein, J.L. (1997). Interneuron migration from basal forebrain to neocortex: dependence on Dlx genes. *Science* **278**, 474-476.
- Angevine, J.B., Jr. and Sidman, R.L. (1961). Autoradiographic study of cell migration during histogenesis of cerebral cortex in the mouse. *Nature* **192**, 766-768.
- Angrand, P.O., Segura, I., Volkel, P., Ghidelli, S., Terry, R., Brajenovic, M., *et al.* (2006). Transgenic mouse proteomics identifies new 14-3-3-associated proteins involved in cytoskeletal rearrangements and cell signaling. *Mol Cell Proteomics* **5**, 2211-2227.
- Arlotta, P., Molyneaux, B.J., Chen, J., Inoue, J., Kominami, R. and Macklis, J.D. (2005). Neuronal subtype-specific genes that control corticospinal motor neuron development in vivo. *Neuron* **45**, 207-221.
- Arnaud, L., Ballif, B.A., Forster, E. and Cooper, J.A. (2003). Fyn tyrosine kinase is a critical regulator of disabled-1 during brain development. *Curr Biol* **13**, 9-17.
- Assadi, A.H., Zhang, G., Beffert, U., McNeil, R.S., Renfro, A.L., Niu, S., *et al.* (2003). Interaction of reelin signaling and Lis1 in brain development. *Nat Genet* **35**, 270-276.
- Austin, C.P. and Cepko, C.L. (1990). Cellular migration patterns in the developing mouse cerebral cortex. *Development* **110**, 713-732.
- Ballif, B.A., Arnaud, L., Arthur, W.T., Guris, D., Imamoto, A. and Cooper, J.A. (2004). Activation of a Dab1/CrkL/C3G/Rap1 pathway in Reelin-stimulated neurons. *Curr Biol* **14**, 606-610.
- Ballif, B.A., Arnaud, L. and Cooper, J.A. (2003). Tyrosine phosphorylation of Disabled-1 is essential for Reelin-stimulated activation of Akt and Src family kinases. *Brain Res Mol Brain Res* **117**, 152-159.
- Bar, I., Lambert De Rouvroit, C., Royaux, I., Krizman, D.B., Derroncourt, C., Ruelle, D., *et al.* (1995). A YAC contig containing the reeler locus with preliminary characterization of candidate gene fragments. *Genomics* **26**, 543-549.
- Bartley, T.D., Hunt, R.W., Welcher, A.A., Boyle, W.J., Parker, V.P., Lindberg, R.A., *et al.* (1994). B61 is a ligand for the ECK receptor protein-tyrosine kinase. *Nature* **368**, 558-560.
- Bayer, S.A. (1980). Development of the hippocampal region in the rat. II. Morphogenesis during embryonic and early postnatal life. *J Comp Neurol* **190**, 115-134.
- Beffert, U., Morfini, G., Bock, H.H., Reyna, H., Brady, S.T. and Herz, J. (2002). Reelin-mediated signaling locally regulates protein kinase B/Akt and glycogen synthase kinase 3beta. *J Biol Chem* **277**, 49958-49964.
- Beffert, U., Weeber, E.J., Durudas, A., Qiu, S., Masiulis, I., Sweatt, J.D., *et al.* (2005). Modulation of synaptic plasticity and memory by Reelin involves differential splicing of the lipoprotein receptor Apoer2. *Neuron* **47**, 567-579.
- Belvindrah, R., Graus-Porta, D., Goebbels, S., Nave, K.A. and Muller, U. (2007). Beta1 integrins in radial glia but not in migrating neurons are essential for the formation of cell layers in the cerebral cortex. *J Neurosci* **27**, 13854-13865.

- Benhayon, D., Magdaleno, S. and Curran, T. (2003). Binding of purified Reelin to ApoER2 and VLDLR mediates tyrosine phosphorylation of Disabled-1. *Brain Res Mol Brain Res* **112**, 33-45.
- Benson, M.D., Romero, M.I., Lush, M.E., Lu, Q.R., Henkemeyer, M. and Parada, L.F. (2005). Ephrin-B3 is a myelin-based inhibitor of neurite outgrowth. *Proc Natl Acad Sci U S A* **102**, 10694-10699.
- Bielas, S.L. and Gleeson, J.G. (2004). Cytoskeletal-associated proteins in the migration of cortical neurons. *J Neurobiol* **58**, 149-159.
- Bock, H.H. and Herz, J. (2003a). Reelin activates SRC family tyrosine kinases in neurons. *Curr Biol* **13**, 18-26.
- Bock, H.H., Jossin, Y., Liu, P., Forster, E., May, P., Goffinet, A.M. and Herz, J. (2003b). Phosphatidylinositol 3-kinase interacts with the adaptor protein Dab1 in response to Reelin signaling and is required for normal cortical lamination. *J Biol Chem* **278**, 38772-38779.
- Bock, H.H., Jossin, Y., May, P., Bergner, O. and Herz, J. (2004). Apolipoprotein E receptors are required for reelin-induced proteasomal degradation of the neuronal adaptor protein Disabled-1. *J Biol Chem* **279**, 33471-33479.
- Bonhoeffer, F. and Huf, J. (1985). Position-dependent properties of retinal axons and their growth cones. *Nature* **315**, 409-410.
- Borrell, V., Del Rio, J.A., Alcántara, S., Derer, M., Martínez, A., D'Arcangelo, G., *et al.* (1999). Reelin regulates the development and synaptogenesis of the layer-specific entorhino-hippocampal connections. *J Neurosci* **19**, 1345-1358.
- Botella-Lopez, A., Burgaya, F., Gavin, R., Garcia-Ayllon, M.S., Gomez-Tortosa, E., Pena-Casanova, J., *et al.* (2006). Reelin expression and glycosylation patterns are altered in Alzheimer's disease. *Proc Natl Acad Sci U S A* **103**, 5573-5578.
- Bouwmeester, T., Bauch, A., Ruffner, H., Angrand, P.O., Bergamini, G., Croughton, K., *et al.* (2004). A physical and functional map of the human TNF-alpha/NF-kappa B signal transduction pathway. *Nat Cell Biol* **6**, 97-105.
- Britanova, O., de Juan Romero, C., Cheung, A., Kwan, K.Y., Schwark, M., Gyorgy, A., *et al.* (2008). Satb2 is a postmitotic determinant for upper-layer neuron specification in the neocortex. *Neuron* **57**, 378-392.
- Bruckner, K., Pablo Labrador, J., Scheiffele, P., Herb, A., Seeburg, P.H. and Klein, R. (1999). EphrinB ligands recruit GRIP family PDZ adaptor proteins into raft membrane microdomains. *Neuron* **22**, 511-524.
- Bruckner, K., Pasquale, E.B. and Klein, R. (1997). Tyrosine phosphorylation of transmembrane ligands for Eph receptors. *Science* **275**, 1640-1643.
- Bulchand, S., Subramanian, L. and Tole, S. (2003). Dynamic spatiotemporal expression of LIM genes and cofactors in the embryonic and postnatal cerebral cortex. *Dev Dyn* **226**, 460-469.
- Bulfone, A., Smiga, S.M., Shimamura, K., Peterson, A., Puelles, L. and Rubenstein, J.L. (1995). T-brain-1: a homolog of Brachyury whose expression defines molecularly distinct domains within the cerebral cortex. *Neuron* **15**, 63-78.
- Burwell, R.D., Witter, M.P. and Amaral, D.G. (1995). Perirhinal and postrhinal cortices of the rat: a review of the neuroanatomical literature and comparison with findings from the monkey brain. *Hippocampus* **5**, 390-408.
- Caviness, V.S., Jr. (1976). Patterns of cell and fiber distribution in the neocortex of the reeler mutant mouse. *J Comp Neurol* **170**, 435-447.
- Caviness, V.S., Jr. (1982). Neocortical histogenesis in normal and reeler mice: a developmental study based upon [3H]thymidine autoradiography. *Brain Res* **256**, 293-302.
- Caviness, V.S., Jr. and Rakic, P. (1978). Mechanisms of cortical development: a view from mutations in mice. *Annu Rev Neurosci* **1**, 297-326.
- Caviness, V.S., Jr. and Sidman, R.L. (1973). Time of origin or corresponding cell classes in the cerebral cortex of normal and reeler mutant mice: an autoradiographic analysis. *J Comp Neurol* **148**, 141-151.

8 Bibliography

- Caviness, V.S., Jr., So, D.K. and Sidman, R.L. (1972). The hybrid reeler mouse. *J Hered* **63**, 241-246.
- Chen, K., Ochalski, P.G., Tran, T.S., Sahir, N., Schubert, M., Pramatarova, A. and Howell, B.W. (2004). Interaction between Dab1 and Crkl is promoted by Reelin signaling. *J Cell Sci* **117**, 4527-4536.
- Cheng, H.J. and Flanagan, J.G. (1994). Identification and cloning of ELF-1, a developmentally expressed ligand for the Mek4 and Sek receptor tyrosine kinases. *Cell* **79**, 157-168.
- Cheresh, D.A., Leng, J. and Klemke, R.L. (1999). Regulation of cell contraction and membrane ruffling by distinct signals in migratory cells. *J Cell Biol* **146**, 1107-1116.
- Chizhikov, V. and Millen, K.J. (2003). Development and malformations of the cerebellum in mice. *Mol Genet Metab* **80**, 54-65.
- Chumley, M.J., Catchpole, T., Silvany, R.E., Kernie, S.G. and Henkemeyer, M. (2007). EphB receptors regulate stem/progenitor cell proliferation, migration, and polarity during hippocampal neurogenesis. *J Neurosci* **27**, 13481-13490.
- Conover, J.C., Doetsch, F., Garcia-Verdugo, J.M., Gale, N.W., Yancopoulos, G.D. and Alvarez-Buylla, A. (2000). Disruption of Eph/ephrin signaling affects migration and proliferation in the adult subventricular zone. *Nat Neurosci* **3**, 1091-1097.
- Coonan, J.R., Greferath, U., Messenger, J., Hartley, L., Murphy, M., Boyd, A.W., et al. (2001). Development and reorganization of corticospinal projections in EphA4 deficient mice. *J Comp Neurol* **436**, 248-262.
- Cooper, J.A. (2008). A mechanism for inside-out lamination in the neocortex. *Trends Neurosci* **31**, 113-119.
- Costa, E., Chen, Y., Davis, J., Dong, E., Noh, J.S., Tremolizzo, L., et al. (2002). REELIN and schizophrenia: a disease at the interface of the genome and the epigenome. *Mol Interv* **2**, 47-57.
- Cowan, C.A. and Henkemeyer, M. (2001). The SH2/SH3 adaptor Grb4 transduces B-ephrin reverse signals. *Nature* **413**, 174-179.
- Cowan, C.A. and Henkemeyer, M. (2002). Ephrins in reverse, park and drive. *Trends Cell Biol* **12**, 339-346.
- Crissman, H.A., Oka, M.S. and Steinkamp, J.A. (1976). Rapid staining methods for analysis of deoxyribonucleic acid and protein in mammalian cells. *J Histochem Cytochem* **24**, 64-71.
- Cuitino, L., Matute, R., Retamal, C., Bu, G., Inestrosa, N.C. and Marzolo, M.P. (2005). ApoER2 is endocytosed by a clathrin-mediated process involving the adaptor protein Dab2 independent of its Rafts' association. *Traffic* **6**, 820-838.
- Curran, T. and D'Arcangelo, G. (1998). Role of reelin in the control of brain development. *Brain Res Brain Res Rev* **26**, 285-294.
- D'Arcangelo, G. (2005). The reeler mouse: anatomy of a mutant. *Int Rev Neurobiol* **71**, 383-417.
- D'Arcangelo, G. and Curran, T. (1998). Reeler: new tales on an old mutant mouse. *Bioessays* **20**, 235-244.
- D'Arcangelo, G., Homayouni, R., Keshvara, L., Rice, D.S., Sheldon, M. and Curran, T. (1999). Reelin is a ligand for lipoprotein receptors. *Neuron* **24**, 471-479.
- D'Arcangelo, G., Miao, G.G., Chen, S.C., Soares, H.D., Morgan, J.I. and Curran, T. (1995). A protein related to extracellular matrix proteins deleted in the mouse mutant reeler. *Nature* **374**, 719-723.
- D'Arcangelo, G., Nakajima, K., Miyata, T., Ogawa, M., Mikoshiba, K. and Curran, T. (1997). Reelin is a secreted glycoprotein recognized by the CR-50 monoclonal antibody. *J Neurosci* **17**, 23-31.
- Davy, A., Gale, N.W., Murray, E.W., Klinghoffer, R.A., Soriano, P., Feuerstein, C. and Robbins, S.M. (1999). Compartmentalized signaling by GPI-anchored ephrin-A5 requires the Fyn tyrosine kinase to regulate cellular adhesion. *Genes Dev* **13**, 3125-3135.
- Davy, A. and Soriano, P. (2005). Ephrin signaling in vivo: look both ways. *Dev Dyn* **232**, 1-10.

- Del Rio, J.A., Heimrich, B., Borrell, V., Forster, E., Drakew, A., Alcantara, S., *et al.* (1997). A role for Cajal-Retzius cells and reelin in the development of hippocampal connections. *Nature* **385**, 70-74.
- Deller, T. (1998). The anatomical organization of the rat fascia dentata: new aspects of laminar organization as revealed by anterograde tracing with Phaseolus vulgaris-Luecoagglutinin (PHAL). *Anat Embryol (Berl)* **197**, 89-103.
- Derer, P. (1985). Comparative localization of Cajal-Retzius cells in the neocortex of normal and reeler mutant mice fetuses. *Neurosci Lett* **54**, 1-6.
- DeSilva, U., D'Arcangelo, G., Braden, V.V., Chen, J., Miao, G.G., Curran, T. and Green, E.D. (1997). The human reelin gene: isolation, sequencing, and mapping on chromosome 7. *Genome Res* **7**, 157-164.
- Drakew, A., Deller, T., Heimrich, B., Gebhardt, C., Del Turco, D., Tielsch, A., *et al.* (2002). Dentate granule cells in reeler mutants and VLDLR and ApoER2 knockout mice. *Exp Neurol* **176**, 12-24.
- Duit, S., Mayer, H., Blake, S.M., Schneider, W.J. and Nimpf, J. (2010). Differential functions of ApoER2 and very low density lipoprotein receptor in Reelin signaling depend on differential sorting of the receptors. *J Biol Chem* **285**, 4896-4908.
- Dulabon, L., Olson, E.C., Taglienti, M.G., Eisenhuth, S., McGrath, B., Walsh, C.A., *et al.* (2000). Reelin binds alpha3beta1 integrin and inhibits neuronal migration. *Neuron* **27**, 33-44.
- Edmondson, J.C. and Hatten, M.E. (1987). Glial-guided granule neuron migration in vitro: a high-resolution time-lapse video microscopic study. *J Neurosci* **7**, 1928-1934.
- Egea, J. and Klein, R. (2007). Bidirectional Eph-ephrin signaling during axon guidance. *Trends Cell Biol* **17**, 230-238.
- Essmann, C.L., Martinez, E., Geiger, J.C., Zimmer, M., Traut, M.H., Stein, V., *et al.* (2008). Serine phosphorylation of ephrinB2 regulates trafficking of synaptic AMPA receptors. *Nat Neurosci* **11**, 1035-1043.
- Fairen, A., Cobas, A. and Fonseca, M. (1986). Times of generation of glutamic acid decarboxylase immunoreactive neurons in mouse somatosensory cortex. *J Comp Neurol* **251**, 67-83.
- Falconer, D.S. (1951) Two new mutants, 'trembler' and 'reeler', with neurological actions in the house mouse (*Mus musculus* L.) pp. 192-205.
- Feng, L., Allen, N.S., Simo, S. and Cooper, J.A. (2007). Cullin 5 regulates Dab1 protein levels and neuron positioning during cortical development. *Genes Dev* **21**, 2717-2730.
- Ferland, R.J., Cherry, T.J., Preware, P.O., Morrisey, E.E. and Walsh, C.A. (2003). Characterization of Foxp2 and Foxp1 mRNA and protein in the developing and mature brain. *J Comp Neurol* **460**, 266-279.
- Ferrere, A., Vitalis, T., Gingras, H., Gaspar, P. and Cases, O. (2006). Expression of Cux-1 and Cux-2 in the developing somatosensory cortex of normal and barrel-defective mice. *Anat Rec A Discov Mol Cell Evol Biol* **288**, 158-165.
- Flanagan, J.G. and Vanderhaeghen, P. (1998). The ephrins and Eph receptors in neural development. *Annu Rev Neurosci* **21**, 309-345.
- Forster, E., Tielsch, A., Saum, B., Weiss, K.H., Johanssen, C., Graus-Porta, D., *et al.* (2002). Reelin, Disabled 1, and beta 1 integrins are required for the formation of the radial glial scaffold in the hippocampus. *Proc Natl Acad Sci U S A* **99**, 13178-13183.
- Forster, E., Zhao, S. and Frotscher, M. (2006). Laminating the hippocampus. *Nat Rev Neurosci* **7**, 259-267.
- Francis, F., Meyer, G., Fallet-Bianco, C., Moreno, S., Kappeler, C., Socorro, A.C., *et al.* (2006). Human disorders of cortical development: from past to present. *Eur J Neurosci* **23**, 877-893.
- Frantz, G.D., Bohner, A.P., Akers, R.M. and McConnell, S.K. (1994). Regulation of the POU domain gene SCIP during cerebral cortical development. *J Neurosci* **14**, 472-485.

8 Bibliography

- Frantz, G.D. and McConnell, S.K. (1996). Restriction of late cerebral cortical progenitors to an upper-layer fate. *Neuron* **17**, 55-61.
- Frotscher, M. (1997). Dual role of Cajal-Retzius cells and reelin in cortical development. *Cell Tissue Res* **290**, 315-322.
- Frotscher, M. (1998). Cajal-Retzius cells, Reelin, and the formation of layers. *Curr Opin Neurobiol* **8**, 570-575.
- Frotscher, M., Haas, C.A. and Forster, E. (2003). Reelin controls granule cell migration in the dentate gyrus by acting on the radial glial scaffold. *Cereb Cortex* **13**, 634-640.
- Fu, W.Y., Chen, Y., Sahin, M., Zhao, X.S., Shi, L., Bikoff, J.B., et al. (2007). Cdk5 regulates EphA4-mediated dendritic spine retraction through an ephexin1-dependent mechanism. *Nat Neurosci* **10**, 67-76.
- Gadisseux, J.F., Evrard, P., Misson, J.P. and Caviness, V.S. (1989). Dynamic structure of the radial glial fiber system of the developing murine cerebral wall. An immunocytochemical analysis. *Brain Res Dev Brain Res* **50**, 55-67.
- Gale, N.W., Flenniken, A., Compton, D.C., Jenkins, N., Copeland, N.G., Gilbert, D.J., et al. (1996). Elk-L3, a novel transmembrane ligand for the Eph family of receptor tyrosine kinases, expressed in embryonic floor plate, roof plate and hindbrain segments. *Oncogene* **13**, 1343-1352.
- Gauthier, L.R. and Robbins, S.M. (2003). Ephrin signaling: One raft to rule them all? One raft to sort them? One raft to spread their call and in signaling bind them? *Life Sci* **74**, 207-216.
- Ghashghaei, H.T., Lai, C. and Anton, E.S. (2007). Neuronal migration in the adult brain: are we there yet? *Nat Rev Neurosci* **8**, 141-151.
- Gleeson, J.G., Allen, K.M., Fox, J.W., Lamperti, E.D., Berkovic, S., Scheffer, I., et al. (1998). Doublecortin, a brain-specific gene mutated in human X-linked lissencephaly and double cortex syndrome, encodes a putative signaling protein. *Cell* **92**, 63-72.
- Goffinet, A.M. (1979). An early development defect in the cerebral cortex of the reeler mouse. A morphological study leading to a hypothesis concerning the action of the mutant gene. *Anat Embryol (Berl)* **157**, 205-216.
- Goffinet, A.M. (1983). The embryonic development of the inferior olivary complex in normal and reeler (rLORL) mutant mice. *J Comp Neurol* **219**, 10-24.
- Goffinet, A.M. (1984). Abnormal development of the facial nerve nucleus in reeler mutant mice. *J Anat* **138 (Pt 2)**, 207-215.
- Goldowitz, D., Cushing, R.C., Laywell, E., D'Arcangelo, G., Sheldon, M., Sweet, H.O., et al. (1997). Cerebellar disorganization characteristic of reeler in scrambler mutant mice despite presence of reelin. *J Neurosci* **17**, 8767-8777.
- Gonzalez, M.I. and Ortega, A. (1997). Regulation of the Na⁺-dependent high affinity glutamate/aspartate transporter in cultured Bergmann glia by phorbol esters. *J Neurosci Res* **50**, 585-590.
- Gotthardt, M., Trommsdorff, M., Nevitt, M.F., Shelton, J., Richardson, J.A., Stockinger, W., et al. (2000). Interactions of the low density lipoprotein receptor gene family with cytosolic adaptor and scaffold proteins suggest diverse biological functions in cellular communication and signal transduction. *J Biol Chem* **275**, 25616-25624.
- Graus-Porta, D., Blaess, S., Senften, M., Littlewood-Evans, A., Damsky, C., Huang, Z., et al. (2001). Beta1-class integrins regulate the development of laminae and folia in the cerebral and cerebellar cortex. *Neuron* **31**, 367-379.
- Grunwald, I.C., Korte, M., Adelmann, G., Plueck, A., Kullander, K., Adams, R.H., et al. (2004). Hippocampal plasticity requires postsynaptic ephrinBs. *Nat Neurosci* **7**, 33-40.
- Gupta, A., Tsai, L.H. and Wynshaw-Boris, A. (2002). Life is a journey: a genetic look at neocortical development. *Nat Rev Genet* **3**, 342-355.
- Hack, I., Bancila, M., Loulier, K., Carroll, P. and Cremer, H. (2002). Reelin is a detachment signal in tangential chain-migration during postnatal neurogenesis. *Nat Neurosci* **5**, 939-945.

- Hack, I., Hellwig, S., Junghans, D., Brunne, B., Bock, H.H., Zhao, S. and Frotscher, M. (2007). Divergent roles of ApoER2 and Vldlr in the migration of cortical neurons. *Development* **134**, 3883-3891.
- Hall, A. and Nobes, C.D. (2000). Rho GTPases: molecular switches that control the organization and dynamics of the actin cytoskeleton. *Philos Trans R Soc Lond B Biol Sci* **355**, 965-970.
- Hamburgh, M. and Vicari, E. (1960). A study of some physiological mechanisms underlying susceptibility to audiogenic seizures in mice. *J Neuropathol Exp Neurol* **19**, 461-472.
- Hammond, V., So, E., Gunnarsen, J., Valcanis, H., Kalloniatis, M. and Tan, S.S. (2006). Layer positioning of late-born cortical interneurons is dependent on Reelin but not p35 signaling. *J Neurosci* **26**, 1646-1655.
- Hatten, M.E. (1999). Central nervous system neuronal migration. *Annu Rev Neurosci* **22**, 511-539.
- Herrick, T.M. and Cooper, J.A. (2002). A hypomorphic allele of dab1 reveals regional differences in reelin-Dab1 signaling during brain development. *Development* **129**, 787-796.
- Herrick, T.M. and Cooper, J.A. (2004). High affinity binding of Dab1 to Reelin receptors promotes normal positioning of upper layer cortical plate neurons. *Brain Res Mol Brain Res* **126**, 121-128.
- Herz, J. and Beffert, U. (2000). Apolipoprotein E receptors: linking brain development and Alzheimer's disease. *Nat Rev Neurosci* **1**, 51-58.
- Herz, J. and Chen, Y. (2006). Reelin, lipoprotein receptors and synaptic plasticity. *Nat Rev Neurosci* **7**, 850-859.
- Hevner, R.F., Daza, R.A., Englund, C., Kohtz, J. and Fink, A. (2004). Postnatal shifts of interneuron position in the neocortex of normal and reeler mice: evidence for inward radial migration. *Neuroscience* **124**, 605-618.
- Hevner, R.F., Daza, R.A., Rubenstein, J.L., Stunnenberg, H., Olavarria, J.F. and Englund, C. (2003). Beyond laminar fate: toward a molecular classification of cortical projection/pyramidal neurons. *Dev Neurosci* **25**, 139-151.
- Hevner, R.F., Shi, L., Justice, N., Hsueh, Y., Sheng, M., Smiga, S., *et al.* (2001). Tbr1 regulates differentiation of the preplate and layer 6. *Neuron* **29**, 353-366.
- Hiesberger, T., Trommsdorff, M., Howell, B.W., Goffinet, A., Mumby, M.C., Cooper, J.A. and Herz, J. (1999). Direct binding of Reelin to VLDL receptor and ApoE receptor 2 induces tyrosine phosphorylation of disabled-1 and modulates tau phosphorylation. *Neuron* **24**, 481-489.
- Himanen, J.P., Chumley, M.J., Lackmann, M., Li, C., Barton, W.A., Jeffrey, P.D., *et al.* (2004). Repelling class discrimination: ephrin-A5 binds to and activates EphB2 receptor signaling. *Nat Neurosci* **7**, 501-509.
- Himanen, J.P., Rajashankar, K.R., Lackmann, M., Cowan, C.A., Henkemeyer, M. and Nikolov, D.B. (2001). Crystal structure of an Eph receptor-ephrin complex. *Nature* **414**, 933-938.
- Hirai, H., Maru, Y., Hagiwara, K., Nishida, J. and Takaku, F. (1987). A novel putative tyrosine kinase receptor encoded by the eph gene. *Science* **238**, 1717-1720.
- Hisaoka, T., Nakamura, Y., Senba, E. and Morikawa, Y. (2009). The forkhead transcription factors, Foxp1 and Foxp2, identify different subpopulations of projection neurons in the mouse cerebral cortex. *Neuroscience* **166**, 551-563.
- Hoffarth, R.M., Johnston, J.G., Krushel, L.A. and van der Kooy, D. (1995). The mouse mutation reeler causes increased adhesion within a subpopulation of early postmitotic cortical neurons. *J Neurosci* **15**, 4838-4850.
- Hong, S.E., Shugart, Y.Y., Huang, D.T., Shahwan, S.A., Grant, P.E., Hourihane, J.O., *et al.* (2000). Autosomal recessive lissencephaly with cerebellar hypoplasia is associated with human RELN mutations. *Nat Genet* **26**, 93-96.
- Horesh, D., Sapir, T., Francis, F., Wolf, S.G., Caspi, M., Elbaum, M., *et al.* (1999). Doublecortin, a stabilizer of microtubules. *Hum Mol Genet* **8**, 1599-1610.
- Horiuchi, D., Collins, C.A., Bhat, P., Barkus, R.V., Diantonio, A. and Saxton, W.M. (2007). Control of a kinesin-cargo linkage mechanism by JNK pathway kinases. *Curr Biol* **17**, 1313-1317.

8 Bibliography

- Howell, B.W., Gertler, F.B. and Cooper, J.A. (1997). Mouse disabled (mDab1): a Src binding protein implicated in neuronal development. *EMBO J* **16**, 121-132.
- Howell, B.W., Herrick, T.M. and Cooper, J.A. (1999a). Reelin-induced tyrosine [corrected] phosphorylation of disabled 1 during neuronal positioning. *Genes Dev* **13**, 643-648.
- Howell, B.W., Herrick, T.M., Hildebrand, J.D., Zhang, Y. and Cooper, J.A. (2000). Dab1 tyrosine phosphorylation sites relay positional signals during mouse brain development. *Curr Biol* **10**, 877-885.
- Howell, B.W., Lanier, L.M., Frank, R., Gertler, F.B. and Cooper, J.A. (1999b). The disabled 1 phosphotyrosine-binding domain binds to the internalization signals of transmembrane glycoproteins and to phospholipids. *Mol Cell Biol* **19**, 5179-5188.
- Huai, J. and Drescher, U. (2001). An ephrin-A-dependent signaling pathway controls integrin function and is linked to the tyrosine phosphorylation of a 120-kDa protein. *J Biol Chem* **276**, 6689-6694.
- Huang, Y., Shah, V., Liu, T. and Keshvara, L. (2005). Signaling through Disabled 1 requires phosphoinositide binding. *Biochem Biophys Res Commun* **331**, 1460-1468.
- Hunter-Schaedle, K.E. (1997). Radial glial cell development and transformation are disturbed in reeler forebrain. *J Neurobiol* **33**, 459-472.
- Iwasato, T., Katoh, H., Nishimaru, H., Ishikawa, Y., Inoue, H., Saito, Y.M., *et al.* (2007). Rac-GAP alpha-chimerin regulates motor-circuit formation as a key mediator of EphrinB3/EphA4 forward signaling. *Cell* **130**, 742-753.
- Jande, S.S., Maler, L. and Lawson, D.E. (1981). Immunohistochemical mapping of vitamin D-dependent calcium-binding protein in brain. *Nature* **294**, 765-767.
- Jossin, Y. and Goffinet, A.M. (2007). Reelin signals through phosphatidylinositol 3-kinase and Akt to control cortical development and through mTor to regulate dendritic growth. *Mol Cell Biol* **27**, 7113-7124.
- Jossin, Y., Ignatova, N., Hiesberger, T., Herz, J., Lambert de Rouvroit, C. and Goffinet, A.M. (2004). The central fragment of Reelin, generated by proteolytic processing in vivo, is critical to its function during cortical plate development. *J Neurosci* **24**, 514-521.
- Kadison, S.R., Makinen, T., Klein, R., Henkemeyer, M. and Kaprielian, Z. (2006). EphB receptors and ephrin-B3 regulate axon guidance at the ventral midline of the embryonic mouse spinal cord. *J Neurosci* **26**, 8909-8914.
- Kalo, M.S. and Pasquale, E.B. (1999). Signal transfer by Eph receptors. *Cell Tissue Res* **298**, 1-9.
- Kalo, M.S., Yu, H.H. and Pasquale, E.B. (2001). In vivo tyrosine phosphorylation sites of activated ephrin-B1 and ephB2 from neural tissue. *J Biol Chem* **276**, 38940-38948.
- Keilani, S. and Sugaya, K. (2008). Reelin induces a radial glial phenotype in human neural progenitor cells by activation of Notch-1. *BMC Dev Biol* **8**, 69.
- Kelemenova, S. and Ostatnikova, D. (2009). Neuroendocrine pathways altered in autism. Special role of reelin. *Neuro Endocrinol Lett* **30**, 429-436.
- Keshvara, L., Benhayon, D., Magdaleno, S. and Curran, T. (2001). Identification of reelin-induced sites of tyrosyl phosphorylation on disabled 1. *J Biol Chem* **276**, 16008-16014.
- Kiecker, C. and Lumsden, A. (2005). Compartments and their boundaries in vertebrate brain development. *Nat Rev Neurosci* **6**, 553-564.
- Kostovic, I. and Rakic, P. (1980). Cytology and time of origin of interstitial neurons in the white matter in infant and adult human and monkey telencephalon. *J Neurocytol* **9**, 219-242.
- Kriegstein, A.R. and Noctor, S.C. (2004). Patterns of neuronal migration in the embryonic cortex. *Trends Neurosci* **27**, 392-399.
- Kullander, K., Butt, S.J., Le Bret, J.M., Lundfald, L., Restrepo, C.E., Rydstrom, A., *et al.* (2003). Role of EphA4 and EphrinB3 in local neuronal circuits that control walking. *Science* **299**, 1889-1892.

- Kullander, K., Croll, S.D., Zimmer, M., Pan, L., McClain, J., Hughes, V., *et al.* (2001a). Ephrin-B3 is the midline barrier that prevents corticospinal tract axons from recrossing, allowing for unilateral motor control. *Genes Dev* **15**, 877-888.
- Kullander, K. and Klein, R. (2002). Mechanisms and functions of Eph and ephrin signalling. *Nat Rev Mol Cell Biol* **3**, 475-486.
- Kullander, K., Mather, N.K., Diella, F., Dottori, M., Boyd, A.W. and Klein, R. (2001b). Kinase-dependent and kinase-independent functions of EphA4 receptors in major axon tract formation in vivo. *Neuron* **29**, 73-84.
- Kuo, G., Arnaud, L., Kronstad-O'Brien, P. and Cooper, J.A. (2005). Absence of Fyn and Src causes a reeler-like phenotype. *J Neurosci* **25**, 8578-8586.
- Lambert de Rouvroit, C., de Bergeyck, V., Cortvrindt, C., Bar, I., Eeckhout, Y. and Goffinet, A.M. (1999). Reelin, the extracellular matrix protein deficient in reeler mutant mice, is processed by a metalloproteinase. *Exp Neurol* **156**, 214-217.
- Lambert de Rouvroit, C. and Goffinet, A.M. (1998). The reeler mouse as a model of brain development. *Adv Anat Embryol Cell Biol* **150**, 1-106.
- Lavdas, A.A., Grigoriou, M., Pachnis, V. and Parnavelas, J.G. (1999). The medial ganglionic eminence gives rise to a population of early neurons in the developing cerebral cortex. *J Neurosci* **19**, 7881-7888.
- Leone, D.P., Srinivasan, K., Chen, B., Alcamo, E. and McConnell, S.K. (2008). The determination of projection neuron identity in the developing cerebral cortex. *Curr Opin Neurobiol* **18**, 28-35.
- Levitt, P. and Rakic, P. (1980). Immunoperoxidase localization of glial fibrillary acidic protein in radial glial cells and astrocytes of the developing rhesus monkey brain. *J Comp Neurol* **193**, 815-840.
- Liebl, D.J., Morris, C.J., Henkemeyer, M. and Parada, L.F. (2003). mRNA expression of ephrins and Eph receptor tyrosine kinases in the neonatal and adult mouse central nervous system. *J Neurosci Res* **71**, 7-22.
- Liu, Y., Fujise, N. and Kosaka, T. (1996). Distribution of calretinin immunoreactivity in the mouse dentate gyrus. I. General description. *Exp Brain Res* **108**, 389-403.
- Lu, Q., Sun, E.E., Klein, R.S. and Flanagan, J.G. (2001). Ephrin-B reverse signaling is mediated by a novel PDZ-RGS protein and selectively inhibits G protein-coupled chemoattraction. *Cell* **105**, 69-79.
- Luque, J.M. (2004). Integrin and the Reelin-Dab1 pathway: a sticky affair? *Brain Res Dev Brain Res* **152**, 269-271.
- Luque, J.M., Morante-Oria, J. and Fairen, A. (2003). Localization of ApoER2, VLDLR and Dab1 in radial glia: groundwork for a new model of reelin action during cortical development. *Brain Res Dev Brain Res* **140**, 195-203.
- Luskin, M.B. and Shatz, C.J. (1985). Studies of the earliest generated cells of the cat's visual cortex: cogeneration of subplate and marginal zones. *J Neurosci* **5**, 1062-1075.
- Magdaleno, S., Keshvara, L. and Curran, T. (2002). Rescue of ataxia and preplate splitting by ectopic expression of Reelin in reeler mice. *Neuron* **33**, 573-586.
- Magdaleno, S.M. and Curran, T. (2001). Brain development: integrins and the Reelin pathway. *Curr Biol* **11**, R1032-1035.
- Mann, F., Ray, S., Harris, W. and Holt, C. (2002). Topographic mapping in dorsoventral axis of the *Xenopus* retinotectal system depends on signaling through ephrin-B ligands. *Neuron* **35**, 461-473.
- Margolis, B. (1996). The PI/PTB domain: a new protein interaction domain involved in growth factor receptor signaling. *J Lab Clin Med* **128**, 235-241.
- Mariani, J., Crepel, F., Mikoshiba, K., Changeux, J.P. and Sotelo, C. (1977). Anatomical, physiological and biochemical studies of the cerebellum from Reeler mutant mouse. *Philos Trans R Soc Lond B Biol Sci* **281**, 1-28.

8 Bibliography

- Marin-Padilla, M. (1998). Cajal-Retzius cells and the development of the neocortex. *Trends Neurosci* **21**, 64-71.
- Marin, O. and Rubenstein, J.L. (2003). Cell migration in the forebrain. *Annu Rev Neurosci* **26**, 441-483.
- Martin, M.R. (1981). Morphology of the cochlear nucleus of the normal and reeler mutant mouse. *J Comp Neurol* **197**, 141-152.
- McConnell, S.K. and Kaznowski, C.E. (1991). Cell cycle dependence of laminar determination in developing neocortex. *Science* **254**, 282-285.
- McEvelly, R.J., de Diaz, M.O., Schonemann, M.D., Hooshmand, F. and Rosenfeld, M.G. (2002). Transcriptional regulation of cortical neuron migration by POU domain factors. *Science* **295**, 1528-1532.
- Meyer, G. and Wahle, P. (1999). The paleocortical ventricle is the origin of reelin-expressing neurons in the marginal zone of the foetal human neocortex. *Eur J Neurosci* **11**, 3937-3944.
- Migani, P., Bartlett, C., Dunlop, S., Beazley, L. and Rodger, J. (2007). Ephrin-B2 immunoreactivity distribution in adult mouse brain. *Brain Res* **1182**, 60-72.
- Migani, P., Bartlett, C., Dunlop, S., Beazley, L. and Rodger, J. (2009). Regional and cellular distribution of ephrin-B1 in adult mouse brain. *Brain Res* **1247**, 50-61.
- Miller, B., Sheppard, A.M., Bicknese, A.R. and Pearlman, A.L. (1995). Chondroitin sulfate proteoglycans in the developing cerebral cortex: the distribution of neurocan distinguishes forming afferent and efferent axonal pathways. *J Comp Neurol* **355**, 615-628.
- Miller, M.W. (1985). Cogeneration of retrogradely labeled corticocortical projection and GABA-immunoreactive local circuit neurons in cerebral cortex. *Brain Res* **355**, 187-192.
- Miller, M.W. (1986). The migration and neurochemical differentiation of gamma-aminobutyric acid (GABA)-immunoreactive neurons in rat visual cortex as demonstrated by a combined immunocytochemical-autoradiographic technique. *Brain Res* **393**, 41-46.
- Miller, M.W. and Pitts, F.A. (2000). Neurotrophin receptors in the somatosensory cortex of the mature rat: co-localization of p75, trk, isoforms and c-neu. *Brain Res* **852**, 355-366.
- Misson, J.P., Austin, C.P., Takahashi, T., Cepko, C.L. and Caviness, V.S., Jr. (1991). The alignment of migrating neural cells in relation to the murine neopallial radial glial fiber system. *Cereb Cortex* **1**, 221-229.
- Misson, J.P., Edwards, M.A., Yamamoto, M. and Caviness, V.S., Jr. (1988). Identification of radial glial cells within the developing murine central nervous system: studies based upon a new immunohistochemical marker. *Brain Res Dev Brain Res* **44**, 95-108.
- Miyata, T., Nakajima, K., Aruga, J., Takahashi, S., Ikenaka, K., Mikoshiba, K. and Ogawa, M. (1996). Distribution of a reeler gene-related antigen in the developing cerebellum: an immunohistochemical study with an allogeneic antibody CR-50 on normal and reeler mice. *J Comp Neurol* **372**, 215-228.
- Molyneaux, B.J., Arlotta, P., Menezes, J.R. and Macklis, J.D. (2007). Neuronal subtype specification in the cerebral cortex. *Nat Rev Neurosci* **8**, 427-437.
- Morimura, T., Hattori, M., Ogawa, M. and Mikoshiba, K. (2005). Disabled1 regulates the intracellular trafficking of reelin receptors. *J Biol Chem* **280**, 16901-16908.
- Morimura, T. and Ogawa, M. (2009). Relative importance of the tyrosine phosphorylation sites of Disabled-1 to the transmission of Reelin signaling. *Brain Res* **1304**, 26-37.
- Muraoka, D., Katsuyama, Y., Kikkawa, S. and Terashima, T. (2007). Postnatal development of entorhinodentate projection of the Reeler mutant mouse. *Dev Neurosci* **29**, 59-72.
- Nadarajah, B. (2003). Radial glia and somal translocation of radial neurons in the developing cerebral cortex. *Glia* **43**, 33-36.
- Nadarajah, B., Brunstrom, J.E., Grutzendler, J., Wong, R.O. and Pearlman, A.L. (2001). Two modes of radial migration in early development of the cerebral cortex. *Nat Neurosci* **4**, 143-150.

- Naimski, P., Bierzynski, A. and Fikus, M. (1980). Quantitative fluorescent analysis of different conformational forms of DNA bound to the Dye, 4',6-diamidine-2-phenylindole, and separated by gel electrophoresis. *Anal Biochem* **106**, 471-475.
- Nakagawa, Y., Johnson, J.E. and O'Leary, D.D. (1999). Graded and areal expression patterns of regulatory genes and cadherins in embryonic neocortex independent of thalamocortical input. *J Neurosci* **19**, 10877-10885.
- Nakano, Y., Kohno, T., Hibi, T., Kohno, S., Baba, A., Mikoshiba, K., *et al.* (2007). The extremely conserved C-terminal region of Reelin is not necessary for secretion but is required for efficient activation of downstream signaling. *J Biol Chem* **282**, 20544-20552.
- Nieto, M., Monuki, E.S., Tang, H., Imitola, J., Haubst, N., Houry, S.J., *et al.* (2004). Expression of Cux-1 and Cux-2 in the subventricular zone and upper layers II-IV of the cerebral cortex. *J Comp Neurol* **479**, 168-180.
- Niu, S., Renfro, A., Quattrocchi, C.C., Sheldon, M. and D'Arcangelo, G. (2004). Reelin promotes hippocampal dendrite development through the VLDLR/ApoER2-Dab1 pathway. *Neuron* **41**, 71-84.
- Niu, S., Yabut, O. and D'Arcangelo, G. (2008). The Reelin signaling pathway promotes dendritic spine development in hippocampal neurons. *J Neurosci* **28**, 10339-10348.
- Noctor, S.C., Flint, A.C., Weissman, T.A., Dammerman, R.S. and Kriegstein, A.R. (2001). Neurons derived from radial glial cells establish radial units in neocortex. *Nature* **409**, 714-720.
- Noctor, S.C., Flint, A.C., Weissman, T.A., Wong, W.S., Clinton, B.K. and Kriegstein, A.R. (2002). Dividing precursor cells of the embryonic cortical ventricular zone have morphological and molecular characteristics of radial glia. *J Neurosci* **22**, 3161-3173.
- Noctor, S.C., Martinez-Cerdeno, V., Ivic, L. and Kriegstein, A.R. (2004). Cortical neurons arise in symmetric and asymmetric division zones and migrate through specific phases. *Nat Neurosci* **7**, 136-144.
- Nowakowski, R.S., Lewin, S.B. and Miller, M.W. (1989). Bromodeoxyuridine immunohistochemical determination of the lengths of the cell cycle and the DNA-synthetic phase for an anatomically defined population. *J Neurocytol* **18**, 311-318.
- O'Rourke, N.A., Sullivan, D.P., Kaznowski, C.E., Jacobs, A.A. and McConnell, S.K. (1995). Tangential migration of neurons in the developing cerebral cortex. *Development* **121**, 2165-2176.
- Ogawa, M., Miyata, T., Nakajima, K., Yagy, K., Seike, M., Ikenaka, K., *et al.* (1995). The reeler gene-associated antigen on Cajal-Retzius neurons is a crucial molecule for laminar organization of cortical neurons. *Neuron* **14**, 899-912.
- Orioli, D. and Klein, R. (1997). The Eph receptor family: axonal guidance by contact repulsion. *Trends Genet* **13**, 354-359.
- Palmer, A. and Klein, R. (2003). Multiple roles of ephrins in morphogenesis, neuronal networking, and brain function. *Genes Dev* **17**, 1429-1450.
- Palmer, A., Zimmer, M., Erdmann, K.S., Eulenburg, V., Porthin, A., Heumann, R., *et al.* (2002). EphrinB phosphorylation and reverse signaling: regulation by Src kinases and PTP-BL phosphatase. *Mol Cell* **9**, 725-737.
- Parnavelas, J.G. (2000). The origin and migration of cortical neurones: new vistas. *Trends Neurosci* **23**, 126-131.
- Pasquale, E.B. (2005). Eph receptor signalling casts a wide net on cell behaviour. *Nat Rev Mol Cell Biol* **6**, 462-475.
- Peduzzi, J.D. (1988). Genesis of GABA-immunoreactive neurons in the ferret visual cortex. *J Neurosci* **8**, 920-931.
- Petit, V., Boyer, B., Lentz, D., Turner, C.E., Thiery, J.P. and Valles, A.M. (2000). Phosphorylation of tyrosine residues 31 and 118 on paxillin regulates cell migration through an association with CRK in NBT-II cells. *J Cell Biol* **148**, 957-970.

8 Bibliography

- Pinto-Lord, M.C., Evrard, P. and Caviness, V.S., Jr. (1982). Obstructed neuronal migration along radial glial fibers in the neocortex of the reeler mouse: a Golgi-EM analysis. *Brain Res* **256**, 379-393.
- Pramatarova, A., Ochalski, P.G., Chen, K., Gropman, A., Myers, S., Min, K.T. and Howell, B.W. (2003). Nck beta interacts with tyrosine-phosphorylated disabled 1 and redistributes in Reelin-stimulated neurons. *Mol Cell Biol* **23**, 7210-7221.
- Qiu, S., Korwek, K.M., Pratt-Davis, A.R., Peters, M., Bergman, M.Y. and Weeber, E.J. (2006). Cognitive disruption and altered hippocampus synaptic function in Reelin haploinsufficient mice. *Neurobiol Learn Mem* **85**, 228-242.
- Quattrocchi, C.C., Wannenes, F., Persico, A.M., Ciafre, S.A., D'Arcangelo, G., Farace, M.G. and Keller, F. (2002). Reelin is a serine protease of the extracellular matrix. *J Biol Chem* **277**, 303-309.
- Rakic, P. (1972). Mode of cell migration to the superficial layers of fetal monkey neocortex. *J Comp Neurol* **145**, 61-83.
- Rakic, P. (1974). Neurons in rhesus monkey visual cortex: systematic relation between time of origin and eventual disposition. *Science* **183**, 425-427.
- Rakic, P. and Caviness, V.S., Jr. (1995). Cortical development: view from neurological mutants two decades later. *Neuron* **14**, 1101-1104.
- Ricard, J., Salinas, J., Garcia, L. and Liebl, D.J. (2006). EphrinB3 regulates cell proliferation and survival in adult neurogenesis. *Mol Cell Neurosci* **31**, 713-722.
- Rice, D.S. and Curran, T. (1999). Mutant mice with scrambled brains: understanding the signaling pathways that control cell positioning in the CNS. *Genes Dev* **13**, 2758-2773.
- Rice, D.S. and Curran, T. (2000). Disabled-1 is expressed in type All amacrine cells in the mouse retina. *J Comp Neurol* **424**, 327-338.
- Rice, D.S. and Curran, T. (2001). Role of the reelin signaling pathway in central nervous system development. *Annu Rev Neurosci* **24**, 1005-1039.
- Rice, D.S., Sheldon, M., D'Arcangelo, G., Nakajima, K., Goldowitz, D. and Curran, T. (1998). Disabled-1 acts downstream of Reelin in a signaling pathway that controls laminar organization in the mammalian brain. *Development* **125**, 3719-3729.
- Rogers, J.T. and Weeber, E.J. (2008). Reelin and apoE actions on signal transduction, synaptic function and memory formation. *Neuron Glia Biol* **4**, 259-270.
- Royaux, I., Lambert de Rouvroit, C., D'Arcangelo, G., Demirov, D. and Goffinet, A.M. (1997). Genomic organization of the mouse reelin gene. *Genomics* **46**, 240-250.
- Sanada, K., Gupta, A. and Tsai, L.H. (2004). Disabled-1-regulated adhesion of migrating neurons to radial glial fiber contributes to neuronal positioning during early corticogenesis. *Neuron* **42**, 197-211.
- Sapir, T., Elbaum, M. and Reiner, O. (1997). Reduction of microtubule catastrophe events by LIS1, platelet-activating factor acetylhydrolase subunit. *EMBO J* **16**, 6977-6984.
- Sawamiphak, S., Seidel, S., Essmann, C.L., Wilkinson, G.A., Pitulescu, M.E., Acker, T. and Acker-Palmer, A. Ephrin-B2 regulates VEGFR2 function in developmental and tumour angiogenesis. *Nature* **465**, 487-491.
- Sawamiphak, S., Seidel, S., Essmann, C.L., Wilkinson, G.A., Pitulescu, M.E., Acker, T. and Acker-Palmer, A. (2010a). Ephrin-B2 regulates VEGFR2 function in developmental and tumour angiogenesis. *Nature* **465**, 487-491.
- Sawamiphak, S., Seidel, S., Essmann, C.L., Wilkinson, G.A., Pitulescu, M.E., Acker, T. and Acker-Palmer, A. (2010b). EphrinB2 regulates VEGFR2 function in developmental and tumour angiogenesis. *Nature* doi:10.1038/nature08995.
- Schaeren-Wiemers, N., Andre, E., Kapfhammer, J.P. and Becker-Andre, M. (1997). The expression pattern of the orphan nuclear receptor RORbeta in the developing and adult rat nervous system suggests a role in the processing of sensory information and in circadian rhythm. *Eur J Neurosci* **9**, 2687-2701.

- Schiffmann, S.N., Bernier, B. and Goffinet, A.M. (1997). Reelin mRNA expression during mouse brain development. *Eur J Neurosci* **9**, 1055-1071.
- Schlessinger, J. (2000). Cell signaling by receptor tyrosine kinases. *Cell* **103**, 211-225.
- Schmechel, D.E. and Rakic, P. (1979). A Golgi study of radial glial cells in developing monkey telencephalon: morphogenesis and transformation into astrocytes. *Anat Embryol (Berl)* **156**, 115-152.
- Schneider, W.J. and Nimpf, J. (2003). LDL receptor relatives at the crossroad of endocytosis and signaling. *Cell Mol Life Sci* **60**, 892-903.
- Segura, I., Essmann, C.L., Weinges, S. and Acker-Palmer, A. (2007). Grb4 and GIT1 transduce ephrinB reverse signals modulating spine morphogenesis and synapse formation. *Nat Neurosci* **10**, 301-310.
- Senzaki, K., Ogawa, M. and Yagi, T. (1999). Proteins of the CNR family are multiple receptors for Reelin. *Cell* **99**, 635-647.
- Shamah, S.M., Lin, M.Z., Goldberg, J.L., Estrach, S., Sahin, M., Hu, L., *et al.* (2001). EphA receptors regulate growth cone dynamics through the novel guanine nucleotide exchange factor ephexin. *Cell* **105**, 233-244.
- Sheen, V.L., Feng, Y., Graham, D., Takafuta, T., Shapiro, S.S. and Walsh, C.A. (2002). Filamin A and Filamin B are co-expressed within neurons during periods of neuronal migration and can physically interact. *Hum Mol Genet* **11**, 2845-2854.
- Sheldon, M., Rice, D.S., D'Arcangelo, G., Yoneshima, H., Nakajima, K., Mikoshiba, K., *et al.* (1997). Scrambler and yotari disrupt the disabled gene and produce a reeler-like phenotype in mice. *Nature* **389**, 730-733.
- Sheppard, A.M., Hamilton, S.K. and Pearlman, A.L. (1991). Changes in the distribution of extracellular matrix components accompany early morphogenetic events of mammalian cortical development. *J Neurosci* **11**, 3928-3942.
- Sheppard, A.M. and Pearlman, A.L. (1997). Abnormal reorganization of preplate neurons and their associated extracellular matrix: an early manifestation of altered neocortical development in the reeler mutant mouse. *J Comp Neurol* **378**, 173-179.
- Shibata, T., Yamada, K., Watanabe, M., Ikenaka, K., Wada, K., Tanaka, K. and Inoue, Y. (1997). Glutamate transporter GLAST is expressed in the radial glia-astrocyte lineage of developing mouse spinal cord. *J Neurosci* **17**, 9212-9219.
- Sholl, D.A. (1953). Dendritic organization in the neurons of the visual and motor cortices of the cat. *J Anat* **87**, 387-406.
- Sidman, R.L., Appel, S.H. and Fullier, J.F. (1965). Neurological Mutants of the Mouse. *Science* **150**, 513-516.
- Simmons, P.A., Lemmon, V. and Pearlman, A.L. (1982). Afferent and efferent connections of the striate and extrastriate visual cortex of the normal and reeler mouse. *J Comp Neurol* **211**, 295-308.
- Simons, K. and Toomre, D. (2000). Lipid rafts and signal transduction. *Nat Rev Mol Cell Biol* **1**, 31-39.
- Stanfield, B.B. and Cowan, W.M. (1979a). The development of the hippocampus and dentate gyrus in normal and reeler mice. *J Comp Neurol* **185**, 423-459.
- Stanfield, B.B. and Cowan, W.M. (1979b). The morphology of the hippocampus and dentate gyrus in normal and reeler mice. *J Comp Neurol* **185**, 393-422.
- Steindler, D.A. and Colwell, S.A. (1976). Reeler mutant mouse: maintenance of appropriate and reciprocal connections in the cerebral cortex and thalamus. *Brain Res* **113**, 386-393.
- Steward, O. and Scoville, S.A. (1976). Cells of origin of entorhinal cortical afferents to the hippocampus and fascia dentata of the rat. *J Comp Neurol* **169**, 347-370.
- Stolt, P.C., Chen, Y., Liu, P., Bock, H.H., Blacklow, S.C. and Herz, J. (2005). Phosphoinositide binding by the disabled-1 PTB domain is necessary for membrane localization and Reelin signal transduction. *J Biol Chem* **280**, 9671-9677.

8 Bibliography

- Storck, T., Schulte, S., Hofmann, K. and Stoffel, W. (1992). Structure, expression, and functional analysis of a Na(+)-dependent glutamate/aspartate transporter from rat brain. *Proc Natl Acad Sci U S A* **89**, 10955-10959.
- Strasser, V., Fasching, D., Hauser, C., Mayer, H., Bock, H.H., Hiesberger, T., *et al.* (2004). Receptor clustering is involved in Reelin signaling. *Mol Cell Biol* **24**, 1378-1386.
- Sugitani, Y., Nakai, S., Minowa, O., Nishi, M., Jishage, K., Kawano, H., *et al.* (2002). Brn-1 and Brn-2 share crucial roles in the production and positioning of mouse neocortical neurons. *Genes Dev* **16**, 1760-1765.
- Super, H., Martinez, A., Del Rio, J.A. and Soriano, E. (1998a). Involvement of distinct pioneer neurons in the formation of layer-specific connections in the hippocampus. *J Neurosci* **18**, 4616-4626.
- Super, H. and Soriano, E. (1994). The organization of the embryonic and early postnatal murine hippocampus. II. Development of entorhinal, commissural, and septal connections studied with the lipophilic tracer Dil. *J Comp Neurol* **344**, 101-120.
- Super, H., Soriano, E. and Uylings, H.B. (1998b). The functions of the preplate in development and evolution of the neocortex and hippocampus. *Brain Res Brain Res Rev* **27**, 40-64.
- Swanson, L.W. and Cowan, W.M. (1977). An autoradiographic study of the organization of the efferent connections of the hippocampal formation in the rat. *J Comp Neurol* **172**, 49-84.
- Sweet, H.O., Bronson, R.T., Johnson, K.R., Cook, S.A. and Davisson, M.T. (1996). Scrambler, a new neurological mutation of the mouse with abnormalities of neuronal migration. *Mamm Genome* **7**, 798-802.
- Tabata, H. and Nakajima, K. (2003). Multipolar migration: the third mode of radial neuronal migration in the developing cerebral cortex. *J Neurosci* **23**, 9996-10001.
- Takahashi, T., Goto, T., Miyama, S., Nowakowski, R.S. and Caviness, V.S., Jr. (1999). Sequence of neuron origin and neocortical laminar fate: relation to cell cycle of origin in the developing murine cerebral wall. *J Neurosci* **19**, 10357-10371.
- Terashima, T., Inoue, K., Inoue, Y., Mikoshiba, K. and Tsukada, Y. (1983). Distribution and morphology of corticospinal tract neurons in reeler mouse cortex by the retrograde HRP method. *J Comp Neurol* **218**, 314-326.
- Tissir, F. and Goffinet, A.M. (2003). Reelin and brain development. *Nat Rev Neurosci* **4**, 496-505.
- Torres, R., Firestein, B.L., Dong, H., Staudinger, J., Olson, E.N., Hagan, R.L., *et al.* (1998). PDZ proteins bind, cluster, and synaptically colocalize with Eph receptors and their ephrin ligands. *Neuron* **21**, 1453-1463.
- Toth, J., Cutforth, T., Gelinas, A.D., Bethoney, K.A., Bard, J. and Harrison, C.J. (2001). Crystal structure of an ephrin ectodomain. *Dev Cell* **1**, 83-92.
- Tremblay, M.E., Riad, M., Bouvier, D., Murai, K.K., Pasquale, E.B., Descarries, L. and Doucet, G. (2007). Localization of EphA4 in axon terminals and dendritic spines of adult rat hippocampus. *J Comp Neurol* **501**, 691-702.
- Trommsdorff, M., Borg, J.P., Margolis, B. and Herz, J. (1998). Interaction of cytosolic adaptor proteins with neuronal apolipoprotein E receptors and the amyloid precursor protein. *J Biol Chem* **273**, 33556-33560.
- Trommsdorff, M., Gotthardt, M., Hiesberger, T., Shelton, J., Stockinger, W., Nimpf, J., *et al.* (1999). Reeler/Disabled-like disruption of neuronal migration in knockout mice lacking the VLDL receptor and ApoE receptor 2. *Cell* **97**, 689-701.
- Utsunomiya-Tate, N., Kubo, K., Tate, S., Kainosho, M., Katayama, E., Nakajima, K. and Mikoshiba, K. (2000). Reelin molecules assemble together to form a large protein complex, which is inhibited by the function-blocking CR-50 antibody. *Proc Natl Acad Sci U S A* **97**, 9729-9734.
- Valcanis, H. and Tan, S.S. (2003). Layer specification of transplanted interneurons in developing mouse neocortex. *J Neurosci* **23**, 5113-5122.
- Varma, R. and Mayor, S. (1998). GPI-anchored proteins are organized in submicron domains at the cell surface. *Nature* **394**, 798-801.

- Verhey, K.J., Meyer, D., Deehan, R., Blenis, J., Schnapp, B.J., Rapoport, T.A. and Margolis, B. (2001). Cargo of kinesin identified as JIP scaffolding proteins and associated signaling molecules. *J Cell Biol* **152**, 959-970.
- Walsh, C.A. and Goffinet, A.M. (2000). Potential mechanisms of mutations that affect neuronal migration in man and mouse. *Curr Opin Genet Dev* **10**, 270-274.
- Wegmeyer, H., Egea, J., Rabe, N., Gezelius, H., Filosa, A., Enjin, A., *et al.* (2007). EphA4-dependent axon guidance is mediated by the RacGAP alpha2-chimaerin. *Neuron* **55**, 756-767.
- Weinges, S. (2006). Molecular dissection of ephrinB reverse signaling. *Dissertation*.
- Weiss, K.H., Johanssen, C., Tielsch, A., Herz, J., Deller, T., Frotscher, M. and Forster, E. (2003). Malformation of the radial glial scaffold in the dentate gyrus of reeler mice, scrambler mice, and ApoER2/VLDLR-deficient mice. *J Comp Neurol* **460**, 56-65.
- Wilkinson, D.G. (2001). Multiple roles of EPH receptors and ephrins in neural development. *Nat Rev Neurosci* **2**, 155-164.
- Woodhams, P.L. and Terashima, T. (1999). Lamina boundaries persist in the hippocampal dentate molecular layer of the mutant Shaking Rat Kawasaki despite aberrant granule cell migration. *J Comp Neurol* **409**, 57-70.
- Woodhams, P.L. and Terashima, T. (2000). Aberrant trajectory of entorhino-dentate axons in the mutant Shaking Rat Kawasaki: a Dil-labelling study. *Eur J Neurosci* **12**, 2707-2720.
- Wybenga-Groot, L.E., Baskin, B., Ong, S.H., Tong, J., Pawson, T. and Sicheri, F. (2001). Structural basis for autoinhibition of the Ephb2 receptor tyrosine kinase by the unphosphorylated juxtamembrane region. *Cell* **106**, 745-757.
- Wyss, J.M., Stanfield, B.B. and Cowan, W.M. (1980). Structural abnormalities in the olfactory bulb of the Reeler mouse. *Brain Res* **188**, 566-571.
- Yacubova, E. and Komuro, H. (2003). Cellular and molecular mechanisms of cerebellar granule cell migration. *Cell Biochem Biophys* **37**, 213-234.
- Yasui, N., Nogi, T., Kitao, T., Nakano, Y., Hattori, M. and Takagi, J. (2007). Structure of a receptor-binding fragment of reelin and mutational analysis reveal a recognition mechanism similar to endocytic receptors. *Proc Natl Acad Sci U S A* **104**, 9988-9993.
- Yip, J.W., Yip, Y.P., Nakajima, K. and Capriotti, C. (2000). Reelin controls position of autonomic neurons in the spinal cord. *Proc Natl Acad Sci U S A* **97**, 8612-8616.
- Yokoyama, N., Romero, M.I., Cowan, C.A., Galvan, P., Helmbacher, F., Charnay, P., *et al.* (2001). Forward signaling mediated by ephrin-B3 prevents contralateral corticospinal axons from recrossing the spinal cord midline. *Neuron* **29**, 85-97.
- Yoshida, M., Assimacopoulos, S., Jones, K.R. and Grove, E.A. (2006). Massive loss of Cajal-Retzius cells does not disrupt neocortical layer order. *Development* **133**, 537-545.
- Yozu, M., Tabata, H. and Nakajima, K. (2004). Birth-date dependent alignment of GABAergic neurons occurs in a different pattern from that of non-GABAergic neurons in the developing mouse visual cortex. *Neurosci Res* **49**, 395-403.
- Yu, H.H., Zisch, A.H., Dodelet, V.C. and Pasquale, E.B. (2001). Multiple signaling interactions of Abl and Arg kinases with the EphB2 receptor. *Oncogene* **20**, 3995-4006.
- Yuasa, S., Kitoh, J., Oda, S. and Kawamura, K. (1993). Obstructed migration of Purkinje cells in the developing cerebellum of the reeler mutant mouse. *Anat Embryol (Berl)* **188**, 317-329.
- Zajchowski, L.D. and Robbins, S.M. (2002). Lipid rafts and little caves. Compartmentalized signalling in membrane microdomains. *Eur J Biochem* **269**, 737-752.
- Zhang, Y. and Bhavnani, B.R. (2005). Glutamate-induced apoptosis in primary cortical neurons is inhibited by equine estrogens via down-regulation of caspase-3 and prevention of mitochondrial cytochrome c release. *BMC Neurosci* **6**, 13.
- Zhao, S., Chai, X., Forster, E. and Frotscher, M. (2004). Reelin is a positional signal for the lamination of dentate granule cells. *Development* **131**, 5117-5125.

8 Bibliography

- Zhao, S., Chai, X. and Frotscher, M. (2007). Balance between neurogenesis and gliogenesis in the adult hippocampus: role for reelin. *Dev Neurosci* **29**, 84-90.
- Zhong, Y. and Wu, C.F. (2004). Neuronal activity and adenylyl cyclase in environment-dependent plasticity of axonal outgrowth in *Drosophila*. *J Neurosci* **24**, 1439-1445.
- Zhou, L., Li, Y. and Yue, B.Y. (1999). Alteration of cytoskeletal structure, integrin distribution, and migratory activity by phagocytic challenge in cells from an ocular tissue--the trabecular meshwork. *In Vitro Cell Dev Biol Anim* **35**, 144-149.
- Zimmer, C., Tiveron, M.C., Bodmer, R. and Cremer, H. (2004). Dynamics of Cux2 expression suggests that an early pool of SVZ precursors is fated to become upper cortical layer neurons. *Cereb Cortex* **14**, 1408-1420.
- Zisch, A.H. and Pasquale, E.B. (1997). The Eph family: a multitude of receptors that mediate cell recognition signals. *Cell Tissue Res* **290**, 217-226.

9 Acknowledgements

It is a pleasure to acknowledge the help of many people who made this thesis possible.

My deepest gratitude goes to my dear supervisor Prof. Amparo Acker-Palmer for giving me the opportunity to carry out my PhD work on this exciting project in a great scientific environment. I greatly appreciate her constant support and interest in my work, expertise and kindness. I am especially grateful for her trust in me and the freedom I had during my thesis work which allowed me to develop my own thoughts and interests. Her positive energy, valuable insights, constant encouragement created a pleasant working environment throughout my thesis work.

My special thanks go to my external thesis committee members, Viktor Tarabykin and Michael Froetscher for their time, sincere interest and scientific advices.

I want to thank to Sylvia Pfenning for her cheerful and fluent collaboration, and friendship, as well as to Katja Burk and Alexander Weiss for their experimental contribution at the initial stages of this project. Help from my summer students, Ozge Yildiz and Ceren Saygi has also been wonderful.

I am especially grateful to Inmaculada Segura as an excellent teacher for being there whenever I needed help and explain with endless patience at the beginning of my PhD, especially for introducing me to the “mice work” and all kinds of help. I am very thankful for her mentorship and friendship which have greatly contributed to my work.

I sincerely appreciated the friendship, scientific suggestions and discussions of my PhD fellow Suphansa Sawamiphak starting from our start to our thesis work on the same day.

I want to thank my past and present colleagues from the Acker-Palmer group, Inmaculada Segura, Suphansa Sawamiphak, Clara Essmann, Helge zum Buttel, Julia Geiger, Elsa Martinez, Stephan Weinges, Sylvia Pfennig, Mathias Ritter, Eva Harde, Kristin Happich, Denis Schmelzer and Ursula

Bauer for providing me a nice, cheerful and friendly working environment in which to learn and grow.

I wish to thank Rudiger Klein for his support and critical questions and suggestions, and all members of Klein lab, especially Joaquim Egea for critical suggestions and discussions during the joined lab-meetings and for their technical help when required during.

Special thanks are dedicated to my fellow colleagues from the Max-Planck-Institute, especially Barbara Cokic, Ali Ertuerk, Joaquim Egea, Christian Erlacher, Alessandro Filosa, Ilona Kadow, Archana Mishra for the nice and relaxed working atmosphere and practical advices, for providing a stimulating and fun environment and friendship especially in the first two years of PhD work.

I also would like to thank Sylvia Pfennig for translating the summary of this thesis into German.

I acknowledge our animal care taker, Kristin Happich for her patience and care for helping me to keep my mice colony, without her it would be impossible to control all several mice lines that I have worked on during my thesis project. I also thank the dozens upon dozens of mice who made the scientific research possible on my behalf.

I offer my regards to those who supported me in any respect during the completion of the project.

Finally, and most importantly, I want to thank to my parents, Nursen and Yilmaz Senturk, for providing me a background which enabled me to make this PhD thesis. I thank my father who has always put education as a first priority in my life and encouraged me to set high goals for myself. Last but not least I want to thank to my brother Onder and my sister Aylin for their love and support, as well as to Serdar Sari and to my best friends for their encouragement and support throughout my life, this thesis is simply impossible without them.

10 Publication List

1. **Senturk A.**, Pfennig S., Weiss A., Burk K. and Acker-Palmer A. (2011). *EphrinBs are functional co-receptors for Reelin signaling to regulate neuronal migration*. Nature, in press.
2. Gregor B. Deutsch, Elisabeth M. Zielonka, Daniel Coutandin, Tobias A. Weber, Birgit Schäfer, Jens Hannewald, Laura M. Luh, Florian G. Durst, Mohamed Ibrahim, Jan Hoffmann, Frank H. Niesen, **Aycan Sentürk**, Hana Kunkel, Bernd Brutschy, Enrico Schleiff, Stefan Knapp, Amparo Acker-Palmer, Manuel Grez, Frank McKeon, Volker Dötsch. *DNA damage in oocytes induces an irreversible switch of the quality control factor TAp63 from dimer to tetramer*. **Cell**, 2011 Feb 18; 144(4): 566-76, 2011.

11 Curriculum Vitae

Personal data

Name	Aycan Senturk
Birth date	27 th of May 1981
Birth place	Olpe, GERMANY
Nationality	Turkish
Parents	Prof. Dr. Yilmaz and Nursen Sentürk

Professional Appointments

August 2010 – present **Postdoc position**

Goethe University Frankfurt
Institute for Cell Biology and Neurosciences
Laboratory of Prof. Acker-Palmer

Education

July 2008-July 2010 **PhD Thesis (continuation)**

Goethe University Frankfurt
Institute for Cell Biology and Neurosciences
Laboratory of Prof. Acker-Palmer

April 2006 July 2008 **PhD Thesis (beginning)**

Max-Planck Institute for Neurobiology, Martinsried
Department of Molecular Neurobiology
Junior research group: Signal Transduction, Prof. Acker-Palmer

Oct 2005-March 2006 **Master Thesis**

Max-Planck Institute for Neurobiology, Martinsried
Department of Molecular Neurobiology
Supervised by Prof. Acker-Palmer
“Crosstalk between Reelin and Ephrin signaling”

11 Curriculum Vitae

Sep 2004-Sep 2005

Master of Science

Georg-August University, Göttingen

Biology Faculty, International Neuroscience Program, IMRPS, Göttingen

1999- 2004

Bachelor in Biological Sciences and Bioengineering

Sabancı University, Istanbul, TURKEY

Major: Biological Sciences and Bioengineering

Minor: Chemistry

1992 – 1999

Abitur

Eskişehir Anatolian High School, Eskişehir, TURKEY

